RADIOLOGY AND ONCOLOGY

vol.47 no.3
september 2013

Halaven®
eribulin

NOVA SMER DO PODALJŠANJA **CELOKUPNEGA PREŽIVETJA**

Eisai

Prva in edina samostojna kemoterapija, ki v primerjavi z ostalimi možnostmi zdravljenja z enim zdravilom, pri bolnicah s predhodno že večkratno zdravljenim metastatskim rakom dojke, dokazano značilno podaljša celokupno preživetje.[1,2]

- **Halaven** (eribulin): ne-taksanski zaviralec dinamike mikrotubulov, prvo zdravilo iz nove skupine kemoterapevtikov, imenovanih *halihondrini*.
- Monoterapija z zdravilom HALAVEN je indicirana za zdravljenje bolnic z lokalno napredovalim ali metastatskim rakom dojke, ki je napredoval po vsaj dveh režimih kemoterapije za napredovalo bolezen. Predhodna zdravljenja morajo vključevati antraciklin in taksan, razen če to zdravljenje za bolnice ni bilo primerno.[1]
- Priporočeni odmerek 1,23 mg/m^2, intravensko, v obliki 2- do 5-minutne infuzije, 1. in 8. dan vsakega 21-dnevnega cikla.
- Ena 2 ml viala vsebuje 0,88 mg eribulina.
- Raztopina, pripravljena za uporabo, redčenje ni potrebno.

SKRAJŠAN POVZETEK GLAVNIH ZNAČILNOSTI ZDRAVILA

HALAVEN 0,44 mg/ml raztopina za injiciranje (eribulin)
TERAPEVTSKE INDIKACIJE: Zdravljenje lokalno napredovalega ali metastatskega raka dojke, ki je napredoval po vsaj dveh režimih kemoterapije za napredovalo bolezen vključno z antraciklinom in taksanom, razen če to ni bilo primerno. **ODMERJANJE IN NAČIN UPORABE:** Halaven se daje v enotah, specializiranih za dajanje citotoksične kemoterapije, in le pod nadzorom usposobljenega zdravnika z izkušnjami v uporabi citotoksičnih zdravil. **ODMERJANJE:** Priporočeni odmerek eribulina v obliki raztopine je 1,23 mg/m^2 i. v. obliki 2- do 5- minutne infuzije 1. in 8. dan vsakega 21-dnevnega cikla. Bolnikom je lahko slabo ali bruhajo. Treba je razmisliti o antiemetični profilaksi, vključno s kortikosteroidi. **Preložitev odmerka med zdravljenjem:** Dajanje Halavena je treba preložiti, če se pojavi kaj od naslednjega: absolutno število nevtrofilcev (ANC) < 1 x 10^9/l, trombociti < 75 x 10^9/l ali nehematološki neželeni učinki 3. ali 4. stopnje. **Zmanjšanje odmerka med zdravljenjem:** Za priporočila za zmanjšanje odmerka ob pojavu hematoloških ali nehematoloških neželenih učinkov glejte celoten povzetek glavnih značilnosti zdravila. **Okvara jeter zaradi zasevkov:** Priporočeni odmerek pri blagi okvari jeter (stopnje A po Child-Pughu) je 0,97 mg/m^2 v obliki 2- do 5- minutne i. v. infuzije 1. in 8. dan 21-dnevnega cikla. Priporočeni odmerek pri zmerni okvari jeter (stopnje B po Child-Pughu) je 0,62 mg/m^2 v obliki 2- do 5- minutne i. v. infuzije 1. in 8. dan 21-dnevnega cikla. Pri hudi okvari jeter (stopnje C) se pričakuje, da je treba dati še manjši odmerek eribulina. **Okvara jeter zaradi ciroze:** Zgornje odmerke se lahko uporabi za blago do zmerno okvaro, vendar se priporoča skrbno nadziranje, saj bo odmerke morda treba ponovno prilagoditi. **Okvara ledvic:** Pri hudi okvari ledvic (očistek kreatinina <40 ml/min) bo morda treba odmerek zmanjšati. Priporoča se skrbno nadziranje varnosti. **NAČIN UPORABE:** Odmerek se lahko razredči z do 100 ml 0,9 % natrijevega klorida (9 mg/ml) za injiciranje. Ne sme se ga redčiti v 5 % infuzijski raztopini glukoze. Pred dajanjem glejte navodila glede redčenja zdravila v celotnem povzetku glavnih značilnosti zdravila ter se prepričajte, da obstaja dober periferni venski dostop ali predhodna centralna linija. Ni znakov, da bi eribulin povzročal mehurje ali dražil. V primeru ekstravazacije mora biti zdravljenje simptomatsko. **KONTRAINDIKACIJE:** Preobčutljivost na zdravilno učinkovino ali katerokoli pomožno snov. Dojenje. **POSEBNA OPOZORILA IN PREVIDNOSTNI UKREPI:** Mielosupresija je odvisna od odmerka in se kaže kot nevtropenija. Pred vsakim odmerkom eribulina je treba opraviti pregled celotne krvne slike. Zdravljenje z eribulinom se lahko uvede le pri bolnikih z vrednostmi ANC ≥ 1,5 x 10^9/l in s trombociti > 100 x 10^9/l. Bolnike, pri katerih se pojavijo febrilna nevtropenija, huda nevtropenija ali trombocitopenija, je treba zdraviti v skladu s priporočili v celotnem povzetku glavnih značilnosti zdravila. Hudo nevtropenijo se lahko zdravi z uporabo G-CSF ali enakovrednim zdravilom v skladu s smernicami. Bolnike je treba skrbno nadzirati za znake periferne motorične in senzorične nevropatije. Pri razvoju hude periferne nevrotoksičnosti je treba odmerek prestaviti ali zmanjšati. Če začnemo zdravljenje pri bolnikih s kongestivnim srčnim popuščanjem, z bradiaritmijami, z zdravili, za katera je znano, da podaljšujejo interval QT, vključno z antiaritmiki razreda Ia in III, in z elektrolitskimi motnjami, je priporočljivo spremljanje EKG. Pred začetkom zdravljenja s Halavenom je treba popraviti hipokaliemijo in hipomagneziemijo in te elektrolite je treba občasno kontrolirati med zdravljenjem. Halavena ne smemo dajati bolnikom s prirojenim sindromom dolgega intervala QT. To zdravilo vsebuje majhne količine etanola (alkohola), manj kot 100 mg na odmerek. Eribulin je pri podganah embriotoksičen, fetotoksičen in teratogen. Halavena se ne sme uporabljati med nosečnostjo, razen kadar je to nujno potrebno. Ženske v rodni dobi naj ne zanosijo v času, ko same ali njihov moški partner dobivajo Halaven, in naj med zdravljenjem in še do 3 mesece po njem uporabljajo učinkovito kontracepcijo. Moški naj se pred zdravljenjem posvetujejo o shranjevanju sperme zaradi možnosti nepopravljive neplodnosti. **INTERAKCIJE:** Eribulin se izloča do 70 % prek žolča. Sočasna uporaba učinkovin, ki zavirajo jetrne transportne beljakovine, kot so beljakovine za prenos organskih anionov, P-glikoprotein, beljakovine, odporne na številna zdravila, z eribulinom se ne priporoča (npr. ciklosporin, ritonavir, sakvinavir, lopinavir in nekateri drugi zaviralci proteaze, efavirenz, emtricitabin, verapamil, klaritromicin, kinin, kinidin, dizopiramid itd). Sočasno zdravljenje z indukcijskimi učinkovinami, kot so rifampicin, karbamazepin, fenitoin, šentjanževka lahko povzroči znižanje koncentracij eribulina v plazmi, zato je ob sočasni uporabi induktorjev potrebna previdnost. Eribulin lahko zavira encim CYP3A4. Pri sočasni uporabi z učinkovinami, ki jih v glavnem presnavlja encim CYP3A4, se priporoča skrbno spremljanje zaradi povečanih koncentracij sočasno uporabljene učinkovine v plazmi. Če ima učinkovina ozek terapevtski razpon, je ne uporabljajte sočasno. **NEŽELENI UČINKI:** *Zelo pogosti (≥1/10):* nevtropenija (54,5 %), (3./4. stopnje: 48,3 %), levkopenija (22,1 %), (3./4. stopnje: 14 %), anemija (20,3 %), (3./4. stopnje: 1,4 %), zmanjšan apetit, periferna nevropatija (32,0 %), (3./4. stopnje: 6,9 %), glavobol, slabost (35,1 %), (3./4. stopnje: 1,1 %), zaprtost, driska, bruhanje, alopecija, artralgija in mialgija, utrujenost/astenija (52,8 %), (3./4. stopnje: 8,4 %), pireksija. *Pogosti (≥1/100 do <1/10):* okužba sečil, ustna kandidiaza, okužba zgornjih dihal, nazofaringitis, rinitis, febrilna nevtropenija (4,7 %), (3./4. stopnje: 4,6 %), trombocitopenija, limfopenija, hipokaliemija, hipomagneziemija, dehidracija, hiperglikemija, hipofosfatemija, nespečnost, depresija, disgevzija, omotičnost, hipoestezija, letargija, nevrotoksičnost, obilnejše solzenje, konjunktivitis, vrtoglavica, tahikardija, vročinski valovi, dispnea, kašelj, orofaringealna bolečina, epistaksa, rinoreja, bolečina v trebuhu, stomatitis, suha usta, dispepsija, gastroezofagealna refluksna bolezen, razjede v ustih, napihnjenost želodca, zvišanje alanin aminotransferaze (3,0 %), (3./4. stopnje: 1,1 %) in aspartat aminotransferaze, izpuščaj, pruritus, bolezni nohtov, nočno potenje, palmarno-plantarna eritrodisestezija, suha koža, eritem, hiperhidroza, bolečina v okončinah, mišični spazmi, mišično-skeletna bolečina in mišično-skeletna bolečina v prsih, mišična oslabelost, bolečina v kosteh, bolečina v hrbtu, vnetje sluznice (9,8 %), (3./4. stopnje: 1,3 %), periferni edem, bolečina, mrzlica, gripi podobna bolezen, bolečina v prsih, zmanjšanje telesne mase. *Občasni (≥1/1.000 do <1/100):* pljučnica, nevtropenična sepsa, ustni herpes, herpes zoster, tinitus, globoka venska tromboza, pljučna embolija, intersticijska pljučna bolezen, hiperbilirubinemija, angioedem, disurija, hematurija, proteinurija, odpoved ledvic. *Redki (≥1/10.000 do <1/1.000):* pankreatitis. Za popoln opis neželenih učinkov glejte celoten povzetek glavnih značilnosti zdravila. **Vrsta ovojnine in vsebina:** viala z 2 ml raztopine. **Režim izdaje:** H. **Imetnik dovoljenja za promet:** Eisai Europe Ltd, Mosquito Way, Hatfield, Hertfordshire, AL10 9SN, Velika Britanija. HAL-161112

Pred predpisovanjem in uporabo zdravila prosimo preberite celoten povzetek glavnih značilnosti zdravila!

Viri: (1) Povzetek glavnih značilnosti zdravila Halaven, november 2012; (2) Cortes J *et al. Lancet* 2011; 377: 914–23

PharmaSwiss
Choose More Life

Odgovoren za trženje v Sloveniji:
PharmaSwiss d.o.o., Dolenjska cesta 242c, 1000 Ljubljana
telefon: +386 1 236 47 00, faks: +386 1 283 38 10

HAL 0113-01, januar 2013

RADIOLOGY AND ONCOLOGY

September 2013
Vol. 47 No. 3
Pages 197-310
ISSN 1318-2099
UDC 616-006
CODEN: RONCEM

Publisher
Association of Radiology and Oncology

Affiliated with
Slovenian Medical Association – Slovenian Association of Radiology, Nuclear Medicine Society,
Slovenian Society for Radiotherapy and Oncology, and Slovenian Cancer Society
Croatian Medical Association – Croatian Society of Radiology
Societas Radiologorum Hungarorum
Friuli-Venezia Giulia regional groups of S.I.R.M.
Italian Society of Medical Radiology

Aims and scope
Radiology and Oncology is a journal devoted to publication of original contributions in diagnostic and interventional radiology, computerized tomography, ultrasound, magnetic resonance, nuclear medicine, radiotherapy, clinical and experimental oncology, radiobiology, radiophysics and radiation protection.

Editorial office

Radiology and Oncology
Zaloška cesta 2
P. O. Box 2217
SI-1000 Ljubljana
Slovenia
Phone: +386 1 5879 369
Phone/Fax: +386 1 5879 434
E-mail: gsersa@onko-i.si

Reader for English

Vida Kološa

Secretary

Mira Klemenčič

Zvezdana Vukmirović

Design

Monika Fink-Serša, Samo Rovan, Ivana Ljubanović

Layout

Matjaž Lužar

Printed by

Tiskarna Ozimek, Slovenia

Published quarterly in 600 copies

Beneficiary name: DRUŠTVO RADIOLOGIJE IN ONKOLOGIJE
Zaloška cesta 2
1000 Ljubljana
Slovenia

Beneficiary bank account number: SI56 02010-0090006751
IBAN: SI56 0201 0009 0006 751
Our bank name: Nova Ljubljanska banka, d.d.,
Ljubljana, Trg republike 2,
1520 Ljubljana; Slovenia

SWIFT: LJBASI2X

Subscription fee for institutions EUR 100, individuals EUR 50

The publication of this journal is subsidized by the Slovenian Research Agency.

Indexed and abstracted by:
Science Citation Index Expanded (SciSearch®)
Journal Citation Reports/Science Edition
Scopus
PubMed
PubMed Central
EMBASE/Excerpta Medica
DOAJ
Open J-gate
Chemical Abstracts
Biomedicina Slovenica
Summon by Serial Solutions (ProQuest)

This journal is printed on acid- free paper

On the web: ISSN 1581-3207
http://www.degruyter.com/view/j/raon
http://www.radioloncol.com

contents

experimental oncology

clinical oncology

radiophysics

RADIOLOGY AND ONCOLOGY is covered in Science Citation Index Expanded (SciSearch®),Journal Citation Reports/Science Edition, Scopus, PubMed, PubMed Central, DOAJ, EMBASE/Excerpta Medica, Open J-gate, Chemical Abstracts, Biomedicina Slovenica, Summon by Serial Solutions (ProQuest)

review

The role of extracellular vesicles in phenotypic cancer transformation

Eva Ogorevc[1], Veronika Kralj-Iglic[2], Peter Veranic[3]

[1] Laboratory of Biophysics, Faculty of Electrical Engineering, University of Ljubljana, Slovenia
[2] Faculty of Health Sciences, University of Ljubljana, Slovenia
[3] Institute of Cell Biology, Faculty of Medicine, University of Ljubljana, Ljubljana, Slovenia

Radiolo Oncol 2013; 47(3): 197-205.

Received: 22 February 2013
Accepted: 2 May 2013

Correspondence to: Prof. Peter Veranič, PhD, Institute of Cell Biology, Faculty of Medicine, University of Ljubljana, Lipičeva 2, Ljubljana, Slovenia. E-mail: peter.veranic@mf.uni-lj.si

Disclosure: No potential conflicts of interest were disclosed.

Background. Cancer has traditionally been considered as a disease resulting from gene mutations. New findings in biology are challenging gene-centered explanations of cancer progression and redirecting them to the non-genetic origins of tumorigenicity. It has become clear that intercellular communication plays a crucial role in cancer progression. Among the most intriguing ways of intercellular communication is that via extracellular vesicles (EVs). EVs are membrane structures released from various types of cells. After separation from the mother membrane, EVs become mobile and may travel from the extracellular space to blood and other body fluids.

Conclusions. Recently it has been shown that tumour cells are particularly prone to vesiculation and that tumour-derived EVs can carry proteins, lipids and nucleic acids causative of cancer progression. The uptake of tumour-derived EVs by noncancerous cells can change their normal phenotype to cancerous. The suppression of vesiculation could slow down tumour growth and the spread of metastases. The purpose of this review is to highlight examples of EV-mediated cancer phenotypic transformation in the light of possible therapeutic applications.

Key words: extracellular vesicles; exosomes; microvesicles; cancer progression

Introduction

Cancer has been traditionally viewed as a consequence of multistep mutations of genetic material that result in transformation of normal to malignant cells. However, nowadays the mainstream paradigms of cancer development and progression are shifting from strictly genocentric towards epigenetic and other nongenetic interpretations. It is thus relevant to explore the possibility that a normal cell could become malignant without previous genetic mutation. In this article several mechanisms of phenotypic transformation are presented mainly involving transfer of membrane attached receptors for growth factors, RNA molecules or even lipids [1,2,3]

It was suggested that intercellular communication plays a crucial role in cancer progression.[1] Exchange of information is attained through release of specific soluble (or immobilized) signalling molecules and their interaction with corresponding receptors[2], or through direct cell-to-cell communication that includes gap junctions[3], cytonems[4] and tunnelling nanotubes.[5] In addition to these mechanisms, a highly conserved way of intercellular communication has recently been revealed - communication via extracellular vesicles (EVs).

It is considered that EVs are membrane-enclosed compartments, released into the surroundings of practically all cell types, both *in vivo* and *in vitro*.[6] After separation from the mother membrane, vesicles with various types of cargo become mobile and may travel from the extracellular/intercellular space to blood (Figure 1). Besides in blood isolates[7,8], EVs were also found in isolates from other body fluids, *i.e.* urine[9,10], ascites[11,12], synovial fluid[8,13], malignant pleural effusions[12,14], bronchial lavage fluid[15], human semen[16], breast milk[17], pregnancy-associated

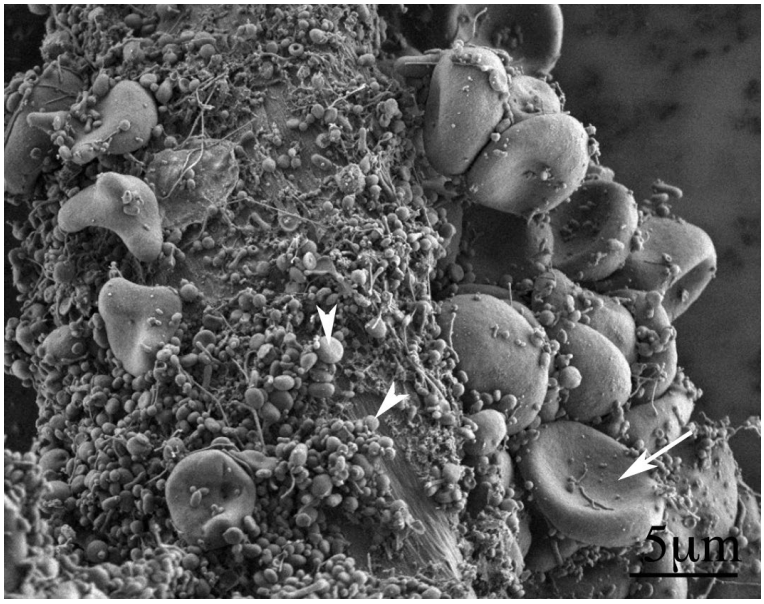

FIGURE 1. Scanning electron micrograph of an isolate from peripheral blood of a healthy human donor (male, 28 years). A mass of extracellular vesicles (arrowhead) and numerous residual erythrocytes (arrow) can be seen. The image was taken using a Quanta TM 250 FEG scanning electron microscope.

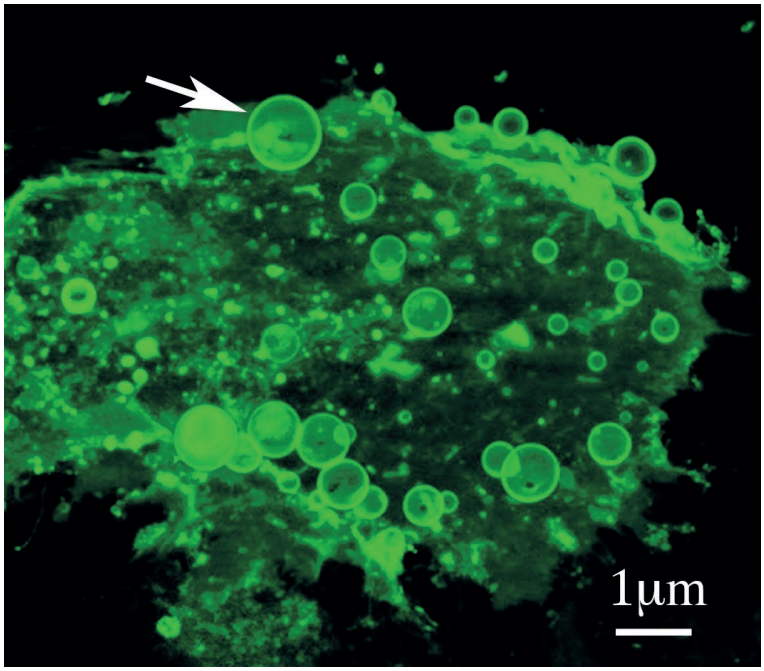

FIGURE 2. A micrograph presenting multiple vesicles budding from a cell of a urothelial cancer cell line T24 labeled with coleratoxin B - FITC. Arrow points to a budding vesicle. The micrograph is a threedimensional reconstruction of optical sections done by a fluorescence microscope.

sera[18], amniotic fluid[19], ocular fluids[20] and human saliva.[21] The vesicles detectable in isolates *in vitro* and *in vivo* represent a mixed population of various sizes and origins. To date no consensus regarding their classification and nomenclature was reached to distinguish between different types of vesicles. In this work we do not consider the apoptotic bodies (usually larger than 1 μm) which are released from the cell in the final stage of programmed cell death.

The content of EVs depends on the cell of origin and the mechanism of vesicle generation. They were found to transfer surface-bound receptors and their ligands, proteins, genetic material, infectious particles, prions and probably even organelles between cells.[22] A fascinating feature of EVs is that they present multiple epitopes to the recipient cells and therefore on one hand carry signalling molecules for phenotypic transformation and, on the other hand, serve as a cell mechanism to get rid of unwanted constitutents.[23]

Tumour-derived EVs (Figure 2) represent an important component of the tumour microenvironment[22], but can also take part in altering non-cancerous counterparts (cells) thus facilitating tumour growth and invasion[11], angiogenesis[24], metastasis[25], chemoresistance[26,27], immune evasion[28,29] and escape from cell death.[30] An increased number of circulating EVs were found in blood isolates of patients with gastrointestinal cancer.[31-33] It is, however, important to bear in mind that the EVs found in blood isolates are not necesarilly the native circulating vesicles but can also be formed during sampling and isolation procedures due to exposure of the cells to thermal and mechanical stress.[6] Nevertheless, studying EVs isolated from blood and other body fluids of cancer patients is of special interest, not only because cancer cells are particularly prone to vesiculation, but also because of greater vulnerability and fragmentation of blood cells (platelets) in cancer patients, which could be reflected in a higher concentration of EVs in blood-isolates[6] which could be used as a valuable diagnostic marker.[2]

Formation of extracellular vesicles

The exact mechanisms underlying the formation of EVs have not yet been fully elucidated, but it seems that vesiculation can be either an extremely well regulated process, or a random, non-specific event associated with, for example, disintegration of the plasma membrane. It is important to realize that general mechanisms of membrane vesicula-

tion can also play a pivotal role in the progression of disease.

Membrane vesiculation takes place in the last phase of membrane budding when the bud is pinched off from the membrane to become a free vesicle (Figure 3A). Budding and vesiculation are essential features of the nonspecific biophysical properties of the membrane that impose local and/or global curvature on the membrane in phospholipid bilayer vesicles[34,35], in erythrocytes[36] and in other cells.[37,38] The packing and distribution of membrane constituents creates local membrane curvature which is consistent with lateral sorting of membrane constituents.[39] During budding, accumulation of molecules that energetically favour large curvature drives the formation of buds and EVs.[40] Vesiculation can also be induced by nonlocal events such as an increase or a decrease in the difference between two membrane areas, as described within the bilayer couple concept.[41-43]

There is a codependence between membrane shape and structure; moreover, membrane curvature is determined by the shapes of membrane constituents and their interactions.[44] Sphingolipids, for example, are located mainly in the outer leaflet of the plasma membrane bilayer, while glycerophospholipids such as phosphatidylserine and phosphatidylethanolamine can under normal circumstances be found only in the inner leaflet.[45,46] Cholesterol is believed to occur in similar proportions in both leaflets.[47] This balance is maintained by several enzymes: scramblase, flippase and translocase.[48] Disruption of membrane asymmetry and consequent bending of the membrane can occur spontaneously or by an energy-requiring process. Further, the composition and configuration of membrane layer areas are affected by pathophysiological processes such as cell activation, hypoxia, irradiation, oxidative injury, exposure to complement proteins and exposure to shear stress.[22] Relocation of phosphatidylserine and phosphatidylethanolamine from the inner to the outer leaflet of the plasma membrane is associated with membrane budding and formation of EVs.[49] EVs are formed in the last stage of the budding process, and thus their surfaces expose large amounts of phosphatidylserine[50] which can be used for the capture of EVs by phosphatidylserine receptors, such as Annexin V.[51]

Additionally EVs seem to be enriched in proteins and lipids associated with membrane rafts.[50,52] Consistent with this, much experimental and theoretical evidence indicates the importance of membrane rafts in the process of membrane budding and vesiculation.[48] Membrane rafts are small (10-200 nm) relatively heterogeneous dynamic structures with an increased concentration of cholesterol and sphingolipids.[53,54] Potential roles of membrane rafts in membrane transport were proposed: they may serve as platforms for the inclusion of sorting receptors and cargo molecules, as sites for organizing the membrane cytoskeleton, or as sites for organizing vesicle docking and fusion processes.[55]

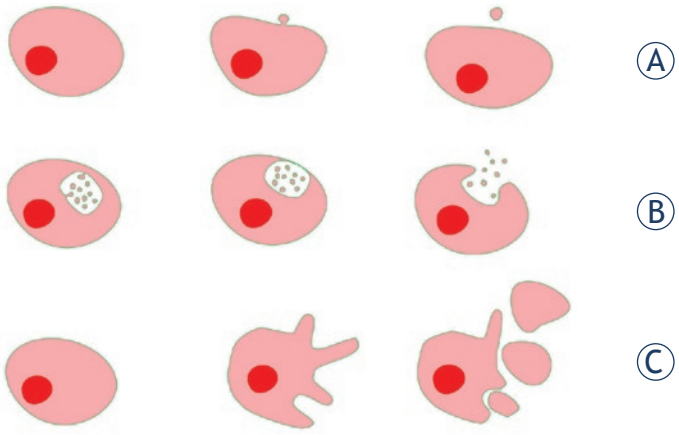

FIGURE 3. Formation of extracellular vesicles in tumor cells. A. Budding of plasma membrane. B. Release of exosomes after fusion of multivesicular body with plasma membrane. C. Non-apoptotic blebbing.

Other pathways leading to curvature and subsequent budding of membranes include an increase of intracellular Ca^{2+} inhibiting translocase, activating scramblase and resulting in loss of membrane asymmetry[48], the reorganization of the cytoskeleton[48,56], and the presence of protein and lipid driving forces since adding a protein or lipid to just one monolayer might cause asymmetry of monolayer areas and thereby increase the intrinsic curvature of the whole bilayer.[57]

Membrane budding can be followed by membrane fission, which is still a subject of some debate, but several ideas supporting the pivotal role of endophilin I and dynamin in this process have been suggested.[58,59]

EVs can also be formed in processes distinct from those already mentioned. EVs smaller than 100 nm, usually called exosomes, are formed by exocytosis after the assembly of several endosomes into a multivesicular body, exiting the endosomal pathway and fusion with the plasma membrane (Figure 3B).[50,60,61] Peculiarly large EVs (1 -10 mm) can be formed as a result of nonapoptotic blebbing (Figure 3C).[62] This relatively rapid process of EV-formation is caused by actomyosin contractions near the cortical cytoskeleton. The force required

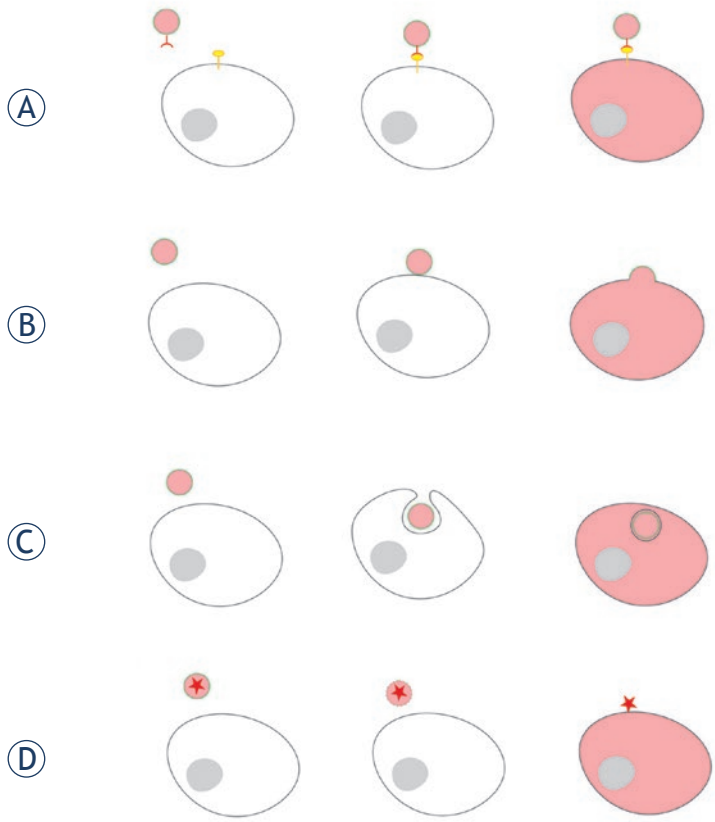

FIGURE 4. Interaction of extracellular vesicles with recipient cell. (A). Adhesion of vesicle molecules to recipient cell surface receptors. (B). Fusion of vesicle with plasma membrane of a recipient cell. (C). Endocytic / phagocytic uptake. D. Extracellular vesicle breakdown and release of its cargo. Transformed cells with pink cytoplasm.

for subsequent bleb retraction is generated by actin filaments.[62]

Interaction of extracellular vesicles with target cells

It is indicated that EVs interact with the membranes of recipient cells. The precise mechanisms of uptake of EVs are still poorly understood, yet it is becoming increasingly evident that their uptake can induce activation of specific signal transduction cascades and thereby influence the physiological or pathological state of recipient cells.[23,63]

Several types of interactions were proposed involving adhesion of vesicle molecules to cellular surface receptors (receptor-mediated uptake), endocytosis (phagocytosis) and fusion with the plasma membrane.[23,64]

Potential receptor candidates for interaction with EV-membranes are, notably, receptors for phosphatidylserine. One such receptor is the T-cell immunoglobulin and mucin-domain-containing molecule (TIM) that was described as mediating vesicle uptake.[65] Segura *et al*.[66] showed that EVs from mature dendritic cells are enriched in intercellular adhesion molecule 1 (ICAM-1), suggesting its role in either helping in capture of EVs by recipient antigen-presenting cells or in favouring T-cell binding of the recipient antigen-presenting cells bearing EVs at their surface (Figure 4A).

The phenomenon of fusion of vesicles with the plasma membrane could be explained by lipid-mediated interactions. Teissier and Pécheur described how lipid rafts, particularly sphingolipids, play a key role in the conformational changes of fusion proteins. These changes lead to interaction of the fusion peptide with the target membrane in viral interactions.[68] Parolini *et al*. showed that exosomes preferentially fuse with the membranes of tumour cells and that in these interactions the microenvironmental pH acts as a key factor by modulating the lipid compostition of the cell and exosome membranes (Figure 4B).[69]

It seems that phagocytosis is the most effective way of EV-uptake; moreover it has been reported that phagocytic cells have a greater ability for the uptake of EVs than non-phagocytic cells.[67] Besides phagocytosis clathrin-dependent endocytosis and macropinocytosis were proposed as mechanisms for the uptake of EVs by the ovarian carcinoma cell line (Figure 4C).[70]

Despite all the above discoveries, it is still a question whether the vesicle cargo can be transfered to the recipient cell without the interaction with the membranes. Taraboletti *et al*. showed that acidic pH can induce breakdown of EVs, leading to pericellular release of their cargo and subsequent paracrine activity (Figure 4D).[71] Furthermore, it has been stated that the breakdown of EVs upon shedding could represent an important signalling mechanism.[72]

Extracellular vesicles as vehicles in phenotypic malignant transformations

When EVs are taken up by recipient cells, they can change the cells' state, either transitionally or in the long term (Figure 5). Transformation of recipient cells due to EV-transfered cargo was shown to be most efficient if the cell was already to some degree pretransformed or immortalized (stem cells).[73] It is still unclear whether EVs may be able to exert long-term genomic changes, such as induction of mutations, but it has been brought to light not only that some oncogenes become incorporated into EV-cargo, but also that they can stimulate EV-formation.[74] Consenquently, EVs can act as vehi-

cles in malignant transformations of normal cells through the transfer of membrane proteins (receptors and receptor-coupled proteins), cytosol proteins, nucleic acids (RNA and DNA) and lipids.[3]

Extracellular vesicle-mediated protein transfer

Al Nedawi *et al*. showed that tumour specific growth receptor EGFRvIII can be transferred between glioma cells by EVs, leading to transfer of oncogenic activity, such as activation of transforming signalling pathways (MAPK and Akt), changes in expression of EGFRvIII-regulating genes (VEGF, Bcl-xL, p27), morphological transformation and increase in anchorage-independent growth capacity.[75]

Similar findings were reported in a study by Skog *et al*., where they detect tumour-specific EGFRvIII in serum EVs of glioblastoma patients.[24] Moreover, they demonstrated that EVs are enriched in angiogenic proteins (interleukin-6, interleukin-8, VEGF) and that they stimulate tubule formation by endothelial cells.[24]

A mechanism that controls metastatic progression through the EV-mediated transfer of another receptor, tyrosine kinase MET, has recently been described. EVs with oncoprotein MET from highly metastatic melanomas increased the metastatic behaviour of primary tumours by permanently educating and mobilizing bone marrow progenitors.[76]

Another example of EV-mediated protein delivery in tumour progession has been described by Sidhu *et al*.[77] The authors showed that extracellular matrix metalloproteinase inducer (EMMPRIN or CD147) is released from the surface of lung carcinoma cells via EVs which rapidly break down to release bioactive EMMPRIN, that stimulates matrix metalloproteinase expression in fibroblasts, thereby facilitating tumour invasion and metastasis.[77]

Many other proteins have been identified in EVs shed from cancer cells, including among others vascular endothelial growth factor (VEGF)[71], tetraspanins[64], heat-shock protein 90α[78], Mart-1/MelanA, carcinoembryogenic antigen[79] and HER2.[79,80]

Extracellular vesicle-mediated horizontal transfer of (epi)genetic information

Recently it has come to light that messenger RNA (mRNA) and various forms of non-coding RNA, such as microRNA (miRNA), act as key players in information transfer between cells.[81] miRNAs are small noncoding RNA gene products believed to negatively regulate other genes' expression. Furthermore, there is evidence that miRNA species might act as tumour suppressors and oncogenes.[82,83] As RNA molecules are unstable in plasma or blood[84,85], they should be in some way protected from degradation during systemic transport. Membrane vesicles appear to be ideal candidates for this kind of protection. In fact, it seems that almost all systemically transfered RNA is stored compactly within EVs and is thereby protected from external RNAse.[24,81] Additionally, more permanent modulation of recipient cells may be achieved through uptake of EVs containing nucleic acids. Interestingly, a microarray comparison of mRNA populations in EVs and their donor cells showed that specific mRNA species were detected exclusively in EVs, suggesting a specific packaging mechanism that encapsulates these mRNAs into EVs.[24,86] Several groups have described the key role of EV-mediated mRNA transfer in tumour progression in various types of cancer, such as colorectal adenocarcinoma[87,88], pancreatic adenocarcinoma[88], lung carcinoma[88] and glioblastoma.[24] The presence of specific miRNA species has been reported in EVs derived either from carcinoma cell-lines or from serum of cancer patients. A study showed that hepatocellular carcinoma cell-derived EVs mediate miRNA transfer and thereby enhance recipient cell growth.[89] Ohshima *et al*. reported that metastatic gastric cancer cell line releases EVs enriched in let-7-miRNAs, known to negatively regulate Ras genes, leading to maintenance of their oncogenesis.[90] Another study showed that EVs from the serum of ovarian cancer patients contain specific miRNA signatures and suggested that circu-

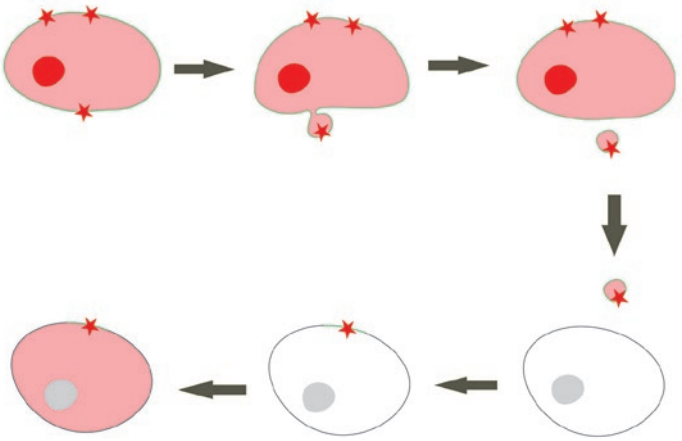

FIGURE 5. Transfer of oncogenic proteins that induce phenotypic transformation. Tumor cell (pink cytoplasm) with a mutated gene (red nucleus) for membrane protein (EGFRvIII – red asterisk) serve as a donor of this protein which is transferred to a nontumor cell (white cytoplasm). Phenotypic transformation (pink cytoplasm) is induced without mutation (gray nucleus)

lating EVs could potentially be used as surrogate diagnostic markers.[91]

EVs have been found to transfer DNA between cells, but it is important to keep in mind that EV fractions can also consist of apoptotic bodies, known to contain DNA fragments, possibly contributing to genetic changes and tumour progression.[92] A group recently showed that brain tumour cells release EVs that contain single stranded DNA (ssDNA), including both cDNA and genomic DNA.[93] The transported DNA contained amplified sequences of the c-Myc oncogene that could be available for horizonzal gene transfer and malignant transformation.[93]

Mitochondrial dysfunction and especially dysfunctions caused by mutations of mtDNA have been implicated with a wide range of age-related pathologies, including cancer.[94] It was reported that EVs from glioblastoma and astrocyte cells contain mitochondrial DNA which can be transferred between cells.[95]

A large part of the mammalian genome is derived from ancient transposable elements, such as DNA-transposons and retrotransposons. While DNA-transposons amplify without any RNA intermediate, retrotransposons need reverse transcriptase to retrotranscribe them before integration into the genome.[96] The expression of retrotransposons is increased in tumour cells through hypomethylation of the genome[97]; further it has been reported that retrotransposon insertion into the genome triggers mutations in tumorigenesis.[98] Balaj *et al*. incubated EVs derived from human medulloblastoma cells and enriched in retrotransposon RNAs, especially HERV-K, with HUVEC cells.[93] After incubation the content of HERV-K in the HUVEC cells was increased up to 60-fold, suggesting the active role of EVs in transfering retrotrasposon sequences to normal surrounding cells.[93]

Extracellular vesicle-mediated lipid delivery

Sphingomyelin is a major membrane phospholipid, mostly localized in the outer leaflet of the mammalian plasma membrane.[99] A significantly increased level of sphingomyelin in the highly metastatic adenocarcinoma cell line was reported in comparison to the lower metastatic variant of adenocarcinoma, suggesting the role of sphingomyelin not only as an important membrane component, but also as a key player in tumour metastasis.[100]

Kim *et al*. showed the importance of sphingomyelin transfer in cancer progression.[101] Namely, they indicated that sphingomyelin is a major active component in angiogenesis. They also found an increased amount of sphingomyelin in EVs derived from tumour cells compared to that from the plasma membrane.[101]

Suppression of oncogenic transformation by extracellular vesicles

It has been shown that heparin, usually used for the treatment of thromboembolisms[102], also has a beneficial effect in suppressing tumour progression in some types of cancer.[103,104] Interestingly, both effects of heparin can be explained by suppression of EV formation on the basis of non-specific biophysical mechanisms. The study, performed on artificial membrane models with controlled lipid composition – giant unilamellar vesicles (GUVs) - showed that budding and vesiculation of membranes can be affected by the surrounding solution.[105] Theoretically and experimentaly it was shown that molecules and ions in the solution can mediate attractive interactions between membranes and cause adhesion.[106,107] The composition and physical properties of the solution in the vicinity of the membrane[108-110] importantly affect these interactions and it was revealed that in the budding process the bud can adhere back to the mother membrane if the mediating effect of the solution is strong enough.[106] It was found that plasma contains molecules that mediate attractive interaction between membranes and that added heparin enhances this effect.[105] A mediating effect was also found for anticoagulant β2-glycoprotein I.[107,111] It was suggested that similar mechanisms may take place in cells, but it is important to note that cell membranes are of more complex composition, making the described mechanisms somewhat distinct.[105] Nevertheless, substances which mediate attractive interaction between membranes (*e.g*. heparin) are suppressors of membrane vesiculation and can therefore have anticoagulant, antimetastatic and anti-inflammatory effect.[105]

Conclusion

Recent investigations revealed that invasive tumours can be spread in the body not only by metastases travelling along tissues or being transported by body fluids and so seeding new tumours after anchoring to targeted tissues. Tumours can also be spread by much smaller carriers in the form of EVs containing genetic information or mutant growth factor receptors that are permanently active and

provoke over-inducing signalling of cell division. Transfer of such vesicles can occur over short distances to neighbouring cells or long distances by body fluids. By finding appropriate target cells the transferred transforming molecules can induce cell transformation and cause cancer progression most efficiently in already immortalized precancerous or stem cells. As tumor cell transformation is usually a multistep process including several consecutive mutations it can be concluded that the transfer of a transforming molecules can serve as one of the steps in this process. By carrying certain enzymes such as metalloproteinases, the EVs can adapt the microenvironment of tumour cells in favour of metastatic dissemination or implantation into certain tissues. Blocking the spreading of EVs, by the use of molecules attaching the vesicles to the vesiculating cells could possibly slow down tumour growth or the spread of metastases. On the other hand, screening of cancer genetic markers transported by EVs could improve diagnostic methods for detection of certain cancerous diseases. A thorough understanding of the biological mechanisms involved in intercellular communication by EVs could provide a key complement to genetic factors in determination of cancer progression, while their controlled manipulation will likely develop into a powerful weapon in the battlefield of oncology.

References

1. Al-Nedawi K, Meehan B, Rak J. Microvesicles: messengers and mediators of tumor progression. *Cell Cycle* 2009; **8:** 2014-18.
2. Rak J. Microparticles in cancer. *Semin Thromb Hemost* 2010; **36:** 888-906.
3. Pap E. The role of microvesicles in malignancies. *Adv Exp Med Biol* 2011; **714:** 183-199.
4. Camussi G, Deregibus MC, Bruno S, Grange C, Fonsato V, Tetta C. Exosome/microvesicle-mediated epigenetic reprogramming of cells. *Am J Cancer Res* 2011; **1:** 98-110.
5. Veranic P, Lokar M, Schutz GJ, Weghuber J, Wieser S, Hagerstrand H, et al. Different types of cell-to-cell connections mediated by nanotubular structures. *Biophys J* 2008; **95:** 4416-25.
6. Sustar V, Bedina-Zavec A, Stukelj R, Frank M, Bobojevic G, Jansa R, et al. Nanoparticles isolated from blood: a reflection of vesiculability of blood cells during the isolation process. *Int J Nanomedicine* 2011; **6:** 2737-48.
7. Wolf P. The nature and significance of platelet products in human plasma. *Br J Haematol* 1967; **13:** 269-88.
8. Junkar I, Sustar V, Frank M, Jansa V, Bedina Zavec A, Rozman B, et al. Blood and synovial microparticles as revealed by atomic force and scanning electron microscope. *Open Autoimmun J* 2009; **1:** 50-58.
9. Pisitkun T, Shen RF, Knepper MA. Identification and proteomic profiling of exosomes in human urine. *Proc Natl Acad Sci USA* 2004; **101:** 13368-73.
10. Gonzales P, Pisitkun T, Knepper MA. Urinary exosomes: is there a future? *Nephrol Dial Transplant* 2008; **23:** 1799-801.
11. Graves LE, Ariztia EV, Navari JR, Matzel HJ, Stack MS, Fishman DA. Proinvasive properties of ovarian cancer ascites-derived membrane vesicles. *Cancer Res* 2004; **64:** 7045-9.
12. Mrvar-Brecko A, Sustar V, Jansa V, Stukelj R, Jansa R, Mujagic E, et al. Isolated microvesicles from peripheral blood and body fluids as observed by scanning electron microscope. *Blood Cells Mol Dis* 2010; **44:** 307-12.
13. Skriner K, Adolph K, Jungblut PR, Burmester GR. Association of citrullinated proteins with synovial exosomes. *Arthritis Rheum* 2006; **54:** 3809-14.
14. Bard MP, Hegmans JP, Hemmes A, Luider TM, Willemsen R, Severijnen LA, et al. Proteomic analysis of exosomes isolated from human malignant pleural effusions. *Am J Respir Cell Mol Biol* 2004; **31:** 114-21.
15. Admyre C, Grunewald J, Thyberg J, Gripenback S, Tornling G, Eklund A, et al. Exosomes with major histocompatibility complex class II and co-stimulatory molecules are present in human BAL fluid. *Eur Respir J* 2003; **22:** 578-583.
16. Sullivan R, Saez F, Girouard J, Frenette G. Role of exosomes in sperm maturation during the transit along the male reproductive tract. *Blood Cells Mol Dis* 2005; **35:** 1-10.
17. Admyre C, Johansson SM, Qazi KR, Filen JJ, Lahesmaa R, Norman M, et al. Exosomes with immune modulatory features are present in human breast milk. *J Immunol* 2007; **179:** 1969-78.
18. Taylor DD, Akyol S, Gercel-Taylor C. Pregnancy-associated exosomes and their modulation of T cell signaling. *J Immunol* 2006; **176:** 1534-42.
19. Asea A, Jean-Pierre C, Kaur P, Rao P, Linhares IM, Skupski D, et al. Heat shock protein-containing exosomes in mid-trimester amniotic fluids. *J Reprod Immunol* 2008; **79:** 12-7.
20. Perkumas KM, Hoffman EA, McKay BS, Allingham RR, Stamer WD. Myocilin-associated exosomes in human ocular samples. *Exp Eye Res* 2007; **84:** 209-12.
21. Ogawa Y, Kanai-Azuma M, Akimoto Y, Kawakami H, Yanoshita R. Exosome-like vesicles with dipeptidyl peptidase IV in human saliva. *Biol Pharm Bull* 2008; **31:** 1059-62.
22. Ratajczak J, Wysoczynski M, Hayek F, Janowska-Wieczorek A, Ratajczak MZ. Membrane-derived microvesicles: important and underappreciated mediators of cell-to-cell communication. *Leukemia* 2006; **20:**1487-95.
23. van der Vos KE, Balaj L, Skog J, Breakefield XO. Brain Tumor Microvesicles: Insights into Intercellular Communication in the Nervous System. *Cell Mol Neurobiol* 2011; **31:** 949-59.
24. Skog J, Wurdinger T, van Rijn S, Meijer DH, Gainche L, Sena-Esteves M, et al. Glioblastoma microvesicles transport RNA and proteins that promote tumour growth and provide diagnostic biomarkers. *Nat Cell Biol* 2008; **10:** 1470-U1209.
25. Janowska-Wieczorek A, Wysoczynski M, Kijowski J, Marquez-Curtis L, Machalinski B, Ratajczak J, et al. Microvesicles derived from activated platelets induce metastasis and angiogenesis in lung cancer. *Int J Cancer* 2005; **113:** 752-60.
26. Safaei R, Larson BJ, Cheng TC, Gibson MA, Otani S, Naerdemann W, et al. Abnormal lysosomal trafficking and enhanced exosomal export of cisplatin in drug-resistant human ovarian carcinoma cells. *Mol Cancer Ther* 2005; **4:** 1595-604.
27. Shedden K, Xie XT, Chandaroy P, Chang YT, Rosania GR. Expulsion of small molecules in vesicles shed by cancer cells: association with gene expression and chemosensitivity profiles. *Cancer Res* 2003; **63:** 4331-7.
28. Hakulinen J, Junnikkala S, Sorsa T, Meri S. Complement inhibitor membrane cofactor protein (MCP; CD46) is constitutively shed from cancer cell membranes in vesicles and converted by a metalloproteinase to a functionally active soluble form. *Eur J Immunol* 2004; **34:** 2620-9.
29. Valenti R, Huber V, Filipazzi P, Pilla L, Sovena G, Villa A, et al. Human tumor-released microvesicles promote the differentiation of myeloid cells with transforming growth factor-beta-mediated suppressive activity on T lymphocytes. *Cancer Res* 2006; **66:** 9290-8.
30. Abid Hussein MN, Boing AN, Sturk A, Hau CM, Nieuwland R. Inhibition of microparticle release triggers endothelial cell apoptosis and detachment. *Thromb Haemost* 2007; **98:** 1096-107.
31. Kim HK, Song KS, Park YS, Kang YH, Lee YJ, Lee KR, et al. Elevated levels of circulating platelet microparticles, VEGF, IL-6 and RANTES in patients with gastric cancer: possible role of a metastasis predictor. *Eur J Cancer* 2003; **39:** 184-91.

32. Jansa R, Sustar V, Frank M, Susanj P, Bester J, Mancek-Keber M, et al. Number of microvesicles in peripheral blood and ability of plasma to induce adhesion between phospholipid membranes in 19 patients with gastrointestinal diseases. *Blood Cells Mol Dis* 2008; **41:** 124-32.

33. Baran J, Baj-Krzyworzeka M, Weglarczyk K, Szatanek R, Zembala M, Barbasz J, et al. Circulating tumour-derived microvesicles in plasma of gastric cancer patients. *Cancer Immunol Immunother* 2010; **59:** 841-50.

34. Lipowsky R. The conformation of membranes. *Nature* 1991; **349:** 475-81.

35. Kralj-Iglic V, Babnik B, Gauger DR, May S, Iglic A. Quadrupolar ordering of phospholipid molecules in narrow necks of phospholipid vesicles. *J Stat Phys* 2006; **125:** 727-52.

36. Hagerstrand H, Isomaa B. Morphological characterization of exovesicles and endovesicles released from human erythrocytes following treatment with amphiphiles. *Biochim Biophys Acta* 1992; **1109**: 117-26.

37. Black PH. Shedding from Normal and Cancer-Cell Surfaces. *New Engl J Med* 1980; **303:** 1415-6.

38. Kralj-Iglic V, Batista U, Hägerstrand H, Iglic A, Majhenc J, Sok M. On mechanisms of cell plasma membrane vesiculation. *Radiol Oncol* 1998; **32:** 119–23.

39. Kralj-Iglic V, Veranic P. Curvature-Induced Sorting of Bilayer Membrane Constituents and Formation of Membrane Rafts**.** In: A. Leitmannova Liu, editor. *Advances in planar lipid bilayers and liposomes*, Vol. 5, Elsevier; 2007. p. 129-49.

40. Kralj-Iglic V, Iglic A, Hagerstrand H, Peterlin P. Stable tubular microexovesicles of the erythrocyte membrane induced by dimeric amphiphiles. *Phys Rev E Stat Phys Plasmas Fluids Relat Interdiscip Topics* 2000; **61:** 4230-4.

41. Sheetz MP, Singer SJ. Biological-membranes as bilayer couples - molecular mechanism of drug-erythrocyte interactions. *Proc Natl Acad Sci USA* 1974; **71:** 4457-61.

42. Helfrich W. Blocked lipid exchange in bilayers and its possible influence on the shape of vesicles. *Z. Naturforsch*. 1974; **29c:** 510.

43. Evans EA. Bending resistance and chemically induced moments in membrane bilayers. *Biophys J* 1974; **14:** 923-31.

44. Kralj-Iglic V. Stability of membranous nanostructures: a possible key mechanism in cancer progression. *Int J Nanomedicine* 2012; **7:** 3579-96.

45. Zachowski A, Devaux PF. Transmembrane movements of lipids. *Experientia* 1990; **46:** 644-56

46. Sims PJ, Wiedmer T. Unraveling the mysteries of phospholipid scrambling. *Thromb Haemost* 2001; **86:** 266-75.

47. Wydro P, Hac-Wydro K. Thermodynamic description of the interactions between lipids in ternary Langmuir monolayers: the study of cholesterol distribution in membranes. *J Phys Chem B* 2007; **111:** 2495-502.

48. Pap E, Pallinger E, Pasztoi M, Falus A. Highlights of a new type of intercellular communication: microvesicle-based information transfer. *Inflamm Res* 2009; **58:** 1-8.

49. van Meer G. Dynamic transbilayer lipid asymmetry. *Csh Perspect Biol* 2011; **3.**

50. Camussi G, Deregibus MC, Bruno S, Cantaluppi V, Biancone L. Exosomes/microvesicles as a mechanism of cell-to-cell communication. *Kidney Int 2010*; **78:** 838-48.

51. Davizon P, Lopez JA. Microparticles and thrombotic disease. *Curr Opin Hematol* 2009; **16:** 334-41.

52. Mrówczyńska L, Salzer U, Iglič A, Hägerstrand H. Curvature factor and membrane solubilisation, with particular reference to membrane rafts**.** *Cell Biol Int,* 2011; **35**: 991-5.

53. Simons K, Ikonen E. Functional rafts in cell membranes. *Nature* 1997; **387:** 569-72.

54. Brown DA, London E. Functions of lipid rafts in biological membranes. *Annu Rev Cell Dev Bi* 1998; **14:** 111-36.

55. Ikonen E. Roles of lipid rafts in membrane transport. *Curr Opin Cell Biol* 2001; **13:** 470-7.

56. Flaumenhaft R. Formation and fate of platelet microparticles. *Blood Cells Mol Dis* 2006; **36:** 182-7.

57. Huttner WB, Zimmerberg J. Implications of lipid microdomains for membrane curvature, budding and fission. *Curr Opin Cell Biol* 2001; **13:** 478-84.

58. Schmidt A, Wolde M, Thiele C, Fest W, Kratzin H, Podtelejnikov AV, et al. Endophilin I mediates synaptic vesicle formation by transfer of arachidonate to lysophosphatidic acid. *Nature* 1999; **401:** 133-41.

59. Kozlov MM. Fission of biological membranes: interplay between dynamin and lipids. *Traffic* 2001; **2:** 51-65.

60. Heijnen HFG, Schiel AE, Fijnheer R, Geuze HJ, Sixma JJ. Activated platelets release two types of membrane vesicles: Microvesicles by surface shedding and exosomes derived from exocytosis of multivesicular bodies and alpha-granules. *Blood* 1999; **94**: 3791-9.

61. Pap E, Pallinger E, Falus A. The role of membrane vesicles in tumorigenesis. *Crit Rev Oncol Hematol* 2011; **79:** 213-23.

62. Di Vizio D, Kim J, Hager MH, Morello M, Yang W, Lafargue CJ, et al. Oncosome formation in prostate cancer: association with a region of frequent chromosomal deletion in metastatic disease. *Cancer Res* 2009; **69:** 5601-9.

63. Del Conde I, Shrimpton CN, Thiagarajan P, Lopez JA. Tissue-factor-bearing microvesicles arise from lipid rafts and fuse with activated platelets to initiate coagulation. *Blood* 2005; **106:** 1604-11.

64. Kharaziha P, Ceder S, Li Q, Panaretakis T. Tumor cell-derived exosomes: A message in a bottle. *Biochim Biophys Acta* 2012; **1826:** 103-11.

65. Miyanishi M, Tada K, Koike M, Uchiyama Y, Kitamura T, Nagata S. Identification of Tim4 as a phosphatidylserine receptor. *Nature* 2007; **450:** 435-9.

66. Segura E, Nicco C, Lombard B, Veron P, Raposo G, Batteux F, et al. ICAM-1 on exosomes from mature dendritic cells is critical for efficient naive T-cell priming. *Blood* 2005; **106:** 216-23.

67. Feng D, Zhao WL, Ye YY, Bai XC, Liu RQ, Chang LF, et al. Cellular Internalization of exosomes occurs through phagocytosis. *Traffic* 2010; **11:** 675-87.

68. Teissier E, Pecheur EI. Lipids as modulators of membrane fusion mediated by viral fusion proteins. *Eur Biophys J* 2007; **36:** 887-99.

69. Parolini I, Federici C, Raggi C, Lugini L, Palleschi S, De Milito A, et al. Microenvironmental pH is a key factor for exosome traffic in tumor cells. *J Biol Chem* 2009; **284:** 34211-22.

70. Escrevente C, Keller S, Altevogt P, Costa J. Interaction and uptake of exosomes by ovarian cancer cells. *BMC Cancer* 2011; **11:** 108.

71. Taraboletti G, D'Ascenzo S, Giusti I, Marchetti D, Borsotti P, Millimaggi D, et al. Bioavailability of VEGF in tumor-shed vesicles depends on vesicle burst induced by acidic pH. *Neoplasia* 2006; **8:** 96-103.

72. Cocucci E, Racchetti G, Meldolesi J. Shedding microvesicles: artefacts no more. *Trends Cell Biol* 2009; **19:** 43-51.

73. Rak J, Guha A. Extracellular vesicles - vehicles that spread cancer genes. *Bioessays* 2012; **34:** 489-97.

74. Lee TH, D'Asti E, Magnus N, Al-Nedawi K, Meehan B, Rak J. Microvesicles as mediators of intercellular communication in cancer - the emerging science of cellular 'debris'. *Semin Immunopathol* 2011; **33:** 455-67.

75. Al-Nedawi K, Meehan B, Micallef J, Lhotak V, May L, Guha A, et al. Intercellular transfer of the oncogenic receptor EGFRvIII by microvesicles derived from tumour cells. *Nat Cell Biol* 2008; **10:** 619-24.

76. Peinado H, Aleckovic M, Lavotshkin S, Matei I, Costa-Silva B, Moreno-Bueno G, et al. Melanoma exosomes educate bone marrow progenitor cells toward a pro-metastatic phenotype through MET. *Nat Med* 2012; **18:** 883-91.

77. Sidhu SS, Mengistab AT, Tauscher AN, LaVail J, Basbaum C. The microvesicle as a vehicle for EMMPRIN in tumor-stromal interactions. *Oncogene* 2004; **23:** 956-963.

78. McCready J, Sims JD, Chan D, Jay DG. Secretion of extracellular hsp90alpha via exosomes increases cancer cell motility: a role for plasminogen activation. *BMC Cancer* 2010; **10:** 294.

79. Andre F, Schartz NE, Movassagh M, Flament C, Pautier P, Morice P. Malignant effusions and immunogenic tumour-derived exosomes. *Lancet* 2002; **360:** 295-305.

80. Koga K, Matsumoto K, Akiyoshi T, Kubo M, Yamanaka N, Tasaki A, et al. Purification, characterization and biological significance of tumor-derived exosomes. *Anticancer Res* 2005; **25:** 3703-7.

81. Dinger ME, Mercer TR, Mattick JS. RNAs as extracellular signaling molecules. *J Mol Endocrinol* 2008; **40:** 151-9.

82. Lagos-Quintana M, Rauhut R, Lendeckel W, Tuschl T. Identification of novel genes coding for small expressed RNAs. *Science* 2001; **294:** 853-8.

83. Esquela-Kerscher A, Slack FJ. Oncomirs - microRNAs with a role in cancer. *Nat Rev Cancer* 2006; **6:** 259-69.

84. Tsui NB, Ng EK, Lo YM. Stability of endogenous and added RNA in blood specimens, serum, and plasma. *Clin Chem* 2002; **48:** 1647-53.

85. Tsui NB, Ng EK, Lo YM. Molecular analysis of circulating RNA in plasma. *Methods Mol Biol* 2006; **336:** 123-34.

86. Valadi H, Ekstrom K, Bossios A, Sjostrand M, Lee JJ, Lotvall JO. Exosome-mediated transfer of mRNAs and microRNAs is a novel mechanism of genetic exchange between cells. *Nat Cell Biol* 2007; **9:** 654-9.

87. Hong BS, Cho JH, Kim H, Choi EJ, Rho S, Kim J, et al. Colorectal cancer cell-derived microvesicles are enriched in cell cycle-related mRNAs that promote proliferation of endothelial cells. *BMC Genomics* 2009; **10:** 556.

88. Baj-Krzyworzeka M, Szatanek R, Weglarczyk K, Baran J, Urbanowicz B, Branski P, et al. Tumour-derived microvesicles carry several surface determinants and mRNA of tumour cells and transfer some of these determinants to monocytes. *Cancer Immunol Immunother* 2006; **55:** 808-18.

89. Kogure T, Lin WL, Yan IK, Braconi C, Patel T. Intercellular nanovesicle-mediated microRNA transfer: a mechanism of environmental modulation of hepatocellular cancer cell growth. *Hepatology* 2011; **54:** 1237-48.

90. Ohshima K, Inoue K, Fujiwara A, Hatakeyama K, Kanto K, Watanabe Y, et al. Let-7 microRNA family is selectively secreted into the extracellular environment via exosomes in a metastatic gastric cancer cell line. *PLoS One* 2010; **5:** e13247.

91. Taylor DD, Gercel-Taylor C. MicroRNA signatures of tumor-derived exosomes as diagnostic biomarkers of ovarian cancer. *Gynecol Oncol* 2008; **110:**13-21.

92. Bergsmedh A, Szeles A, Henriksson M, Bratt A, Folkman MJ, Spetz AL, et al. Horizontal transfer of oncogenes by uptake of apoptotic bodies. *Proc Natl Acad Sci USA* 2001; **98:** 6407-11.

93. Balaj L, Lessard R, Dai L, Cho YJ, Pomeroy SL, Breakefield XO, et al. Tumour microvesicles contain retrotransposon elements and amplified oncogene sequences. *Nat Commun* 2011; **2:** 180.

94. Desler C, Marcker ML, Singh KK, Rasmussen LJ. The importance of mitochondrial DNA in aging and cancer. *J Aging Res* 2011; **2011:** 407536.

95. Guescini M, Genedani S, Stocchi V, Agnati LF. Astrocytes and Glioblastoma cells release exosomes carrying mtDNA. *J Neural Transm* 2010; **117:** 1-4.

96. Bannert N, Kurth R. Retroelements and the human genome: new perspectives on an old relation. *Proc Natl Acad Sci USA* 2004; **101:** 14572-9.

97. Cordaux R, Batzer MA. The impact of retrotransposons on human genome evolution. *Nat Rev Genet* 2009; **10:** 691-703.

98. Wiemels JL, Hofmann J, Kang M, Selzer R, Green R, Zhou M, et al. Chromosome 12p deletions in TEL-AML1 childhood acute lymphoblastic leukemia are associated with retrotransposon elements and occur postnatally. *Cancer Res* 2008; **68:** 9935-44.

99. Bretscher MS. Membrane structure: some general principles. *Science* 1973; **181:** 622-9.

100. Dahiya R, Boyle B, Goldberg BC, Yoon WH, Konety B, Chen K, et al. Metastasis-associated alterations in phospholipids and fatty acids of human prostatic adenocarcinoma cell lines. *Biochem Cell Biol* 1992; **70:** 548-54.

101. Kim CW, Lee HM, Lee TH, Kang C, Kleinman HK, Gho YS. Extracellular membrane vesicles from tumor cells promote angiogenesis via sphingomyelin. *Cancer Res* 2002; **62:** 6312-7.

102. McGarry LJ, Thompson D. Retrospective database analysis of the prevention of venous thromboembolism with low-molecular-weight heparin in acutely III medical inpatients in community practice. *Clin Ther* 2004; **26:** 419-30.

103. Smorenburg SM, Hettiarachchi RJ, Vink R, Buller HR. The effects of unfractionated heparin on survival in patients with malignancy-a systematic review. *Thromb Haemost* 1999; **82:** 1600-4.

104. Stevenson JL, Choi SH, Wahrenbrock M, Varki A, Varki NM. Heparin effects in metastasis and Trouseeau syndrome: anticoagulation is not the primary mechanism. *Haem Rep* 2005; **1:** 59–60.

105. Sustar V, Jansa R, Frank M, Hagerstrand H, Krzan M, Iglic A et al. Suppression of membrane microvesiculation - a possible anticoagulant and anti-tumor progression effect of heparin. *Blood Cells Mol Dis* 2009; **42:** 223-7.

106. Urbanija J, Tomsic N, Lokar M, Ambrozic A, Cucnik S, Rozman B, et al. Coalescence of phospholipid membranes as a possible origin of anticoagulant effect of serum proteins. *Chem Phys Lipids* 2007; **150:** 49-57.

107. Urbanija J, Babnik B, Frank M, Tomsic N, Rozman B, Kralj-Iglic V, et al. Attachment of beta 2-glycoprotein I to negatively charged liposomes may prevent the release of daughter vesicles from the parent membrane. *Eur Biophys J* 2008; **37:** 1085-95.

108. May S, Iglič A, Reščič J, Maset S., Bohinc K. Bridging like-charged macroions through long divalent rod-like ions. *J Phys Chem B* 2008; **112**: 1685-92.

109. Velikonja A, Perutkova Š, Gongadze E, Kramar P, Polak A, Maček-Lebar A, Iglič A. Monovalent ions and water dipoles in contact with dipolar zwitterionic lipid headroups - theory and MD simulations, *Int J Mol Sci* 2013; **14**: 2846-61.

110. Gongadze E, Iglič A. Excluded volume effect of counterions and water dipoles near a highly charged surface due to a rotationally averaged Boltzmann factor for water dipoles. *Gen Phys Biophys* 2013; **21:** 143-5..

111. Ambrožič A, Čučnik S, Tomšič N, Urbanija J, Lokar M, Babnik B et al. Interaction of giant phospholipid vesicles containing cardiolipin and cholesterol with beta 2-glycoprotein-I and anti-beta2-glycoprotein-I antibodies. *Autoimmun Rev* 2006; **6:** 10-5.

review

Comparison between whole-body MRI and Fluorine-18-Fluorodeoxyglucose PET or PET/CT in oncology: a systematic review

Mario Ciliberto[1*], Fabio Maggi[1], Giorgio Treglia[2*], Federico Padovano[1], Lucio Calandriello[1], Alessandro Giordano[2], Lorenzo Bonomo[1]

[1] Institute of Radiology, Università Cattolica del Sacro Cuore, Rome, Italy
[2] Institute of Nuclear Medicine, Università Cattolica del Sacro Cuore, Rome, Italy

Radiol Oncol 2013; 47(3): 206-218.

Received 19 september 2012
Accepted 23 october 2012

Correspondence to: Dr. Giorgio Treglia, Institute of Nuclear Medicine, Università Cattolica del Sacro Cuore, Largo Gemelli 8, 00168 Rome, Italy. Phone:+39-0630156200; Fax:+39-063013745; E-mail: giorgiomednuc@libero.it

* Authors Mario Ciliberto and Giorgio Treglia equally contributed to this article, sharing the first authorship.

Disclosure: No potential conflicts of interest were disclosed.

Background. The aim of the article is to systematically review published data about the comparison between positron emission tomography (PET) or PET/computed tomography (PET/CT) using Fluorine-18-Fluorodeoxyglucose (FDG) and whole-body magnetic resonance imaging (WB-MRI) in patients with different tumours.

Methods. A comprehensive literature search of studies published in PubMed/MEDLINE, Scopus and Embase databases through April 2012 and regarding the comparison between FDG-PET or PET/CT and WB-MRI in patients with various tumours was carried out.

Results. Forty-four articles comprising 2287 patients were retrieved in full-text version, included and discussed in this systematic review. Several articles evaluated mixed tumours with both diagnostic methods. Concerning the specific tumour types, more evidence exists for lymphomas, bone tumours, head and neck tumours and lung tumours, whereas there is less evidence for other tumour types.

Conclusions. Overall, based on the literature findings, WB-MRI seems to be a valid alternative method compared to PET/CT in oncology. Further larger prospective studies and in particular cost-effectiveness analysis comparing these two whole-body imaging techniques are needed to better assess the role of WB-MRI compared to FDG-PET or PET/CT in specific tumour types.

Key words: positron emission tomography; PET/CT; fluorodeoxyglucose; whole-body magnetic resonance imaging; diffusion-weighted imaging; oncology

Introduction

Accurate staging and thorough tumour surveillance are essential in patients with a neoplastic disease to assess prognosis and to decide the most appropriate therapeutic options. Imaging plays a key role in these evaluation steps: multi-slice computed tomography (CT) and, recently, positron emission tomography/CT (PET/CT) are widely used in order to get an integrated diagnostic approach to cancer as a systemic disease.[1] In particular, the use of Fluorine-18-Fluorodeoxyglucose (FDG) tracer made, up to now, PET contribution to oncologic imaging matchless by any other functional imaging modality.[2] However, this technique uses ionizing radiations and has some limitations for what concerns spatial and contrast resolution; false positive and false negative results of FDG-PET are well known, too.

Magnetic resonance imaging (MRI), with its lack of ionizing radiation, high soft tissue contrast and good spatial resolution, is a useful application for tumour detection and staging of malignancies and could overcome the limits of FDG-PET/CT.[3]

In recent years, significant improvements in hardware and important innovations in sequence design and image acquisition have allowed a whole-body imaging with MRI in a suitable acquisition time without impairment of spatial resolution.[4] Furthermore, the introduction of diffusion-weighted MRI (DWI) has increased the potential for the detection of malignancies throughout the body.[5] Whole body MRI (WB-MRI) has then emerged as an excellent candidate for staging and surveillance of patients with neoplastic disease and many authors have compared FDG-PET/CT and WB-MRI in oncology.

Our article aims to systematically review the current evidence on the comparison between PET or PET/CT using FDG and WB-MRI in patients with different tumours.

Methods

A comprehensive literature search of studies published in PubMed/MEDLINE, Scopus and Embase databases was carried out to find relevant peer-reviewed articles on the comparison of FDG-PET or PET/CT and WB-MRI in patients with different tumours.

A search algorithm based on a combination of the terms: a) ''PET'' OR "positron emission tomography" AND b) "whole body MR" OR "whole-body MR" OR "whole body magnetic resonance" OR "whole-body magnetic resonance" OR "whole body MRI" OR "whole-body MRI" was used. No beginning date limit was used and the search was updated until April 2012.

All the studies which compared FDG-PET or PET/CT and WB-MRI in oncology were considered eligible for inclusion in this systematic review.

The exclusion criteria were: a) articles not within the field of interest of this review; b) review articles, editorials or letters, comments, conference proceedings; c) case reports or small case series (less than seven patients included); d) articles not in English, Spanish, French or German language; e) possible data overlap (in this case the most complete article was included).

Two researchers (MC and GT) reviewed the titles and the abstracts of the retrieved articles, applying the inclusion and exclusion criteria mentioned above. The full-text version of the retrieved articles was reviewed to confirm their eligibility for inclusion. Disagreements were resolved in a consensus meeting.

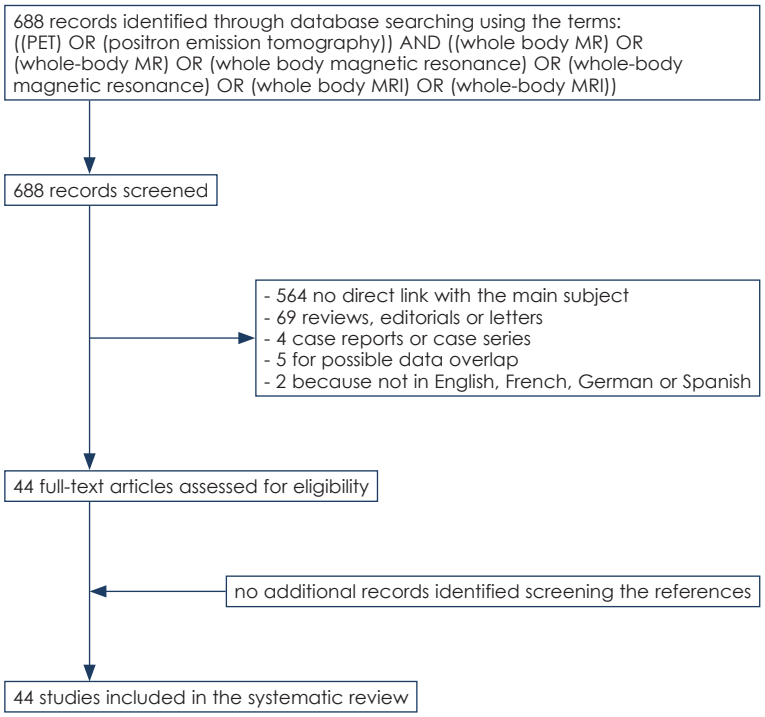

FIGURE 1. Flow chart of the search for eligible studies on the comparison of FDG-PET or PET/CT and WB-MRI in oncology.

For each included study, information was collected concerning basic study (authors, journal, year of publication, country of origin, type of study), patient characteristics (number of patients, mean age, gender and type of tumours evaluated), methodological aspects about PET imaging (device used, injected activity, time between tracer injection and image acquisition, PET acquisition protocol, image analysis), methodological aspects about WB-MRI (field strength, sequences used, slice thickness, contrast media, diffusion-weighted imaging, apparent diffusion coefficient, acquisition time) and reference standard used.

Results

Literature search

The comprehensive literature search revealed 688 articles. Reviewing titles and abstracts, 644 articles were excluded applying the criteria mentioned above: 564 studies were excluded because not within the range of interest of this review; 69 articles were excluded because review articles, editorials or letters, comments, conference proceedings; 4 articles were excluded because case reports or small case series (less than seven patients included)[6-9];

2 articles were excluded because not in English, Spanish, French or German language[10,11]; 5 articles were excluded for possible data overlap.[12-16]

Lastly, forty-four articles comprising 2287 patients were retrieved in full-text version and included in this systematic review (Figure 1).[17-60] No additional studies were found screening the references of these articles.[6-16] The characteristics of the included studies are presented in Tables 1-3.

Mixed tumours were evaluated in 12 articles[17-28], lymphomas in 7[29-35]; bone tumours in 7[36-42]; head and neck tumours in 5[43-47]; lung tumours in 4[48-51]; melanoma in 3[52-54]; breast cancer in 2[55,56]; colorectal tumours in 2[57,58]; neuroendocrine tumours in 2.[59,60]

Literature data discussion

Mixed tumours

First of all, Antoch *et al*.[17] performing both FDG-PET/CT and WB-MRI in 98 patients with different malignancies, recommended the use of FDG-PET/CT as first-line whole-body imaging modality for tumour staging. In fact, the overall TNM stage was correctly determined in 75 cases with PET/CT (77%) and in 53 with WB-MRI (54%). Compared with WB-MRI, PET/CT had a direct impact on patient management in 12 patients. WB-MRI findings changed the therapy regimen in 2 patients compared with PET/CT.[17]

In 2005, Schmidt *et al*.[18] evaluating 41 patients with mixed tumours using both methods found that WB-MRI was highly sensitive in detecting distant metastases (sensitivity was 96% for WB-MRI and 82% for FDG-PET/CT; specificity was 82% for both methods), whereas PET/CT was superior in lymph node staging (sensitivity was 98% for PET/CT and 80% for WB-MRI; specificity was 83% for PET/CT and 75% for WB-MRI). Accuracy for correct TNM staging was 96% for PET/CT and 91% for WB-MRI.[18]

In 2007 Komori *et al*.[19] comparing FDG-PET/CT and DWI WB-MRI in 16 patients with malignant tumours reported that DWI WB-MRI may be useful in detecting malignancies, even if differentiating malignant and benign tumours may be difficult with this method. Twenty-five (92.6%) of the 27 malignant lesions were detected by DWI WB-MRI whereas 22 malignant tumours (81.5%) were detected by FDG-PET/CT.[19]

Also Li *et al*.[20] reported that DWI WB-MRI is a feasible imaging method in oncology, providing comparable results to PET imaging in 30 oncologic patients evaluated.

Brauck *et al*.[21] evaluated a WB-MRI protocol by using unenhanced T2-weighted and contrast-enhanced T1-weighted real-time sequences during continuous table movement in 11 patients with FDG-PET/CT positive for metastases. Seventy-three of 75 metastases detected by PET/CT were correctly diagnosed by using WB-MRI, demonstrating the feasibility of this method in detecting metastases.[21]

In 2008, Yang *et al*.[22] evaluated 56 patients with different tumours demonstrating the valuable role of DWI WB-MRI in tumour detection. Twelve patients underwent also FDG-PET. Among the diagnostic imaging methods DWI WB-MRI showed the highest sensitivity and specificity in detecting bone metastases. Among the twelve results compared with PET, eight were identical (concordance of 66.7%), one was found to be false-positive at MRI, two were found false-negative at MRI, one case was false-negative at PET and true-positive at MRI.[22]

In 2009, Stecco *et al*.[23] compared FDG-PET/CT and DWI WB-MRI in staging 29 oncologic patients. Using FDG-PET/CT as reference standard, DWI WB-MRI interpreted by two readers had a sensitivity of 87-89%, a specificity of 98-99%, and an accuracy of 98-99%. These authors underlined the usefulness of DWI WB-MRI in cancer screening, staging, restaging and follow-up.[23]

Krohmer *et al*.[24] evaluated 24 paediatric tumours with WB-MRI and FDG-PET, showing that WB-MRI had high sensitivity for the detection of malignant disease. Overall 190 lesions were detected by WB-MRI and 155 lesions were found by FDG-PET. In patients with suspected bone lesions, WB-MRI should be considered for initial disease evaluation prior to specific and regional imaging methods to reduce the overall number of imaging examinations and radiation exposure.[24]

In 2011, Fischer *et al*.[25] prospectively evaluated the diagnostic accuracy of WB-MRI with and without DWI compared with PET/CT (as reference standard) in 66 oncologic patients. PET/CT revealed 374 malignant lesions in 48/64 (75%) patients. Detection rates of WB-MRI with and without DWI were 84% and 64%, respectively. The detection rate was significantly higher with side-by-side analysis and fused image analysis compared with WB-MRI alone.[25]

Recently, Schmidt *et al*.[26] demonstrated that both FDG-PET/CT and WB-MRI were efficient diagnostic triage methods in 135 patients planned for radioembolisation of liver metastases. Overall, FDG-PET/CT showed a higher diagnostic accuracy compared to WB-MRI. Both modalities, combined, exhibited high sensitivity for the diagnosis of extrahepatic tumour manifestations. Patient-based sen-

TABLE 1. Basic studies and patient characteristics

Authors	Year	Country	Study type	No. of patients	Mean Age	% Male	Type of tumors
Antoch *et al.*[17]	2003	Germany	Prospective	98	58	64%	Mixed
Schmidt *et al.*[18]	2005	Germany	Prospective	41	56	44%	Mixed
Komori *et al.*[19]	2007	Japan	NR	16	66	70%	Mixed
Li *et al.*[20][18]	2007	China	NR	30	48	37%	Mixed
Brauck *et al.*[21]	2008	Germany	Prospective	11	53	63%	Mixed
Yang *et al.*[22]	2008	China	NR	56	57	71%	Mixed
Stecco *et al.*[23]	2009	Italy	Prospective	29	NR	NR	Mixed
Krohmer *et al.*[24]	2010	Germany	Prospective	24	11	NR	Mixed
Fischer *et al.*[25]	2011	Switzerland	Prospective	66	60	66%	Mixed
Schmidt *et al.*[26]	2012	Germany	Retrospective	135	61	45%	Mixed
Cafagna *et al.*[27]	2012	Italy	Retrospective	38	60	47%	Mixed
Manenti *et al.*[28]	2012	Italy	Retrospective	45	66	53%	Mixed
Punwani *et al.*[29]	2010	England	NR	31	13	58%	Lymphoma
van Ufford *et al.*[30]	2011	Netherlands	Prospective	22	49	68%	Lymphoma
Abdulqadhr *et al.*[31]	2011	Sweden	Prospective	31	47	64%	Lymphoma
Gu *et al.*[32]	2011	China	NR	17	50	65%	Lymphoma
Lin *et al.*[33]	2011	France	Prospective	15	48	60%	Lymphoma
Wu *et al.*[34]	2011	Finland	Prospective	8	54	50%	Lymphoma
Chen *et al.*[35]	2012	China	Prospective	10	45	40%	Lymphoma
Shortt *et al.*[36]	2009	Ireland	NR	24	67	46%	Multiple Mieloma
Daldrup-Link *et al.*[37]	2001	Germany	NR	39	13	69%	Bone
Schmidt *et al.*[38]	2007	Germany	Prospective	30	58	60%	Bone
Ribrag *et al.*[39]	2008	France	Prospective	47	50	50%	Bone
Kumar *et al.*[40]	2008	India	NR	26	NR	NR	Bone
Takenaka *et al.*[41]	2009	Japan	Prospective	115	72	57%	Bone
Heusner *et al.*[42]	2011	Germany	Prospective	109	57	60%	Bone
Ng *et al.*[43]	2010	Taiwan	Prospective	179	47	75%	Head and neck
O'Neill *et al.*[44]	2010	Ireland	Prospective	15	59	66%	Head and neck
Ng *et al.*[45]	2011	Taiwan	Prospective	79	52	88%	Head and neck
Chan *et al.*[46]	2011	Taiwan	Prospective	103	53	94%	Head and neck
Eiber *et al.*[47]	2012	Germany	Prospective	20	56	80%	Head and neck
Plathow *et al.*[48]	2008	Germany	NR	52	62	69%	Lung
Ohno *et al.*[49]	2008	Japan	Prospective	203	72	53%	Lung
Yi *et al.*[50]	2008	Korea	Prospective	165	61	72%	Lung
Chen *et al.*[51]	2010	China	NR	56	51	62%	Lung
Pfannenberg *et al.*[52]	2007	Germany	Prospective	64	58	41%	Melanoma
Laurent *et al.*[53]	2010	France	Prospective	35	NR	NR	Melanoma
Dellestable *et al.*[54]	2011	France	Prospective	40	57	50%	Melanoma
Schmidt *et al.*[55]	2008	Germany	NR	33	55	0%	Breast
Heusner *et al.*[56]	2010	Germany	Prospective	20	54	0%	Breast
Squillaci *et al.*[57]	2008	Italy	NR	20	56	60%	Colorectal
Schmidt *et al.*[58]	2009	Germany	Retrospective	24	62	NR	Colorectal
Giraudet *et al.*[59]	2007	France	Prospective	55	56	62%	Neuroendocrine tumors
Takano *et al.*[60]	2008	Japan	Prospective	11	40	55%	Neuroendocrine tumors

NR = not reported

TABLE 2. Technical aspects of the included studies

Authors	Device	Injected activity	Time between tracer injection and image acquisition (min)	PET acquisition protocol	Image analysis	Field strenght (T)	Sequences used	Slice thickness	Contrast media administration	DWI	ADC	Acquisition time (min)	Reference standard
Antoch *et al.*[17]	PET/CT	350 MBq	60	Static acquisition (3-5min per bed position)	Qualitative	1.5	T1w(chest,abdomen), T2w(chest,abdomen), T1w(chest,abdomen)afterCM, T2w(chest,abdomen)after CM	7mm	Yes	No	No	26	Histology and/ or follow up
Schmidt *et al.*[18]	PET/CT	200 MBq	60	Static acquisition (3min per bed position)	Qualitative, semi-quantitative	1.5	STIR(WB), HASTE(chest), T1w(WB), 3D-VIBE(abdomen,pelvis)after CM	5mm	Yes	No	No	55	Histology and PET/CT
Komori *et al.*[19]	PET/CT	3.7 MBq/kg	60	Static acquisition	Qualitative, semi-quantitative	1.5	DW-EPI(WB)	6mm	No	Yes (Bvalue0-1000mm2/s)	Yes	9	Histology and/ or follow up
Li *et al.*[20]	PET	NR	NR	Static aquisition	Qualitative, semi-quantitative	1.5	DW-EPI-STIR(WB)	7mm	No	Yes (Bvalue0-800mm2/s)	Yes	30	Follow up
Brauck *et al.*[21]	PET/CT	300-340 MBq	60	Static aquisition	Qualitative	1.5	T1wSSFP(WB), T1wSSFP(WB) after CM, T2wSSFP(WB)	5mm	Yes	No	No	6	PET/CT
Yang *et al.*[22]	PET	NR	NR	Static acquisition	Qualitative	1.5	DW-EPI-STIR(WB)	7mm	No	Yes (Bvalue0-400-600mm2/s)	No	17-21	Follow up
Stecco *et al.*[23]	PET/CT	3.5 MBq/kg	60	Static acquisition	Qualitative, semi-quantitative	1.5	DW-EPI-STIR(WB)	5mm	No	Yes (Bvalue0-500-1000mm2/s)	No	20	PET/CT
Krohmer *et al.*[24]	PET	NR	NR	Static aquisition	Qualitative	1.5	T2w-STIR(WB), T1wTSE(WB)	6-8mm	No	No	No	45	Follow up
Fischer *et al.*[25]	PET/CT	350 MBq	60	Static acquisition	Qualitative	1.5	DW-EPI-FS(WB), T2wFIESTA(WB)	7mm	No	Yes (Bvalue0-700mm2/s)	Yes	40	PET/CT
Schmidt *et al.*[26]	PET/CT	294 MBq	60	Static acquisition	Qualitative, semi-quantitative	1.5	STIR(WB), HASTE(abdomen), HASTE(lung), STIR-lung, T2w-FS-TSE(liver), T1wTSE(WB), T1wTSE(spine), STIR(spine), VIBE(liver), T1-FS- GE(pelvis), T1wTSE(brain), T2wTSE(brain)	3-5mm	Yes	No	No	51	Follow up
Cafagna *et al.*[27]	PET/CT	370-550 MBq	60	Static acquisition (3min per bed position)	Qualitative, semi-quantitative	1.5	TSE(WB), DW-EPI-STIR(WB)	5mm	No	Yes (B-value0-500-1000mm2/s)	Yes	51	Follow up
Manenti *et al.*[28]	PET/CT	NR	NR	Static acquisition (4min per bed position)	Qualitative	3.0	T1wTFE(WB), T2wTFE(WB), THRIVE-FFE(WB), DW-EPI-STIR(WB)	4-6mm	Yes	Yes (B-value 0-1000mm2/s)	No	35	Histology and/ or follow up
Punwani *et al.*[29]	PET/CT	370 MBq	60	Static acquisition	Qualitative, semi-quantitative	1.5	STIR-RARE(WB)	7mm	No	No	No	25-30	PET/CT
van Ufford *et al.*[30]	PET/CT	3 MBq/kg	60	Static acquisition(3min per bed position)	Qualitative	1.5	T1wTSE(WB), T1wSTIR(WB), DW-EPI(head,neck), DW-EPI-FS(chest,abdomen,pelvis)	6mm	No	Yes (Bvalue0-1000mm2/s)	No	55	Follow up
Abdulqadhr *et al.*[31]	PET/CT	5 MBq/kg	60	Static acquisition (3min per bed position)	Qualitative	1.5	T1wTSE(WB), T2wSTIR-FS, DWIBS(WB), T2wTSE, T1wGE(chest,abdomen)	6mm	No	Yes (Bvalue0-1000mm2/s)	No	50	Histology and/ or follow up
Gu *et al.*[32]	PET/CT	4.8 MBq/kg	60	Static acquisition (4min per bed position)	Qualitative	3.0	T2wSPAIR-FS, DW-EPI-STIR	5mm	No	Yes (B-value0-1000mm2/sec)	No	48	PET/CT
Lin *et al.*[33]	PET/CT	5 MBq/kg	60	Static acquisition (2min per bed position)	Qualitative, semi-quantitative	1.5	DW-EPI-FS(WB)	5mm	No	Yes (Bvalue50-400-800mm2/s)	Yes	30-45	PET/CT
Wu *et al.*[34]	PET/CT	370 MBq	60	Static acquisition (3min per bed position)	Qualitative, semi-quantitative	3.0	T1wTSE(WB), T2wIR(WB), T1wGEVIBE(neck,abdomen), T1wGE-VIBE(neck,abdomen)after CM, T2wTSE(neck,abdomen), T2wTSE-FS(abdomen), DW-EPI(WB)	1-5mm	Yes	Yes (Bvalue0-800mm2/s)	Yes	27	Follow up
Chen *et al.*[35]	PET and PET/CT	NR	NR	NR	NR	1.5	DW-EPI-STIR, FSE	6-7mm	No	Yes (B-value 0-800mm2/s)	Yes	43	Histology
Shortt *et al.*[36]	PET/CT	250-440 MBq	90	Static acquisition	Qualitative, semi-quantitative	1.5	STIR(WB), T1wTSE(WB)	8mm	No	No	No	20	Histology
Daldrup-Link *et al.*[37]	PET	3.7 MBq/kg	60	Static acquisition(4-6min per bed position)	Qualitative	1.5	T1wSE, T2wSTIR-FS	4-6mm	No	No	No	45-60	Histology and/ or follow up
Schmidt *et al.*[38]	PET/CT	202-372 MBq	60	Static acquisition (3min per bed position)	Qualitative, semi-quantitative	1.5	STIR(WB), HASTE-STIR(lung), T2wSE(liver), T1wSE(WB), T1w+STIR(spine), 3D-VIBE(liver)after CM, T1wGE-FS(abdomen)after CM, T1w+T2w(skull)	5mm	Yes	No	No	55	Histology and/ or follow up
Ribrag *et al.*[39]	PET/CT	539 MBq	46-184	Static acquisition (7-8min per bed position)	Qualitative, semi-quantitative	1.5	STIR(WB), T1wSE(WB)	8mm	No	No	No	20	Histology
Kumar *et al.*[40]	PET/CT	5.2 MBq/kg	45	Static acquisition	Qualitative	1.5	SE-STIR(WB)	NR	No	No	No	40-60	Histology and/ or follow up
Takenaka *et al.*[41]	PET/CT	3.3 MBq/kg	60	Static acquisition (2min per bed position)	Qualitative, semi-quantitative	1.5	T1wGE(WB), T1wGE(WB)after CM, Opposed-phase T1 GE(WB), STIR-TSE(WB), DW-EPI-STIR(WB)	8mm	Yes	Yes (Bvalue0-1000mm2/s)	No	75	Follow up
Heusner *et al.*[42]	PET/CT	260 MBq	60	Static acquisition (4-6min per bed position)	Qualitative, semi-quantitative	1.5	T1wGE(chest,abdomen), T2wHASTE(chest,abdomen), T1wVIBE(abdomen)after CM, T1wVIBE(head,chest pelvis) after CM	3-7mm	Yes	No	No	NR	Follow up

Authors	Device	Injected activity	Time between tracer injection and image acquisition (min)	PET acquisition protocol	Image analysis	Field strenght (T)	Sequences used	Slice thickness	Contrast media administration	DWI	ADC	Acquisition time (min)	Reference standard
Ng *et al.*[43]	PET/CT	370 MBq	50-70	Static acquisition (3min per bed position)	Qualitative	3.0	T2wTSE-FS(head,neck, T1wTSE(head,neck), T1wTSE(spine), STIR(spine)T1wTSE-WB, STIR-WB, T2wHASTE(chest,abdomen), T1wVIBE(abdomen), T1wVIBE(abdomen in artery,portal,equilibrium phase) after CM, T1wVIBE(chest,pelvis) after CM, T1wTSE-FS after CM	3-5mm	Yes	No	No	37	Histology and/ or follow up
O'Neill *et al.*[44]	PET/CT	NR	NR	NR	Qualitative	1.5	NR	NR	NR	No	No	20	NR
Ng *et al.*[45]	PET/CT	370 MBq	50-70	Static acquisition (3min per bed position)	Qualitative	3.0	T2wTSE-FS(head,neck), T1wTSE(head,neck), T1wTSE(spine), STIR(spine), T1wTSE(WB), STIR(WB), T2wHASTE(chest,abdomen), T1wVIBE(abdomen), T1wVIBE(abdomen)after CM, T1wVIBE(chest,pelvis)after CM, T1wTSE-FS after CM	3-5mm	Yes	No	No	37	Histology and/ or follow up
Chan *et al.*[46]	PET/CT	370 MBq	50-70	Static acquisition(2min per bed position)	Qualitative, semi-quantitative	3.0	T2wTSE-FS(head,neck), T1wTSE(head,neck), T1wTSE(spine), STIR(spine)T1wTSE(WB), STIR(WB), T2wHASTE(chest,liver), T1wVIBE(abdomen), T1wVIBE(abdomen)after CM, T1wVIBE(chest,pelvis)after CM, T1wTSE-FS after CM	3-5mm	Yes	No	No	50	Histology and/ or follow up
Eiber *et al.*[47]	PET/CT	350-500 MBq	90	Static acquisition (2min per bed position)	Qualitative	3.0	Dixon VIBE T1w(WB), T2 STIR(neck), T1 TSE(neck), T1 TSE after CM(neck), T1 TSE FS after CM(neck), VIBE T1w dynamic(liver), VIBE T1w after CM(lungs)	2.6-5mm	Yes	No	No	23	Histology and/ or follow up
Plathow *et al.*[48]	PET/CT	360-400 MBq	55-65	Static acquisition(3min per bed position)	Qualitative	1.5	STIR(chest), VIBE-FS	NR	NR	No	No	60	Histology and/ or follow up
Ohno *et al.*[49]	PET/CT	3.3 MBq/kg	60	Static acquisition (2min per bed position)	Qualitative	1.5	T1wGE(WB), T1wGE(WB)after CM, Opposed-phase T1wGE(WB), STIR-TSE(WB, DW-EPI-STIR(WB)	NR	Yes	Yes (Bvalue0-1000mm2/s)	No	75	Histology and/ or follow up
Yi *et al.*[50]	PET/CT	370 MBq	45	Static acquisition	Qualitative	3.0	T2wTSE-FS(WB), T1wTFE(WB) after CM	4-8mm	Yes	No	No	40	Histology and/ or follow up
Chen *et al.*[51]	PET/CT	3.3 MBq/kg	60	Static acquisition	Qualitative	1.5	DW-EPI(WB)	6mm	No	Yes (Bvalue0-1000mm2/s)	No	12	Histology and/ or follow up
Pfannenberg *et al.*[52]	PET/CT	370 MBq	55-65	Static acquisition (3min per bed position)	Qualitative, semi-quantitative	1.5	NR	NR	NR	No	No	NR	Histology and/ or follow up
Laurent *et al.*[53]	PET/CT	5.5 MBq/kg	60	Static acquisition (3-4 min per bed position	Qualitative	1.5	2D-STIR(WB), 3D-T1w(WB)after CM, DW-EPI(WB)	7-8mm	Yes	Yes (Bvalue0-600mm2/s)	No	60	Histology and/ or follow up
Dellestable *et al.*[54]	PET/CT	5.5 MBq/kg	60	Static acquisition	Qualitative, semi-quantitative	1.5	T2wSTIR(WB), T1(WB), DWI(WB), T1w3D-GE(WB)after CM	NR	Yes	Yes (Bvalue NR)	No	60	Histology and/ or follow up
Schmidt *et al.*[55]	PET/CT	200 MBq	60	Static acqusition	Qualitative, semi-quantitative	1.5-3.0	STIR(WB), HASTE(abdomen), HASTE(lung), STIR(lung), T2w-SE FS(liver), T1wTSE(WB), T1wTSE(spine), STIR(spine), Dyn. VIBE(liver)after CM, Static VIBE(lung,breast)after CM, T1wGE-FS(pelvis)after CM, T1wSE(brain) after CM, T1wGE(brain), T2wSE(brain)after CM	NR	Yes	No	No	43-52	Histology and/ or follow up
Heusner *et al.*[56]	PET/CT	300 MBq	60	Static acquisition(4min per bed position)	Qualitative, semi-quantitative	1.5	DW-EPI(WB), HASTE-FS(spine), DW-EPI(spine), T2wSPAIR(WB), T1wFLASH(WB), T2wHASTE(WB), T1wVIBE(WB)after CM	3-6mm	Yes	Yes (Bvalue50-600-800mm2/s)	Yes	NR	Histology and/ or follow up
Squillaci *et al.*[57]	PET/CT	370 MBq	45-60	Static acquisition (4min per bed position)	Qualitative, semi-quantitative	3.0	T1wFFE(WB), T2wTSE(WB), T2wTSE-STIR(WB), THRIVE-SPAIR(WB), T1wFFE(WB)after CM	4-6mm	Yes	No	No	47-55	Histology and/ or clinical/ imaging follow up
Schmidt *et al.*[58]	PET/CT	197-390 MBq	60	Static acquisition	Qualitative, semi-quantitative	1.5-3.0	STIR(WB), T1wTSE(WB), HASTE(lung), STIR(lung), T2wTSE-FS(liver), STIR(spine), T1wTSE(spine), VIBE(liver)after CM, T1wTSE(brain) after CM, T2wTSE(brain)after CM, T1wGE-FS(abdomen)after CM	1.5-6mm	Yes	No	No	42-51	Follow up
Giraudet *et al.*[59]	PET/CT	5 MBq/kg	60	Static acquisition	Qualitative, semi-quantitative	1.5	T2wFSE(liver), dynamic contrast-enhanced MRI, T1-weighted sequences with fast multiplanar spoiled gradient-recalled echo imaging, STIR(WB), T1wSE(WB)	7mm	No	No	No	NR	Follow up
Takano *et al.*[60]	PET	5 MBq/kg	50	Static acquisition (8min per bed position)	Qualitative	1.5	T1wGE(WB), T2wFSE(WB), DW-EPI-STIR(WB)	4mm	No	Yes (Bvalue 0-1000 mm2/s)	No	NR	Histology and/ or follow up

NR = not reported; CM = contrast media; DWIBS = diffusion weighted imaging with background body signal suppression; WB = whole-body

sitivity for detection of extra-hepatic disease was 94% for PET/CT and 91% for WB-MRI. Overall, by combining both modalities, the specificity for inclusion to radioembolisation therapy was 99%.[26]

Cafagna *et al*.[27] evaluating 38 cancer patients demonstrated that DWI WB-MRI may be used in detecting tumours but is less effective in characterizing lymph nodal and bone lesions compared to FDG-PET/CT. The qualitative analysis of DWI WB-MRI and FDG-PET/CT showed that two patients were negative at both techniques. DWI WB-MRI was positive in 36 patients, 34 of whom were positive and two negative at FDG-PET/CT, respectively. A significant discordance was found between the two methods (255 lesions were identified by DWI WB-MRI and 184 by FDG-PET/CT).[27]

Lastly, Manenti *et al*.[28] reported that DWI WB-MRI should be considered as alternative tool to conventional whole-body methods for tumour staging in cancer patients. Evaluating 45 patients using both methods, detection rates of malignancy did not differ between DWI WB-MRI and FDG-PET/CT.[28]

Lymphomas

Staging

Punwani *et al*.[29] evaluated 31 subjects with lymphoma using both WB-MRI and enhanced FDG-PET/CT (used as reference standard) demonstrating that WB-MRI can accurately depict nodal and extranodal disease and may provide an alternative non-ionizing imaging method for initial staging. WB-MRI and enhanced PET/CT showed a good agreement for nodal and extranodal staging. The sensitivity and specificity of WB-MRI were 98% and 99%, respectively, for nodal disease; 91% and 99%, respectively, for extranodal disease.[29]

van Ufford *et al*.[30] compared DWI WB-MRI with FDG-PET/CT in the staging of 22 patients with newly diagnosed lymphoma. These authors found a moderate overall agreement between DWI WB-MRI and FDG-PET/CT. Ann Arbor staging, according to DWI WB-MRI findings, was concordant with that of FDG PET/CT findings in 77% (17/22) of patients. In the care of patients with newly diagnosed lymphoma, staging with DWI WB-MRI did not result in underestimation of stage relative to the results with FDG-PET/CT. In a minority of patients, reliance on DWI WB-MRI led to clinically important overstaging relative to the results with FDG-PET/CT.[30]

Recently, Abdulqadhr *et al*.[31] compared DWI WB-MRI with FDG-PET/CT in the staging of 31 lymphoma patients (8 with Hodgkin's lymphoma and 23 with non-Hodgkin's lymphomas). The staging was the same for DWI WB-MRI and FDG-PET/CT in 28 (90.3%) patients and different in three (9.7%). No Hodgkin lymphoma or aggressive non-Hodgkin's lymphoma patients had different staging using both methods. Three indolent lymphocytic lymphomas had higher staging with DWI WB-MRI when compared with FDG-PET/CT.[31]

Gu *et al*.[32] evaluated the diagnostic performance of WB-MRI with or without DWI in the detection of 17 patients with newly diagnosed lymphomas, using FDG-PET/CT as the reference standard. The addition of DWI to conventional WB-MRI improved diagnostic accuracy for lymphomas. These authors suggested that WB-MRI could be useful as an alternative method to FDG-PET/CT in the management of lymphomas.[32]

Treatment response assessment

Lin *et al*.[33] assessed post-treatment changes in 15 patients with diffuse large B-cell lymphomas on DWI WB-MRI using PET/CT as the reference standard. After chemotherapy, among 85 examined lymph nodal regions, residual nodes were present in 62 (73%) regions on DWI WB-MRI. Of these 62 regions, 26 had persistent lymph nodes with longest transverse diameter > 10mm (MRI size criteria for positivity). Only 6 of these 26 regions were considered positive on PET/CT. DWI with ADC mapping showed a significant increase in ADC values of residual masses persisting after treatment and were helpful to assess the treatment response in patients with diffuse large B-cell lymphomas.[33]

Wu *et al*.[34] evaluated the feasibility of DWI WB-MRI in the early chemotherapeutic response assessment of 8 patients with large B-cell lymphomas. These authors found that the results of WB-MRI with or without DWI were comparable with those of FDG-PET/CT.[34]

Recently, Chen *et al*.[35] reported that DWI WB-MRI, combined with the dynamic changes of ADC value, was a valid alternative method compared to FDG PET/CT in assessing treatment response to chemotherapy in 10 patients with non-Hodgkin's lymphoma.[35]

Bone tumours

Primary tumours

Shortt *et al*.[36] found that WB-MRI performed better than FDG-PET/CT in the assessment of disease activity in 24 patients with multiple myeloma. FDG-PET/CT had a sensitivity of 59%, specificity of 75%, and accuracy of 65%. WB-MRI had a sensitivity of 68%, specificity of 83% and accuracy of 74%. In 62% of cases, FDG-PET/CT and WB-MRI findings were

concordant. When PET and WB-MRI findings were concordant and positive, specificity was 100%.[36]

Bone metastases

Daldrup-Link *et al*.[37] compared the diagnostic accuracy of WB-MRI and FDG-PET for the detection of bone metastases in 39 children. Sensitivity for the detection of bone metastases were 90% for FDG-PET and 82% for WB-MRI.[37]

In 2007, Schmidt *et al*.[38] prospectively compared the diagnostic accuracy of WB-MRI and FDG-PET/CT for the detection of bone metastases in 30 patients with different oncologic diseases. WB-MRI showed a sensitivity, specificity and accuracy of 94%, 76% and 91%, respectively. PET/CT achieved a sensitivity, specificity and accuracy of 78%, 80% and 78%, respectively. Cut-off size for the detection of malignant bone lesions was 2 mm for WB-MRI and 5 mm for PET/CT.[38]

In 2008, Ribrag *et al*.[39] suggested that non-invasive morphological procedures (WB-MRI and FDG-PET/CT) could be superior to bone marrow biopsy for bone marrow assessment in aggressive lymphomas. Both WB-MRI and PET/CT detected bone marrow lesions in the 9/43 patients, but two patients with multiple lesions had more lesions detected by PET/CT compared to MRI.[39]

Kumar *et al*.[40] compared WB-MRI and FDG-PET/CT for the detection of bone marrow metastases in 26 children with small-cell neoplasms. WB-MRI showed a sensitivity, specificity and accuracy of 97.5%, 99.4%, and 99% respectively. FDG-PET/CT showed a sensitivity, specificity and accuracy of 90.0%, 100%, and 98%. Both WB-MRI and FDG-PET/CT showed excellent agreement with the final diagnosis.[40]

In 2009, Takenaka *et al*.[41] prospectively compared WB-MRI (with and without DWI) and FDG-PET/CT in the detection of bone metastases in 115 patients with non-small cell lung cancer. These authors suggested that DWI WB-MRI can be used for bone metastases assessment in patients with non-small cell lung cancer being more accurate than bone scintigraphy and FDG-PET/CT.[41]

Recently, Heusner *et al*.[42] found that FDG-PET/CT and WB-MRI were equally suitable for the detection of bone metastases in 109 patients with non-small cell lung cancer and malignant melanoma. The sensitivity, specificity, and accuracy for the detection of bone metastases was 45%, 99%, and 94% with FDG-PET/CT and 64%, 94%, and 91% with WB-MRI.[42]

Head and neck tumours

In 2010, Ng *et al*.[43] prospectively compared WB-MRI and FDG-PET/CT for the detection of residual/recurrent nasopharyngeal carcinoma in 179 patients. On a per patient-based analysis, sensitivity and specificity of WB-MRI were similar to those of FDG-PET/CT (90.9% *vs*. 87.3%, and 91.1% vs. 90.3%, respectively). A combined interpretation of both methods increased the sensitivity to 94.5%.[43]

In the same year, O'Neill *et al*.[44] compared WB-MRI and FDG-PET/CT for the staging of 15 patients with head and neck tumours. This study found radiological staging discordance between the two imaging modalities: T-staging showed a 74% of concordance, N-staging a 80% of concordance and M-stage a 100% of concordance.[44]

Recently, Ng *et al*.[45] compared WB-MRI and FDG-PET/CT in 79 treated oropharyngeal or hypopharyngeal squamous cell carcinoma. PET/CT showed a trend towards higher diagnostic accuracy than WB-MRI in detecting residual/recurrent tumours or second primary tumours. The combined use of PET/CT and WB-MRI provided more added value to WB-MRI alone than to PET/CT alone. Sensitivity and specificity of FDG-PET/CT on a patient-based analysis were 72% and 94%. Sensitivity and specificity of WB-MRI on a patient-based analysis were 55% and 90%.[45]

The same group prospectively compared the diagnostic value of FDG-PET/CT and WB-MRI for the assessment of distant metastases and second primary cancers in 103 patients with untreated oropharyngeal or hypopharyngeal squamous cell carcinoma. Again, FDG-PET/CT showed a consistent trend toward higher sensitivity compared to WB-MRI for the detection of distant metastases and secondary primary cancers in these patients.[46]

Lastly, Eiber *et al*.[47] reported that a combination of FDG-PET/CT and WB-MRI increased the diagnostic accuracy in the staging of 20 patients with head and neck tumours.[47]

Lung cancer

In 2008, Plathow *et al*.[48] evaluated and compared FDG-PET/CT with WB-MRI in the correct staging of 52 patients with advanced non-small cell lung cancer (NSCLC). In the correct staging of advanced NSCLC, PET/CT had advantages in N-staging, whereas WB-MRI had certain advantages in T-staging. WB-MRI correctly T-staged all patients. PET/CT did not correctly stage chest wall infiltration in 4 cases (sensitivity: 92.3%; specificity: 100%). PET/CT correctly N-staged 51 patients (sensitivity: 96.1%; specificity: 100%). WB-MRI showed a significant tendency to understage N-status (sensitivity: 88.5%; specificity: 96.1%). In 2 patients, distant metastases were detected by both techniques.[48]

TABLE 3. Diagnostic performance of PET and WB-MRI in the included studies

Authors	Sensitivity (%)				Specificity (%)				Accuracy(%)			
	PET		MRI		PET		MRI		PET		MRI	
	Pt	Les	Pt	Les	Pt	Les	Pt	Les	Pt	Les	Pt	Les
Antoch *et al.*[17]	NR	NR	NR	NR	NR	NR	NR	NR	NR	NR	NR	NR
Schmidt *et al.*[18]	NR	RS	NR	89	NR	RS	NR	86	NR	RS	NR	88
Komori *et al.*[19]	NR	NR	NR	NR	NR	NR	NR	NR	NR	NR	NR	NR
Li *et al.*[20]	NR	NR	NR	NR	NR	NR	NR	NR	NR	NR	NR	NR
Brauck *et al.*[21]	NR	NR	NR	NR	NR	NR	NR	NR	NR	NR	NR	NR
Yang *et al.*[22]	NR	NR	NR	NR	NR	NR	NR	NR	NR	NR	NR	NR
Stecco *et al.*[23]	NR	RS	NR	87-89	NR	RS	NR	98-99	NR	RS	NR	97-99
Krohmer *et al.*[24]	NR	RS	NR	96	NR	NR	NR	NR	NR	NR	NR	NR
Fischer *et al.*[25]	RS	RS	85(WB-MRI), 88(DWI)	57(WB-MRI), 64(DWI)	RS	NR	81(WB-MRI), 69(DWI)	NR	RS	NR	84(WB-MRI), 83(DWI)	NR
Schmidt *et al.*[26]	94	NR	91	NR	97	NR	88	NR	96	NR	89	NR
Cafagna *et al.*[27]	NR	NR	NR	NR	NR	NR	NR	NR	NR	NR	NR	NR
Manenti *et al.*[28]	NR	RS	NR	96(WB-MRI), 94(DWI)	NR	RS	NR	100(WB-MRI), 100(DWI)	NR	RS	NR	97(WB-MRI), 96(DWI)
Punwani *et al.*[29]	NR	100 (nodal) 96(extranodal)	NR	98(nodal) 91(extranodal)	NR	100(nodal) 100(extranodal)	NR	99 (nodal) 99 (extranodal)	NR	100 (nodal) 100(extranodal)	NR	99 (nodal) 99(extranodal)
van Ufford *et al.*[30]	NR	NR	NR	NR	NR	NR	NR	NR	NR	NR	NR	NR
Abdulqadhr *et al.*[31]	NR	NR	NR	NR	NR	NR	NR	NR	NR	NR	NR	NR
Gu *et al.*[32]	NR	RS	NR	89(WB-MRI), 97(DWI)	NR	NR	NR	NR	NR	NR	NR	NR
Lin *et al.*[33]	NR	NR	NR	NR	NR	NR	NR	NR	NR	NR	NR	NR
Wu *et al.*[34]	NR	NR	NR	NR	NR	NR	NR	NR	NR	NR	NR	NR
Chen *et al.*[35]	NR	NR	NR	NR	NR	NR	NR	NR	NR	NR	NR	NR
Shortt *et al.*[36]	NR	59	NR	68	NR	75	NR	83	NR	65	NR	74
Daldrup-Link *et al.*[37]	86	90	76	82	89	NR	100	NR	87	NR	87	NR
Schmidt *et al.*[38]	NR	98(N-stage), 82(M-stage)	NR	80(N-stage), 96(M-stage)	NR	83(N-stage), 82(M-stage)	NR	75(N-stage), 82(M-stage)	NR	96(TNM)	NR	91(TNM)
Ribrag *et al.*[39]	100(bone lesions), 29 (bone marrow)	96(bone lesions), 95(bone marrow)	100(bone lesions), 100(bone marrow)	83(bone lesions), 90(bone marrow)	NR	NR	NR	NR	NR	NR	NR	NR
Kumar *et al.*[40]	NR	90	NR	97	NR	100	NR	99	NR	98	NR	99
Takenaka *et al.*[41]	96	97	64(WB-MRI), 96(DWI)	73(WB-MRI), 95(DWI)	86	95	90(WB-MRI) 79(DWI)	96(WB-MRI), 94(DWI)	88	95	84(WB-MRI), 83(DWI)	95(WB-MRI), 94(DWI)
Heusner *et al.*[42]	45	NR	64	NR	99	NR	94	NR	94	NR	91	NR
Ng *et al.*[43]	87	87	91	89	90	96	91	97	89	95	91	96
O'Neill *et al.*[44]	NR	NR	NR	NR	NR	NR	NR	NR	NR	NR	NR	NR
Ng *et al.*[45]	72	71	55	64	94	96	90	96	86	92	76	91
Chan *et al.*[46]	NR	81	NR	62	NR	99	NR	99	NR	99	NR	98
Eiber *et al.*[47]	NR	NR	NR	NR	NR	NR	NR	NR	NR	NR	NR	NR
Plathow *et al.*[48]	92(T-stage), 96(N-stage), 100(M-stage)	NR	100(T-stage), 88(N-stage), 100(M-stage)	NR	100(T-stage), 100(N-stage), 100(M-stage)	NR	100(T-stage), 96(N-stage), 100(M-stage)	NR	NR	NR	NR	NR
Ohno *et al.*[49]	62-70	NR	56-60(WB-MRI), 57-67(DWI)	NR	94	NR	92(WB-MRI), 88(DWI)	NR	88-90	NR	86(WB-MRI),82-84(DWI)	NR
Yi *et al.*[50]	48	NR	52	NR	96	NR	94	NR	86	NR	86	NR
Chen *et al.*[51]	NR	98	NR	91	NR	98	NR	92	NR	97	NR	91
Pfannenberg *et al.*[52]	NR	90	NR	80	NR	77	NR	76	NR	87	NR	79
Laurent *et al.*[53]	NR	73	NR	83	NR	93	NR	98	NR	NR	NR	NR
Dellestable *et al.*[54]	NR	74	NR	83	NR	89	NR	96	NR	74	NR	81
Schmidt *et al.*[55]	NR	91	NR	90	NR	90	NR	86	NR	91	NR	91
Heusner *et al.*[56]	75-100	94	66-100	91	94-100	99	0-100	72	93-100	98	30-100	76
Squillaci *et al.*[57]	NR	NR	NR	NR	NR	NR	NR	NR	NR	NR	NR	NR
Schmidt *et al.*[58]	NR	86	NR	72	NR	96	NR	93	NR	91	NR	83
Giraudet *et al.*[59]	NR	NR	NR	NR	NR	NR	NR	NR	NR	NR	NR	NR
Takano *et al.*[60]	NR	NR	NR	NR	NR	NR	NR	NR	NR	NR	NR	NR

NR = not reported; Pt = per patient-based analysis; Les = per lesion-based analysis; DWI = diffusion weighted imaging; WB-MRI = whole body magnetic resonance imaging

In the same year, Ohno *et al*.[49] prospectively compared WB-MRI with and without DWI and FDG-PET/CT for M-stage assessment in 203 NSCLC patients. These authors found that DWI WB-MRI can be used for M-stage assessment in NSCLC patients with accuracy as good as that of PET/CT. The area under the ROC curve was 0.89 for FDG-PET/CT, 0.85 for DWI WB-MRI and 0.81 for WB-MRI without DWI, excluding brain metastases (due to the low accuracy of FDG-PET/CT in detecting brain metastases).[49]

Yi *et al*.[51] prospectively compared the diagnostic accuracy of FDG-PET/CT and WB-MRI for TNM stage of 165 patients with NSCLC. WB-MRI was more useful for detecting brain and hepatic metastases, whereas PET/CT was more useful for detecting lymph node and soft-tissue metastases. Primary tumours (n=123 patients) were correctly staged in 101 (82%) patients at PET/CT and in 106 (86%) patients at WB-MRI. N stages (n=150 patients) were correctly determined in 105 (70%) patients at PET/CT and in 102 (68%) patients at WB-MRI. Thirty-one (20%) of 154 patients had metastatic lesions. Accuracy for detecting metastases was comparable between PET/CT and WB-MRI (86%). WB-MRI was more useful for detecting brain and hepatic metastases, whereas PET/CT was more useful for detecting lymph node and soft-tissue metastases.[50]

Chen *et al*.[51] compared the diagnostic accuracy of DWI WB-MRI and FDG-PET/CT for assessment of 56 NSCLC patients. DWI WB-MRI was a feasible imaging method for the assessment of lymph nodal and metastatic spread with high accuracy, but it was limited in the evaluation of neck lymph nodal metastases and small metastatic lung nodules. Primary tumours were correctly detected in 56 (100%) patients by both PET/CT and DWI WB-MRI. Sensitivity, specificity and accuracy for lymph nodal metastases were 91%, 90% and 90% with DWI WB-MRI and 98%, 97% and 97% with PET/CT, respectively. Sensitivity, specificity and accuracy for other metastases were 90%, 95% and 92% with DWI WB-MRI and 98%, 100% and 98% with PET/CT.[51]

Melanoma

Pfannenberg *et al*.[52] compared the diagnostic accuracy and impact on patient management of FDG-PET/CT and WB-MRI in staging of 64 patients with advanced melanoma. The overall accuracy of PET/CT was 86.7% compared to 78.8% for WB-MRI. PET/CT was significantly more accurate in N-staging and in detecting skin and subcutaneous metastases, whereas WB-MRI was more sensitive in detecting liver, bone and brain metastases. WB-MRI was less sensitive but more specific than PET/CT in classifying pulmonary lesions.[52]

Laurent *et al*.[53] compared WB-MRI (with and without DWI) and FDG-PET/CT for staging of 35 patients with advanced melanoma. The sensitivity and specificity for WB-MRI without DWI were 82% and 97%, respectively, while for PET/CT were 72.8% and 92.7%, respectively. DWI allowed the detection of 14 supplementary malignant lesions (20%) in comparison with standard MRI protocol.[51] In particular WB-MRI has been shown to be the most accurate method for detecting metastases in the liver, bone, subcutaneous and intra-peritoneal sites.[53]

Recently, Dellestable *et al*.[54] found that DWI WB-MRI was superior compared to FDG-PET/CT in the staging of 40 patients with melanoma. Sensitivity and specificity were 74% and 89% for FDG-PET/CT, 83% and 96% for DWI WB-MRI. The sensitivity of MRI was distinctly superior compared to that of PET/CT for both hepatic and pulmonary lesions.[54]

Breast cancer

Schmidt *et al*.[55] compared the diagnostic accuracy of WB-MRI and FDG-PET/CT for the detection of tumour recurrence in 33 patients with breast cancer. WB-MRI and PET/CT were both useful for the detection of tumour recurrence. WB-MRI was highly sensitive to detect distant metastatic disease. PET/CT was more sensitive in detecting lymph node involvement. Overall sensitivity was 91% for PET/CT and 90% for WB-MRI. Overall specificity was 90% for FDG-PET/CT and 86% for WB-MRI.[55]

Heusner *et al*.[56] prospectively compared the diagnostic value of DWI WB-MRI and FDG-PET/CT for breast cancer staging in 20 patients. DWI resulted a sensitive but unspecific method for the detection of locoregional or metastatic breast cancer. These authors suggested that DWI WB-MRI is not alternative to FDG-PET/CT in staging breast cancer. The sensitivity, specificity, and accuracy for FDG-PET/CT were 94%, 99%, and 98%, respectively, whereas for DWI WB-MRI were 91%, 72%, and 76%, respectively.[56]

Colorectal cancer

Squillaci *et al*.[57] assessed the accuracy of WB-MRI in comparison with FDG-PET/CT in staging 20 patients with colorectal carcinoma. These authors found that WB-MRI was a feasible method for staging colorectal cancer but could not substitute PET/CT. Lymph-nodal metastases were detected in 10/20 cases at WB-MRI and in 15/20 at PET/CT.

M-stage was evaluated for liver metastases (27 lesions detected in 15 patients with WB/MRI; 23 lesions detected in 15 patients with PET/CT), lung metastases (19 lesions detected in 5 patients with WB-MRI, 25 lesions detected in 7 patients with PET/CT), and bone (9 lesions detected in 3 patients with both methods).[57]

Schmidt *et al*.[58] assessed the diagnostic accuracy of WB-MRI compared with FDG-PET/CT in the follow-up of 24 patients suffering from colorectal cancer. Malignant foci were detected in 71% of patients with both methods. Lymph nodal metastases were better detected using PET/CT (sensitivity was 93% for PET/CT and 63% for WB-MRI), whereas distant metastases were depicted equally well by both investigations (sensitivity was 80% for PET/CT and 78% for WB-MRI). Overall sensitivity, specificity and diagnostic accuracy was 86%, 96% and 91% for PET/CT, and 72%, 93% and 83% for WB-MRI.[58]

Neuroendocrine tumours

Giraudet *et al*.[59] comparing FDG-PET/CT and WB-MRI in 50 patients with suspected recurrent medullary thyroid carcinoma found a superior diagnostic accuracy of WB-MRI compared to FDG-PET/CT.[59]

Takano *et al*.[60] found that DWI WB-MRI had a higher detection rate of metastatic lesions in 11 patients with paraganglioma when compared with metaiodobenzylguanidine scintigraphy or FDG-PET, particularly for lymph nodal and liver metastases. The limitations of DWI WB-MRI were possible false-positive findings and lower detectability of mediastinal lymph nodes and lung metastases.[60]

General remarks and conclusions

On the basis of our systematic review, we found several articles in which mixed tumour types were evaluated using both imaging methods.[17-28] For what concerns the specific tumour types, more evidence exists for lymphomas[29-35], bone tumours[36-42], head and neck tumours[43-47] and lung tumours[48-51], whereas there is less evidence for other tumour types.

Overall, based on the literature findings, WB-MRI seems to be a valid alternative method compared to PET/CT in oncology. Nevertheless, it should be considered that the studies included in this systematic review were highly heterogeneous not only about the patient population evaluated (Table 1), but also for those technical aspects related to PET imaging and WB-MRI (Table 2). In particular, DWI, when performed, seemed to provide an added value to WB-MRI compared to FDG-PET/CT, increasing the sensitivity (due to a better lesion to background contrast).

A possible limitation of some studies evaluated in this systematic review is the reference standard used. In fact, in some articles the diagnostic performance of WB-MRI was assessed considering PET or PET/CT as a reference standard. This is a possible source of bias, because FDG-PET or PET/CT has its own limitations, mainly due to the possibility of false-positive or false-negative results, which could affect the diagnostic accuracy calculated for WB-MRI (Table 3).

Possible advantages of WB-MRI compared to FDG-PET or PET/CT are: the lack of ionizing radiation, the higher soft-tissue contrast, the higher spatial resolution, the better assessment of non FDG-avid tumour types or sites of physiological FDG uptake. On the other hand, it should be considered that WB-MRI has a longer examination time compared to PET/CT and more variable acquisition protocols.

Both these imaging techniques still show limited worldwide availability if compared to other conventional imaging methods.

Referring to the costs, Plathow *et al*.[61], performing a cost-analysis study, demonstrated that both whole-body imaging techniques allow substantial reduction of health care costs in many tumour types. On the basis of a simple full cost analysis, total costs of whole-body PET/CT were higher than those of whole-body MRI by a factor of about 2.0.[61]

Further larger prospective studies and in particular cost-effectiveness analysis comparing these two whole-body imaging techniques is needed to better assess the role of WB-MRI compared to FDG-PET or PET/CT in specific tumour types. Furthermore, emerging hybrid PET/MRI devices will increase the number of studies comparing PET to WB-MRI.

References

1. Hodolic M. Role of F-18-choline PET/CT in evaluation of patients with prostate carcinoma. *Radiol Oncol* 2011; **45:** 17-21.
2. Basu S, Alavi A. Unparalleled contribution of 18F-FDG PET to medicine over 3 decades. *J Nucl Med* 2008; **49:** 17N-21N, 37N.
3. Wang X, Xu M, Liang H, Xu LS. Comparison of CT and MRI in diagnosis of cerebrospinal leak induced by multiple fractures of skull base. *Radiol Oncol* 2011; **45**: 91-6.
4. Schmidt GP, Reiser MF, Baur-Melnyk A. Whole-body MRI for the staging and follow-up of patients with metastasis. *Eur J Radiol* 2009; **70:** 393-400.
5. Lambregts DM, Maas M, Cappendijk VC, Prompers LM, Mottaghy FM, Beets GL, et al. Whole-body diffusion-weighted magnetic resonance imaging: Current evidence in oncology and potential role in colorectal cancer staging. *Eur J Cancer* 2011; **47:** 2107-16.

6. Thomson V, Pialat JB, Gay F, Coulon A, Voloch A, Granier A, et al. Whole-body MRI for metastases screening: a preliminary study using 3D VIBE sequences with automatic subtraction between noncontrast and contrast enhanced images. *Am J Clin Oncol* 2008; **31:** 285-92.
7. Mürtz P, Krautmacher C, Träber F, Gieseke J, Schild HH, Willinek WA. Diffusion-weighted whole-body MR imaging with background body signal suppression: a feasibility study at 3.0 Tesla. *Eur Radiol* 2007; **17:** 3031-7.
8. Seemann MD, Meisetschlaeger G, Gaa J, Rummeny EJ. Assessment of the extent of metastases of gastrointestinal carcinoid tumors using whole-body PET, CT, MRI, PET/CT and PET/MRI. *Eur J Med Res* 2006; **11:** 58-65.
9. Furth C, Amthauer H, Denecke T, Ruf J, Henze G, Gutberlet M. Impact of whole-body MRI and FDG-PET on staging and assessment of therapy response in a patient with Ewing sarcoma. *Pediatr Blood Cancer* 2006; **47:** 607-11.
10. Yan RZ, Yang C, Zhang Q, Gu XM. [Whole-body diffusion weighted imaging manifestation of oral squamous cell carcinoma with metastatic lymph nodes]. [Chinese]. *Zhonghua Kou Qiang Yi Xue Za Zhi* 2009; **44:** 144-6.
11. Wang JW, Zhao S, Liu Y, Li J, Xu LM. [Preliminary study on the validity of whole body diffusion-weighted imaging for the detection of malignant lesions]. [Chinese]. *Zhonghua Kou Qiang Yi Xue Za Zhi* 2010; **32:** 304-8.
12. Lin C, Luciani A, Itti E, El-Gnaoui T, Vignaud A, Beaussart P, et al. Whole-body diffusion-weighted magnetic resonance imaging with apparent diffusion coefficient mapping for staging patients with diffuse large B-cell lymphoma. *Eur Radiol* 2010; **20:** 2027-38.
13. Schmidt GP, Baur-Melnyk A, Tiling R, Hahn K, Reiser MF, Schoenberg SO. [Comparison of high resolution whole-body MRI using parallel imaging and PET-CT. First experiences with a 32-channel MRI system.] [German]. *Radiologe* 2004; **44:** 889-98.
14. Reiner CS, Fischer MA, Hany T, Stolzmann P, Nanz D, Donati OF, et al. Molecular imaging of malignant tumor metabolism: whole-body image fusion of DWI/CT vs. PET/CT. *Acad Radiol* 2011; **18:** 940-6.
15. Ohno Y, Koyama H, Nogami M, Takenaka D, Yoshikawa T, Yoshimura M, et al. Whole-body MR imaging vs. FDG-PET: comparison of accuracy of M-stage diagnosis for lung cancer patients. *J Magn Reson Imaging* 2007; **26:** 498-509.
16. Ng SH, Chan SC, Yen TC, Chang JT, Liao CT, Ko SF, et al. Pretreatment evaluation of distant-site status in patients with nasopharyngeal carcinoma: accuracy of whole-body MRI at 3-Tesla and FDG-PET-CT. *Eur Radiol* 2009; **19:** 2965-76.
17. Antoch G, Vogt FM, Freudenberg LS, Nazaradeh F, Goehde SC, Barkhausen J, et al. Whole-body dual-modality PET/CT and whole-body MRI for tumor staging in oncology. *JAMA* 2003; **290:** 3199-206.
18. Schmidt GP, Baur-Melnyk A, Herzog P, Schmid R, Tiling R, Schmidt M, et al. High-resolution whole-body magnetic resonance image tumor staging with the use of parallel imaging versus dual-modality positron emission tomography-computed tomography: experience on a 32-channel system. *Invest Radiol* 2005; **40:** 743-53.
19. Komori T, Narabayashi I, Matsumura K, Matsuki M, Akagi H, Ogura Y, et al. 2-[Fluorine-18]-fluoro-2-deoxy-D-glucose positron emission tomography/computed tomography versus whole-body diffusion-weighted MRI for detection of malignant lesions: initial experience. *Ann Nucl Med* 2007; **21:** 209-15.
20. Li S, Sun F, Jin ZY, Xue HD, Li ML. Whole-body diffusion-weighted imaging: technical improvement and preliminary results. *J Magn Reson Imaging* 2007; **26:** 1139-44.
21. Brauck K, Zenge MO, Vogt FM, Quick HH, Stock F, Trarbach T, et al. Feasibility of whole-body MR with T2- and T1-weighted real-time steady-state free precession sequences during continuous table movement to depict metastases. *Radiology* 2008; **246:** 910-6.
22. Yang TH, Lin JZ, Wang X, Lu JH, Chen Z. Preliminary study of feasibility of whole body diffusion weighted imaging in diagnosis of metastasis of tumor. *Chin Med Sci J* 2008; **23:** 187-92.
23. Stecco A, Romano G, Negru M, Volpe D, Saponaro A, Costantino S, et al. Whole-body diffusion-weighted magnetic resonance imaging in the staging of oncologic patients: comparison with positron emission tomography computed tomography (PET-CT) in a pilot study. *Radiol Med* 2009; **114:** 1-17.
24. Krohmer S, Sorge I, Krausse A, Kluge R, Bierbach U, Marwede D, et al. Whole-body MRI for primary evaluation of malignant disease in children. *Eur J Radiol* 2010; **74:** 256-61.
25. Fischer MA, Nanz D, Hany T, Reiner CS, Stolzmann P, Donati OF, et al. Diagnostic accuracy of whole-body MRI/DWI image fusion for detection of malignant tumours: a comparison with PET/CT. *Eur Radiol* 2011; **21:** 246-55.
26. Schmidt GP, Paprottka P, Jakobs TF, Hoffmann RT, Baur-Melnyk A, Haug A, et al. FDG-PET-CT and whole-body MRI for triage in patients planned for radioembolisation therapy. *Eur J Radiol* 2012; **81:** 269-76.
27. Cafagna D, Rubini G, Iuele F, Maggialetti N, Notaristefano A, Pinto D, et al. Whole-body MR-DWIBS vs. [(18)F]-FDG-PET/CT in the study of malignant tumors: a retrospective study. *Radiol Med* 2012; **117:** 293-311.
28. Manenti G, Cicciò C, Squillaci E, Strigari L, Calabria F, Danieli R, et al. Role of combined DWIBS/3D-CE-T1w whole-body MRI in tumor staging: Comparison with PET-CT. *Eur J Radiol* 2012 doi:10.1016/j.ejrad.2011.08.005
29. Punwani S, Taylor SA, Bainbridge A, Prakash V, Bandula S, De Vita E, et al. Pediatric and adolescent lymphoma: comparison of whole-body STIR half-Fourier RARE MR imaging with an enhanced PET/CT reference for initial staging. *Radiology* 2010; **255:** 182-90.
30. van Ufford HM, Kwee TC, Beek FJ, van Leeuwen MS, Takahara T, Fijnheer R, et al. Newly diagnosed lymphoma: initial results with whole-body T1-weighted, STIR, and diffusion-weighted MRI compared with 18F-FDG PET/CT. *AJR Am J Roentgenol* 2011; **196:** 662-9.
31. Abdulqadhr G, Molin D, Aström G, Suurküla M, Johansson L, Hagberg H, et al. Whole-body diffusion-weighted imaging compared with FDG-PET/CT in staging of lymphoma patients. *Acta Radiol* 2011; **52:** 173-80.
32. Gu J, Chan T, Zhang J, Leung AY, Kwong YL, Khong PL. Whole-body diffusion-weighted imaging: the added value to whole-body MRI at initial diagnosis of lymphoma. *AJR Am J Roentgenol* 2011; **197:** w384-91.
33. Lin C, Itti E, Luciani A, Zegai B, Lin SJ, Kuhnowski F, et al. Whole-body diffusion-weighted imaging with apparent diffusion coefficient mapping for treatment response assessment in patients with diffuse large B-cell lymphoma:pilot study. *Invest Radiol* 2011; **46:** 341-9.
34. Wu X, Kellokumpu-Lehtinen PL, Pertovaara H, Korkola P, Soimakallio S, Eskola H, et al. Diffusion-weighted MRI in early chemotherapy response evaluation of patients with diffuse large B-cell lymphoma--a pilot study: comparison with 2-deoxy-2-fluoro-D-glucose-positron emission tomography/computed tomography. *NMR Biomed* 2011; **24:** 1181-90.
35. Chen Y, Zhong J, Wu H, Chen N. The clinical application of whole-body diffusion-weighted imaging in the early assessment of chemotherapeutic effects in lymphoma: the initial experience. *Magn Reson Imaging* 2012; **30:** 165-70.
36. Shortt CP, Gleeson TG, Breen KA, McHugh J, O'Connell MJ, O'Gorman PJ, et al. Whole-Body MRI versus PET in assessment of multiple myeloma disease activity. *AJR Am J Roentgenol* 2009; **192:** 980-6.
37. Daldrup-Link HE, Franzius C, Link TM, Laukamp D, Sciuk J, Jürgens H, et al. Whole-body MR imaging for detection of bone metastases in children and young adults: comparison with skeletal scintigraphy and FDG PET. *AJR Am J Roentgenol* 2001; **177:** 229-36.
38. Schmidt GP, Schoenberg SO, Schmid R, Stahl R, Tiling R, Becker CR, et al. Screening for bone metastases: whole-body MRI using a 32-channel system versus dual-modality PET-CT. *Eur Radiol* 2007; **17:** 939-49.
39. Ribrag V, Vanel D, Leboulleux S, Lumbroso J, Couanet D, Bonniaud G, et al. Prospective study of bone marrow infiltration in aggressive lymphoma by three independent methods: whole-body MRI, PET/CT and bone marrow biopsy. *Eur J Radiol* 2008; **66:** 325-31.
40. Kumar J, Seith A, Kumar A, Sharma R, Bakhshi S, Kumar R, et al. Whole-body MR imaging with the use of parallel imaging for detection of skeletal metastases in pediatric patients with small-cell neoplasms: comparison with skeletal scintigraphy and FDG PET/CT. *Pediatr Radiol* 2008; **38:** 953-62.
41. Takenaka D, Ohno Y, Matsumoto K, Aoyama N, Onishi Y, Koyama H, et al. Detection of bone metastases in non-small cell lung cancer patients: comparison of whole-body diffusion-weighted imaging (DWI), whole-body MR imaging without and with DWI, whole-body FDG-PET/CT, and bone scintigraphy. *J Magn Reson Imaging* 2009; **30:** 298-308.
42. Heusner T, Gölitz P, Hamami M, Eberhardt W, Esser S, Forsting M, et al. "One-stop-shop" staging: should we prefer FDG-PET/CT or MRI for the detection of bone metastases? *Eur J Radiol* 2011; **78:** 430-5.

43. Ng SH, Chan SC, Yen TC, Liao CT, Chang JT, Ko SF, et al. Comprehensive imaging of residual/ recurrent nasopharyngeal carcinoma using whole-body MRI at 3 T compared with FDG-PET-CT. *Eur Radiol* 2010; **20:** 2229-40.

44. O'Neill JP, Moynagh M, Kavanagh E, O'Dwyer T. Prospective, blinded trial of whole-body magnetic resonance imaging versus computed tomography positron emission tomography in staging primary and recurrent cancer of the head and neck. *J Laryngol Otol* 2010; **124:** 1274-7.

45. Ng SH, Chan SC, Yen TC, Liao CT, Lin CY, Tung-Chieh Chang J, et al. PET/CT and 3-T whole-body MRI in the detection of malignancy in treated oropharyngeal and hypopharyngeal carcinoma. *Eur J Nucl Med Mol Imaging* 2011; **38:** 996-1008.

46. Chan SC, Wang HM, Yen TC, Lin CY, Chin SC, Liao CT, et al. ^{18}F-FDG PET/CT and 3.0-T whole-body MRI for the detection of distant metastases and second primary tumours in patients with untreated oropharyngeal/hypopharyngeal carcinoma: a comparative study. *Eur J Nucl Med Mol Imaging* 2011; **38:** 1607-19.

47. Eiber M, Souvatzoglou M, Pickhard A, Loeffelbein DJ, Knopf A, Holzapfel K, et al. Simulation of a MR-PET protocol for staging of head-and-neck cancer including Dixon MR for attenuation correction. *Eur J Radiol* 2012; **81:** 2658-65.

48. Plathow C, Aschoff P, Lichy MP, Eschmann S, Hehr T, Brink I, et al. Positron emission tomography/computed tomography and whole-body magnetic resonance imaging in staging of advanced nonsmall cell lung cancer—initial results. *Invest Radiol* 2008; **43:** 290-7.

49. Ohno Y, Koyama H, Onishi Y, Takenaka D, Nogami M, Yoshikawa T, et al. Non-small cell lung cancer: whole-body MR examination for M-stage assessment--utility for whole-body diffusion-weighted imaging compared with integrated FDG PET/CT. *Radiology* 2008; **248:** 643-54.

50. Yi CA, Shin KM, Lee KS, Kim BT, Kim H, Kwon OJ, et al. Non-small cell lung cancer staging: efficacy comparison of integrated PET/CT versus 3.0-T whole-body MR imaging. *Radiology* 2008; **248:** 632-42.

51. Chen W, Jian W, Li HT, Li C, Zhang YK, Xie B, et al. Whole-body diffusion-weighted imaging vs. FDG-PET for the detection of non-small-cell lung cancer. How do they measure up? *Magn Reson Imaging* 2010; **28:** 613-70.

52. Pfannenberg C, Aschoff P, Schanz S, Eschmann SM, Plathow C, Eigentler TK, et al. Prospective comparison of 18F-fluorodeoxyglucose positron emission tomography/computed tomography and whole-body magnetic resonance imaging in staging of advanced malignant melanoma. *Eur J Cancer* 2007; **43:** 557-64.

53. Laurent V, Trausch G, Bruot O, Olivier P, Felblinger J, Régent D. Comparative study of two whole-body imaging techniques in the case of melanoma metastases: advantages of multi-contrast MRI examination including a diffusion-weighted sequence in comparison with PET-CT. *Eur J Radiol* 2010; **75:** 376-83.

54. Dellestable P, Granel-Brocard F, Rat AC, Olivier P, Régent D, Schmutz JL. [Impact of whole body magnetic resonance imaging (MRI) in the management of melanoma patients, in comparison with positron emission tomography/computed tomography (TEP/CT) and CT.] [French]. *Ann Dermatol Venereol* 2011; **138:** 377-83.

55. Schmidt GP, Baur-Melnyk A, Haug A, Heinemann V, Bauerfeind I, Reiser MF, et al. Comprehensive imaging of tumor recurrence in breast cancer patients using whole-body MRI at 1.5 and 3 T compared to FDG-PET-CT. *Eur J Radiol* 2008; **65:** 47-58.

56. Heusner TA, Kuemmel S, Koeninger A, Hamami ME, Hahn S, Quinsten A, et al. Diagnostic value of diffusion-weighted magnetic resonance imaging (DWI) compared to FDG PET/CT for whole-body breast cancer staging. *Eur J Nucl Med Mol Imaging* 2010; **37:** 1077-86.

57. Squillaci E, Manenti G, Mancino S, Cicciò C, Calabria F, Danieli R, et al. Staging of colon cancer: whole-body MRI vs. whole-body PET-CT--initial clinical experience. *Abdom Imaging* 2008; **33:** 676-88.

58. Schmidt GP, Baur-Melnyk A, Haug A, Utzschneider S, Becker CR, Tiling R, et al. Whole-body MRI at 1.5 T and 3 T compared with FDG-PET-CT for the detection of tumour recurrence in patients with colorectal cancer. *Eur Radiol* 2009; **19:** 1366-78.

59. Giraudet AL, Vanel D, Leboulleux S, Aupérin A, Dromain C, Chami L, et al. Imaging medullary thyroid carcinoma with persistent elevated calcitonin levels. *J Clin Endocrinol Metab* 2007; **92:** 4185-90.

60. Takano A, Oriuchi N, Tsushima Y, Taketomi-Takahashi A, Nakajima T, Arisaka Y, et al. Detection of metastatic lesions from malignant pheochromocytoma and paraganglioma with diffusion-weighted magnetic resonance imaging: comparison with 18F-FDG positron emission tomography and 123I-MIBG scintigraphy. *Ann Nucl Med* 2008; **22:** 395-401.

61. Plathow C, Walz M, Lichy MP, Aschoff P, Pfannenberg C, Bock H, et al. [Cost considerations for whole-body MRI and PET/CT as part of oncologic staging.] [German]. *Radiologe* 2008; **48:** 384-96.

research article

Prediction of 2 years-survival in patients with stage I and II non-small cell lung cancer utilizing ^{18}F-FDG PET/CT SUV quantification

Angelina Cistaro[1], Natale Quartuccio[2], Alireza Mojtahedi[3], Piercarlo Fania[1], Pier Luigi Filosso[4], Alfredo Campenni[2], Umberto Ficola[5], Sergio Baldari[2]

[1] Positron Emission Tomography Centre IRMET S.p.A., Euromedic inc., Turin, Italy
[2] Nuclear Medicine Unit, Department of Biomedical Sciences and of the Morphological and Functional Images, University of Messina, Messina, Italy
[3] Nuclear Medicine Service, Memorial Sloan-Kettering Cancer Center, New York, USA
[4] Department of Thoracic Surgery, S. Giovanni Battista Hospital, Turin, Italy
[5] Department of Nuclear Medicine, La Maddalena Hospital, Palermo, Italy

Radiol Oncol 2013; 47(3): 219-223.

Received 15 October 2012
Accepted 4 March 2013

Correspondence to: Angelina Cistaro, MD, Positron Emission Tomography Centre IRMET S.p.A, V.O. Vigliani 89, Turin 10136, Italy. Phone: +390113160158; Fax: +390113160828; E-mail: a.cistaro@irmet.com

Disclosure: No potential conflicts of interest were disclosed.

Background. The purpose of the study was to evaluate the correlation between the maximum standardized uptake value (SUVmax), size of primary lung lesion, disease-free survival (DFS) and overall survival (OS) in patients with stage I and II non-small cell lung cancer (NSCLC) in 2 years follow-up.

Patients and methods. Forty-nine patients with stage I-II NSCLC were included in this study. Pre-surgical 2-deoxy-2-[18F]fluoro-D-glucose positron-emission tomography (^{18}F-FDG PET/CT) study was performed for all patients. The relationship between SUVmax, tumour size and clinical outcome was measured. The cut-off value for SUVmax and tumour size with the best prognostic significance, probability of DFS and the correlation between SUVmax and the response to therapy were calculated.

Results. There was a statistically significant correlation between SUVmax and DFS ($p = 0.029$). The optimal cut-offs were 9.00 for SUVmax ($p = 0.0013$) and 30mm for tumour size ($p = 0.0028$). Patients with SUVmax > 9 and primary lesion size > 30 mm had an expected 2years-DFS of 37.5%, while this rose to 90% if the tumour was <30 mm and/or SUVmax was <9.

Conclusions. In stage I-II, SUVmax and tumour size might be helpful to identify the subgroup of patients with high chance for recurrence.

Key words: 2-deoxy-2-[18F]fluoro-D-glucose positron emission tomography; non-small cell lung cancer; maximum standardized uptake value; disease-free survival; overall survival.

Introduction

Lung cancer (LC) is the major cause of death in the developing countries, with an incidence of about 65-70 new cases per 100.000.[1] 2-deoxy-2-[18F] fluoro-D-glucose positron-emission tomography (^{18}F-FDG PET/CT) is widely used in lung cancer for staging, restaging and evaluation of the treatment response.[2,3] Multiple studies demonstrate that PET/CT is more sensitive and specific than PET alone in evaluating the lung cancer since it provides combined morphological and functional information of the tumour.[4-7] High accuracy of PET/CT has been observed in the early assessment of response to therapy, showing a close correlation between the reduction of tumour metabolic activity measured after a course of therapy and the clinical outcome of patients after the previewed cycles of therapy in patients in advanced stage.[8-9] In early stage, Tumour Node Metastasis (TNM) staging system,

it is still the most reliable prognostic factor to predict the outcome after surgery. However, many patients in stage I or II may experience a worse outcome than expected and an early relapse even after a successful tumour resection.[10] Also magnetic resonance imaging (MRI) [11], computed tomography (CT) [12] and endobronchial ultrasonography (EBUS) [13] have a role in the staging of lung cancer but, unlike PET/CT, lack in providing functional information, which may provide clinicians additional prognostic indications regarding the survival and the estimate risk of relapse by means of the assessment of the maximum standardized uptake value (SUVmax).

The aim of this study was to estimate the cut-off value for combined SUVmax and size of primary lung lesion that correspond with poor disease-free survival (DFS) in patients with stage I and II non-small cell lung cancer (NSCLC) in 2 years follow-up.

Patients and methods

Between 2004 and 2009, forty-nine patients (36 males = 73%; 13 females = 27%; M/F Ratio = 2.77:1; mean age = 67.2 years; range = 44-79 years) were referred to Positron Emission Tomography Centre IRMET S.p.A., Euromedic inc. in Turin, Italy and Unit of Nuclear Medicine of La Maddalena Hospital in Palermo, Italy for the evaluation of their non-small cell lung cancer. According to the inclusion criteria 49 patients included in this study received a complete tumour resection and systematic lymph node dissection.

All patients have been staged according to TNM 7th edition.[14] Survival and death information were obtained from the hospitals databases and through phone calls to the patient families. The research proposal was approved by Institutional Review Board and Ethics Committee.

The inclusion criteria were histologically proven NSCLC, glycaemia lower than 140 mg/dl at the time of the exam, availability of pre-surgical FDG-PET/CT and tumour size > 20 mm to minimize the underestimation of SUV. Exclusion criteria were as follows: (a) poor performance status; (b) diabetes (due to poor uptake of FDG); (c) pregnancy; (d) Charlson Combined Age-Comorbidity Index ≥ 6; (e) histological diagnosis of "bronchioloalveolar cell carcinoma" (BAC) subtype.

Preoperative TNM staging was obtained via information gathered through patient's chart including physical examination, routine blood test, bronchoscopy, contrast-enhanced CT of the chest and upper abdomen, brain CT and total-body ^{18}F-FDG PET/CT scan.

TABLE 1. Characteristics of population

Number of Patients	49	
Sex	36 M	13 F
Mean Age	67.2 y (range: 44-79)	
Histotypes:		
Adenocarcinoma	28	
Squamous	15	
Large cell	2	
Undetermined	4	

The PET/CT images were acquired using integrated PET/CT scanner (Discovery ST, General Electric Medical System, Milwaukee, WI, USA), 60 minutes after the injection of the 260-420 MBq of ^{18}F-FDG, following 6 hours of fasting from the cranial base to the pelvis (total body) in 3D modality. Blood glucose was measured before the injection of the tracer to ensure glucose blood levels < 140 mg/dL. The PET images were reconstructed iteratively on a 128 × 128 matrix. The SUVmax, within a spherical region of interest encompassing the entire volume, was calculated using a dedicated workstation (Xeleris, General Electric medical Systems, Milwaukee, WI, USA). The formula used for SUV calculation was: activity (MBq/ml) x body weight / injected dose (MBq/ml). The anatomical size of lung lesion was measured considering the maximum diameter of the lesion in the three planes on CT.[15]

PET, CT, and fused PET/CT images were reviewed, by two experienced nuclear medicine physicians. Images were assessed visually and semi-quantitatively. Patients were followed up for 24 months with a frequency of clinical examination of every 3 months during the first year and every 6 months in the second year. A contrast-enhanced CT scan of the thorax was performed in all cases at 6 and 12 months, while the additional PET/CT scans were used in case of suspected morphological findings.

The overall survival (OS) was calculated. The disease-free survival (DFS) was considered as the time between surgery and recurrence of disease. The correlation between SUVmax and clinical outcome (2 years-DFS) was assessed by the Student-t test (the hypothesis was considered significant if p </= 0.05). The chi-square test was used to identify the SUVmax cut-off value at the time of the initial staging with the best correlation to prognosis.

TABLE 2A. Summary of (stage I-II) patients' outcome at a follow-up period of 24 months

DFS	36 disease free	13 recurrence of disease
OS	41 alive	8 dead

TABLE 2B. Stratification of disease-free survival for the maximum standardized uptake value (SUVmax) cut-off at a follow-up period of 24 months. (Chi-square test) p = 0.0013

DFS	SUVmax < 9	SUVmax > 9
Disease-free	26	10
Recurrence of disease	2	11

TABLE 2C. Stratification of disease-free survival for a size threshold of 30 mm at a follow-up period of 24 months. (Chi-square test) p = 0.0028

DFS	Size < 30 mm	Size > 30 mm
Disease-free	22	14
Recurrence of disease	1	12

TABLE 2D. Stratification of disease-free survival for the combined maximum standardized uptake value (SUVmax) and size cut-offs at a follow-up period of 24 months. (Chi-square test) p = 0.0003

DFS	SUV max < 9 and/or Size < 30 mm	SUV max > 9 and Size > 30 mm
Disease-free	30	6
Recurrence of disease	3	10

Finally, the estimated probability of disease-free time according to the SUVmax cut-off and the dimensional threshold was calculated using the Kaplan-Meier method.

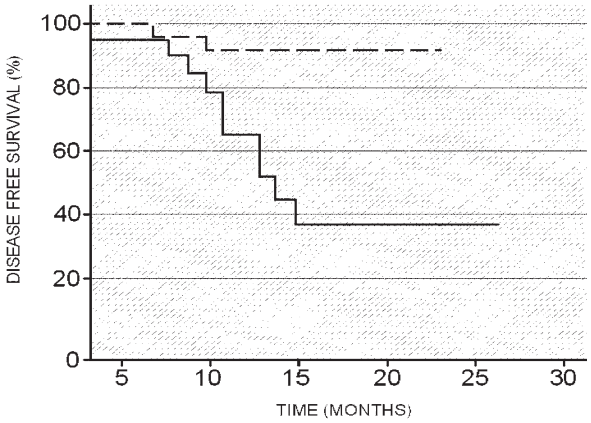

FIGURE 1. Disease-free survival (DFS) curves (Kaplan-Meier) based on a dimensional cut-off of 30 mm. The disease-free survival curves illustrate that patients with a lung cancer with dimension < 30 mm present a better prognosis (significant longer DFS) than patients with lung cancer size > 30 mm.

Dashed line = DFS for patients in stage I-II with lesion diameter < 30 mm.

Continuous line = DFS for patients in stage I-II with lesion diameter > 30 mm.

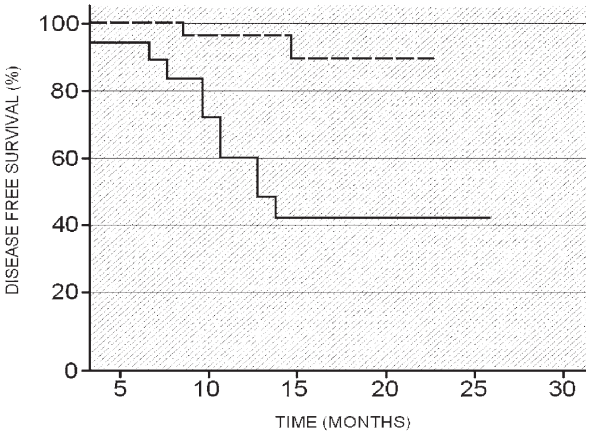

FIGURE 2. Disease-free survival (DFS) curves (Kaplan-Meier) based on a cut-off maximum standardized uptake value (SUVmax) of nine. The disease-free survival curves illustrate that patients with lung cancer SUVmax < 9 present a significant longer DFS than patients with lung cancer SUVmax > 9.

Dashed line = DFS for patients in stage I-II with SUVmax < 9;

Continuous line = DFS for patients in stage I-II with SUVmax > 9.

Results

Twenty-eight out of 49 patients (M = 36, F = 13, M/F Ratio = 2.77: 1; mean age = 67.2 years, range: 44–79) diagnosed with adenocarcinoma (BAC excluded according to exclusion criteria) which was the most frequent tumour histologic subtype (57%). Squamous cell carcinoma was observed in 15 patients (31%), and large cell carcinoma in 2 cases (4%). In 4 patients (8%) no sufficient data about pathological examination were available and they were classified as undetermined (Table 1).

At the time of the pre-surgical PET/CT scan, the patients in stage I-II showed an average SUVmax value of 10 ± 5.5 and an average size of primary lung lesion of 33 mm ± 17.00; at the follow-up period of 24 months, DFS and OS were respectively 73.4% and 83,6 %. 36 patients (average SUVmax value of 8.96 ± 5.26; mean size of primary lung lesions of 31.27 mm ± 18.65) were 2 years disease-free and presented an OS of 100%. 13 patients (average SUVmax = 12.8 ± 5.3; mean size of primary lung lesion = 40.5 ± 9.4 mm) had recurrence of disease (median DFS = 10 months, OS = 39.5%). There was a statistically significant correlation between SUVmax and DFS (p = 0.029, Student-t test). Using

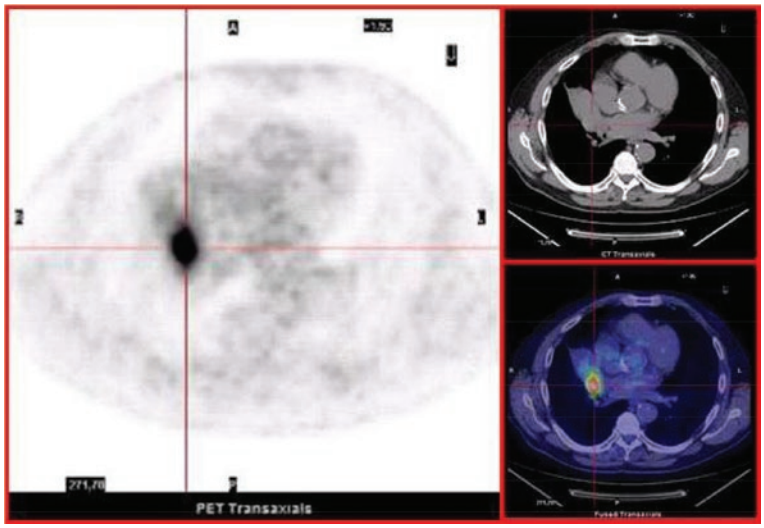

FIGURE 3A. Pre-surgical ^{18}F-FDG PET/CT axial images. Abnormal 18F-FDG uptake (SUVmax < 9) in a cancer lesion located in the perihilar region of the right lung (size < 30 mm).

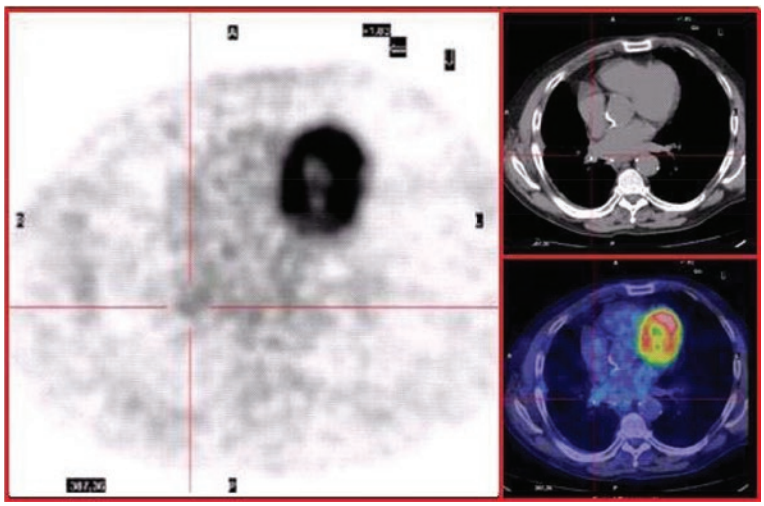

FIGURE 3B. Post-surgical ^{18}F-FDG PET/CT axial images. No pathological ^{18}F-FDG uptake can be detected in the perihilar region of the right lung.

the chi-square test, the SUVmax cut-off and the dimensional cut-off with the best prognostic significance were 9.00 (p = 0.0013) and 30 mm (p = 0.0028) respectively. In the subgroup of 26 patients presenting with a primitive lung lesion larger than 30 mm, there were 12 recurrence of disease events (Table 2A-D), 2 of them with a SUV max <9 and 10 of them with a SUV max > 9.

Combining metabolic and dimensional parameters, patients with SUV > 9 and primary lesion size >30 mm had an expected 2 years-DFS of 37.5%, while the expected 2 years-DFS raised to 90% if the tumour was smaller than 30 mm and/or the SUVmax was below 9.00 (one or both cut-offs) (Table 2A-D).

With cut-off values (SUVmax = 9, size = 30 mm) and using the univariate statistical analysis according to the Kaplan-Meier method, two different disease-free survival curves were generated (Figures 1, 2). The analysis of the disease-free survival curves illustrated that patients with SUVmax < 9 and patients with a primary lung cancer size below 30 mm demonstrated a significant longer DFS (Figure 3A,B) in comparison with patients with SUVmax > 9 or patients with a primitive lesion > 30 mm.

Discussion

Among several prognostic staging systems of NSCLC, the TNM system still remains the most widely used. Despite this, the clinical outcome doesn't always follow the clinical prognostic assessment, so the disease can sometimes result in more unfavorable outcome than expected.[2,16] Even if a complete surgical resection is accomplished, NSCLCs can relapse. These data are extremely dramatic in patients in stage I and II, in whom recurrences of disease will happen and a more aggressive treatment would have been beneficial.[2] In NSCLC, the use of SUV measurements previously reported to be accurate and reproducible in the assessment of the outcome.[17-22]

In our study with patients in stage I-II it has been attempted to focus on the prognostic significance of SUVmax and dimensional parameter of the primitive neoplastic lung lesion in reference with the 2 years disease-free survival. In the present study we accurately selected patients undergoing only the surgical procedure. The cut-off value of a SUVmax in a 2 years follow-up period has not been clearly defined in literature.[23-28] Jeong *et al.* determined a cut-off value of 7 to be indicator of poor disease-free survival (DFS) [24], while Goodgame and colleagues found the threshold value of SUV to be 5.5.[12] Our data showed that in stages I and II, the increased size more than threshold (30 mm) and SUVmax cut-off (9.00) could help to identify a subgroup of patients with a high risk of recurrence within 2 years after curative surgery. The relative estimated risk for patients with SUVmax < 9 and/or tumour size < 30 mm is lower (10%) (p = 0.004) compared to the group above these cut-offs. Similar results had been documented by the Leuven Lung Cancer Group which reported a 2-year survival rate of 86% if the resected tumour was smaller than 3 cm and the SUV was below 7.[27]

Our data showed that, in the early stages of disease, SUVmax and dimension of the primitive lesion were independent prognostic factors and this correlated with 3 previously published papers.[11,25,28] In our series, the additional prognostic information provided by the SUVmax cut-off showed the most powerful impact in case of tumour > 30 mm. In fact the highest rate of recurrence (62.5%) was recorded in case of tumour SUVmax >9 and size >30 mm (10 recurrence of disease and 6 disease-free patients), while patients with SUVmax <9 and tumour dimension >30 mm, presented a lower rate of recurrence (20%; 8 disease –free and 2 recurrence of disease events). However, due to the small number of patients it was not possible to attempt to demonstrate any statistical correlation.

Our study, however, had several limitations including a limited number of patient, lack of SUV quantification in each single histotype, and different cut off value for each subtype of NSCLC. Additional studies are required to further accurately assess the correlation between SUVmax and size of primary lung lesion with DFS and OS in different histotypes in 2 years period.

Conclusions

Our data suggested that in patients with NSCLC stage I-II the combination of a dimensional cut-off (30 mm) and of a SUVmax cut-off (9) could identify a subgroup of patients that would have a high risk of recurrence of disease within 2 years from surgery.

References

1. WHO Department of Gender, Women and Health. *Gender in lung cancer and smoking research.* Geneva: World Health Organization; January 2004. p. 8.
2. Lardinois D, Weder W, Hany TF, Kamel EM, Korom S, Seifert B, et al. Staging of non-small-cell lung cancer with integrated positron-emission tomography and computed tomography. *N Engl J Med* 2003; **348:** 2500-7.
3. Baum RP, Hellwig D, Mezzetti M. Position of nuclear medicine modalities in the diagnostic workup of cancer patients: lung cancer. *Q J Nucl Med Mol Imaging* 2004; **48:** 119-42.
4. Hellwig D, Baum RP, Kirsch C. FDG PET, PET/CT and conventional nuclear medicine procedures in the evaluation of lung cancer: a systematic review. *Nuklearmedizin* 2009; **48:** 59-69.
5. Vansteenkiste J, Fisher BM, Dooms C, Mortensen J. Positron-emission tomography in prognostic and therapeutic assessment of lung cancer: systematic review. *Lancet Oncol* 2004; **5:** 531-40.
6. Chen HH, Chiu NT, Su WC, Guo HR, Lee BF. Prognostic value of whole-body total lesion glycolysis at pretreatment FDG PET/CT in non-small cell lung cancer. *Radiology* 2012; **264:** 559-66.
7. Goodgame B, Pillot GA, Yang Z, Shriki J, Meyers BF, Zoole J, *et al*. Prognostic value of preoperative positron emission tomography in resected stage I non-small cell lung cancer. *J Thorac Oncol* 2008; **3:** 130-4.
8. Huang W, Zhou T, Ma L, Sun H, Gong H, Wang J, et al. Standard uptake value and metabolic tumour volume of ^{18}F-FDG PET/CT predict short-term outcome early in the course of chemoradiotherapy in advanced non-small cell lung cancer. *Eur J Nucl Med Mol Imaging* 2011; **38:** 1628-35.
9. Benz MR, Herrmann K, Walter F, Garon EB, Reckamp KL, Figlin R, et al. (18) F-FDG PET/CT for monitoring treatment responses to the epidermal growth factor receptor inhibitor erlotinib. *J Nucl Med* 2011; **52:** 1684-9.
10. Nesbitt JC, Putnam JB Jr, Walsh GL, Roth JA, Mountain CF. Survival in early-stage non-small cell lung cancer. *Ann Thorac Surg* 1995; **60:** 466-72.
11. Gümüştaş S, Inan N, Akansel G, Ciftçi E, Demirci A, Ozkara SK. Differentiation of malignant and benign lung lesions with diffusion-weighted MR imaging. *Radiol Oncol* 2012; **46:** 106-13.
12. Collins LG, Haines C, Perkel R, Enck RE. Lung cancer: diagnosis and management. *Am Fam Physician* 2007; **75:** 56-63.
13. Andrade RS, Odell DD, D'Cunha J, Maddaus MA. Endobronchial ultrasonography (EBUS)-Its role in staging of non-small cell lung cancer and who should do it? *J Thorac Cardiovasc Surg* 2012; **144:** S9-S13.
14. American Joint Committee on Cancer. *AJCC Cancer Staging Manual*. 7th edition. New York: Springer; 2010. p. 299-324.
15. Eisenhauera EA, Therasse P, Bogaerts J, Schwartz LH, Sargent D, Ford R, et al. New response evaluation criteria in solid tumours: Revised RECIST guideline (version 1.1). *Eur J Cancer* 2009; **45:** 228-47.
16. Beadsmoore CJ, Screton NJ. Classification, staging and prognosis of lung cancer. *Eur J Radiol* 2003; **45:** 8-17.
17. Weber WA, Ziegler SI, Thodtmann R, Hanauske AR, Schwaiger M. Reproducibility of metabolic measurements in malignant tumors using FDG PET. *J Nucl Med* 1999; **40:** 1771-7.
18. Huang SC. Anatomy of SUV. Standardized uptake value. *Nucl Med Biol* 2000; **27:** 643-6.
19. Adams MC, Turkington TG, Wilson JM, Wong TZ. A systematic review of the factors affecting accuracy of SUV Measurements. *AJR Am J Roentgenol* 2010; **195:** 1043.
20. Boellaard R, O'Doherty MJ, Weber WA, Mottaghy FM, Lonsdale MN, Stroobants SG, et al. FDG PET and PET/CT: EANM procedure guidelines for tumour PET imaging: version 1.0. *Eur J Nucl Med Mol Imaging* 2010; **37:** 181-200.
21. Cerfolio RJ, Bryant AS, Ohja B, Bartolucci AA. The maximum standardized uptake values on positron emission tomography of a non-small cell lung cancer predict stage, recurrence, and survival. *J Thorac Cardiovasc Surg* 2005; **130:** 151-9.
22. Van Baardwijk A, Dooms C, Van Suylen RJ, Verbeken E, Hochstenbag M, Dehing-Oberije C, et al. The maximum uptake of (18)F-deoxyglucose on positron emission tomography scan correlates with survival, hypoxia inducible factor-1alpha and GLUT-1 in non-small cell lung cancer. *Eur J Cancer* 2007; **43:** 1392-8.
23. Sasaki R, Komaki R, Macapinlac H. [18F]fluorodeoxyglucose uptake by positron emission tomography predicts outcome of non-small-cell lung cancer. *J Clin Oncol* 2005; **23:** 1136-43.
24. Jeong HJ, Min JJ, Park JM, Kim BT, Jeong JM, Lee DS, et al. Determination of the prognostic value of [(18)F] fluorodeoxyglucose uptake by using positron emission tomography in patients with non-small cell lung cancer. *Nucl Med Commun* 2002; **23:** 865-70.
25. Downey RJ, Akhurst T, Gonen M, Vincent A, Bains MS, Larson S, et al. Preoperative F-18 fluorodeoxyglucose-positron emission tomography maximal standardized uptake value predicts survival after lung cancer resection. *J Clin Oncol* 2004; **22:** 3255-60.
26. Vesselle H, Freeman JD, Wiens L, Stern J, Nguyen HQ, Hawes SE, et al. Fluorodeoxyglucose uptake of primary non-small cell lung cancer at positron emission tomography: New contrary data on prognostic role. *Clin Cancer Res* 2007; **13:** 3255-63.
27. Vansteenkiste JF, Stroobants SG, Dupont PJ, De Leyn PR, Verbeken EK, Deneffe GJ, et al. Prognostic importance of the standardized uptake value on (18)F-fluoro-2-deoxy-glucose-positron emission tomography scan in non-small-cell lung cancer: an analysis of 125 cases. Leuven Lung Cancer Group. *J Clin Oncol* 1999; **17:** 3201-6.
28. Hanin FX, Lonneux M, Cornet J, Noirhomme P, Coulon C, Distexhe J, et al. Prognostic value of FDG uptake in early stage non-small cell lung cancer. *Eur J Cardiothorac Surg* 2008; **33:** 819-23.

research article

Advanced ultrasonography technologies to assess the effects of radiofrequency ablation on hepatocellular carcinoma

Nobuyuki Toshikuni, Hisakazu Shiroeda, Kazuaki Ozaki, Yasuhiro Matsue, Takahiro Minato, Tomoe Nomura, Nobuhiko Hayashi, Tomiyasu Arisawa, Mikihiro Tsutsumi

Department of Gastroenterology, Kanazawa Medical University, Ishikawa, Japan

Radiol Oncol 2013; 47(3): 224-229.

Received 21 November 2012
Accepted 24 March 2013

Correspondence to: Nobuyuki Toshikuni, MD, Department of Gastroenterology, Kanazawa Medical University, 1-1 Daigaku, Uchinada-machi, Kahoku, Ishikawa 920-0293, Japan. Phone: +81 76 286 2211; Fax: +81 76 286 0892; E-mail: n.toshikuni@gmail.com

Disclosure: No potential conflicts of interest were disclosed.

Background. Radiofrequency ablation (RFA) is a curative therapy for hepatocellular carcinoma (HCC). In RFA, ultrasonography (US) is most commonly used to guide tumor puncture, while its effects are assessed using dynamic computed tomography or magnetic resonance. The differences in modalities used for RFA and assessment of its effects complicate RFA. We developed a method for assessing the effects of RFA on HCC by combining contrast-enhanced (CE) US and real-time virtual sonography with three-dimensional US data.

Patients and methods. Before RFA, we performed a sweep scan of the target HCC nodule and the surrounding hepatic parenchyma to generate three-dimensional US data. After RFA, we synchronized multi-planar reconstruction images derived from stored three-dimensional US data with real-time US images on the same US monitor and performed CEUS and real-time virtual sonography. Using a marking function, we drew a sphere marker along the target HCC nodule contour on pre-treatment US- multi-planar reconstruction images so that the automatically synchronized sphere marker represented the original HCC nodule contour on post-treatment real-time CEUS images. Ablation was considered sufficient when an avascular area with a margin of several millimeters in all directions surrounded the sphere marker on CEUS.

Results. This method was feasible and useful for assessing therapeutic effects in 13 consecutive patients with HCC who underwent RFA. In 2 patients who underwent multiple sessions of RFA, HCC-nodule portions requiring additional RFA were easily identified on US images.

Conclusions. This method using advanced US technologies will facilitate assessment of the effects of RFA on HCC.

Key words: hepatocellular carcinoma; radiofrequency ablation; contrast-enhanced ultrasonography; real-time virtual sonography; three-dimensional ultrasonography

Introduction

Percutaneous radiofrequency ablation (RFA) is a minimally invasive curative therapy for unresectable hepatocellular carcinoma (HCC).[1] During RFA, ultrasonography (US) is most commonly used to guide tumor puncture, while side-by-side comparisons of pre- and post-treatment contrast-enhanced computed tomography (CT) or magnetic resonance (MR) images are typically used to assess the therapeutic effects of RFA. Differences in the modalities for RFA and the techniques for assessing its effects complicate RFA. Furthermore, side-by-side comparisons of images can often make assessment of ablated margins difficult.

Recent advances in imaging modalities have enabled the synthesis of high-resolution multiplanar reconstruction (MPR) images from three-dimensional (3D) data.[2] This technology and position-tracking systems with magnetic navigation allow the synchronization of CT- or MR-MPR images with real-time US images or real-time virtual sonography

(RVS) images.[3] With this method, one can utilize MPR images during US examinations. RVS has been shown to be useful for detecting small hepatic nodules [4] and guiding the puncture of HCC nodules that are difficult to detect with conventional US but detectable with CT and/or MR imaging.[5-8]

Contrast-enhanced US (CEUS) with perflubutane (Sonazoid; GE Healthcare, Oslo, Norway), a microbubble contrast agent, has been routinely used in Japan to scrutinize hepatic tumors.[9] Recent studies have demonstrated that the use of this contrast agent during CEUS improved HCC detection by conventional US, thereby facilitating accurate nodule puncture.[10-12]

The combination of CEUS and RVS provides information on the accurate position and vascular flow of the target lesion. We hypothesized that CEUS and RVS using 3DUS data may be useful for assessing the effects of RFA and reducing its complexity. Here we describe our preliminary results of this promising method.

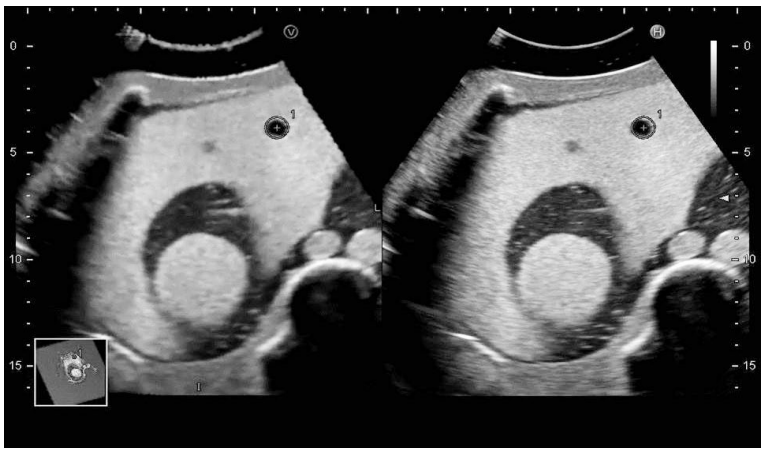

FIGURE 1. RVS synchronization using 3DUS data from a phantom model. US-MPR images from the 3D data (left) and real-time US images (right) are synchronized on the same US monitor. Furthermore, synchronized spherical markers (+, the center of the spherical marker) are displayed along the contour of a spherical structure of the phantom model on synchronized US-MPR and real-time US images.

RVS = real-time virtual sonography; 3DUS = three-dimensional ultrasonography; MPR = multiplanar reconstruction

Patients and methods

In vitro experiments using a phantom model

To verify whether CEUS and RVS using 3DUS data could be applied to assess the effects of RFA on HCC, an operator (N.T.) with 20 years of experience in performing US examinations used 3DUS data from a phantom model (Model 057 Triple Modality 3D Abdominal Phantom; CIRS, Norfolk, USA) that contained structures representing abdominal organs to conduct an RVS synchronization experiment. The operator performed a manual sweep scan with a US machine (HI VISION Preirus; Hitachi Medical Corporation, Tokyo, Japan) and a convex probe (EUP-C715; Hitachi Medical Corporation) at an arbitrary site on the surface of the phantom model. The scan time was set for 15 s. The 3DUS data sets were automatically generated and manually stored on the hard disk of the US machine. Immediately after storage of the 3D data, the same site was scanned and examined to determine whether US-MPR images from the 3D data were synchronized with real-time US images on the same US monitor. The US machine had a marking function that automatically displayed synchronized straight and spherical markers on US-MPR and real-time US images, respectively. The size of a spherical marker was designed to change inversely with the distance between the center of the marker and scanning section. Then, the operator drew a spherical marker along the contour of a spherical structure to show its maximum diameter on the US-MPR image and determined that the synchronized spherical markers were displayed along the contour of the spherical structure in all directions on the synchronized US-MPR and real-time US images. The operator repeated the same procedures five times.

Patients

This study was conducted in accordance with the guidelines of the Declaration of Helsinki and the standards of the institutional ethics committee. Informed consent was obtained from all patients. The study included 13 consecutive patients with 14 HCC nodules who underwent RFA between December 2011 and April 2012. HCC diagnoses were based on the results of CEUS, dynamic CT, and dynamic MR imaging.[13] RFA was indicated according to the Clinical Practice Guidelines for Hepatocellular Carcinoma (the J-HCC guidelines), the first evidence-based clinical practice guidelines for the treatment of HCC in Japan, which were compiled by an expert panel supported by the Japanese Ministry of Health, Labour and Welfare.[14]

RFA

Two operators (N.T. and H.S.) with 7 years and 3 years of experience with the technique performed RFA using a cooled-tip RFA system (Covidien, Mansfield, MA, USA) on the enrolled patients. A

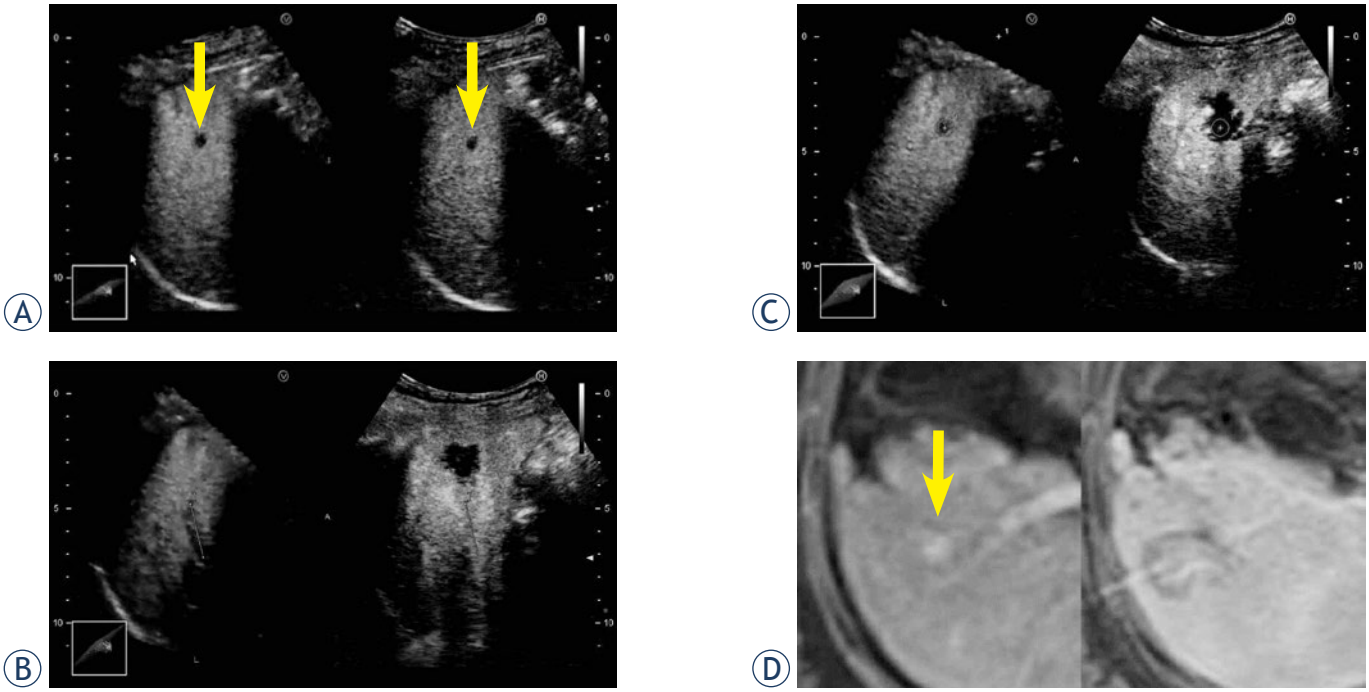

FIGURE 2. Assessment of the effects of RFA on HCC by combination of CEUS and RVS using 3DUS data. A 57-year-old female patient had a 7-mm HCC in segment 5. Sufficient ablation was achieved in a single session of RFA. **A.** CEUS and RVS using 3DUS data before RFA. The Kupffer phase data set was selected for RVS. The HCC nodule is shown as a perfusion defect (arrow). The US-MPR and real-time CEUS images are synchronized. **B.** CEUS and RVS using 3DUS data after RFA. The US-MPR (left) and real-time CEUS (right) images are adjusted with synchronized straight markers. Each marker is drawn on the same anterior branch of the right branch of the portal vein. **C.** CEUS and RVS using 3DUS data after RFA. Automatically synchronized spherical markers represent the HCC contour. An avascular area surrounds the sphere marker (+, the center of the spherical marker) with a margin of several millimeters on CEUS images, suggesting sufficient ablation. **D.** Dynamic MR imaging. Before RFA (left), the HCC nodule is shown as a hypervascular lesion (arrow). MR image obtained after RFA (right) shows a sufficient ablation zone.

CEUS = contrast-enhanced ultrasonography; HCC = hepatocellular carcinoma; MR = magnetic resonance MPR = multiplanar reconstruction; RFA = radiofrequency ablation; RVS = real-time virtual sonography; 3DUS = three-dimensional ultrasonography

17-gauge, internally cooled-tip electrode with a 2- or 3-cm tip that was attached to a 480-kHz monopolar RF generator was percutaneously inserted into the target HCC under real-time US guidance using an US machine (HI VISION Preirus; Hitachi Medical Corporation) and a 3.5-MHz microconvex probe (EUP-B512; Hitachi Medical Corporation). The generator output was slowly increased to 80–120 watts and maintained for up to 12 min. In some cases, multiple RF electrode insertions were required to obtain sufficient ablation.

CEUS and RVS using 3DUS data

Before RFA, the operators (N.T. and H.S.) and their assistants (K.O. and N.H.) used a US machine (HI VISION Preirus) to perform planning B-mode US and CEUS with perflubutane (Sonazoid). A manual sweep scan with a convex probe (EUP-C715; Hitachi Medical Corporation) was performed at the planned puncture site in B-mode US and during the vascular and Kupffer phases of CEUS. The sweep scan covered the target HCC nodule and surrounding hepatic parenchyma. The scan time was set for 15 s. CEUS, RVS, and the stored 3DUS data were used by the operators (N.T. and H.S.) to assess by consensus the therapeutic effects of a single RFA session 1 to 2 days after the session. A scan with a US machine (HI VISION Preirus) and a convex probe (EUP-C715) was performed at the puncture site. We selected the data set with the clearest images of the target HCC nodule. While a patient held his/her breath, the operators manually moved and rotated the 3DUS data to synchronize the US-MPR images with real-time US images on the same US monitor. Straight markers were used to adjust both-side images; the markers were drawn on linear structures such as intrahepatic vessels. Then the operators drew a spherical marker along the target HCC nodule contour on the pretreatment US-MPR images so that the automatically synchronized spherical marker represented the original HCC contour on the post-treatment real-time US images. After completion of image synchronization, CEUS with perflubutane (Sonazoid)

TABLE 1. Patient profiles

Parameter	
Age (years)	70 ± 11[a]
Sex, Male/Female	5/8
Etiology of liver disease, HBV/HCV/Others	2/10/1
Child–Pugh grade, A/B	6/7
Location of HCC, Segment 3/4/5/6/7/8	1/2/2/3/2/4
Naive HCC nodule/Local recurrence nodule/Distant recurrence nodule	5/4/5
Maximum diameter (mm)	17 ± 6[a]
Electrode-tip exposure, 2 cm/3 cm	5/9
Number of electrode insertions, 1/2/3	8/4/2
Number of RFA sessions, 1/2/3	12/1/1

[a] Data are expressed as mean ± standard deviation

HBV = hepatitis B virus; HCC = hepatocellular carcinoma; HCV = hepatitis C virus; RFA = radiofrequency ablation

and RVS was performed. The acoustic power of the US machine was set at a mechanical index of 0.2. After bolus injection of perflubutane (Sonazoid) into an antecubital vein at a dose of 0.7 ml, the operators scanned regions covering the original target HCC nodules and surrounding hepatic parenchyma for up to 30 s, during which the patient kept holding his/her breath. Simultaneously, motion images were recorded. Injection of the contrast agent and scans were repeated as necessary.

Assessments of RFA effects

Assessment of RFA effects was performed in real time and during frame-by-frame playbacks of the recorded motion images. Ablation was considered sufficient when an avascular area with a margin of several millimeters surrounded the spherical marker in all directions on the CEUS images.[15] When HCC nodules were adjacent to vessels or near the liver surface, treatment was considered complete even if a margin was not obtained. When the US findings did not meet these criteria, additional RFAs were performed and CEUS and RVS with 3DUS data were used to assess the therapeutic effects again. Around the time that the CEUS and RVS using 3DUS data were performed, contrast-enhanced CT (CECT) or contrast-enhanced MR (CEMR) imaging was also performed, and their therapeutic effects were assessed by experienced radiologists in a blinded manner. The agreement rate for the therapeutic assessments between CEUS and RVS using 3DUS data and CECT or CEMR was calculated.

Results

In every *in vitro* experiment, the US-MPR images from the 3D data and real-time US images were synchronized on the same US monitor (Figure 1). Furthermore, synchronized spherical markers were displayed along the contour of a spherical structure of the phantom model on the synchronized US-MPR and real-time US images.

Patient profiles are shown in Table 1. All patients were safely treated with RFA. The time required for RVS synchronization using stored 3D data ranged approximately from 10 to 15 min. The time tended to be prolonged in patients who could not continuously holding their breath. During CEUS and RVS, it was possible to assess whether an avascular area surrounded a spherical marker representing an original HCC contour. Furthermore, frame-by-frame playbacks of the recorded motion images permitted detailed reviews of the images, including measurement of ablated margins (Figure 2). Of the 13 patients, 2 underwent multiple sessions of RFA. In those patients, HCC-nodule portions requiring additional RFA were easily identified on US images (Figure 3). Additional sessions of RFA resulted in sufficient ablation for the patients. The total time required for RVS synchronization, CEUS, and RVS, including review of the recorded motion images, ranged approximately from 20 to 30 min. The agreement rate for the therapeutic assessments between CEUS and RVS using 3DUS data and CECT or CEMR was 100% in our series.

Discussion

CECT and CEMR are standard methods for assessing the effects of RFA on HCC. By contrast, CEUS is currently employed as an adjunct method, although several studies have suggested that the usefulness of CEUS is comparable to that of the standard methods.[16, 17] In the present study, we intended to actively use CEUS by combining RVS in the therapeutic assessment. On the basis of the feasibility, accuracy, and reproducibility of RVS synchronization using 3DUS data in *in vitro* experiments, we confirmed the applicability of CEUS and RVS using 3DUS data to the assessment of the effects of RFA on HCC. Our results showed that this method was feasible and its usefulness was comparable to that of CECT or CEMR. Furthermore, we noted that the present method has advantages over the standard methods. First, if post-treatment CECT or CEMR images suggest insufficient ablation, HCC-nodule portions re-

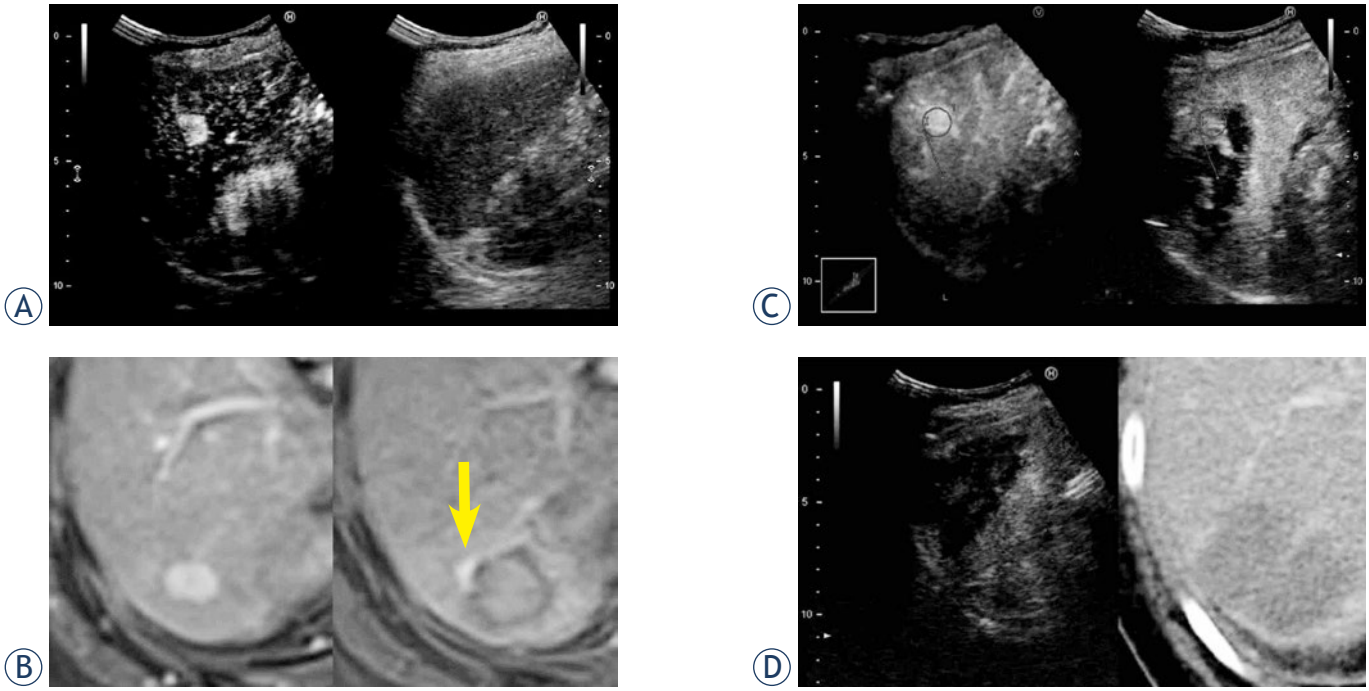

FIGURE 3. Usefulness of CEUS and RVS using 3DUS data in identifying HCC nodules requiring additional RFA. A 66-year-old female patient had a 13-mm HCC in segment 6. Because HCC was poorly visualized with conventional US, RFA was performed under CEUS guidance. After the first RFA session, dynamic MR showed a residual viable portion, but the second RFA session failed to ablate that portion. CEUS and RVS using 3DUS data clearly showed the portion requiring additional RFA. Therefore, a third RFA session was performed, which ablated the portion. **A.** CEUS before RFA. **B.** Dynamic MR imaging before RFA (left) and after the first RFA session (right). A residual viable portion is shown (arrow). **C.** CEUS and RVS using 3DUS data displays the portion requiring additional RFA (spherical marker). Each synchronized straight marker is drawn on the same posterior branch of the right branch of the portal vein. **D.** CEUS (left) and dynamic CT (right) suggest sufficient ablation.

CEUS = contrast-enhanced ultrasonography; CT = computed tomography; HCC = hepatocellular carcinoma; MR = magnetic resonance; RFA = radiofrequency ablation; RVS = real-time virtual sonography; 3DUS, three-dimensional ultrasonography

quiring additional RFA need to be identified by US. Our method uses a single modality to enable both RFA and assessment of its effects. Furthermore, conventional side-by-side comparisons between pre- and post-treatment CECT or CEMR images often make accurate assessment of ablated margins difficult, especially when an ablated area is slightly larger than the original target HCC nodule. Our method uses a marking function that allows direct comparison of an avascular area formed by RFA with a spherical marker representing the original target nodule contour on real-time CEUS images.

The present method is unique in that it provides positional information about original HCC nodules on post-treatment real-time US images. Some earlier studies have shown the usefulness of synchronized MPR images in CEUS-based assessment of the effects of RFA on HCC.[18,19] In those studies, CT-MPR images were used as reference images that were synchronized with CEUS images. The positions of target HCC nodules were identified by measuring the distance from the edge of the nodules to the architecture such as the surrounding organs. The researchers highlighted the usefulness of their method in decreasing the number of CECT images required for the therapeutic assessment. Our method is more advanced and convenient; therefore, it can be incorporated into the routine assessment of RFA effects, even though CECT and CEMR are currently the main assessment methods.

Patients who are allergic to contrast agents used during CT and MR imaging or those suffering from renal insufficiency are unsuitable for therapeutic assessments using CECT or CEMR. For these patients, other CE imaging methods are required. Perflubutane (Sonazoid) is less allergenic, and it can be used regardless of the patient's renal function because it is excreted during exhalation.[20] Therefore, our CEUS-based method is particularly useful for such patients.

Hiraoka *et al*. described the usefulness of RVS using 3DUS data in predicting the effects of RFA on HCC.[21] The RVS system runs on a workstation connected to a US machine (EUB7500; Hitachi Medical Corporation). In their study, they used the system's marking function to compare pretreatment

US-MPR images with real-time US images 5 min after RFA. Because the extent of hyperechoic microbubbles induced by RFA is mostly proportional to the degree of ablation, they predicted that a sufficient margin was obtained when the microbubbles completely surrounded the spherical marker representing the original HCC nodule contour. The RVS system resulted in sufficient ablation and decreased the number of RFA sessions. The therapeutic effects were assessed by conventional CECT in the study conducted by Hiraoka *et al*. In contrast, we aimed to establish a US-based method to assess the effects of RFA. However, it is worth testing to see whether assessment of the extent of microbubbles immediately after RFA by our method is useful in predicting therapeutic effects.

The present method had some limitations. First, US image synchronization required the patients to hold their breath continuously, which was a difficult task for some patients. Second, our method may not be applied to HCC nodules located near US beam obstacles such as pulmonary air and calcium deposits. Third, the spherical marker contour did not completely overlap HCC nodules because their shapes were not perfect spheres. In cases with irregularly shaped HCC nodules, spherical marker contours should overlap HCC nodule portions that possibly have insufficient ablation margins.

This study suggested that the combination of CEUS and RVS using 3DUS data is feasible and useful for assessing the effects of RFA on HCC. The method uses advanced US technologies, and although its accuracy and reproducibility should be verified in a blinded study with a larger number of patients, we believe that the method will become an important modality and provide even greater benefits of US than those demonstrated previously for assessing the effects of RFA on HCC.

Acknowledgements

We are grateful to Mr. Makoto Mishita, Hitachi Medical Corporation, for his excellent technical support.

References

1. Tiong LMaddern GJ. Systematic review and meta-analysis of survival and disease recurrence after radiofrequency ablation for hepatocellular carcinoma. *Br J Surg* 2011; **98:** 1210-24.
2. Fuchs T, Kachelriess MKalender WA. Technical advances in multi-slice spiral CT. *Eur J Radiol* 2000; **36:** 69-73.
3. Kudo M. New sonographic techniques for the diagnosis and treatment of hepatocellular carcinoma. *Hepatol Res* 2007; **37(Suppl 2):** S193-9.
4. Okamoto E, Sato S, Sanchez-Siles AA, Ishine J, Miyake T, Amano Y, et al. Evaluation of virtual CT sonography for enhanced detection of small hepatic nodules: a prospective pilot study. *AJR Am J Roentgenol* 2010; **194:** 1272-8.
5. Minami Y, Kudo M, Chung H, Inoue T, Takahashi S, Hatanaka K, et al. Percutaneous radiofrequency ablation of sonographically unidentifiable liver tumors. Feasibility and usefulness of a novel guiding technique with an integrated system of computed tomography and sonographic images. *Oncology* 2007; **72(Suppl 1):** 111-6.
6. Kitada T, Murakami T, Kuzushita N, Minamitani K, Nakajo K, Osuga K, et al. Effectiveness of real-time virtual sonography-guided radiofrequency ablation treatment for patients with hepatocellular carcinomas. *Hepatol Res* 2008; **38:** 565-71.
7. Kawasoe H, Eguchi Y, Mizuta T, Yasutake T, Ozaki I, Shimonishi T, et al. Radiofrequency ablation with the real-time virtual sonography system for treating hepatocellular carcinoma difficult to detect by ultrasonography. *J Clin Biochem Nutr* 2007; **40:** 66-72.
8. Nakai M, Sato M, Sahara S, Takasaka I, Kawai N, Minamiguchi H, et al. Radiofrequency ablation assisted by real-time virtual sonography and CT for hepatocellular carcinoma undetectable by conventional sonography. *Cardiovasc Intervent Radiol* 2009; **32:** 62-9.
9. Numata K, Luo W, Morimoto M, Kondo M, Kunishi Y, Sasaki T, et al. Contrast enhanced ultrasound of hepatocellular carcinoma. *World J Radiol* 2010; **2:** 68-82.
10. Minami Y, Kudo M, Hatanaka K, Kitai S, Inoue T, Hagiwara S, et al. Radiofrequency ablation guided by contrast harmonic sonography using perfluorocarbon microbubbles (Sonazoid) for hepatic malignancies: an initial experience. *Liver Int* 2010; **30:** 759-64.
11. Masuzaki R, Shiina S, Tateishi R, Yoshida H, Goto E, Sugioka Y, et al. Utility of contrast-enhanced ultrasonography with Sonazoid in radiofrequency ablation for hepatocellular carcinoma. *J Gastroenterol Hepatol* 2011; **26:** 759-64.
12. Numata K, Morimoto M, Ogura T, Sugimori K, Takebayashi S, Okada M, et al. Ablation therapy guided by contrast-enhanced sonography with Sonazoid for hepatocellular carcinoma lesions not detected by conventional sonography. *J Ultrasound Med* 2008; **27:** 395-406.
13. Bruix JSherman M. Management of hepatocellular carcinoma. *Hepatology* 2005; **42:** 1208-36.
14. Kokudo NMakuuchi M. Evidence-based clinical practice guidelines for hepatocellular carcinoma in Japan: the J-HCC guidelines. *J Gastroenterol* 2009; **44(Suppl 19):** 119-21.
15. Kim YS, Lee WJ, Rhim H, Lim HK, Choi DLee JY. The minimal ablative margin of radiofrequency ablation of hepatocellular carcinoma (> 2 and < 5 cm) needed to prevent local tumor progression: 3D quantitative assessment using CT image fusion. *AJR Am J Roentgenol* 2010; **195:** 758-65.
16. Kim CK, Choi D, Lim HK, Kim SH, Lee WJ, Kim MJ, et al. Therapeutic response assessment of percutaneous radiofrequency ablation for hepatocellular carcinoma: utility of contrast-enhanced agent detection imaging. *Eur J Radiol* 2005; **56:** 66-73.
17. Lu MD, Yu XL, Li AH, Jiang TA, Chen MH, Zhao BZ, et al. Comparison of contrast enhanced ultrasound and contrast enhanced CT or MRI in monitoring percutaneous thermal ablation procedure in patients with hepatocellular carcinoma: a multi-center study in China. *Ultrasound Med Biol* 2007; **33:** 1736-49.
18. Kisaka Y, Hirooka M, Kumagi T, Uehara T, Hiasa Y, Kumano S, et al. Usefulness of contrast-enhanced ultrasonography with abdominal virtual ultrasonography in assessing therapeutic response in hepatocellular carcinoma treated with radiofrequency ablation. *Liver Int* 2006; **26:** 1241-7.
19. Kisaka Y, Hirooka M, Koizumi Y, Abe M, Matsuura B, Hiasa Y, et al. Contrast-enhanced sonography with abdominal virtual sonography in monitoring radiofrequency ablation of hepatocellular carcinoma. *J Clin Ultrasound* 2010; **38:** 138-44.
20. Landmark KE, Johansen PW, Johnson JA, Johansen B, Uran SSkotland T. Pharmacokinetics of perfluorobutane following intravenous bolus injection and continuous infusion of sonazoid in healthy volunteers and in patients with reduced pulmonary diffusing capacity. *Ultrasound Med Biol* 2008; **34:** 494-501.
21. Hiraoka A, Hirooka M, Koizumi Y, Hidaka S, Uehara T, Ichikawa S, et al. Modified technique for determining therapeutic response to radiofrequency ablation therapy for hepatocellular carcinoma using US-volume system. *Oncol Rep* 2010; **23:** 493-7.

research article

Intrathoracic malignant peripheral nerve sheath tumors: imaging features and implications for management

Sophia Constance Kamran[1,2,4], Atul Bhanudas Shinagare[1,2,4], Stephanie Anne Holler Howard[1,2,4], Mizuki Nishino[1,2,4], Jason Laurence Hornick[3,4], Katherine Margaret Krajewski[1,2,4], Nikhil Himmatsinh Ramaiya[1,2,4]

[1] Department of Imaging, Dana-Farber Cancer Institute, 450 Brookline Ave, Boston, MA 02115, USA
[2] Department of Radiology, Brigham and Women's Hospital, 75 Francis Street, Boston, MA 02115, USA
[3] Department of Pathology, Brigham and Women's Hospital, 75 Francis Street, Boston, MA 02115, USA
[4] Harvard Medical School, Boston MA 02115, USA

Radiol Oncol 2013; 47(3): 230-238.

Received 11 January 2013
Accepted 5 April 2013

Correspondence to: Atul B. Shinagare, MD, Department of Imaging, Dana-Farber Cancer Institute, 450 Brookline Ave, Boston, MA 02115, USA. Phone: +1 617 650 7465; Fax: + 617 582 8574; E-mail: ashinagare@partners.org

Disclosure: No potential conflicts of interest were disclosed. In financial disclosures the authors stated that the investigator Mizuki Nishino (MN) had been supported by 1K23CA157631 (NCI) from the National Institutes of Health.

Background. The aim of the study was to analyze the clinical and imaging characteristics of primary intrathoracic malignant peripheral nerve sheath tumors (MPNSTs).

Patients and methods. In this institutional review board (IRB)-approved retrospective study, clinical and imaging features of 15 patients (eight men; mean age 50 years [range 18–83)] with pathologically proven malignant peripheral nerve sheath tumors seen from January 1999 to December 2011 were analyzed. Imaging features (CT in 15, MRI in 5 and PET/CT in 4) of primary tumors were evaluated by three radiologists and correlated with clinical management.

Results. Of the 15 tumors, six were located in the mediastinum (two each in anterior, middle and posterior mediastinum), four in chest wall, two were paraspinal, and three in the lung. Four patients had neurofibromatosis-1 (NF1); four tumors had heterologous rhabdomyoblastic differentiation (malignant triton tumor). Masses typically were elongated along the direction of nerves, with mean size of 11 cm. The masses were hypo- or isodense to muscles on CT, isointense on T1-weighted images, hyperintense on T2-weighted images and intensely fluorodeoxyglucose (FDG) avid (mean standardized uptake value $[SUV]_{max}$ of 10.5 [range 4.4–23.6]). Necrosis and calcification was seen in four tumors each. Finding of invasion of adjacent structures on imaging led to change in management in seven patients; patients with invasion received chemoradiation.

Conclusions. Intrathoracic MPNSTs appear as large elongated masses involving mediastinum, lung or chest wall. Radiological identification of invasion of adjacent structures is crucial and alters therapy, with patients with invasion receiving neoadjuvant or adjuvant chemoradiation.

Key words: malignant peripheral nerve sheath tumors; chest; neurofibromatosis; imaging; malignant triton tumor

Introduction

Malignant peripheral nerve sheath tumors (MPNSTs) are rare, accounting for 5-10% of all soft tissue sarcomas.[1] MPNSTs usually demonstrate nerve sheath differentiation, and although they grossly appear similar to benign peripheral nerve sheath tumors such as schwannomas and neurofibromas, MPNSTs commonly contain hyperchromatic spindle cells with nuclear atypia, mitotic activity, and areas of tumor necrosis on histology.[1,2] Rapid enlargement, pain, or associated neurological symptoms favor MPNST over a benign nerve sheath tumor.[1] MPNSTs are most often sporadic,

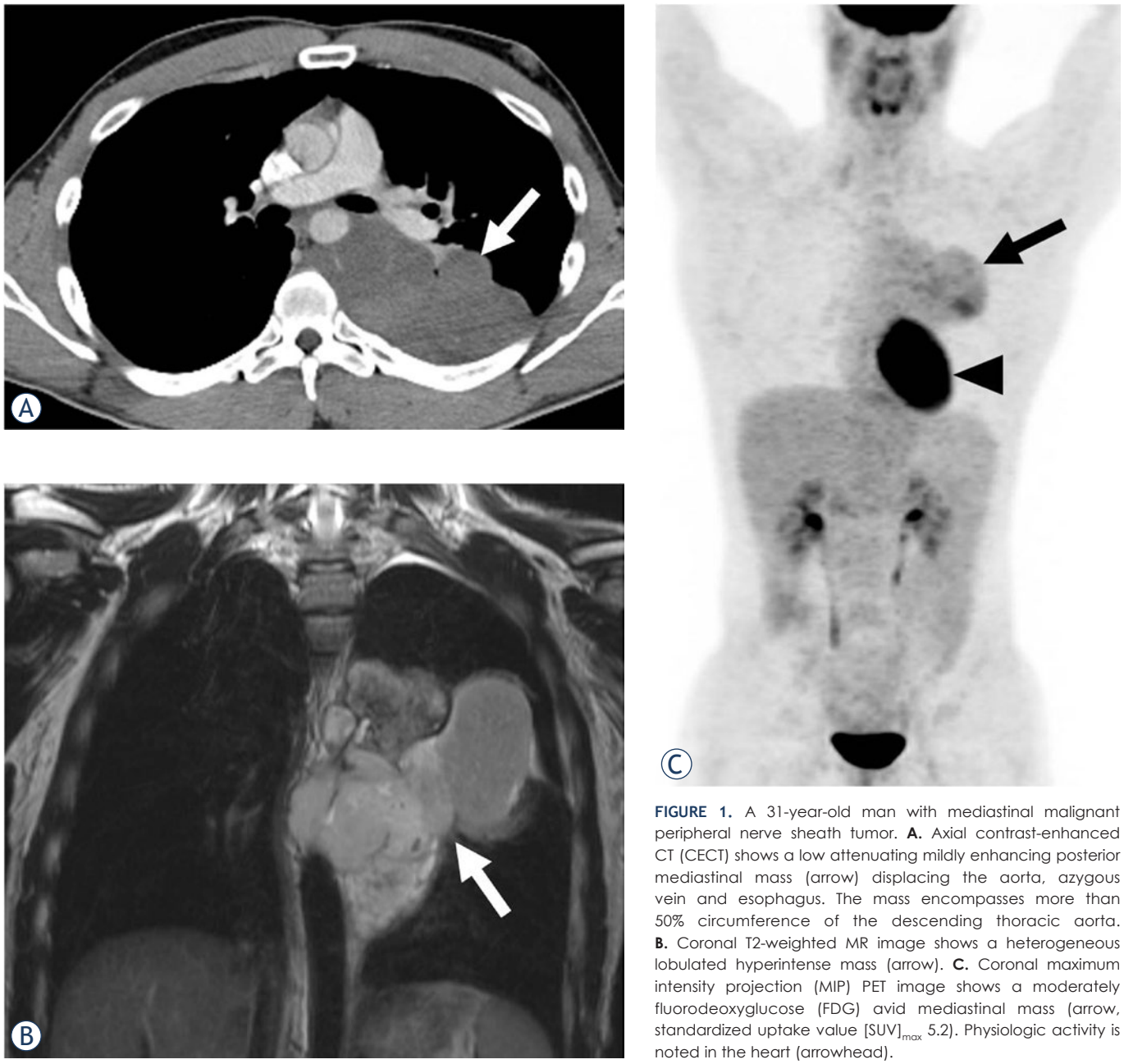

FIGURE 1. A 31-year-old man with mediastinal malignant peripheral nerve sheath tumor. **A.** Axial contrast-enhanced CT (CECT) shows a low attenuating mildly enhancing posterior mediastinal mass (arrow) displacing the aorta, azygous vein and esophagus. The mass encompasses more than 50% circumference of the descending thoracic aorta. **B.** Coronal T2-weighted MR image shows a heterogeneous lobulated hyperintense mass (arrow). **C.** Coronal maximum intensity projection (MIP) PET image shows a moderately fluorodeoxyglucose (FDG) avid mediastinal mass (arrow, standardized uptake value $[SUV]_{max}$ 5.2). Physiologic activity is noted in the heart (arrowhead).

although 20–30% occur in association with neurofibromatosis-1 (NF1).[1] Patients typically present around age 40–50[1], although patients with NF1 often present earlier (mean age 30 years).[3] MPNSTs most often occur in the extremities[1], followed by trunk and head and neck, however MPNSTs can arise anywhere in the body. Intrathoracic MPNST are particularly rare.[4] Pathologically, MPNSTs typically have a fascicular growth pattern and are composed of spindle cells with variable nuclear atypia and mitotic activity. MPNSTs with heterologous rhabdomyoblastic (*i.e.* skeletal muscle) differentiation are called malignant triton tumors (MTTs). MPNSTs have an aggressive clinical course with 5- and 10-year survival rates of 34–60% and 22–45% respectively.[1,5] MTT is associated with an even worse clinical outcome, with a 5-year survival rate of 11–15%.[6] Location also plays a role in outcome, with tumors in the trunk associated with poorer prognosis, likely attributable to difficulty in achieving negative surgical margins and consequent local or regional recurrence.[1,5] While studying the impact of rhabdomyoblastic differentiation (MTT), presence of NF1 and location on the out-

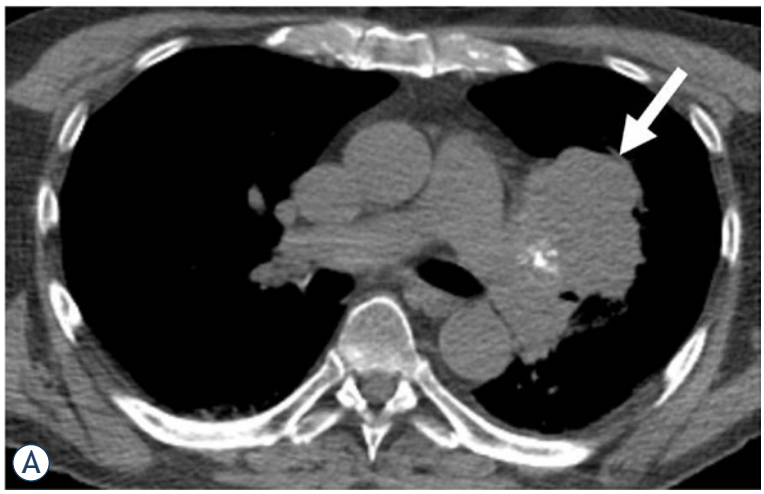

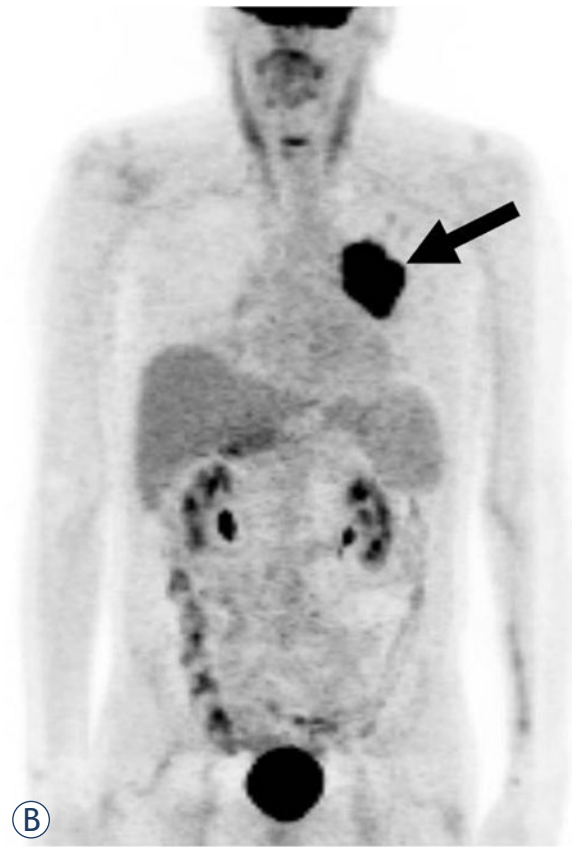

FIGURE 2. A 67-year-old man with MPNST involving the left lung. **A.** Unenhanced CT image of the chest at the level of main pulmonary arteries shows a lobulated mass abutting the left hilum with peripheral foci of calcification (arrow). **B.** Coronal maximum intensity projection (MIP) image from PET/CT shows an intensely fluorodeoxyglucose (FDG) avid mass (arrow, standardized uptake value $[SUV]_{max}$ 23.6). Patient underwent left pneumonectomy on which intrapulmonary location of the mass was confirmed. Rhabdomyoblastic differentiation (malignant triton tumor) was noted on pathology.

come of 84 consecutive patients with MPNST[7], we noticed that the imaging literature on intrathoracic MPNST is extremely limited, consisting mostly of case reports with little information on imaging findings.[4,8–14] Therefore, the purpose of this study was to assess the clinical and imaging characteristics of primary intrathoracic MPNST.

Patients and methods

Patients

In this institutional review board-approved study, the electronic pathology patient database was reviewed to identify patients with pathologically proven primary intrathoracic MPNSTs (mediastinum, lung, and chest wall tumors) evaluated at our institution from January 1999 to December 2011. First, we identified a total of 110 patients with pathologically proven MPNSTs. Among them, 26 patients were excluded because they were referred from outside institution and the pathology of the primary tumor was not confirmed by review at our institution. Among the remaining 84 patients, 21 patients had intrathoracic MPNSTs. Of these 21 patients, 6 were excluded because imaging of the primary tumor was not available. Therefore, the final study population consisted of 15 patients with pathologically proven intrathoracic MPNST who had imaging of primary tumors available for review. Mediastinal tumor localization was determined by an adaptation of the Felson methodology. For large tumors, we used the epicenter of the tumor to define its location. Clinical features including clinical presentation and treatment were correlated with imaging findings.

Image Analysis

All imaging analysis was performed, in consensus, by three radiologists (N.R., S.H. and A.S.) with 13, 10 and 7 years of experience. Images were reviewed on the picture archiving and communication system (PACS) using commercially available workstations (Centricity, General Electric, Barrington, IL).

A systematic review of available imaging studies was performed and location, size (single longest dimension was selected by manually placing caliper on the axial or coronal images), and imaging features (CT in 15, MRI in 5 and PET/CT in 4) of the primary tumors were recorded. CT attenuation of the tumor was compared to muscles by placing a circular region of interest (ROI) in the most representative portion of the tumor. Image inten-

sity on T1 and T2-weighted images was visually compared to muscles. Degree of enhancement was evaluated in comparison with skeletal muscle and graded as mild if less enhancement than skeletal muscle, moderate if similar degree of enhancement as muscle (considered similar for the purpose of this study if the ROI values were within 10% the muscle), and intense if more enhancement than muscle using ROI measurements, similar to previous reports.[15] Homogeneous or heterogeneous appearance of the tumors on CT and MRI, presence of hemorrhage (defined as areas that are hyperdense on unenhanced CT images or T1-hyperintense areas on T1-weighted MR images), necrosis (defined as hypodense and/or T2-hyperintense, non-enhancing area within the tumor), and calcifications were also recorded. Degree of fluorodeoxyglucose (FDG) uptake was measured on PET/CT images by manually placing a circular ROI over the most FDG avid portion of the lesion on a commercially available workstation (Hermes, Hermes Medical Solutions Inc, Greenville, NC, USA). Standardized uptake value $(SUV)_{max}$ was used to represent the FDG uptake of the tumor. Invasion of adjacent structures, seen as extension of tumor invading and distorting the adjacent tissues, was noted and its impact on management was studied.

Differentiation between malignant and benign nerve sheath tumors is challenging, especially in NF1 patients. Signs of malignancy in this context on imaging include high attenuation and necrosis/hemorrhage on CT, heterogeneity on T1 weighted images in MR, and rapidly increasing size.[16,17]

Results

Patients

Among 15 eligible patients, there were eight men and seven women (Table 1). The average age at diagnosis was 49 years (range: 18–83 years). Eleven patients had conventional MPNSTs, and 4 patients had MTT (27%). The average age of the MPNST patients was 50 (range 18–83) while the average age of the MTT patients was 40 (range 27–67). Four patients (27%) had NF1 (2 patients with MPNST, 2 patients with MTT).

Six tumors (40%) were located in the mediastinum (two anterior, two middle and two in posterior mediastinum) (Figure 1), four (27%) were in the chest wall (Figure 2), three (20%) involved the lung, and two were paraspinal (13%) (Figure 3).

Of the six mediastinal tumors, all were conventional MPNSTs and 2 were associated with NF1 (33%). Of the four chest wall tumors, 2 were MTT, both of which were associated with NF1 (50%), while the other two were conventional sporadic MNPST. Of the three lung tumors, 1 was a MTT (33%); none of these patients had NF1. Of the two paraspinal tumors, 1 was a MTT (50%) and none of the patients had NF1.

Nine patients presented with a chief complaint of pain, three with back pain, three with pleuritic chest pain, two with painful chest wall lumps, and one with right arm pain. Six patients presented with dyspnea or respiratory distress. One patient presented with right arm tingling/swelling. Table 2 summarizes the clinical presentation of the patients with intrathoracic MPNST. Only one patient was asymptomatic, with a large subxiphoid mass detected on surveillance imaging; the patient had received chemotherapy and radiation for Hodgkin's lymphoma 14 years prior to developing an MPNST. Clinical information regarding presentation was unavailable for one patient.

Imaging features of primary tumors

All patients had a single tumor representing MPNST. Average tumor size was 11 cm (range 3–32 cm) (Table 3). Patients with MTT tended to have larger tumors at diagnosis (mean size 15 cm) than those with conventional MPNSTs (mean size 9 cm). However, this difference could not be statistically assessed due to a small sample size.

On CT, eight tumors (53%) had lower attenuation than muscle and seven (47%) were isoattenuating. On MRI, all five masses were isointense to muscles on T1-weighted images and hyperintense on T2-weighted images. Ten masses demonstrated mild enhancement, four had moderate enhancement, and one patient only had unenhanced CT. Eight (53%) masses were heterogeneous and seven (47%) were homogeneous.

Calcifications were seen in four lesions (27%) and four (27%) had features suggestive of necrosis. Three patients had punctate calcifications and one had chunky, nodular calcifications; calcifications were peripheral in two patients, central in one patient, and diffusely scattered in one. Of the four masses with appearance suggestive of necrosis on imaging, two had necrosis on pathology and one had cystic degeneration. No necrosis or cystic degeneration was noted on pathology in the fourth patient. Hemorrhage was seen in two masses (13%).

The four masses that underwent PET/CT were intensely FDG—avid with mean SUV_{max} of 10.5

TABLE 1. Clinical features of patients with malignant peripheral nerve sheath tumor (MPNST) of chest

Sr No	Age	Sex	NF1	Location	Size (cm)	Histology (MPNST/MTT)	Management
1	38	F	Yes	Middle mediastinum	16	MPNST	Chemoradiation
2	31	M	No	Posterior mediastinum	14	MPNST	Neoadjuvant chemoradiation, followed by surgery
3	48	M	No	Anterior mediastinum	13.6	MPNST	Chemoradiation
4	18	F	Yes	Middle mediastinum	8	MPNST	Neoadjuvant chemoradiation, followed by surgery
5	65	M	No	Posterior mediastinum	5.5	MPNST	Neoadjuvant chemotherapy and surgery
6	33	F	No	Anterior mediastinum-subxiphoid	4	MPNST	Surgery
7	83	F	No	Chest wall	17	MPNST	Surgery, followed by chemoradiation
8	60	M	No	Chest wall	3	MPNST	Surgery
9	27	M	Yes	Chest wall	4	MTT	Surgery, followed by chemoradiation
10	44	F	Yes	Chest wall	32	MTT	None
11	51	F	No	Left lung	4.5	MPNST	Neoadjuvant chemotherapy and surgery
12	63	M	No	Left lung	unknown	MPNST	Chemotherapy
13	67	M	No	Left lung	12.8	MTT	Surgery
14	58	M	No	Paraspinal	2.5	MPNST	Chemoradiation
15	61	F	No	Paraspinal	10	MTT	Chemotherapy

(range 4.4–23.6). One of these had MTT, and we noticed that this tumor had higher SUV_{max} (23.6) than those without MTT (mean 6.1, range 4.4–8.9). Again, this difference could not be statistically analyzed given the small number of patients with this rare entity.

Neuroforaminal extension was seen in one posterior mediastinum patient and one paraspinal patient. Two patients had evidence of rib erosion on imaging, while two patients had evidence of rib displacement. Of the six mediastinal cases, four had invasion or encasement of adjacent structures on imaging such as trachea, mediastinal great vessels and esophagus, and one had intraspinal extension. Of the chest wall cases, one had invasion of adjacent tissues (4 cm) and another large mass had extensive invasion and displacement of multiple adjacent structures. All three of the lung cases had invasion of nearby structures including chest wall, diaphragm and mediastinum. Of the paraspinal cases, one patient presented with lung metastases, and the other patient had invasion into paraspinal musculature and extrapleural fat.

Management

In general, surgery was the treatment of choice whenever possible. Large masses which were initially deemed unresectable received neoadjuvant chemotherapy or chemoradiation, following which they were surgically resected if there was response and if they were considered resectable. Patients with nonradical resection received adjuvant chemotherapy.

Two posterior mediastinal masses and one middle mediastinal mass were treated with neoadjuvant chemoradiation or chemotherapy followed by surgery. The patient with the 14cm posterior mediastinal mass received concurrent chemotherapy (etoposide/ifosfamide) and radiation followed by surgical resection, as the tumor was initially deemed unresectable. One patient with middle mediastinal mass and another with an anterior mediastinal mass underwent chemoradiation alone as they were deemed unresectable. The patient with the anterior mediastinal mass received chemotherapy (etoposide/cisplatin) followed by radiation, the patient with the middle mediastinal mass received concurrent chemotherapy (adriamycin/ifosfamide) and radiation. Another patient with a 4 cm subxiphoid mass was resected without neoadjuvant therapy.

Of the four patients with chest wall masses, the 4 cm invasive mass and another large mass (17 cm) underwent surgery and chemoradiation, and one small mass (3 cm) was treated with surgical resection. The patient with the 4 cm invasive mass initially underwent non-radical resection, followed

TABLE 2. Initial presentation of patients with malignant peripheral nerve sheath tumor (MPNST) of the chest

Sr No	Location	Size (cm)	Histology (MPNST/MTT)	Presentation
1	Middle mediastinum	16	MPNST	Right arm pain with radiation to axilla
2	Posterior mediastinum	14	MPNST	Back pain
3	Anterior mediastinum	13.6	MPNST	Dyspnea, found to have mass with partial obstruction of right mainstem bronchus
4	Middle mediastinum	8	MPNST	Dyspnea/pleuritic chest pain and pleural effusion
5	Posterior mediastinum	5.5	MPNST	Back pain
6	Anterior mediastinum-subxiphoid	4	MPNST	Asymptomatic, found on routine screening
7	Chest wall	17	MPNST	Right arm tingling/swelling
8	Chest wall	3	MPNST	Painful chest wall lump
9	Chest wall	4	MTT	Painful chest wall lump
10	Chest wall	32	MTT	Dyspnea/pleuritic chest pain and pleural effusion
11	Left lung	4.5	MPNST	PNA, tx'd, with continuing decline and respiratory distress
12	Left lung	unknown	MPNST	Dyspnea/pleuritic chest pain and pleural effusion
13	Left lung	12.8	MTT	Unknown
14	Paraspinal	2.5	MPNST	Back pain
15	Paraspinal	10	MTT	Lung mets and dyspnea on exertion

MTT = malignant triton tumors; Sr No = serial number

by radiation therapy, re-resection, and then chemotherapy with vincristine/actinomycin/cyclophosphamide/mesna; exact details of chemotherapy were not available for the 17cm chest wall mass as patient received chemotherapy at an outside institution. The one patient with the 32 cm mass and extensive invasion of adjacent structures died prior to any treatment.

Of the three lung tumors, one case with mediastinal invasion was treated with neoadjuvant chemotherapy followed by surgery, one case with a chest wall and diaphragmatic invasion was treated with chemotherapy, and a hilar mass with invasion of the pulmonary artery was treated with total pneumonectomy.

Of the two paraspinal cases, one patient was treated with chemoradiation (further details not available), while the other was treated with chemotherapy alone, as the patient presented initially with widespread metastatic disease.

Discussion

Thoracic MPNSTs may involve mediastinum, lung or chest wall, with those in the mediastinum or chest wall manifesting as large elongated masses. They are often heterogeneous on CT and MRI, and intensely FDG-avid on PET. To our knowledge, this is the largest study of imaging findings of intrathoracic MPNST.

MPNSTs are rare, aggressive soft tissue sarcomas occurring anywhere in the body. They often occur in association with NF1, with an incidence ranging from 20–30%.[1,3,5] Four patients in our study had NF1 (27%); this number is consistent with the reported incidence. MPNSTs most commonly occur in the extremities; intrathoracic MPNST are rarely reported, mostly in the form of isolated case reports. If MPNSTs arise in the nerves of the deep tissue, as occurs frequently with thoracic tumors, early diagnosis is clinically more difficult.[4] Pain was the most common complaint and presenting symptom in others (7/15 patients). In a recent series of 175 patients with MPNSTs conducted at Mayo Clinic, the median tumor size was 6.0 cm[1]; our average tumor size was 11 cm.

MTT, defined by the presence of rhabdomyoblasts in an MPNST on pathology, account for < 10% of MPNSTs.[6] MTTs behave more aggressively than conventional MPNSTs. Out of the 15 patients in our study, 4 had the MTT subtype (27%). These patients had a larger tumor size at diagnosis, measuring 15 cm compared to 9 cm for conventional MPNSTs.

MPNSTs typically are ovoid, occurring along a nerve[18], and presenting as a non-specific soft tissue mass. MPNSTs have low attenuation on CT.[9]

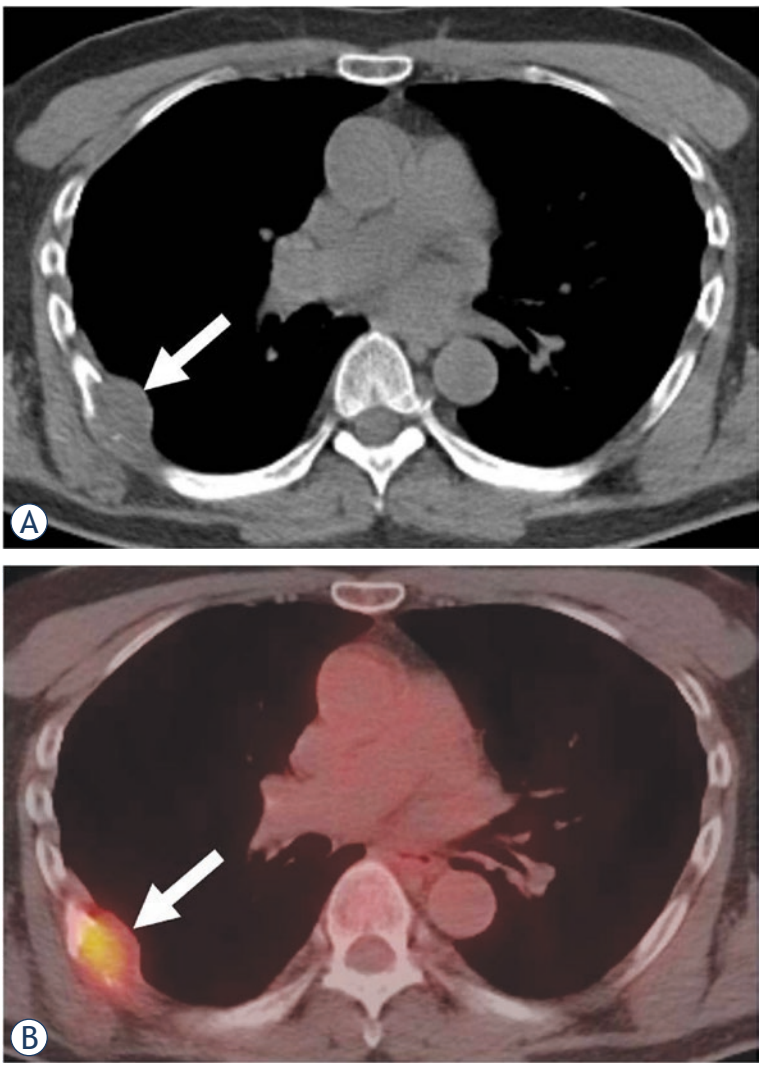

FIGURE 3. A 60-year-old man with left chest wall MPNST. **A.** Axial unenhanced CT image shows a low attenuation right chest wall mass abutting a rib (arrow) causing rib destruction and adjacent pleural thickening. **B.** Axial fused PET/CT image shows presence of moderate fluorodeoxyglucose (FDG) uptake (arrow, standardized uptake value $[SUV]_{max}$ 4.4).

On MR, MPNSTs are isointense on T1 and hyperintense on T2.[8] Our findings for intrathoracic MPNST are similar, as 8/15 patients had hypoattenuating lesions on CT, and of the five patients with MR, all had isointense lesions on T1 and hyperintense lesions on T2. MPNSTs present as FDG-avid masses and can therefore be evaluated using PET/CT.[19]

Differentiation between malignant and benign nerve sheath tumors is challenging, especially in NF1 patients. Signs of MPNST on imaging include high attenuation and necrosis/hemorrhage on CT, heterogeneity on T1 weighted images in MR, and rapidly increasing size.[16,17] A "target sign", or a central hypodense region on T2-weighted images, was previously implicated as an indicator for MPNST, but this has not been corroborated by other groups.[2,20,21] Our data also did not confirm this finding, as a target sign was only seen in one patient. MPNST should be considered in the differential diagnosis for large thoracic masses found on imaging, especially if they are located along major nerves. MPNST should be especially high on the differential diagnosis if a thoracic mass is found in a patient with NF1.

Treatment of MPNST relies primarily on surgical resection.[4] Neoadjuvant chemoradiation is often used for initially unresectable tumors with an intention to downstage the mass pre-resection. Radiation therapy can be given in addition to surgical resection for improved local control.[5] Chemotherapy is typically reserved for aggressive cases, and also when there is tumor rupture, positive margins, or metastases, although improvement in survival has not been demonstrated.[1] In an analysis of MPNST patients who received either surgery alone or multimodality treatment, the rate of recurrence was not significantly affected[7], however, given the aggressive nature of MPNSTs, multimodality treatment is typically recommended. To the best of our knowledge, there are no studies comparing the efficacy of sequential versus concurrent chemoradiation in the treatment of MPNSTs.

Imaging assists with management of these patients, as tumors visualized to have invasion or compression of nearby structures often undergo additional therapy prior to surgical resection. PET/CT may play an important role in MPNST management, as increased FDG uptake is associated with malignant transformation, and PET/CT has 72% specificity for diagnosis of malignancy.[19] In addition, whole-body MRI adequately assesses tumor burden in patients with NF1, and can allow visualization of tumors not observed on physical examination. This technique allows close surveillance of neurofibromas in NF1 patients and may allow for earlier detection of malignant transformation.[21,23]

An important limitation to this study was small sample size. However, intrathoracic MPNST are rare, and there are no prior reports on imaging features of series of these tumors. Due to the retrospective nature of the study with patients undergoing imaging evaluation as clinically indicated, we do not have MRI or PET/CTs for all 15 patients. As these are rare tumors, there is no fixed protocol for imaging evaluation of these masses.

In summary, intrathoracic MPNST may involve the mediastinum, lung and chest wall; mediastinal and chest wall tumors are usually large

TABLE 3. Imaging features of patients with malignant peripheral nerve sheath tumor (MPNST) of the chest

Sr No	Location	CT density	MR T1	MR T2	Enhancement	Homogeneity	Calcification	Necrosis	Hemorrhage	PET SUVmax
1	Middle mediastinum	Hypo	-	-	Mild	Homogenous	Yes	-	-	-
2	Posterior mediastinum	Hypo	Iso	Hyper	Moderate	Heterogenous	-	-	Yes	5.2
3	Anterior mediastinum	Hypo	-	-	Mild	Homogenous	-	-	-	-
4	Middle mediastinum	Iso	Iso	Hyper	Mild	Heterogenous	-	-	-	-
5	Posterior mediastinum	Iso	Iso	Hyper	Moderate	Heterogenous	-	-	-	-
6	Anterior mediastinum-subxiphoid	Hypo	-	-	Mild	Heterogenous	-	-	-	-
7	Chest wall	Iso	-	-	Mild	Heterogenous	Yes	Yes	Yes	-
8	Chest wall	Iso	-	-	Mild	Homogenous	-	-	-	4.4
9	Chest wall	Iso	Iso	Hyper	Moderate	Homogenous	-	-	-	-
10	Chest wall	Hypo	-	-	Mild	Heterogenous	-	Yes	-	-
11	Left lung	Hypo	-	-	Mild	Heterogenous	Yes	Yes	-	-
12	Left lung	Hypo	-	-	Moderate	Homogenous	-	Yes	-	8.9
13	Left lung	Iso	-	-	-	Homogenous	Yes	-	-	23.6
14	Paraspinal	Iso	Iso	Hyper	Mild	Homogenous	-	-	-	-
15	Paraspinal	Hypo		-	Mild	Heterogenous	-	-	-	-

Sr No = serial number; SUV_{max} = standardized uptake value

elongated masses along the course of nerves. They are usually hypoattenuating on CT, hyperintense on T2-weighted images, are often heterogeneous, and are intensely FDG-avid masses. Comparison with previously published data on MPNSTs suggests that intrathoracic MPNST are similar in appearance to MPNSTs in other locations, but these tumors may present larger in size. For MPNSTs, imaging is often nonspecific, and although we as radiologists can raise the possibility, an accurate diagnosis always needs histologic confirmation. MPNST should be considered in the differential diagnosis when a large, elongated intrathoracic mass is found. The role of the radiologist lies in identification of invasion of adjacent structures as patients with invasion receive neoadjuvant or adjuvant chemoradiation.

References

1. Stucky CC, Johnson KN, Gray RJ, Stucky CC, Johnson KN, Gray RJ, et al. Malignant peripheral nerve sheath tumors (MPNST): the Mayo Clinic experience. *Ann Surg Oncol* 2012; **19:** 878-85.
2. Van Herendael BH, Heyman SR, Vanhoenacker FM, De Temmerman G, Bloem JL, Parizel PM, et al. The value of magnetic resonance imaging in the differentiation between malignant peripheral nerve-sheath tumors and non-neurogenic malignant soft-tissue tumors. *Skeletal Radiol* 2006; **35:** 745-53.
3. Ramanathan RC, Thomas JM. Malignant peripheral nerve sheath tumours associated with von Recklinghausen's neurofibromatosis. *Eur J Surg Oncol* 1999; **25:** 190-3.
4. Shimizu J, Arano Y, Murata T, Ishikawa N, Yachi T, Nomura T, et al. A case of intrathoracic giant malignant peripheral nerve sheath tumor in neurofibromatosis type I (von Recklinghausen's disease). *Ann Thorac Cardiovasc Surg* 2008; **14:** 42-7.
5. Anghileri M, Miceli R, Fiore M, Mariani L, Ferrari A, Mussi C, et al. Malignant peripheral nerve sheath tumors: prognostic factors and survival in a series of patients treated at a single institution. *Cancer* 2006; **107:** 1065-74.
6. McConnell YJ, Giacomantonio CA. Malignant triton tumors-complete surgical resection and adjuvant radiotherapy associated with improved survival. *J Surg Oncol* 2012; **106:** 51-6.
7. Kamran SC, Howard SA, Shinagare AB, Krajewski KM, Jagannathan JP, Hornick JL, et al. Malignant peripheral nerve sheath tumors: Prognostic impact of rhabdomyoblastic differentiation (malignant triton tumors), neurofibromatosis 1 status and location. *Eur J Surg Oncol* 2013; **39:** 46-52.
8. Kim JG, Sung WJ, Kim DH, Kim YH, Sohn SK, Lee KB. Malignant peripheral nerve sheath tumor in neurofibromatosis type I: unusual presentation of intraabdominal or intrathoracic mass. *Korean J Intern Med* 2005; **20:** 100-4.
9. Chu YC, Yoon YH, Han HS, Han JY, Kim JM, Park IS. Malignant transformation of intrathoracic ancient neurilemmoma in a patient without von Recklinghausen's disease. *J Korean Med Sci* 2003; **18:** 295-8.
10. McLaughlin EJ, Heuer GG, Whitmore RG, Birknes JK, Belasco J, Sterman D, et al. Treatment of a malignant peripheral nerve sheath tumor and its complications through a multidisciplinary approach. *J Neurosurg Pediatr* 2011; **7:** 543-8.
11. Patel VS, St Louis JD, Oduntan O, Landolfo KP. Intrathoracic peripheral nerve sheath tumors in patients with neurofibromatosis type 1 (von Recklinghausen disease). *J Thorac Cardiovasc Surg* 2006; **131:** 736-7.
12. Park JH, Choi KH, Lee HB, Rhee YK, Lee YC, Chung MJ. Intrathoracic malignant peripheral nerve sheath tumor in von Recklinghausen's disease. *Korean J Intern Med* 2001; **16:** 201-4.

13. Chao BH, Stogner-Underwood KA, Kiev J, Smith TJ. Intrathoracic malignant peripheral nerve sheath tumor in neurofibromatosis 1. *J Clin Oncol* 2008; **26:** 2216-8.

14. Yamaguchi M, Yoshino I, Fukuyama S, Osoegawa A, Kameyama T, Tagawa T, et al. Surgical treatment of neurogenic tumors of the chest. *Ann Thorac Cardiovasc Surg* 2004; **10:** 148-51.

15. Podobnik J, Kocijancic I, Kovac V, Sersa I. 3T MRI in evaluation of asbestos-related thoracic diseases-preliminary results. *Radiol Oncol* 2012; **44:** 92-6.

16. Levy AD, Patel N, Dow N, Abbott RM, Miettinen M, Sobin LH. From the archives of the AFIP: abdominal neoplasms in patients with neurofibromatosis type 1: radiologic-pathologic correlation. *Radiographics* 2005; **25:** 455-80.

17. Murphey MD, Smith WS, Smith SE, Kransdorf MJ, Temple HT. From the archives of the AFIP. Imaging of musculoskeletal neurogenic tumors: radiologic-pathologic correlation. *Radiographics* 1999; **19:** 1253-80.

18. Li CS, Huang GS, Wu HD, Chen WT, Shih LS, Lii JM, et al. Differentiation of soft tissue benign and malignant peripheral nerve sheath tumors with magnetic resonance imaging. *Clin Imaging* 2008; **32:** 121-7.

19. Bredella MA, Torriani M, Hornicek F, Ouellette HA, Plamer WE, Williams Z, et al. Value of PET in the assessment of patients with neurofibromatosis type 1. *AJR Am J Roentgenol* 2007; **189:** 928-35.

20. Wasa J, Nishida Y, Tsukushi S, Shido Y, Sugiura H, Nakashima H, et al. MRI features in the differentiation of malignant peripheral nerve sheath tumors and neurofibromas. *AJR Am J Roentgenol* 2010; **194:** 1568-74.

21. Bhargava R, Parham DM, Lasater OE, Chari RS, Chen G, Fletcher BD. MR imaging differentiation of benign and malignant peripheral nerve sheath tumors: use of the target sign. *Pediatr Radiol* 1997; **27:** 124-9.

22. Mautner VF, Asuagbor FA, Dombi E, Fünsterer C, Kluwe L, Wenzel R, et al. Assessment of benign tumor burden by whole-body MRI in patients with neurofibromatosis 1. *Neuro Oncol* 2008; **10:** 593-8.

23. Van Meerbeeck SF, Verstraete KL, Janssens S, Mortier G. Whole body MR imaging in neurofibromatosis type 1. *Eur J Radiol* 2009; **69:** 236-42.

case report

Percutaneous mechanical thrombectomy of superior mesenteric artery embolism

Dimitrij Kuhelj, Pavel Kavcic, Peter Popovic

Clinical Radiology Institute, University Medical Centre Ljubljana, Ljubljana, Slovenia

Radiol Oncol 2013; 47(3): 239-243.

Received 29 December 2012
Accepted 24 January 2013

Correspondence to: Assist. Dimitrij Kuhelj, MD, MSc, Clinical Radiology Institute, University Medical Centre Ljubljana, Zaloška 7, 1000 Ljubljana, Slovenia. Phone: +386 1 522 8530; Fax: +386 1 522 2481; E-mail: dimitrij.kuhelj@guest.arnes.si

Disclosure: No potential conflicts of interest were disclosed.

Background. The present series present three consecutive cases of successful percutaneous mechanical embolectomy in acute superior mesenteric artery ischemia. Superior mesenteric artery embolism is a rare abdominal emergency that commonly leads to bowel infarction and has a very high mortality rate. Prompt recognition and treatment are crucial for successful outcome. Endovascular therapeutic approach in patients with acute SMA embolism in median portion of its stem is proposed.

Case reports. Three male patients had experienced a sudden abdominal pain and acute superior mesenteric artery embolism in median portion of its stem was revealed on computed tomography angiography. No signs of intestinal infarction were present. The decision for endovascular treatment was made in concordance with the surgeons. In one patient 6 French gauge Rotarex® device was used while in others 6 French gauge Aspirex® device were used. All patients experienced sudden relief of pain after the procedure with no signs of intestinal infarction. Minor procedural complication – rupture of a smaller branch of SMA during Aspirex® treatment was successfully managed by coiling while transient paralytic ileus presented in one patient resolved spontaneously. All three patients remained symptom-free with patent superior mesenteric artery during the follow-up period.

Conclusions. Percutaneous mechanical thrombectomy seems to be a rapid and effective treatment of acute superior mesenteric artery embolism in median portion of its stem in absence of bowel necrosis. Follow-up of our patients showed excellent short- and long-term results.

Key words: acute mesenteric ischemia; superior mesenteric artery embolism; percutaneous mechanical thrombectomy; Aspirex®; Rotarex®

Introduction

Acute mesenteric ischemia (AMI) is a serious abdominal emergency characterized by sudden interruption of intestinal blood flow that commonly leads to bowel infarction. Its occurrence is relatively infrequent; accounting for 0.1% of hospital admissions.[1] It typically affects elderly with increased risk of cardiovascular events. The most common cause of acute AMI is embolism (40-50% of cases).[2] The majority of mesenteric emboli originate from the heart, most commonly in patients with atrial fibrillation.[3]

Despite considerable improvements in diagnostics and AMI treatment over the last decades, the condition still has a poor prognosis, with an in-hospital mortality rate of 59 to 93%.[4] Early recognition and treatment are crucial for successful outcome.[4] Delay in diagnosis results in intestinal infarction and gangrene that cannot be reversed by blood flow restoration. The treatment of choice has been surgical laparotomy with thrombectomy.[5] Alternatively, cases of percutaneous thrombectomy were reported.[6-12] The two main percutaneous methods are aspiration thrombectomy, in which thrombus is removed by suction, and mechanical thrombectomy, using different automated devices to fragment and remove embolus.

Aspirex S® and Rotarex S® (Straub Medical, Wangs, Switzerland) are mechanical thrombecto-

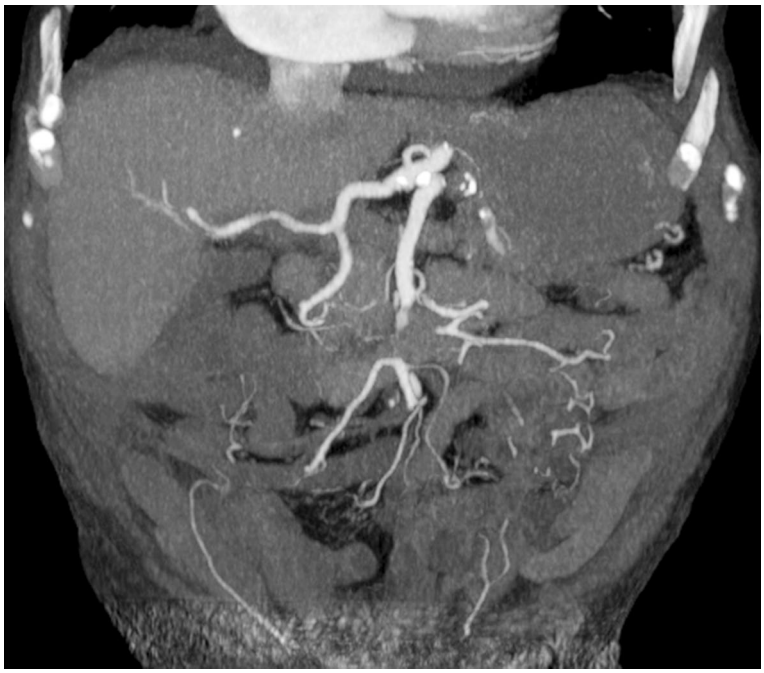

FIGURE 1. Coronal MIP reconstructions of CTA, revealing a segmental, occlusive acute embolism of the mid portion of SMA stem.

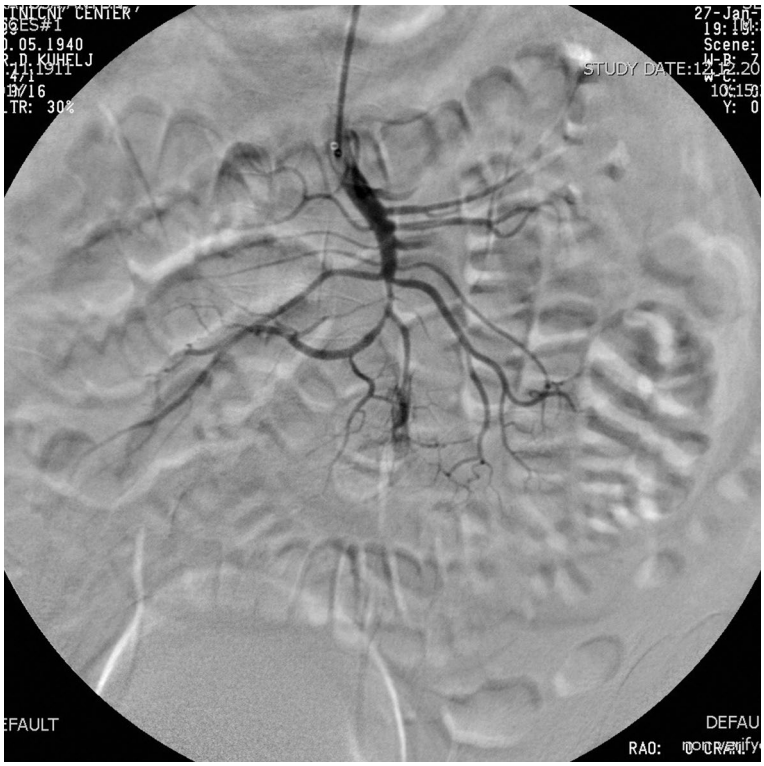

FIGURE 2. Control angiography after third pass with Aspirex® showing patent SMA with extravasation of contrast medium due to a small branch rupture.

my devices that are often used in our department to treat acute and sub-acute peripheral arterial occlusions with good results and low complication rate. They are rotating over-the-wire devices designed for efficient and rapid removal of the occluding material. The rotations produce a continuous vacuum inside the catheter, which leads to aspiration of the material into the catheter and transportation into the collecting bag. Rotarex® catheter features a rotating head detaching occlusion material in acute, subacute and chronic occlusions. Aspirex® catheter is designed for the use in acute occlusions, since its head does not rotate, therefore the risk for vessel trauma should be lower as in Rotarex® catheters. Both are 6 French gauge (Fr, F) and 8 Fr systems, suitable for the use in arteries with a diameter larger than 3 mm.[13,14]

The present series present three consecutive cases of successful percutaneous mechanical thrombectomy in acute superior mesenteric artery (SMA) embolism treated in our institution. Also, up to 45 months follow-up is presented.

Case reports

Three male patients, age 63-97 years, with sudden abdominal pain and also thoracic pain in one case were admitted to our hospital. Only one patient had known atrial fibrillation with congestive heart failure and was on Aspirin, while in two patients atrial fibrillation was newly discovered. Except for mild normocytic anaemia in one patient, no abnormal laboratory findings were present. Abdominal ischemia was suspected in two and dissection of thoracic aorta was suspected in patient with thoracic pain. Contrast enhanced computed tomography angiography (CTA) was performed accordingly. Segmental occlusion of the medial portion of SMA stem was revealed in all three patients. The occlusion of mid portion of SMA in one of our patients is shown on Figure 1. SMA proximally and distally from occlusion was of normal size in all three cases, suggesting embolism rather than thrombosis. No signs of irreversible bowel wall ischemia were found, though circumferential wall thickening of the cecum with normal, homogenous wall enhancement was noted in one patient.

The decision for endovascular treatment was reached in concordance with abdominal surgeons.

According to exiting angle of SMA from the aorta, transaxillary approach was used in two patients and transfemoral in one, local anaesthesia was used in all cases. Fifty-five cm long straight sheaths

were used to catheterise SMA ostium. Initial SMA angiography confirmed acute occlusion in the mid portion of the SMA trunk with a few distal embolic occlusions in some jejunal and colic branches.

Six F Aspirex® was used in two patients while in one case 6F Rotarex® was used, since 6F Aspirex® was not available at that time. Five thousand IU of heparin were infused intraarterially prior to the procedure in all cases. Two passes with catheter were performed in all patients, resulting in normal blood flow in the majority of peripheral branches with only minimal wall irregularity in SMA stem. During the third catheter manipulation in one patient, the guidewire slipped into the smaller branch and the third pass with the Aspirex® ruptured it. The patient experienced acute pain and after angiographic confirmation of the rupture (Figure 2) embolization with coils sealed the rupture (Figure 3).

No adjunctive endovascular procedure was applied and the remaining distal embolic occlusions in jejunal and colic branches were left untreated. Patients' symptoms improved immediately after the procedure in all cases. After a few days all patients underwent a colour Doppler ultrasound examination that confirmed patent SMA (Figure 4). In the patient with circumferential wall thickening of cecum control abdominal CTA due to distended and painful abdomen was performed also. A paralytic ileus of small bowel was found with no signs of bowel ischemia. SMA was patent with few non-occlusive wall thrombi. Ileus was treated conservatively and resolved spontaneously after 4 days. Lifelong warfarin therapy was introduced after discharge in two patients, while anaemia of unknown origin prevented it in one.

Six-month follow-up excluded any clinical symptoms of abdominal ischemia in all patients and no follow-up was planned. 45 months after the treatment, the first patient treated had a CTA of abdominal and peripheral arteries prior to femoropopliteal bypass surgery. Normally patent SMA with no symptoms or signs consistent with recurrence of acute mesenteric ischemia was observed (Figure 5).

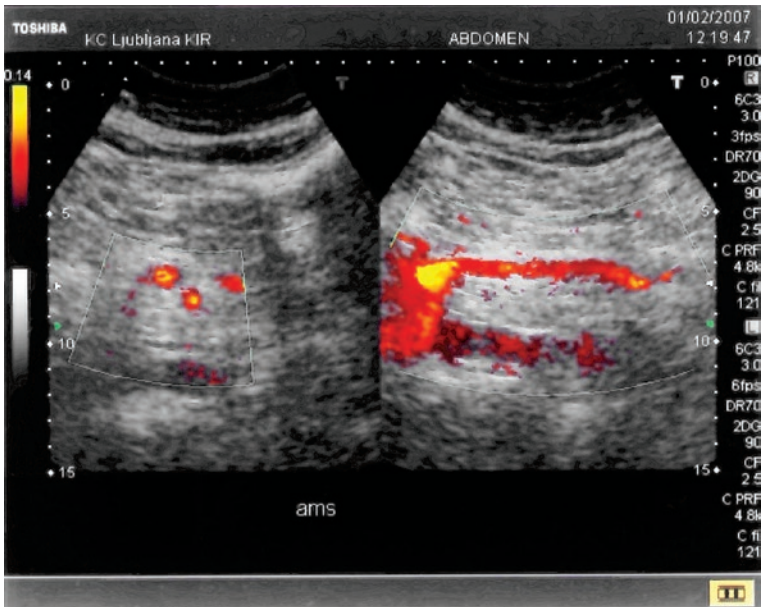

FIGURE 3. Control angiography after embolisation of ruptured branch with coils.

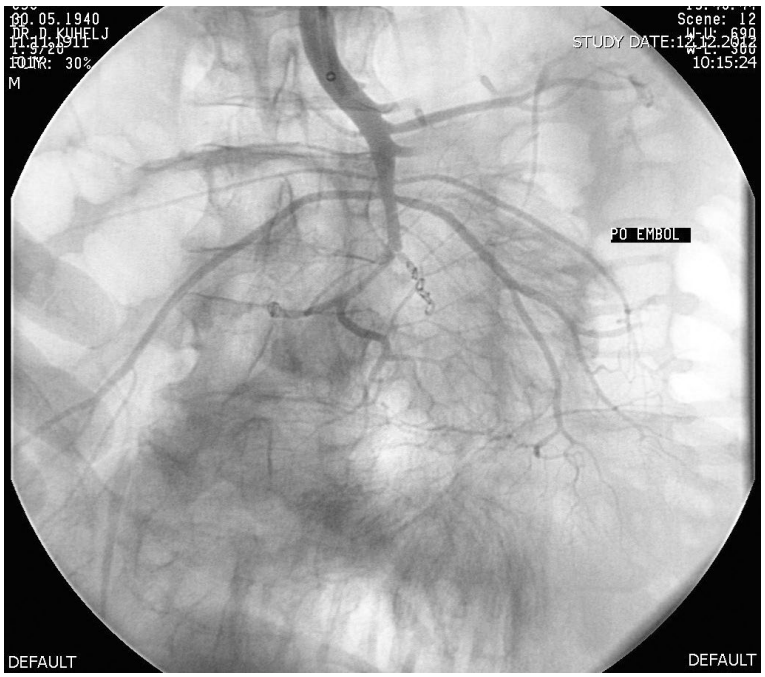

FIGURE 4. Doppler US control 5 days after the treatment showing patent SMA.

Discussion

AMI is a life-threatening condition that commonly leads to bowel infarction. The reasons for the high mortality rate are late recognition due to non-specific clinical findings, infrequency of the condition as well as complex surgical treatment. The diagnosis of AMI depends on the ability of the attending physician to suspect and recognize it.[15] In patients with acute abdominal pain and disproportionate lack of clinical, laboratory or ultrasound findings, AMI should be considered, especially if risk factors like atrial fibrillation, general atherosclerosis or hypercoagulability are present. Once AMI is suspected, CTA should be performed immediately in order to proceed with therapy as soon as possible.

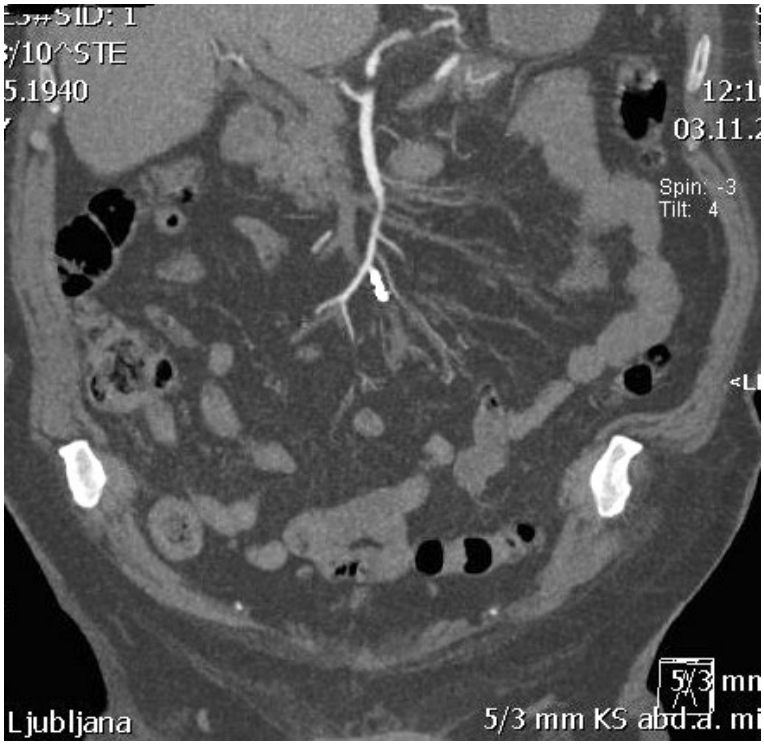

FIGURE 5. Coronal MIP reconstructions of CTA 45 months after the treatment, revealing patent SMA and branches. Coils permanently occluded ruptured branch.

If there are clinical or CT signs of bowel necrosis, urgent surgery is needed. However, if there is no clear evidence of bowel necrosis, endovascular treatment can be a promising alternative[11,12,16,17], as also confirmed in our series. Minimal bowel changes, such as circumferential wall thickening of cecum with normal, homogenous wall enhancement is not a contraidication for endovascular procedure. As follow-up showed also in our patient, there is no need for additional surgery, since the changes were due to oedema and not to prolonged, irreversible acute intestinal ischemia.[18]

To our knowledge, there are just few reports of using mechanical thrombectomy in SMA embolism treatment. One is the first case performed in our department[19] and another is a case report of treatment with AngioJet® hydrodynamic mechanical thrombectomy and EKOS® catheter pharmacological thrombolysis.[12] There are also some reports with a very high success rate (90%) for local fibrinolysis of the embolus in patients with SMA embolism.[20,21] However, while the endovascular approach may rapidly restore the blood flow to the bowel, the time needed for local lysis is variable and the bowel viability cannot be assessed with laparotomy after, if needed.[22] Also, numerous reports of complications after local thrombolysis were reported, possibly compromising the outcome.[21,23,24]

Percutaneous mechanical thrombectomy showed good results in our series with dramatic improvement of symptoms present immediately in all patients. No post procedural complications were present in our patients, probably due to absence of any additional pharmacologic lysis.

The main advantages of this technique are rapid and effective removal of large thrombus without the need for local thrombolysis and its minimal invasiveness, thus avoiding the complications associated with surgery. The seriousness of potential vessel damage should not be disregarded and the risk probably increases with smaller vessel diameters. Still, such complications can be easily managed by simple coiling, as performed in one of our patients.

It is of outmost importance that two phases of CTA for bowel ischemia exclusion should be performed prior to the treatment, since SMA recanalisation in patients with necrosed bowel could have disastrous consequences. Also, the location of the embolus should be considered. The recanalisation of completely occluded SMA ostium might be technically challenging and potentially dangerous due to risk of distal arterial embolization; mechanical recanalization of distal branches is difficult and might cause a rupture.

The three patients reported here represent the only patients with occluded AMI, treated with percutaneous mechanical thrombectomy devices at our Institution until now. No permanent complications were observed and good long-term results suggests that Aspirex® and Rotarex® thrombectomy is a good alternative to established surgical treatment in selected cases. Still, by avoiding surgery, the bowel ischemia or necrosis may progress, during the time between CTA and percutaneous procedure, and if the patient's condition does not improve, laparotomy may follow.

References

1. Kozuch PL, Brandt LJ. Review article: diagnosis and management of mesenteric ischemia with an emphasis on pharmacotherapy. *Aliment Pharmacol Ther* 2005; **21:** 201-215.

2. Shih MC, Hagspiel KD. CTA and MRA in mesenteric ischemia: part 1, Role in diagnosis and differential diagnosis. *AJR Am J Roentgenol* 2007; **188:** 452-61.

3. Stanley JC. Mesenteric arterial occlusive and aneurysmal disease. *Cardiol Clin* 2002; **20:** 611-22.

4. Schoots IG, Koffeman GI, Legemate DA, Levy M, Van Gulik TM. Systematic review of survival after acute mesenteric ischemia according to disease aetiology. *Br J Surg* 2004; **91:** 17-21.

5. Bingol H, Zeybek N, Cingöz F, Yilmaz AT, Tatar H, Sen D. Surgical therapy for acute superior mesenteric artery embolism. *Am J Surg* 2004; **188:** 68-70.

6. Kawarada O, Sonomura T, Yokoi Y. Direct aspiration using rapid-exchange and low-profile device for acute thrombo-embolic occlusion of the superior mesenteric artery. *Catheter Cardiovasc Interv* 2006; **68:** 862-6.

7. Heiss P, Loewenhardt B, Manke C, Hellinger A, Dietl KH, Schlitt HJ, et al. Primary percutaneous aspiration and thrombolysis for the treatment of acute embolic superior mesenteric artery occlusion. *Eur Radiol* 2010; **20:** 2948-58.

8. Sonoda K, Ikeda S, Koga S, Fukui J, Ishino T, Kohno S. Successful treatment of acute occlusion in superior mesenteric artery of an elderly man by thrombus aspiration. *J Clin Gastroenterol* 2007; **41:** 933-4.

9. Rousseau H, Sapoval M, Ballini P, Dube M, Joffre F, Gaux JC, et al. Percutaneous recanalization of acutely thrombosed vessels by hydrodynamic thrombectomy (Hydrolyser). *Eur Radiol* 1997; **7:** 935-41.

10. Wakabayashi H, Shiode T, Kurose M, Moritani H, Fujiki S, Morimoto N, et al. Emergent treatment of acute embolic superior mesenteric ischemia with combination of thrombolysis and angioplasty: report of two cases. *Cardiovasc Intervent Radiol* 2004; **27:** 389-93.

11. Arthurs ZM, Titus J, Bannazadeh M, Eagleton MJ, Srivastava S, Sarac TP, et al. A comparison of endovascular revascularization with traditional therapy for the treatment of acute mesenteric ischemia. *J Vasc Surg* 2011; **53:** 698-704.

12. Ballehaninna UK, Hingorani A, Ascher E, Shiferson A, Marks N, Aboian E, et al. Acute superior mesenteric artery embolism: reperfusion with AngioJet hydrodynamic suction thrombectomy and pharmacologic thrombolysis with the EKOS catheter. *Vascular.* Published online first: 22 March 2012. doi: 10.1258/vasc.2011.cr0311.

13. Bérczi V, Deutschmann HA, Schedlbauer P, Tauss J, Hausegger KA. Early experience and midterm follow-up results with a new, rotational thrombectomy catheter. *Cardiovasc Intervent Radiol* 2002; **25**: 275-281.

14. Zeller T, Frank U, Bürgelin K, Müller C, Flügel P, Horn B, et al. Early experience with a rotational thrombectomy device for treatment of acute and subacute infra-aortic arterial occlusions. *J Endovasc Ther* 2003; **10:** 322-31.

15. Jayaprakash S. Diagnosis and management of intestinal ischemic disorders. *BMJ* 2003; **326**: 1372-6.

16. Block TA, Acosta S, Björck M. Endovascular and open surgery for acute occlusion of the superior mesenteric artery. *J Vasc Surg* 2010; **52**: 959-66.

17. Hawkins BM, Khan Z, Abu-Fadel MS, Exaire JE, Saucedo JF, Hennebry TA. Endovascular treatment of mesenteric ischemia. *Catheter Cardiovasc Interv* 2011; **78:** 948-52.

18. Macari M, Balthazar EJ. CT of bowel wall thickening: significance and pitfalls of interpretation. *AJR Am J Roentgenol* 2001; **176:** 1105-16.

19. Popovič P, Kuhelj D, Bunc M. Superior mesenteric artery embolism treated with percutaneous mechanical thrombectomy. *Cardiovasc Intervent Radiol* 2011; **34:** 67-9.

20. Simó G, Echenagusia AJ, Camúñez F, Turégano F, Cabrera A, Urbano J. Superior mesenteric arterial embolism: local fibrinolytic treatment with urokinase. *Radiology* 1997; **204:** 775-9.

21. Björnsson S, Björck M, Block T, Resch T, Acosta S. Thrombolysis for acute occlusion of the superior mesenteric artery. *J Vasc Surg* 2011; **54:** 1734-42.

22. Barakate MS, Cappe I, Curtin A, Engel KD, Li-Kim-Moy J, Poon MS, Sandeman MD. Management of acute superior mesenteric artery occlusion. *ANZ J Surg* 2002; **72:** 25-9.

23. Yamaguchi T, Saeki M, Iwasaki Y, Ishikawa M, Hayakawa M, Sakuyama K, et al. Local thrombolytic therapy for superior mesenteric artery embolism: complications and long-term clinical follow-up. *Radiat Med* 1999; **17:** 27-33.

24. Kuoppala M, Åkeson J, Svensson P, Lindblad B, Franzen S, Acosta S. Risk factors for haemorrhage during local intra-arterial thrombolysis for lower limb ischaemia. *J Thromb Thrombolysis* 2011; **31:** 226-32.

case report

Magnetic resonance imaging of vulvar dermatofibrosarcoma protuberans - report of a case

Evrim Ozmen[1], Güven Güney[2], Oktay Algin[1]

[1] Department of Radiology, [2] Department of Pathology, Ataturk Training and Research Hospital, Bilkent, Ankara, Turkey

Radiol Oncol 2013; 47(3): 244-246.

Received 21 April 2012
Accepted 30 September 2012

Correspondence to: Evrim Ozmen, Department of Radiology, Ataturk Training and Research hospital, 06050, Ankara, Turkey. Phone: +903 122238130; Fax: +903 122912707; E-mail: evrimkilicdr@gmail.com

Disclosure: No potential conflicts of interest were disclosed.

Background. Dermatofibrosarcoma protuberans (DFSP) of the vulva is a rare low-grade soft tissue sarcoma. Magnetic resonance imaging (MRI) findings of vulvar DFSP were essentially unreported in the literature.

Case report. We report a DFSP of vulva with its clinical, histological and MRI features. As far we know this is the first case of histologically confirmed vulvar DFSP presenting with MR images. The diagnosis of DFSP is usually made by histopathologic and clinical findings.

Conclusions. MRI is useful both for the diagnosis of DFSP and following up the patients since it has high soft tissue resolution and no risk of radiation exposure. With MRI the relation to the adjacent anatomical structures, extension and depth of the tumour and possible lymph node involvement can also be demonstrated.

Key words: dermatofibrosarcoma protuberans; imaging features; MRI; vulvar sarcoma; vulvar carcinoma

Introduction

Dermatofibrosarcoma protuberans (DFSP) is a rare low-grade soft tissue sarcoma that occurs in dermis and usually invades the subcutaneous tissue and muscles.[1] The incidence of DFSP is approximately 0.1% of all tissue cancers and 5-6% of all soft tissue sarcomas.[2,3] As far as we know only 28 cases with vulvar DFSP were reported.[2,3] However, detailed magnetic resonance imaging (MRI) findings of vulvar DFSP were essentially unreported in the literature.[1] Here in we report a DFSP of vulva with its clinical, pathological and MRI features.

Case report

A 60-year-old woman complaining of slowly growing foci of nodular mass extending beyond left vulva towards the left groin was admitted to our hospital. Physical examination revealed an approximately 6 cm erythematous plaque. MRI including T1 and T2 weighted (W), short tau inversion recovery (STIR) and contrast enhanced fat-suppressed T1W sequences were performed. On T1W sequence, the lesion was hypo intense; on T2W and STIR sequences it was hyper intense and after the administration of contrast-material it was enhanced heterogeneously (Figure 1). There was a lipomatous area at the centre of the lesion on all of the sequences. The contour of the lesion was irregular with spicular extension to the adjacent fat tissue. The lesion was limited with the subcutaneous fat tissue.

The patient was operated. Wide resection was performed and rectus abdominis muscle-skin flap was adapted to the defect area. Histologic examination revealed a tumour specimen in a storiform and honeycomb pattern which was stained positive for CD 34 and vimentin indicating DFSP (Figure 2). The patient was followed up by regular dressing and she was discharged with recommendations. At the control of the second year the patient had no complaint. Control MRI images demonstrated post-operative changes and there was no MRI signs of illness relapse (Figure 3).

Discussion

DFSP is a rare low grade soft tissue malignancy and is characterized by local invasion and recurrence.[1] Males and females are affected equally.[1-3] Although DFSP can occur in all ages, it most commonly occurs in young and middle aged people especially in fourth decade.[2] DFSP may involve any part of the body but is mostly seen in trunk (42–62%).[1-3] It occurs on extremities in 16% to 30% of cases, followed by head and neck (10–16%).[3] Involvement of the vulva is extremely rare.[1,2]

American Musculoskeletal Tumour Society set a staging system considering the tumour grade and compartment.[4] According to this system; stage IA represents the tumours that are low-grade intracompartmental lesions without involvement of subcutaneous compartment. In stage IB, tumours are low-grade extra-compartmental lesions which extend beyond to the underlying fascia, muscle, or bone.[4] According to German Guidelines for DFSP; stage I represents locally invasive primary tumour, stage II indicates regional lymph node metastases and stage III describes distant metastases.[5] In our patient DFSP was stage IA according to American Musculoskeletal Tumour Society staging system as we , myxoid, giant cell angiofibroma, palisaded (reminiscent of schwannoma), atrophic, fibrosarcomatoid, mixed, granular cell and sclerosing type.[6,7] DFSP is composed of spindled cells in a storiform pattern and infiltrates the surrounding subcutaneous fat. It stains strongly with CD 34 and vimentin as seen on immune-histochemical studies in our case.[3,8]

DFSP may be asymptomatic with its characteristic clinical appearance as an irregular flesh-coloured, reddish-brown to bluish nodule or violaceous plaque. It usually occurs as a solitary lesion but multiple foci could be seen.[3,8] In our patient, there were multiple primary lesions that extend between the left vulva and left groin with total size of 6 cm.

DFSP could dedifferentiate to the high grade sarcomas with an increased risk of local recurrence and metastasis. Advanced age, high mitotic index and increased cellularity are associated with poor outcome as well.[3] Our patient had a history of recurrences but had no metastases.

Ultrasonography (US) or computed tomography (CT) could demonstrate DFSP as a heterogeneous subcutaneous solid mass with spiculated or lobulated margins.[2,4,5,9] MRI can show the extension and depth of the lesion with its relation to the adjacent structures.[1,9] The impact of MRI in DFSP was first described by Kransdorf in 1994.[9] Up to now, Kransdorf and Meis-Kindbom reported eleven cases and Torreggiani reported another ten patients with MR imaging findings.[1,9] However, to the best of our knowledge in the literature there is only one DFSP case of the vulva mentioned with MR examination but without added MR image or mentioned MRI features of the lesion in the report.[10]

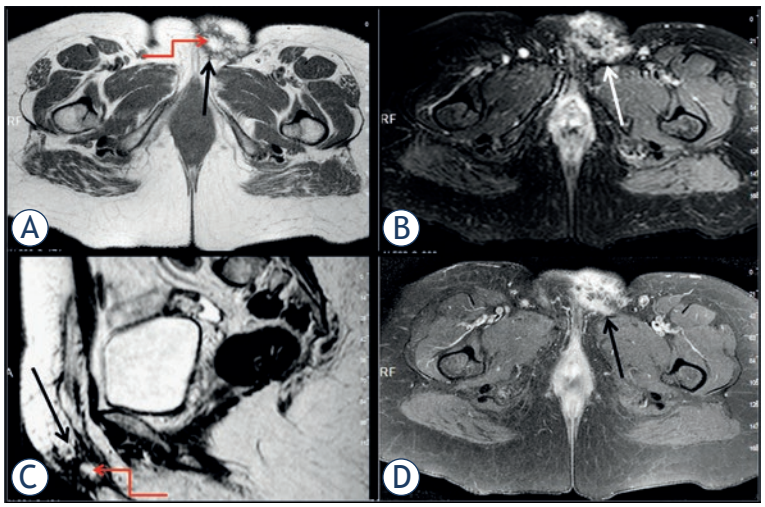

FIGURE 1. Axial T1W **A.**, axial STIR **B.**, sagittal T2W **C.**, and axial contrast enhanced T1W **D.** images. A lesion located at the vulva with irregular contours and spicular extension to the adjacent subcutaneous fat tissue (arrows). Lipomatous area at the centre of lesion (curved arrows **A.** and **C.**). Multiple foci with variable signal characteristics and fibrotic changes around the lesion. Marked contrast-material enhancement of the lesion after intravenous administration of the contrast media (arrow, **D.**).

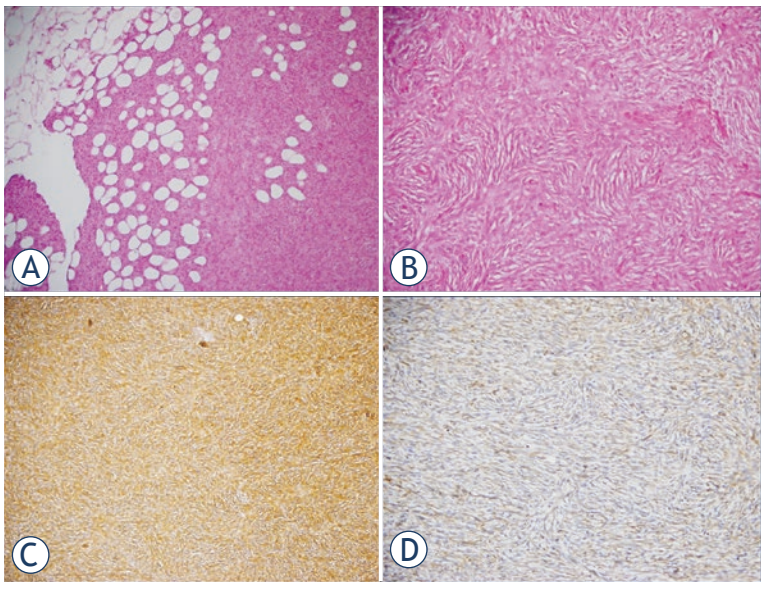

FIGURE 2. Photomicrographs of the patient. Honeycomb pattern interdigitates with lobules of subcutaneous fat (H and E, ×100) **A.** Uniform population of slender fibroblasts arranged in storiform pattern (H and E, ×200) **B.** Diffuse cytoplasmic CD34 (C; H and E, ×100) and vimentin (D; H and E, ×200) positivity **C., D.**

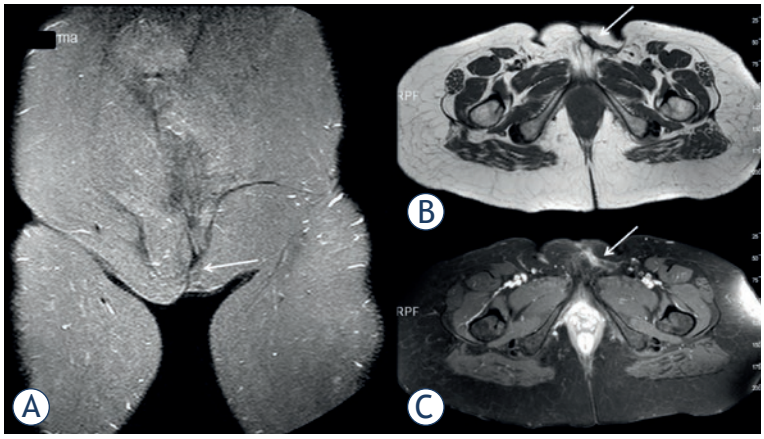

FIGURE 3. Coronal STIR **A.**, axial T1W **B.**, and axial contrast enhanced T1W **C.** MR images obtained 2 years after the surgery: postoperative changes in the operation area (arrows), no sign detected related to the recurrence.

DFSP is frequently iso intense or hypo intense to muscle on T1W images, and iso intense or hyper intense on T2W sequences. The margin of the lesion is best seen on short tau inversion recovery (STIR) sequences. On contrast-material enhanced images, it enhances heterogeneously due to the foci of haemorrhage, myxoid change, and tumour necrosis.[1,10] We detected an intensive heterogeneous contrast enhancement on fat suppressed contrast-material enhanced T1W images consistent with the literature. This finding may indicate the hyper vascularity of tumour.

All of the preoperative MR sequences of the presented patient demonstrated that the contour of the lesion was irregular and there were some multiple millimetres' foci with variable signal characteristics. We believed that these foci represented the haemorrhage, myxoid change, and/or tumour necrosis as reported in the literature. Besides, the existence of lipomatous area at the centre of the lesion could be important in the diagnosis of DFSP as in our case. All of these mentioned MRI findings which were not clearly indicated in literature could be useful in differentiating DFSP from the other soft tissue sarcomas, but however it can overlap.[1,9]

DFSP can also be distinguished from other soft tissue since it is generally a large-sized tumour, it has suspicious deeper component, and it has history of recurrent lesion and recurrent excision with positive surgical margins.[3,7,10]

DFSP of our patient had the characteristic clinical appearance and it was diagnosed by histological examinations after the patient was operated. Thus, we performed only MRI after the physical examination since US or CT was unnecessary for our patient.

A wide surgical resection with a margin of 2–3 cm of normal tissue is recommended as the optimal treatment for both primary and recurrent DFSP. Mohs micrographic surgery has presented as an alternative approach as well. Wide surgical resection with skin-muscle flapping was preferred for our patient.

Conclusions

DFSP of vulva is a rare low grade soft tissue sarcoma. The diagnosis is usually made by histological examinations after suspecting clinical findings. Radiologic examinations are necessary in some conditions including large tumour size, suspicious deeper component, recurrent tumours, critical locations and recurrent excision of DFSPs with positive surgical margins. MR is the most appropriate radiologic methods since it has good soft tissue contrast resolution can demonstrate the relation to the adjacent anatomical structures, extension and depth of the tumour and show the possible lymph node involvement. Also it is useful as a follow up method.

References

1. Torreggiani WC, Al-Ismail K, Munk PL, Nicolaou S, O'Connell JX, Knowling MA. Dermatofibrosarcoma protuberans: MR imaging features. *AJR Am J Roentgenol* 2002; **178:** 989–93.
2. Liu SZ, Ho TL, Hsu SM, Zhan HL, Chou CP. Imaging of dermatofibrosarcoma protuberans of breast. *Breast J* 2010; **16:** 541-3.
3. Hammonds LM, Hendi A. Dermatofibrosarcoma protuberans of the vulva treated using mohs micrographic surgery. *Dermatol Surg* 2010; **36:** 558-63.
4. Mendenhall W, Zlotecki R, Scarborough M. Dermatofibrosarcoma protuberans. *Cancer* 2004; **101:** 2503-8.
5. Ugurel S, Kortmann RD, Mohr P, Mentzel T, Garbe C, Breuninger H. Dermatofibrosarcoma protuberans: Short German guidelines. *J Dtsch Dermatol Ges* 2008; **6:** 17-8.
6. Angouridakis N, Kafas P, Jerjes W, Triaridis S, Upile T, Karkavelas G, et al. Dermatofibrosarcoma protuberans with fibrosarcomatous transformation of the head and neck. *Head Neck Oncol* 2011; **3:** 5.
7. Bergin P, Rezaei S, Lau Q, Coucher J. Dermatofibrosarcoma protuberans, magnetic resonance imaging and pathological correlation. *Australas Radiol* 2007; **51:** B64-6.
8. Lee SJ, Mahoney MC, Shaughnessy E. Dermatofibrosarcoma protuberans of the breast: imaging features and review of the literature. *AJR Am J Roentgenol* 2009; **193:** W64-9.
9. Krandorf Kransdorf MJ. Meis-Kindblom JM. Dermatofibrosarcoma protuberans: Radiologic appearance. *AJR Am J Roentgenol* 1994; **163:** 391-4.
10. Ohlinger R, Kühl A, Schwesinger G, Bock P, Lorenz G, Köhler G. Dermatofibrosarcoma protuberans of the vulva. *Acta Obstet Gynecol Scand* 2004; **83:** 685–6.

research article

The potential value of the neutral comet assay and γH2AX foci assay in assessing the radiosensitivity of carbon beam in human tumor cell lines

Jin Zhao[1*], Zhong Guo[1*], Hong Zhang[2], Zhenhua Wang[3], Lei Song[1], Jianxiu Ma[1], Shuyan Pei[1], Chenjing Wang[1]

[1] Medical College of Northwest University for Nationalities, Lanzhou 730030, PR China
[2] Institution of Modern Physics, Chinese Academy of Science, Lanzhou 730000, PR China
[3] School of Life Sciences, Yantai University, Yantai, 264005, PR China

Radiol Oncol 2013; 47(3): 247-257.

Received 21 November 2012
Accepted 19 May 2013

Correspondence to: Prof. Jin Zhao, PhD, Medical College of Northwest University for Nationalities, Lanzhou 730030, PR China.
Phone/Fax: +86 931 293 8152; E-mail: gz6768@163.com

* The authors contributed equally

Disclosure: No potential conflicts of interest were disclosed.

Background. Carbon ions ($^{12}C^{6+}$) are high linear energy transfer (LET) radiation characterized by higher relative biological effectiveness than low LET radiation. The assessment of tumour radiosensitivity would be particularly useful in optimizing the radiation dose during radiotherapy. The aim of the current study was to evaluate the potential value of the neutral comet assay and γH2AX foci assay in assessing $^{12}C^{6+}$ radiosensitivity of tumour cells.

Materials and methods. The doses of $^{12}C^{6+}$ and X-rays used in the present study were 2 and 4 Gy. The survival fraction, DNA double-strand breaks (DSB) and repair kinetics of DSB were assayed with clonogenic survival, neutral comet assay and γH2AX foci assay in human cervical carcinoma HeLa cells, hepatoma HepG2 cells, and mucoepidermoid carcinoma MEC-1 cells at the time points of 0.5, 4, 16 and 24 h after $^{12}C^{6+}$ and X-rays irradiation.

Results. The survival fraction for 12C6+ irradiation was much more inhibited than for X-rays ($p < 0.05$) in all three tumour cell lines tested. Substantial amounts of residual damage, assessed by the neutral comet assay, were present after irradiation ($p < 0.05$). The highest residual damage was observed at 0.5 or 4 h, both for $^{12}C^{6+}$ and X-ray irradiation. However, the residual damage in HeLa and MEC-1 cells was higher for $^{12}C^{6+}$ than X-rays ($p < 0.05$). The strongest induction of γH2AX foci was observed after 30 min, for all three tumour cell lines ($p < 0.01$). The franction of γH2AX foci persisted for at least 24 h after $^{12}C^{6+}$ irradiation; in HeLa cells and MEC-1 was higher than after X-ray irradiation ($p < 0.05$). The correlation coefficients between the clonogenic survival, neutral comet assay and γH2AX foci assay were not statistically significant, except for some tumour cells at individual irradiation doses and types.

Conclusions. Our study demonstrated that the neutral comet assay and γ-H2AX foci assay could be used to assess the radiosensitivity of $^{12}C^{6+}$ in human tumour cells.

Key words: human tumour cells; carbon ions; X-rays; radiation sensitivity; DNA double strand breaks; γH2AX

Introduction

Due to their physical and radiobiological properties, high linear energy transfer (LET) radiation qualities are of special interest for tumour therapy. Carbon ions radiotherapy has the potential to broaden the spectrum of primary radiotherapy, as first reports on favourable results for 'radio-resistant tumours' like primary renal cell carcinoma have become available and particle irradiation was shown to suppress metastatic potential of cancer cells.[1,2]

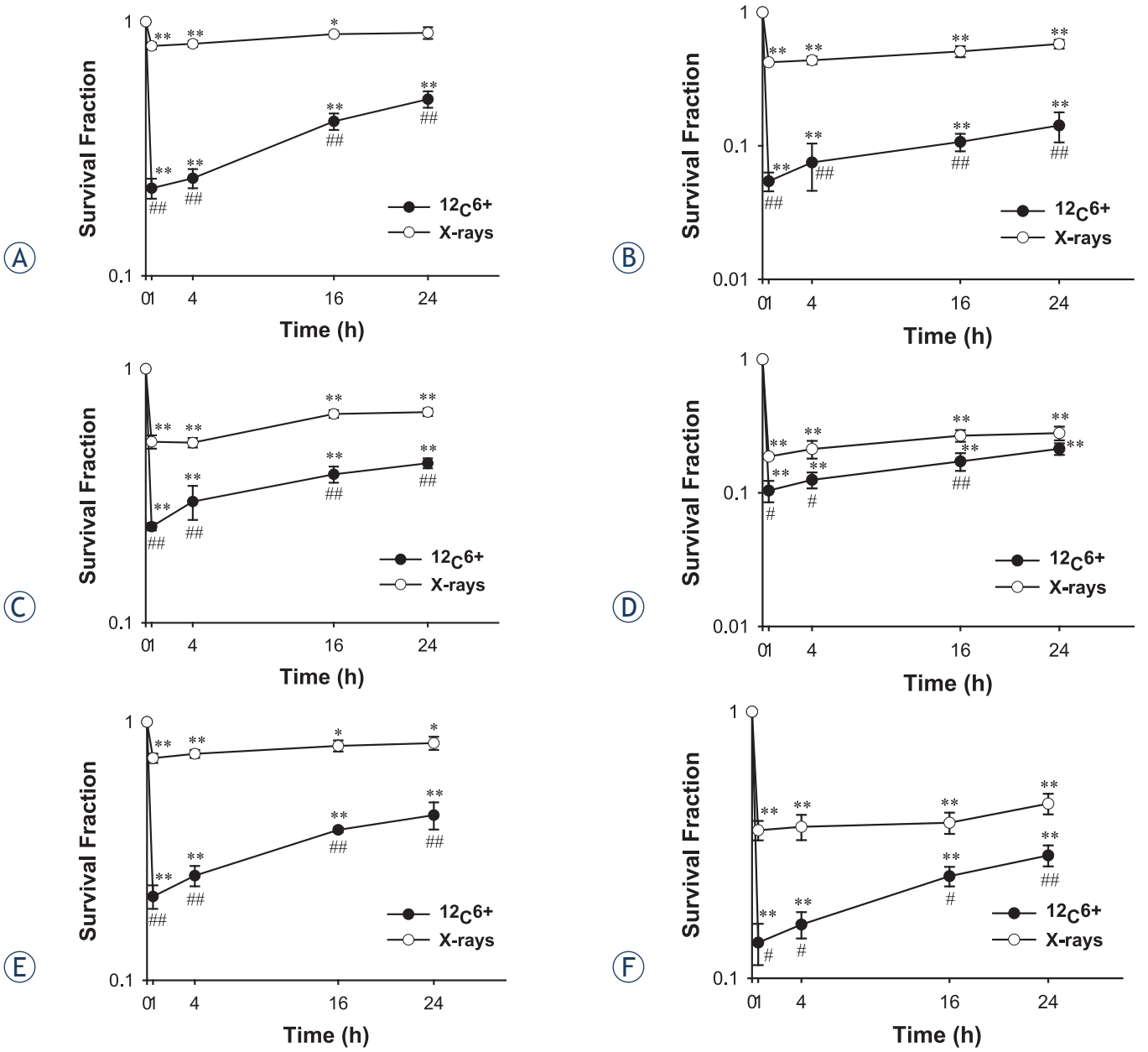

FIGURE 1. A survival curve for the Hela,HepG2 and MEC-1 cell lines, as determined by clonogenic assay. Exponentially growing cells were plated and irradiated, the cells were taken at the indicated time intervals after irradiation of $^{12}C^{6+}$ and X-rays and a clonogenic assay was performed. The means and SD are shown for three independent experiments with 4 replicates in each experiment. Untreated cells served as a control. After incubation for two weeks, colonies with cells greater than 50 were counted (**A.** Hela-2Gy; **B.** Hela-4Gy; **C.** HepG2-2Gy; **D.** HepG2-4Gy; **E.** MEC-1-2Gy; **F.** MEC-1-4Gy.)

*: *P*<0.05 *vs.* 0Gy irradiation; **: *P*<0.01 *vs.* 0Gy irradiation; #: *P*<0.05 *vs.* the same dose x-rays irradiation; ##: *P*<0.01 *vs.* the same dose x-rays irradiation.

In order to obtain more insight into this promising strategy some features of the underlying molecular mechanisms inducing the cellular response to carbon ions radiation are currently analyzed. Ionizing radiation causes various DNA lesions such as base damage, DNA-protein cross-links, DNA single-strand breaks and DNA double-strand breaks (DSB). An important prerequisite for a better understanding of such high- LET radiation on the DNA is the mechanistic description of the processing of DSB. It is well-known that the extremely large localized energy deposition and energy ions can lead to particularly complex types of DSB.[3] Although these effects can lead to cell death, mutations, genomic instability, or carcinogenesis, problems associated with the repair of the high-LET induced DSB are not fully understood.

An estimation of the DNA damage would seem a likely surrogate marker for radiosensitivity because DNA is considered as a primary target of ionizing radiation. The comet assay, which is widely used to quantify DNA damage after exposure to various genotoxic agents, can be a fast and reliable assay system for determining cellular radiosensitivity. Many reporters also have shown that there was a close correlation between γH2AX residual foci and radiosensitivity in some tumour cell lines and γH2AX foci could be used as a sensitive detector of low dose ionizing radiation. The clonogenic assay is the gold standard technique in determining the cellular radiosensitivity. Attempts have been made in the past to correlate DNA damage with the clonogenic survival of the tumour cells using the comet assay and γH2AX assay.[4,5] However, this correlation was not profound, observed in tumour cells with carbon ions ($^{12}C^{6+}$) irradiation, suggesting for more studies in this direction for the potential application of the comet assay and γH2AX foci assay in determining the $^{12}C^{6+}$ radiosensitivity of tumour cells.

In the present study, the neutral comet assay and γH2AX foci assay were evaluated for their usefulness in assessing radiosensitivity and the correlation between clonogenic survival, neutral comet assay and γH2AX foci assay in human cervical carcinoma Hela cells, hepatoma HepG2 cells and mucoepidermoid carcinoma MEC-1 after irradiation with $^{12}C^{6+}$ as compared to X-rays. Our studies emphasize the usefulness of the neutral comet assay and γH2AX foci assay in the assessment of the $^{12}C^{6+}$ radiosensitivity of tumour cells.

Materials and methods

Cell lines and treatments

Human cervical carcinoma HeLa cell and human hepatoma HepG2 cell were purchased from shanghai institute of biochemistry and cell biology. Human mucoepidermoid carcinoma MEC-1 cell was purchased from School of Stomatology Fourth Military Medical University. The cells were routinely subcultured in Dulbecco's Modified Eagle Medium (DMEM) (GIBCO, USA), containing 10% newborn calf serum, 100U/mL penicillin, 125 ug/mL streptomycin, and 0.03% glutamine. Exponentially growing cells were seeded at 2×10^4 cells/100 mm dish and were exposed to different dose of carbon ions ($^{12}C^{6+}$) or X-rays. Immediately following irradiation medium was quickly removed and cells were then incubated for various time intervals at 37°C to allow repair.

Irradiation using carbon ions beam and X-rays

Carbon ions beam was supplied by the Heavy Ion Research Facility in Lanzhou (HIRFL) at the Institute of Modern Physics, Chinese Academy of Sciences (IMP-CAS). Cell exposures were conducted at the therapy terminal of the HIRFL, which had a vertical beam line. Due to the energy degradation by the vacuum window, air gap, Petri dish cover and medium, the energy of the ion beam on cell samples was calculated to be 300 Mev/u, corresponding to a LET of 15 keV/um and the dose rate was adjusted to be about 0.4 Gy/min. The ion beam was calibrated by absolute ionization chamber. The tumour cells were irradiated by plateau of carbon ions LET curve and the dose of scatter off the walls of the plate has been calculated and incorporated into the total dose. The acquisition of the data (preset numbers converted to absorbed dose of particle radiation) was automatically obtained using a microcomputer during irradiation.

Low-LET irradiations were performed using Faxitron Cabinet X-ray System, (Model RX-650, 130kVp, 5mA, USA) operated at 100 kVp. The dose rate was approximately 1.38 Gy/min and the dose used for each irradiation ($^{12}C^{6+}$ or X-rays) was 0,2 and 4 Gy. All irradiations were performed once for each dish of cells at room temperature on the same day.

Clonogenic survival assays

The cells were cultured for 0.5, 4, 16 and 24 h after irradiation and then were washed with phosphate-buffered saline, trypsinized, and counted using a Coulter counter, replated at a density of 5×10^2 ~ 3×10^4 cells in duplicate using 100 mm dishes for cell-survival assays. Plates were stained and colonies were counted two weeks later. Counts from the two plates were averaged, and surviving fraction was calculated as the ratio of the plating efficiency of the treated cells divided by the plating efficiency of the control cells. Experiments were repeated 3-4 times.[6] The survival fraction was calculated using the following formula:

$$\text{Survival fraction} = \frac{\text{no.of colonies}}{\text{no.of cells plated} \times (\text{plating efficiency}/100)}$$

Double-strand break detection using the neutral comet assay

The neutral comet assay was used as described previously.[7] After the trypsin treatment to produce

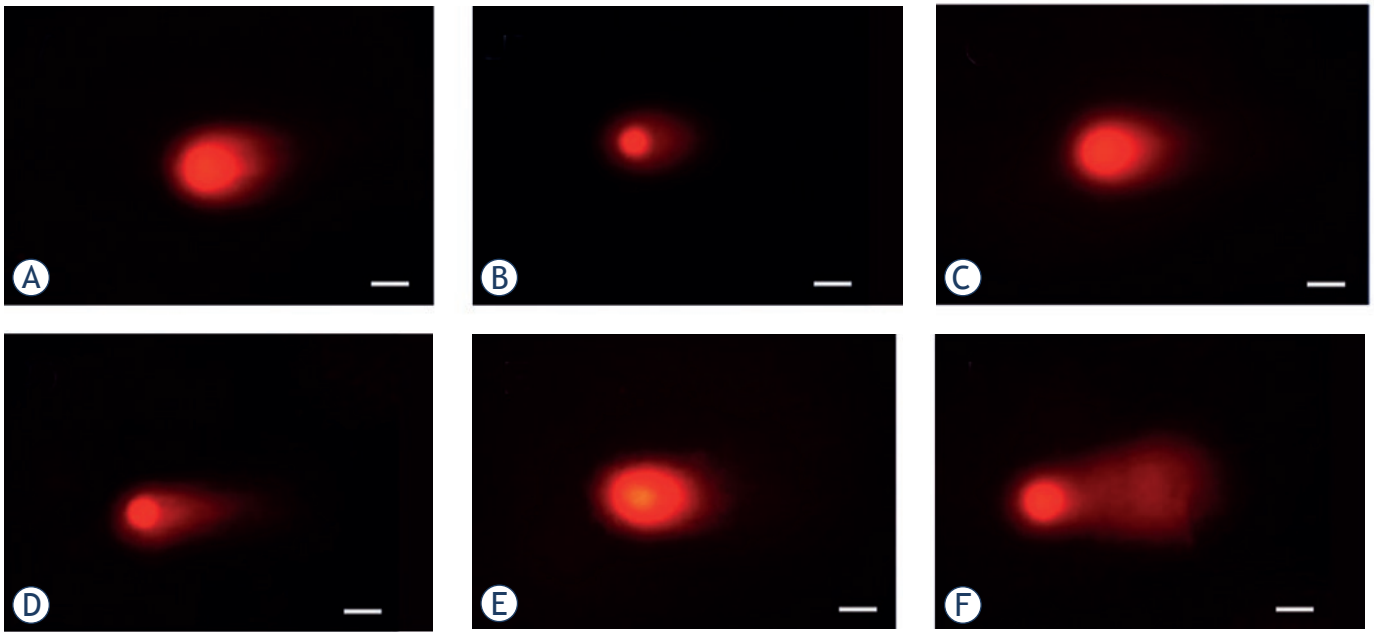

FIGURE 2. Comet images of DSB detected by neutral comet assay 4 h post-irradiation of $^{12}C^{6+}$ (**A.** Hela-Control; **B.** Hela-4Gy; **C.** HepG2-Control; **D.** HepG2-4Gy; **E.** MEC-1-Control; **F.** MEC-1-4Gy. Scale bar, 50um).

a single cell suspension, approximately 1.5×10^4 cells were embedded in 0.75% low-gelling-temperature agarose and rapidly pipetted onto a precoated microscope slide. Samples were lysed for 4 h at 50°C in 0.5% SDS, 30 mM EDTA, pH 8.0. After rinsing overnight at room temperature in Tris/borate/ EDTA buffer, pH 8.0, samples were electrophoresed for 25 min at 0.6 V/cm, then stained with propidium iodide. Slides were viewed using a fluorescence microscope with a CCD camera, and 150 individual comet images were analyzed from each sample for tail moment, DNA content, and percentage DNA in tail using CASP software (www.casplab.com). CASP is a tool to image analysis in comet assay. An unlimited number of images can be marked, CASP could load them successively into an "image view" window. Only comets oriented from left (head) to right (tail) can be analyzed correctly. In addition to such parameter as head radius, tail length etc., the program calculates the tail moment (TM) and the Olive tail moment (OTM). Three independent experiments were performed.

Immunofluorescence microscopy for γH2AX

Immunofluorescent microscopy was conducted essentially as described earlier with some modifications.[8] Briefly, 2×10^4 cells were seeded into 35 mm dishes containing a glass cover slip in each well. After irradiation, slides were air-dried, and fixed for 30 min in 2% paraformaldehyde in TBS. Cells were rinsed in TBS, placed in -20°C methanol for 1 min, rinsed, then placed for 20 min in TBS plus 1% bovine serum albumin and 0.2% Tween-20 (TTN) and finally incubated for 2 h with diluted anti-phospho-histone H2AX (Ser-139) mAb (Upstate, Lake Placid, NY) diluted 1:500 in TTN. Slides were washed and incubated with FITC-conjugated anti-mouse goat F (ab') ^{2} fragment (DAKO, Carpinteria,CA) diluted 1:200 in TTN for 1 h at room temperature. Slides were rinsed and then immersed in 0.05 mg/mL DAPI for 15 min, rinsed and mounted with cover slips using 10 uL Fluorogard (Bio-Rad) as the antifade mounting medium, and sealed. To prevent bias in selection of cells that display foci, over 800 randomly selected cells were counted. Cells with three or more foci of any size were classified as positive. Experiments were repeated at least three times.

Statistical analysis

SPSS version 13.0 software program was employed for the statistical analysis. Data were expressed as mean ± standard error (SD). A two-tailed Student's t-test was also performed to compare the differences between 2 groups. The significance of the correlation coefficient was also calculated. A value of $P < 0.05$ was considered statistically significant.

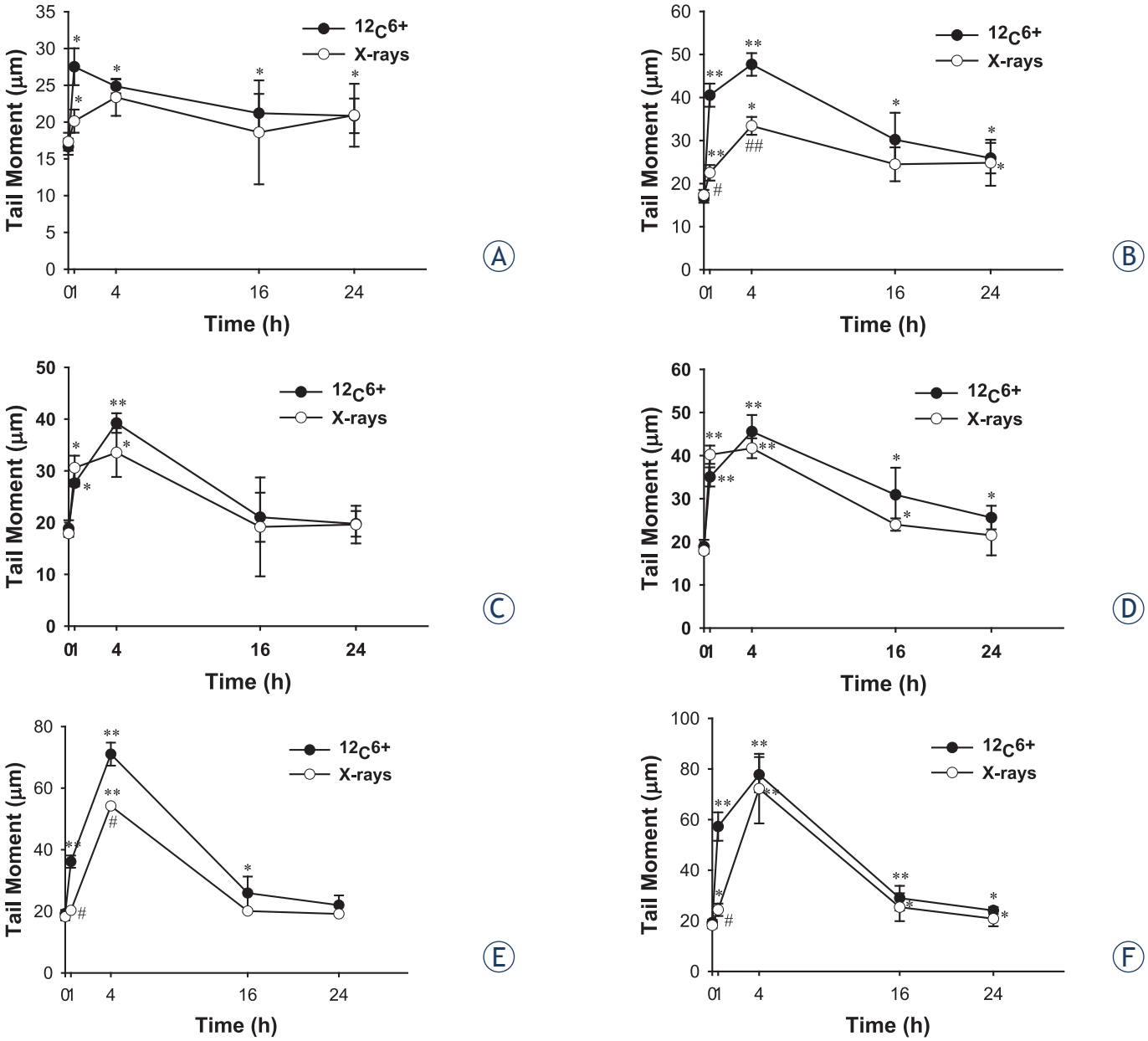

FIGURE 3. DNA damage induction and repair profiles measured by the neutral comet assay in Hela, HepG2 and MEC-1 cell lines irradiated with 2 and 4 Gy of $^{12}C^{6+}$ and X-rays in vitro. The extent of DNA damage was measured quantitatively by the comet tail moment (TM). Immediately after irradiation, the cell samples were placed at 37° C in a 5% CO2 incubator. The cells were taken at the indicated time intervals after $^{12}C^{6+}$ and X-rays exposure and subjected to the comet assay. The means and SD of TM are shown for three independent experiments with 2 replicates in each experiment. Thirty cells were analyzed for each slide (**A.** Hela-2Gy; **B.** Hela-4Gy; **C.** HepG2-2Gy; **D.** HepG2-4Gy; **E.** MEC-1-2wGy; **F.** MEC-1-4Gy.)

*: P<0.05 vs. 0Gy irradiation; **: P<0.01 vs. 0Gy irradiation; #: P<0.05 vs. the same dose x-rays irradiation; ##: P<0.01 vs. the same dose x-rays irradiation.

Results

Growth dynamics of colony survival assay

Colony assay experiments were performed to compare the differences in terms of the clonogenic growth dynamics of $^{12}C^{6+}$ and X-rays (Figure 1). Clonogenics cells were inactivated immediatedly, but in turn, significantly increased during 24 h after $^{12}C^{6+}$ and X-rays irradiation ($p < 0.05$). At each time point after irradiation, the increase in the survival for $^{12}C^{6+}$ was much more inhibited rather than for X-rays ($p < 0.05$), except for HepG2 cell at 4 Gy irradiation ($p > 0.05$, 24 h). For Hela cells after 2 Gy X-rays irradiation, the survival fraction almost reached the control level at 24 h ($p > 0.05$), however, the survival fraction for $^{12}C^{6+}$ was still lower ($p < 0.01$).

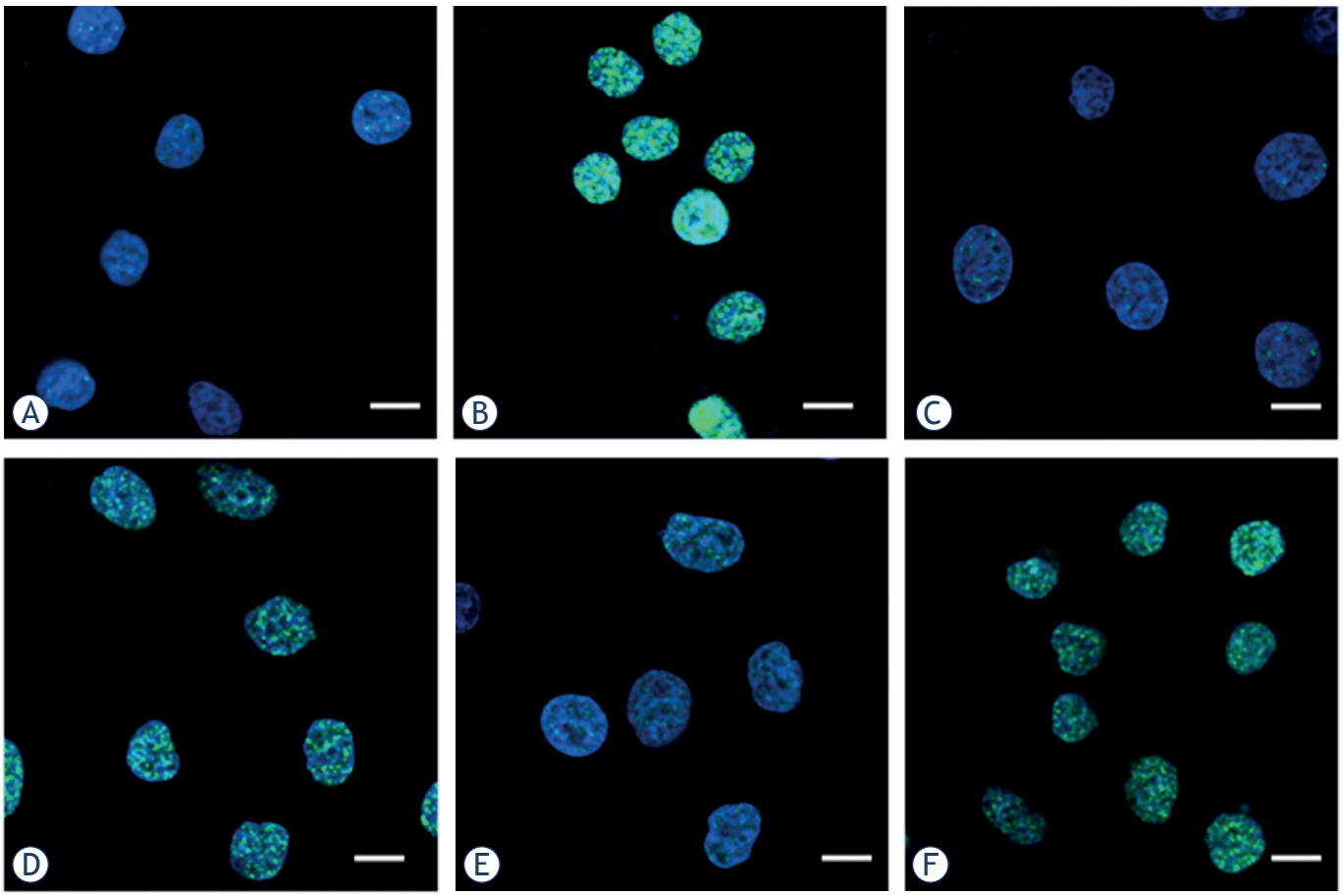

FIGURE 4. Digitized images of γH2AX foci in Hela, HepG2 and MEC-1 cell lines. After exposure to 4 Gy $^{12}C^{6+}$ followed incubated for 30 min, cells were grown and irradiated on cover slips. DNA was stained with DAPI and γH2AX was detected using an Alexa488- conjugated secondary antibody after staining using a monoclonal anti-γH2AX antibody. (**A.** Hela-Control; **B.** Hela-4Gy; **C.** HepG2-Control; **D.** HepG2-4Gy; **E.** MEC-1- Control; **F.** MEC-1-4Gy. Scale bar, 15um)

Neutral comet assay

The neutral comet assays were applied to tumour cell lines exposed to $^{12}C^{6+}$ and X-rays and allowed 0.5, 4, 16 and 24 h for double strand break rejoining and then examined for DSB. Typical comet images were shown at Figure 2. The fraction of residual damage is given in Figure 3. Substantial amounts of residual damage were present for tumour cells after irradiation ($p < 0.05$) and the highest residual damage was almost all shown at 0.5 or 4 h either for $^{12}C^{6+}$ or X-rays. After 0.5 or 4 h of irradiation, the residual damages, contained in HeLa cells and MEC-1, was higher for $^{12}C^{6+}$ than for X-rays ($p < 0.05$).

Immunofluorescence staining of phosphorylated H2AX foci

Since DSB are the primary toxic lesions induced by radiation, the number of DSB was scored by examining the foci of phosphorylated H2AX in irradiated cells. γH2AX foci were observed with anti-γH2AX antibodies (green) and the nuclei were stained with DAPI (blue). Typical images of $^{12}C^{6+}$ and X-rays induced γH2AX foci are shown in Figure 4. The formation of γH2AX foci in untreated cells was kept at lower levels and no significantly difference was seen between cell lines and culture times (data not shown). After 30 min of radiation, γH2AX foci, visualized as bright spots, were present in all the cells. The time-dependent induction of γH2AX foci by $^{12}C^{6+}$ and X-rays were counted in all tumour cell lines. It was noted the strongest inductions of γH2AX foci at 0.5 h for all three tumour cell lines ($p < 0.01$) and then decreased over time. A fraction of γH2AX foci persisted for at least 24 h after $^{12}C^{6+}$ radiation in HeLa cells (2 and 4 Gy) and MEC-1 (4 Gy), in contrast to foci induced by X-rays that had a lower level after 24 h ($p < 0.05$, Figure 5).

TABLE 1. Correlation coefficient obtained from TM by correlating expression with the SF

Cell lines	X-ray/$^{12}C^{6+}$(2Gy)		X-ray/$^{12}C^{6+}$(4Gy)	
	r-values	P-values	r-values	P-values
Hela	-0.447/-0.934	0.55/0.07	-0.270/-0.847	0.73/0.15
HepG2	-0.987/-0.641	**0.01**/0.36	-0.956/-0.758	**0.04**/0.24
MEC-1	-0.377/-0.647	0.62/0.35	-0.402/-0.874	0.60/0.13

TABLE 2. Correlation coefficient obtained from γH2AX by correlating expression with the SF

Cell lines	X-ray/$^{12}C^{6+}$(2Gy)		X-ray/$^{12}C^{6+}$(4Gy)	
	r-values	P-values	r-values	P-values
Hela	-0.945/-0.987	0.05/**0.01**	-0.894/-0.892	0.11/0.11
HepG2	-0.935/-0.948	0.06/0.05	-0.936/-0.870	0.06/0.13
MEC-1	-0.973/-0.976	**0.03**/**0.02**	-0.989/-0.773	**0.01**/0.23

TABLE 3. Correlation coefficient obtained from TM by correlating expression with the γH2AX

Cell lines	X-ray/$^{12}C^{6+}$(2Gy)		X-ray/$^{12}C^{6+}$(4Gy)	
	r-values	P-values	r-values	P-values
Hela	0.242/0.872	0.76/0.13	0.232/0.776	0.77/0.22
HepG2	0.892/0.818	0.11/0.18	0.957/0.736	**0.04**/0.26
MEC-1	0.519/0.743	0.47/0.26	0.452/0.607	0.55/0.39

The correlation between the clonogenic survival, neutral comet assay and γH2AX foci in $^{12}C^{6+}$ and X-rays irradiated tumour cells

A negative correlation was observed between the clonogenic survival and tail moment assessed by neutral comet assay. The negative correlation was also shown between the clonogenic survival and γH2AX foci. However, a positive correlation was shown between the tail moment and γH2AX foci. However, the correlation coefficients for the most parameters we used, such as different doses and irradiated types, were not statistically significant ($P > 0.05$, Tables 1, 2 and 3).

Discussion

In general, it is believed that the DNA damage induced by high-LET heavy ions radiation is more complex than that by X- or gamma rays and leads to more severe biological consequences including cell death, mutation and transformation.[9,10] This complex DNA damage is also referred to as clustered damage or multiply damaged sites, which was originally introduced by Ward.[11-13] These damages could be generated during the processing period of the initially induced DNA lesions. Ionizing radiation even at low doses such as 1 Gy could induce this kind of damage, and with high-LET radiation, the degree of complexity may increase depending on the LET of the particular radiation.[14] The clustered DNA damage is thought to be more difficult to repair when compared with simple or isolated DNA damage, probably because of retarded enzymatic activities leading to serious biological consequences.[15]

A substantial number of studies on DSB and its repair in cells exposed to high-LET heavy ions have been reported.[16,17] In general, DSB repair is inhibited as a function of LET (up to 200 keV/μm), and the degree of rejoining correlates with the cell survival. If the rejoining is inefficient, a high number of remaining DSB persist after irradiation, leading to a lower cell survival.

In the present study, radiosensitivities of different tumour cell lines to $^{12}C^{6+}$ and X-rays were established using the clonogenic assay and this was correlated with DSB and repair assessed by the

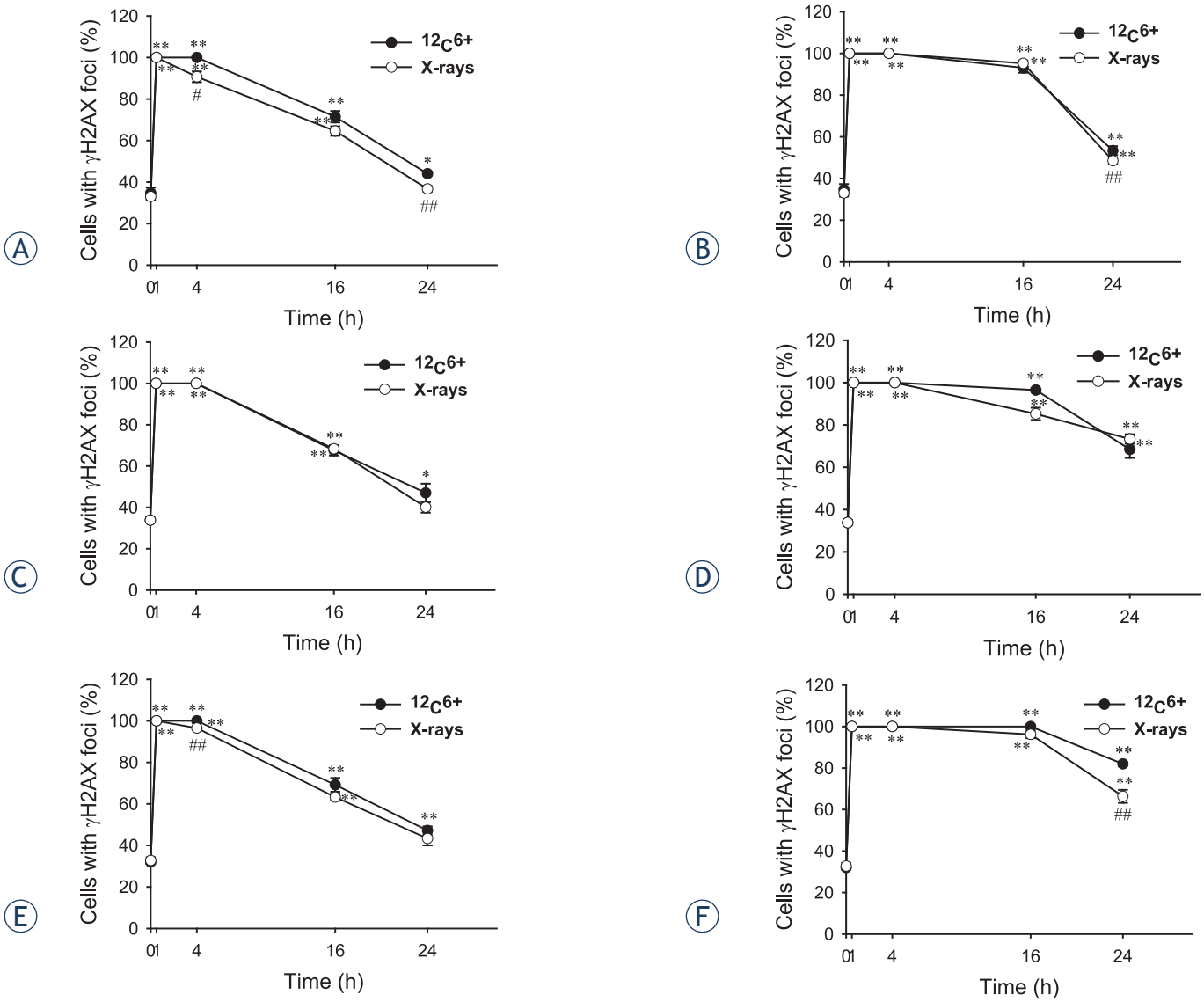

FIGURE 5. The percentage of γH2AX foci of Hela, HepG2 and MEC-1 cell lines after exposure to 2 and 4 Gy $^{12}C^{6+}$ and X-rays followed incubation for 0.5, 4, 16 and 24 h in *vitro*. Over 800 randomly selected cells were counted. Cells with three or more foci of any size were classified as positive. Results are the means and SD for three experiments (**A.** Hela-2Gy; **B.** Hela-4Gy; **C.** HepG2-2Gy; **D.** HepG2-4Gy; **E.** MEC-1-2Gy; **F.** MEC-1-4Gy).

*: P<0.05 vs. 0Gy irradiation; **: P<0.01 vs. 0Gy irradiation; #: P<0.05 vs. the same dose x-rays irradiation; ##: P<0.01 vs. the same dose x-rays irradiation.

neutral comet assay and γH2AX foci. We selected three tumour cell lines which were of different tissue origins. The different cell types were used to ensure that the assay was able to distinguish the radiosensitivity across different tumour types. In the clonogenic assay, a significantly survival inhibition was shown in $^{12}C^{6+}$ and X-rays irradiation over time (Figure 1). It, therefore, seemed reasonable to conclude that an early significant increase in the survival fraction within 24 h occurred after X-rays irradiation, whereas the increase in survival was inhibited after $^{12}C^{6+}$ irradiation. These results obviously showed that $^{12}C^{6+}$ was more cytotoxic than X-rays.

The comet assay can be used when combined with repair enzymes as damage probes to detect DSB for high-LET.[18-20] This method has been shown to correlate radiosensitivity with residual damage, measured at longer times after irradiation.[21] The assay requires little specialized equipment other than a microscope and under neutral conditions assesses primarily the repair of DSB. From

the DNA damage repair analysis, which was performed by measuring the DSB at different time intervals (0.5, 4, 16 and 24 h) and irradiation types, the differences of DSB depended on repair time and irradiation types. For example, the most severe damage was observed after 0.5 or 4 h repair and the damage decreased with time of repair. At 0.5 or 4 h, the residual damages contained in HeLa and MEC-1 cells were much higher for $^{12}C^{6+}$ compared to X-rays (Figure 3).

The results of the neutral comet assay were also compared with those of clonogenic assay in determining the radiosensitivity of the tumour cell lines for different irradiation types. For the three cell lines, the DNA repair kinetics after $^{12}C^{6+}$ and X-rays irradiation, as measured using the neutral comet assay, failed to strongly correlate with the radiosensitivity of clonogenicity, which is in agreement with some of the earlier reports but not with other studies.[4,22] Though DNA repair capacity is one major determinant of the radiosensitivity of the cell, a comet assay may not be sensitive enough to resolve the smaller differences in the residual DNA damage between the cell lines and irradiation types. Our results also showed that the tail moments of the comets had mostly returned to control by 24 h, whereas the survival fraction had not. The reason was that the higher doses (> 10 Gy) were usually used in comet studies, which was significantly higher than the dose range used for the cell survival.[23,24] For example, pulsed-field gel electrophoresis experiments have established that high LET radiation induces persistent DNA double-strand breaks for doses in the range of 25–80 Gy.[25,26] In the present study the doses of 2 and 4 Gy were used for both clonogenic assay and comet assay. The smaller doses usually produced lesser DSB results in the residual damages after 24h contained in cells almost could not be detected by the comet assay.

In 1998, Bonner's group identified a site in histone molecules, namely H2AX, which is phosphorylated after DSB is induced.[27] The ''so-called'' γH2AX assay was introduced to detect DSB by simply counting foci in cells using an antibody of γH2AX.[27-30] γH2AX foci along with other radiation induced foci (RIF) were also used to observe the spatial distribution of the radiation tracks from high-LET heavy ion particles.[31-35] Asaithamby *et al*. indicated that high- LET iron ions induced more clustered DNA damage than low-LET radiation; more colocalized foci from three markers were observed with iron ions.[36] They also showed that high- LET iron ions led to a significantly higher number of chromosome aberrations per mitotic cell than low-LET radiation.[36] Although many reporters have shown γH2AX foci could be used as a sensitive detector of low dose ionizing radiation, Tomohiro's research showed that there was not a close correlation between residual foci and radiosensitivity in some tumour cell lines which showed high expression of endogenous γH2AX foci.[37] In the present study, we firstly compared the background values of γH2AX in three tumour cell lines. The expression of endogenous γH2AX foci was lower and there was not a significant difference between the three tumour cell lines we used ($p > 0.05$). We, then, measured foci frequency for up to 24 h and found that a fraction of γH2AX foci persisted for at least 24 h after high LET carbon ions radiation in Hela and MEC-1 cells, in contrast to foci induced by X-rays that had a lower level after 24 h (Figure 5). This confirms the earlier studies that these persistent γH2AX foci as evidence of persistent DSB. Karlsson and Stenerlöw found persistent γH2AX foci for up to 24 h after 1 Gy of high LET nitrogen-ion irradiation in non-proliferating normal human fibroblasts.[38] Takahashi *et al*. showed a slower decrease in the γH2AX intensity using flow cytometry after exposure to 500 MeV/amu iron ions compared to X-rays irradiation in exponentially growing human AG01522 fibroblasts.[39] Desai *et al*. also showed a LET dependency for the disappearance of γH2AX clusters in confluent normal human fibroblasts between iron (176 keV/mm) and silicon (54 keV/mm) ions.[40] A recent study using γH2AX fluorescence indicated that high-LET carbon irradiation contributed significantly to the slow component of γH2AX loss kinetics than X-irradiation (80% after carbon irradiation vs. 47% after X-irradiation) confirming the complex nature of DSB by high-LET radiation.[41]

Some results showed the DNA damage measured right after X-rays exposure could be a better reflection of the radiosensitivity than the residual damage[5], however, for $^{12}C^{6+}$ irradiation, the results were not clear. For both $^{12}C^{6+}$ and X-rays irradiation, although our results clearly indicated that the γH2AX assay could predict the radiosensitivity of different tumour cells and irradiation types, which was not in line with the results of the clonogenic survival assay and tail moment of comet. This problem can be attributed to that for three tumour cells we used, the highest level of DSB were at 0.5 and 4 h for the comet assay and the strongest inductions of γH2AX foci were at 0.5 h for γH2AX assay, however, the lowest survival fractions should be right after the radiation exposure.

Conclusions

Our studies showed that the neutral comet assay and γH2AX assay could be used in assessing the radiosensitivity of tumour cells in $^{12}C^{6+}$ irradiation. However, to gain greater confidence in use of these techniques in determining the $^{12}C^{6+}$ radiosensitivity of tumour cells, a larger number of cell lines and validation in a clinical scenario using biopsy samples may be needed.

Acknowledgements

This work was supported in part by grants from the National Natural Science Foundation of China (Nos.31060127 and 81260442), Gansu Provincial Natural Science Foundation (No.1010RJZA078 and No.1208RJZA246) and the Project Sponsored by the Scientific Research Foundation for the Returned Overseas Chinese Scholars, State Education Ministry([2011]1568).

References

1. Nomiya T, Tsuji H, Hirasawa N, Kato H, Kamada T, Mizoe J, et al. Carbon ion radiation therapy for primary renal cell carcinoma: initial clinical experience. *Int J Radiat Oncol Biol Phys* 2008; **72:** 828-33.
2. Ogata T, Teshima T, Kagawa K, Hishikawa Y, Takahashi Y, Kawaguchi A, et al. Particle irradiation suppresses metastatic potential of cancer cells. *Cancer Res* 2005; **65:** 113-20.
3. Prise KM, Folkard M, Newman HC, Michael BD. Effect of radiation quality on lesion complexity in cellular DNA. *Int J Radiat Biol* 1994; **66:** 537-42.
4. El-Awady RA, Dikomey E, Dahm-Daphi J. Radiosensitivity of human tumour cells is correlated with the induction but not with the repair of DNA double-strand breaks. *Br J Cancer* 2003; **89:** 593-601.
5. Jayakumar S, Bhilwade HN, Pandey BN, Sandur SK, Chaubey RC. The potential value of the neutral comet assay and the expression of genes associated with DNA damage in assessing the radiosensitivity of tumor cells. *Mutat Res* 2012; **748:** 52-9.
6. Olive PL, Banáth JP, Durand RE. Development of apoptosis and polyploidy in human lymphoblast cells as a function of position in the cell cycle at the time of irradiation. *Radiat Res* 1996; **146:** 595-602.
7. Olive PL, Banáth JP, Durand RE. Heterogeneity in radiation-induced DNA damage and repair in tumor and normal cells measured using the "comet" assay. *Radiat Res* 2012; **178:** AV35-42.
8. Banuelos CA, Banáth JP, MacPhail SH, Zhao J, Reitsema T, Olive PL. Radiosensitization by the histone deacetylase inhibitor PCI-24781. *Clin Cancer Res* 2007; **13:** 6816-26.
9. Terato H, Tanaka R, Nakaarai Y, Nohara T, Doi Y, Iwai S, et al. Quantitative analysis of isolated and clustered DNA damage induced by gamma-rays, carbon ion beams, and iron ion beams. *J Radiat Res* 2008; **49:** 133-46.
10. Hada M, Georgakilas AG. Formation of clustered DNA damage after high-LET irradiation: a review. *J Radiat Res* 2008; **49:** 203-10.
11. Chatterjee A, Holley WR. Biochemical mechanisms and clusters of damage for high-LET radiation. *Adv Space Res* 1992; **12:** 33-43.
12. Ward JF. Biochemistry of DNA lesions. *Radiat Res Suppl* 1985; **8:** S103-11.
13. Ward JF. The complexity of DNA damage: relevance to biological consequences. *Int J Radiat Biol* 1994; **66:** 427-32.
14. Hada M, Sutherland BM. Spectrum of complex DNA damages depends on the incident radiation. *Radiat Res* 2006; **165:** 223-30.
15. Georgakilas AG, Bennett PV, Sutherland BM. High efficiency detection of bi-stranded abasic clusters in gammairradiated DNA by putrescine. *Nucleic Acids Res* 2002; **30:** 2800-8.
16. Rydberg B, Lobrich M and Cooper PK. DNA double-strand breaks induced by high-energy neon and iron ions in human fibroblasts. I. Pulsed-field gel electrophoresis method. *Radiat Res* 1994; **139:** 133-41.
17. Taucher-Scholz G, Heilmann J, Kraft G. Induction and rejoining of DNA double-strand breaks in CHO cells after heavy ion irradiation. *Adv Space Res* 1996; **18:** 83-92.
18. Ostling O, Johanson KJ. Microelectrophoretic study of radiationinduced DNA damages in individual mammalian cells. *Biochem Biophys Res Commun* 1984; **123:** 291-8.
19. Blaisdell JO, Wallace SS. Abortive baseexcision repair of radiation-induced clustered DNA lesions in Escherichia coli. *Proc Natl Acad Sci USA* 2001; **98:** 7426-30.
20. Holt SM, Georgakilas AG. Detection of complex DNA damage in gammair-radiated acute lymphoblastic leukemia Pre-b NALM-6 cells. *Radiat Res* 2007; **168:** 527-34.
21. Olive PL. Impact of the comet assay in radiobiology. *Mutat Res* 2009; **681:** 13-23.
22. Nahas SA, Davies R, Fike F, Nakamura K, Du L, Kayali R, et al. Comprehensive profiling of radiosensitive human cell lines with DNA damage response assays identifies the neutral comet assay as a potential surrogate for clonogenic survival. *Radiat Res* 2012; **177:** 176-86.
23. Iliakis G, Mehta R, Jackson M. Level of DNA double-strand break rejoining in Chinese hamster xrs-5 cells is dose-dependent: implications for the mechanism of radiosensitivity. *Int J Radiat Biol* 1992; **61:** 315-21.
24. Noguchi M, Yu D, Hirayama R, Ninomiya Y, Sekine E, Kubota N, et al. Inhibition of homologous recombination repair in irradiated tumor cells pretreated with Hsp90 inhibitor 17-allylamino-17-demethoxygeldanamycin. *Biochem Biophys Res Commun* 2006; **351:** 658-63.
25. Stenerlöw B, Höglund E, Carlsson J, Blomquist E. Rejoining of DNA fragments produced by radiations of different linear energy transfer. *Int J Radiat Biol* 2000; **76:** 549-57.
26. Rydberg B, Cooper B, Cooper PK, Holley WR, Chatterjee A. Dose-dependent misrejoining of radiation-induced DNA double-strand breaks in human fibroblasts: experimental and theoretical study for high- and low-LET radiation. *Radiat Res* 2005; **163:** 526-34.
27. Rogakou EP, Pilch DR, Orr AH, Ivanova VS, Bonner WM. DNA double-stranded breaks induce histone H2AX phosphorylation on serine 139. *J Biol Chem* 1998; **273:** 5858-68.
28. Rothkamm K, Lobrich M. Evidence for a lack of DNA double-strand break repair in human cells exposed to very low x-ray doses. *Proc Natl Acad Sci USA* 2003; **100:** 5057-62.
29. Kato TA, Nagasawa H, Weil MM, Genik PC, Little JB, Bedford JS. Gamma-H2AX foci after low-dose-rate irradiation reveal atm haploinsufficiency in mice. *Radiat Res* 2006; **166:** 47-54.
30. Kinner A, Wu W, Staudt C, Iliakis G. Gamma-H2AX in recognition and signaling of DNA double-strand breaks in the context of chromatin. *Nucleic Acids Res* 2008; **36:** 5678-94.
31. Desai N, Davis E, O'Neill P, Durante M, Cucinotta FA, Wu H. Immunofluorescence detection of clustered gamma-H2AX foci induced by HZE-particle radiation. *Radiat Res* 2005; **164:** 518-22.
32. Okayasu R, Okada M, Okabe A, Noguchi M, Takakura K, Takahashi S. Repair of DNA damage induced by accelerated heavy ions in mammalian cells proficient and deficient in the non-homologous endjoining pathway. *Radiat Res* 2006; **165:** 59-67.
33. Costes SV, Ponomarev A, Chen JL, Nguyen D, Cucinotta FA, Barcellos-Hoff MH. Image-based modeling reveals dynamic redistribution of DNA damage into nuclear sub-domains. *PLoS Comput Biol* 2007; **3:** e155.
34. Takahashi A, Yamakawa N, Kirita T, Omori K, Ishioka N, Furusawa Y, et al. DNA damage recognition proteins localize along heavy ion induced tracks in the cell nucleus. *J Radiat Res* 2008; **49:** 645-52.

35. Jakob B, Splinter J, Durante M, Taucher- Scholz G. Live cell microscopy analysis of radiation-induced DNA double-strand break motion. *Proc Natl Acad Sci USA* 2009; **106:** 3172-7.

36. Asaithamby A, Hu B, Chen DJ. Unrepaired clustered DNA lesions induce chromosome breakage in human cells. *Proc Natl Acad Sci USA* 2011; **108:** 8293-8.

37. Yoshikawa T, Kashino G, Ono K, Watanabe M. Phosphorylated H2AX foci in tumor cells have no correlation with their radiation sensitivities. *J Radiat Res* 2009; **50:** 151-60.

38. Karlsson KH, Stenerlöw B. Focus formation of DNA repair proteins in normal and repair-deficient cells irradiated with high-LET ions. *Radiat Res* 2004; **161:** 517-27.

39. Takahashi A, Yamakawa N, Kirita T, Omori K, Ishioka N, Furusawa Y, et al. DNA damage recognition proteins localize along heavy ion induced tracks in the cell nucleus. *J Radiat Res* 2008; **49:** 645-52.

40. Desai N, Davis E, O'Neill P, Durante M, Cucinotta FA, Wu H. Immunofluorescence detection of clustered gamma-H2AX foci induced by HZE-particle radiation. *Radiat Res* 2005; **164:** 518-22.

41. Schmid TE, Dollinger G, Beisker W, Hable V, Greubel C, Auer S, et al. Differences in the kinetics of gamma-H2AX fluorescence decay after exposure to low and high LET radiation. *Int J Radiat Biol* 2010; **86:** 682-91.

research article

Inhibition of cathepsin X enzyme influences the immune response of THP-1 cells and dendritic cells infected with *Helicobacter pylori*

Miha Skvarc[1], David Stubljar[1], Andreja Natasa Kopitar[1], Samo Jeverica[1], Bojan Tepes[2], Janko Kos[3, 4], Alojz Ihan[1]

[1] University of Ljubljana, Faculty of Medicine, Institute of Microbiology and Immunology, Ljubljana, Slovenia
[2] AM - Rogaska Diagnostic Centre, Rogaska Slatina, Slovenia
[3] Faculty of Pharmacy, University of Ljubljana, Ljubljana, Slovenia
[4] Department of Biotechnology, Jožef Stefan Institute, Ljubljana, Slovenia

Radiol Oncol 2013; 47(3): 258-265.

Received 8 April 2013
Accepted 11 May 2013

Correspondence to: Miha Skvarč, MD, Institute of Microbiology and Immunology, Faculty of Medicine, University of Ljubljana, Zaloška 4, SI - 1000 Ljubljana, Slovenia. E-mail: miha.skvarc@mf.uni-lj.si

Disclosure: No potential conflicts of interest were disclosed.

Background. The immune response to *Helicobacter pylori* importantly determines the outcome of infection as well as the success of eradication therapy. We demonstrate the role of a cysteine protease cathepsin X in the immune response to *H. pylori* infection.

Materials and methods. We analysed how the inhibition of cathepsin X influenced the immune response in experiments when THP-1 cells or dendritic cells isolated from patients were stimulated with 48 strains of *H. pylori* isolated from gastric biopsy samples of patients which had problems with the eradication of bacteria.

Results. The experiments, performed with the help of a flow cytometer, showed that the expression of Toll-like receptors (TLRs), especially TLR-4 molecules, on the membranes of THP-1 cells or dendritic cells was higher when we stimulated cells with *H. pylori* together with inhibitor of cathepsin X 2F12 compared to THP-1 cells or dendritic cells stimulated with *H. pylori* only, and also in comparison with negative control samples. We also demonstrated that when we inhibited the action of cathepsin X in THP-1 cells, the concentrations of pro-inflammatory cytokines were lower than when THP-1 cell were stimulated with *H. pylori* only.

Conclusions. We demonstrated that inhibition of cathepsin X influences the internalization of TLR-2 and TLR-4. TLR-2 and TLR-4 redistribution to intra-cytoplasmic compartments is hampered if cathepsin X is blocked. The beginning of a successful immune response against *H. pylori* in the case of inhibition of cathepsin X is delayed.

Key words: cathepsin X; macrophages; dendritic cells; hampered immune response; toll-like receptors; cytokines

Introduction

One of the important host factors that affect cure rates for *Helicobacter pylori* infections is the immune response to the infection. *H. pylori* antigens are recognised by epithelial cells, macrophages, and dendritic cells with the help of Toll-like receptors (TLRs) and Nod-like receptors (NLRs).[1] Activation of immune cells leads to *H. pylori*–specific adaptive T helper type 1 response.[2] In the case of impaired host immunity, a defective immune response to *H. pylori* may be a reason for *H. pylori* eradication failure.[3] Chronic infection with *H. pylori* can also be the result of the host's inability to induce an appropriate immune response.[4]

The discovery of cathepsin X brought new knowledge to how different proteins contribute to the immune response to *H. pylori*.[5] Patients infected with *H. pylori* expressed more cathepsin X than the healthy control group. Cathepsin X was located in macrophages gathered from gastric mucosa. Afterwards it was discovered that patients with *H. pylori* gastritis had a higher concentration of cathepsin X protein and cathepsin X mRNA levels in gastric mucosa compared to *H. pylori* negative patients.[6] Cathepsin X was also up regulated in the gastric mucosa of patients with gastric cancer in contrast to those without gastric cancer.[7]

Cathepsin X is a lysosomal cysteine protease found predominantly in the cells of monocyte/macrophage lineage. It acts as a monocarboxypepidase and has strict positional and narrower substrate specificity relative to other human cathepsins.[8] Cathepsin X is capable of cleaving regulatory motifs at the C-terminus affecting the function of the β_2 subunit of integrin receptors and alpha and gamma enolase. It was demonstrated that via activation of β_2 integrin receptor Mac-1 (CD11b/CD18), active cathepsin X enhances the adhesion of monocytes/macrophages to fibrinogen and regulates phagocytosis.[9] By activating the Mac-1 receptor, cathepsin X may also regulate the maturation of dendritic cells (DCs), a process that is crucial in the initiation of adaptive immunity.[10] Cathepsin X also activates the other β_2 integrin receptor, LFA-1 (CD11a/CD18), which is involved in the proliferation of T lymphocytes.[11]

In our study we wanted to test the hypothesis that inhibition of cathepsin X influences the successful immune response to an infection with *H. pylori.*

Materials and methods

Strains of *H. pylori* and patients

We analysed the influence of 40 *H. pylori* strains on the immune response of THP-1 cells. 20 strains of the bacteria were sensitive to all tested antibiotics. 20 strains of the bacteria were resistant to clarithromycin. The strains were isolated from gastric biopsies of patients with chronic gastritis. We also included a total of 8 strains of bacteria from dyspeptic patients with chronic gastritis that had problems with eradication of *H. pylori.* These patients gave 24 ml of blood that was later used to isolate DCs. Ethical approval was obtained for this study (National Medical Ethics Committee of the Republic of Slovenia).

Isolation of *H. pylori* and antibiotic susceptibility testing

Gastric biopsy samples were inoculated onto BHI agar with 10% horse blood and checked every 3 days for the total of 12 days for the presence of colonies typical of *H. pylori* and the identity confirmed with urease, catalase and oxidase enzyme activity. Antimicrobial susceptibility was determined with an Etest (bioMerieux, France) using ISO Sensitest agar supplemented with 10% horse blood. Antimicrobial susceptibility against clarithromycin, metronidazole, amoxicillin, tetracycline, and levofloxacin was determined. Metronidazole susceptibility was additionally tested with the breakpoint agar dilution method with the metronidazole concentration of 8 mg/L. Susceptibility breakpoints used to determine resistance were in accordance with the EUCAST standards. The presence of *cagA* and v*acA* genes was determined with PCR method as stated in the previous article.[12]

The number of bacteria used in the experiment with THP-1 and DCs was determined by the absorption at A_{550}, with 0.8 optical density (OD) units corresponding to 10^8 CFU/ml of bacteria. *H. pylori* bacteria were washed three times with PBS and stored at −20°C.

Flow cytometer analysis

All the data was collected on a FACSCanto flow cytometer and expression of different proteins was measured as MFI of various markers. We also assessed the MFI of molecules on the cell membranes using FlowJo (TreeStar, USA) and FACSDiva™ (BD Biosciences, UK) analysis software.

Isolation and culture of THP-1 cells and DCs

The medium used throughout the experiment was Advanced RPMI 1640 supplemented with 2 mM L-glutamine, 5% FCS, and antibiotics (Hyclone, Logan, UT, USA). THP-1 cells (TIB-202™) were obtained from LGC Promochem, UK. We cultured the cells for 7 days. Cells were allowed to differentiate to monocytes/macrophages at 37°C for 24 h in a 5% CO_2 humidified atmosphere. The flasks were washed gently with PBS to remove non-adherent cells. Adherent cells were detached with PBS containing EDTA.

Peripheral blood mononuclear cells (PBMCs) were obtained through Ficoll-Paque (PAA Laboratories Ltd., UK) gradient centrifugation.

Monocyte-derived DCs were generated from $CD14^+$ cells isolated by using CD14 coated immunomagnetic beads (DynabeadsFlowComp, Dynal, Norway). To differentiate dendritic cells from PBMCs we used recombinant human IL-4 (Sigma, USA) at 500 U/ml, and granulocyte-macrophage colony-stimulating factor (GM-CSF) (Sigma, USA) at 50ng/ml. We added them every 2 days before the cells were harvested on day five. Immature DCs were routinely characterized by the expression of HLA-DR, CD80, CD83, CD86, and CD14.[13] The control of cell viability (LIVE/DEAD kit, Molecular Probes, USA) was included in the analysis.

In vitro stimulation of THP-1 cells and DCs by *H. pylori*

THP-1 cells were adjusted to a final concentration of 10^6 cells/ml and 900 µl of cell suspension was added to a 24-well plate (Corning Costar, USA). 100 µl of *H. pylori* suspension was added to each well. The experiments were performed in duplicates. In the negative control samples, the bacteria were omitted and we also added polymixin B (Sigma, USA) to block any LPS effects. In the negative control samples we also added inhibitor of cathepsin X 2F12, neutralizing cathepsin X carboxypeptidase activity to see if it has any effect on the immune response in concentration 0.5 µM.[8] THP-1 cells were incubated in the presence of bacteria for 48 hours at 37°C. Expression of TLRs was investigated using the following antibodies: TLR-2 PE and TLR-4 FITC (e-Bioscience, UK). The 1×10^6 of THP-1 or DCs were co-cultured for two days with defrosted *H. pylori* at a 1:10 (DCs-to-*H. pylori*) ratio. We used the patients' *H. pylori* to stimulate their isolated DCs cells.

Inhibition of cathepsin X and analysis of TLR-2 and TLR-4 expression

To block cathepsin X effects, we added inhibitor of cathepsin X 2F12, as previously described[14] to THP-1 cells and DCs with *H. pylori* at the concentration of 0.5 µM. The concentration used proved to be the most appropriate in the previous experiments.[10] The inhibitor 2F12 was added at the beginning of the experiments and again after 24 hours. Cells were grown for two days, than harvested and the expression of different molecules on the cell membrane was investigated. To control the influence of inhibitor of cathepsin X 212F, the population of unstimulated THP-1 cells and DCs with inhibitor of cathepsin X 2F12 was analysed.

Cytokines concentrations in the supernatant of *H. pylori* primed THP-1 cells and DCs

We collected the supernatant of THP-1 cells and DCs that were stimulated with *H. pylori* only or with *H. pylori* plus cathepsin X inhibitor 2F12. The cytokines (tumour necrosis factor (TNF)-α, interleukin (IL)-1b, IL-6, IL-8, IL-10, and IL-12p70) in the supernatants were measured with the help of BD CBA Flex Set (Becton Dickinson, USA).

Statistical analysis

Differences between study groups were analysed for statistical significance using the unpaired Student's *t* test, with $P<0.05$ taken as significant. Differences between the concentrations of cytokines of the two study groups were analysed with Mann-Whitney test, with $P<0.05$ taken as significant. Differences between the expression of TLRs in cathepsin X inhibited and cathepsin X non-inhibited THP-1 cells or DCs primed with *H. pylori* were analysed with Student's *t* test and with non-parametric Wilcox Signed rank test. $P<0.05$ differences were taken as significant. All the calculations were done with the SPSS PASW Statistics 19 program (IBM, USA).

Results

In vitro stimulation of THP-1 cells by *H. pylori* and expression of TLR-2 and TLR-4

We first measured the expression of TLR-2 and TLR-4 on THP-1 cells after stimulating the cells with *H. pylori* with or without the addition of cathepsin X inhibitor 2F12. We did not find any differences in the expression of TLRs and cytokine production between un-stimulated THP-1 cells and un-stimulated THP-1 cells with the added inhibitor of cathepsin X 2F12.

When we compared the expression of TLRs between two groups of strains, one group being *H. pylori* strains sensitive to clarithromycin (HpS), the other strains resistant to clarithromycin (HpR), we noticed that resistant strains stimulated more THP-1 cells (% ± standard deviation-SD) to express more TLR-4 (MFI ± SD) than sensitive strains (81.51% ± 3.05 and 3656.03 MFI ± 301.05 HpR *vs*. 77.36% ± 4.85 and 3224.82 MFI ± 705.83 HpS). The difference was statistically significant ($P<0.05$). A similar effect was observed when we added inhibitor of cathepsin X

2F12. The TLR-4 MFI was statistically significantly higher (P<0.05) when THP-1 cells were stimulated with resistant strains (3519.33 MFI ± 428.65 HpR vs. 3172.03 MFI ± 535.67 HpS) (Figure 1).

We did not notice a statistically significant difference when we analysed the expression of TLR-2 on THP-1 cells stimulated with *H. pylori* with or without inhibitor of cathepsin X 2F12 or when we analysed the possible difference of clarithromycin sensitive or resistant strains on TLR-2.

Such a difference was not seen if we compared all strains with or without the inhibitor of cathepsin X. The mean MFI for the TLR-4 was almost the same (3440.42 ± 578.47 Hp *vs*. 3345.67 ± 510.13 Hp + inhibitor 2F12). The same was observed in the case of TLR-2 (5702.1795 ± 949.74 Hp *vs*. 5383.54 ± 741.14 Hp + inhibitor 2F12).

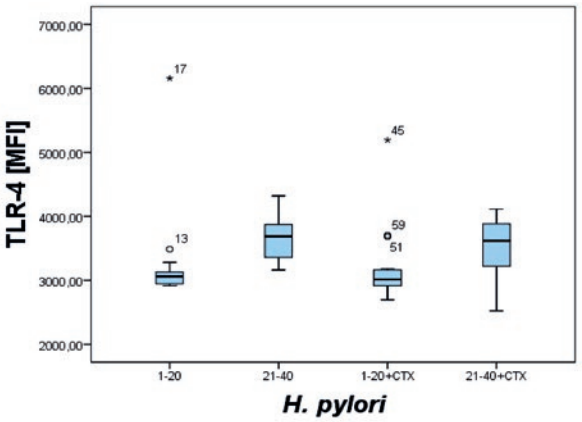

FIGURE 1. Expression of TLR-4 on THP-1 cells after stimulation with *H. pylori* or with *H. pylori* plus inhibitor of cathepsin X. 1-20 strains of *H. pylori* sensitive to clarithromycin, 21-40 strains of *H. pylori* resistant to clarithromycin, CTX inhibitor of cathepsin X.

Cytokines concentrations in the supernatant of *H. pylori* primed THP-1 cells

We measured the *in vitro* secretion of IL-1b, IL-12, IL-6, IL-8, TNF-α, and IL-10 by THP-1 cells primed with *H. pylori* with different susceptibility patterns and with or without inhibitor of cathepsin X 2F12. In the negative control sample (supernatants of THP–1 cells without *H. pylori* stimulation), we detected just very small concentrations of the above mentioned cytokines. The same occurred when we measured cytokines in the supernatant, where the THP-1 cells were primed only with inhibitor of cathepsin X 2F12.

After stimulation of THP-1 cells with *H. pylori* and with *H. pylori* plus inhibitor of cathepsin X 2F12, we noticed that inhibited action of cathepsin X lowers the concentration of cytokines in the group of 20 strains that are clarithromycin sensitive. Inhibition of cathepsin X influenced the cytokines IL-1b and IL-6 (P<0.01 and P<0.05) but not the others. Inhibition of cathepsin X influenced the production of IL-1b when we stimulated THP-1 cells with the group of 20 strains resistant to clarithromycin (P<0.05). The concentration of cytokines was lower in the case of the inhibited action of cathepsin X (Figure 2). The concentrations of all the other cytokines measured were lower when we added the inhibitor of cathepsin X 2F12, but did not reach statistical significance.

When we compared the concentrations of cytokines in the supernatant of THP-1 cells between 20 clarithromycin resistant and 20 sensitive strains of *H. pylori* without adding the inhibitor of cathepsin X 2F12, we noticed that clarithromycin resistant strains were weaker stimulators of cytokine production. The concentrations were statistically significantly lower for IL-6, IL-1b, IL-8, and IL-10 (P<0.01 in all comparisons). The concentrations of TNF-α and IL-12 were very low in both groups of strains, just above the limit of positivity, and were not included in the statistical analysis.

When we added the inhibitor of cathepsin X 2F12 we noticed the same phenomena between 20 clarithromycin resistant and 20 sensitive strains of *H. pylori* as in the above mentioned in the experiments without the inhibitor of cathepsin X 2F12. The concentrations of cytokines IL-8 and IL-10 (Figure 2) were again much lower where clarithromycin resistant strains plus inhibitor of cathepsin X 2F12 were used (P<0.01) in comparison to clarithromycin sensitive strains. We noticed that the biggest differences between the clarithromycin sensitive and clarithromycin resistant strains occurred in the cases of IL-1b and IL-10 where calculated F values were higher than 19.

In vitro stimulation of DCs by *H. pylori* and expression of TLR-2 and TLR-4

We continued with the clinical part of the study where we wanted to know how different strains from people that had problems with the eradication of *H. pylori* influence the immune response of the DCs isolated from their blood. We first checked the phenotypic features of *H. pylori* (Table 1). All strains were sensitive to amoxicillin and tetracycline (data not shown).

For negative control we also used DCs co-cultivated with RPMI medium alone or we added an inhibitor of cathepsin X 2F12. We did not find any

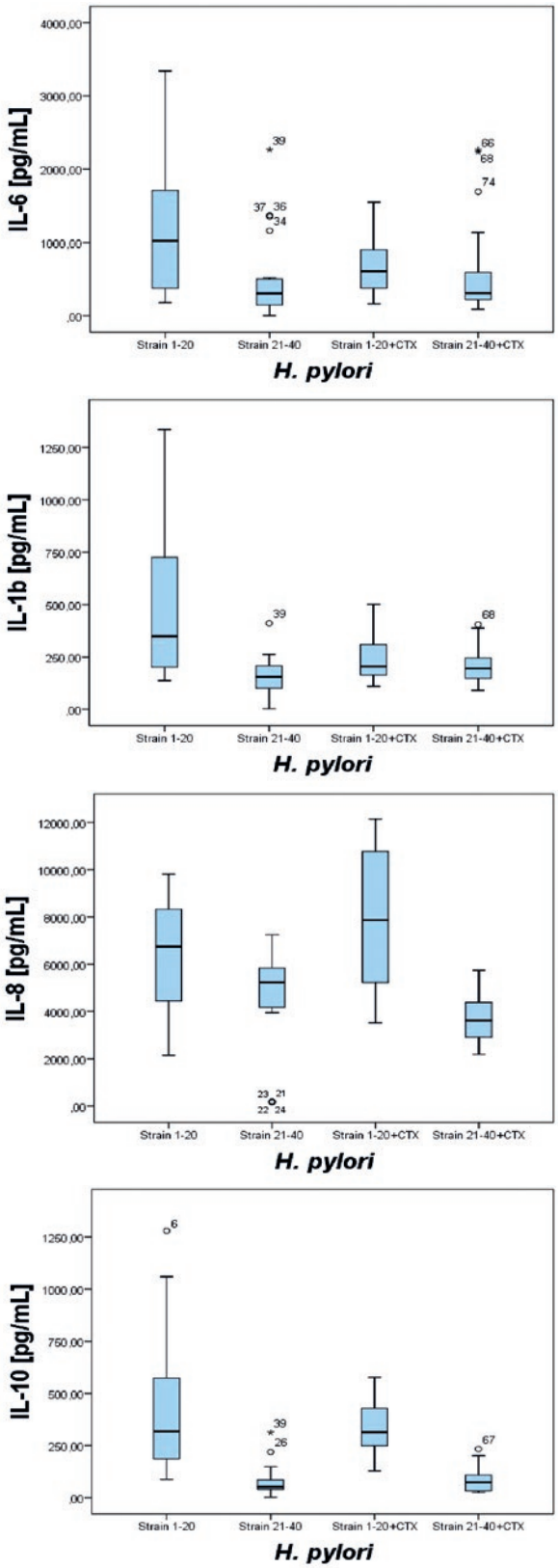

FIGURE 2. Concentrations of cytokines (pg/ml) IL-6, IL-1b, IL-8, IL-10 in the supernatant of THP-1 cells after stimulation with *H. pylori* strains or with *H. pylori* strains plus inhibitor of cathepsin X (CTX). 1-20 strains of *H. pylori* sensitive to clarithromycin, 21-40 strains of *H. pylori* resistant to clarithromycin.

TABLE 1. Susceptibility of *H. pylori* strains to antibiotics and *CagA*/*VacA* status

Patient's strains	E-test Cla/Metro/ Cipro*	CagA status	VacA status
1	S/S/S	P	P
2	S/S/R	P	P
3	S/S/S	P	P
4	S/S/S	P	P
5	R/R/S	P	P
6	S/R/S	N	P
7	R/S/S	P	P
8	S/R/S	P	P

*Cla = clarithromycin; Metro = metronidazole; Cipro = ciprofloxacin; S = sensitive, R = resistant; P = positive; N = negative.

differences in the expression of HLA-DR and cytokine production between un-stimulated DCs and un-stimulated DCs when we added an inhibitor of cathepsin X 2F12 (data not shown).

In the negative control sample (DCs without any stimulation) we detected a statistically significantly lower expression of TLR-4 and TLR-2 in comparison with dendritic cells stimulated with *H. pylori* only (Figure 3).

We checked the expression of TLR-2 and TLR-4 (Figure 3) on the membrane of DCs. Statistically, the expression of TLR-4 and TLR-2 presented as MFI was significantly higher ($P<0.05$) in the group where cathepsin X was inhibited with 2F12 (TLR-4 - *H. pylori* stimulation 161.91(146.88-232.61) *vs. H. pylori* + 2F12 inhibition 219.25 (164.38-388.83); TLR-2 - *H. pylori* stimulation 133.54(128.18-189.59) *vs. H. pylori* + 2F12 inhibition 151.045 (133.2-324.59)).

Cytokines concentrations in the supernatant of *H. pylori* primed DCs

We measured the *in vitro* secretion of IL-12, IL-8, and IL-10 by DCs primed with *H. pylori* and with inhibitor of cathepsin X 2F12 added to *H. pylori*. In the negative control samples (supernatants of DCs without any stimulation), we did not detect any of the above mentioned cytokines. After priming DCs with *H. pylori* or with *H. pylori* + inhibitor of cathepsin X 2F12, we did not detect any statistical difference between the groups in cytokine concentrations but cytokine concentrations were lower in the dendritic cells group *H. pylori* + inhibitor of cathepsin X 2F12 - inhibition. The concentrations of TNF-α and IL-6, IL-1b detected were very low, just

above the limit of positivity, and were not included in the statistical analysis.

Discussion

For the first time, we have shown the involvement of cathepsin X in the antigen presentation with TLRs. When we stimulated THP-1 cells with different strains of *H. pylori* we noticed that the addition of the inhibitor of cathepsin X 2F12 resulted in a higher expression of TLR-4 on the membranes of THP-1 cells. This was especially true if we compared clarithromycin sensitive strains of *H. pylori* to resistant strains stimulated THP-1 cells, the resistant strains expressed more TLR-4. Our results in the clinical part of the study have shown that the expression of TLR-4 and TLR-2 was significantly higher when *H. pylori* stimulated DCs were cultivated together with cathepsin X inhibitor 2F12 compared to the dendritic cells stimulated with *H. pylori* only and also in comparison with negative control samples.

Cathepsin X is in some way responsible for the regulation of an immune response. The patients with eradication failure, despite having taken the appropriate empiric antibiotic therapy prescribed by gastroenterologist, expressed cathepsin X after stimulation with *H. pylori* antigens on the membrane of the THP-1 cell line different from the patients with successful *H pylori* eradication.[14] How does cathepsin X influence the action of TLR-4 and TLR-2 and consequently the antigen presenting cells? *In vitro* studies have demonstrated that upon stimulation with LPS or peptidoglycan, which occurs with constant exposure to commensal bacteria, TLR-2 and TLR-4 are redistributed from the apical surface to intra-cytoplasmic compartments adjacent to the basolateral membrane.[15] TLR-4 is redistributed to the Golgi apparatus.[16] It was shown that during maturation, cathepsin X translocates to the plasma membrane of maturing dendritic cells, enabling Mac-1 activation and consequently cell adhesion.[10,14]

In our opinion, inhibition of cathepsin X hampers the internalization of TLRs, because the membrane (in the case of cathepsin X inhibition) becomes more rigid and internalization is delayed or even not possible. If cathepsin X is blocked it cannot cleave regulatory motifs at the C-terminus and this affects the function of the β2 subunit of integrin receptors of gamma enolase.[9]

We checked the influence of higher expression of TLR-4 on the membranes of THP-1 cells on the production of cytokines IL-1b, IL-8, IL-10, and IL-6, three pro-inflammatory cytokines, and one regulatory cytokine. The concentrations were lower in the group of *H. pylori* strains that were resistant to clarithromycin. The same phenomena were seen in the experiments with THP-1 cells where we added bacteria along with the inhibitor of cathepsin X 2F12. It seems that the inhibition of cathepsin X influences the concentrations of cytokines, as well on the TLRs, that are crucial for efficient regulation of immune response to *H. pylori.* We discovered that strains that are resistant to clarithromycin are less immunogenic than clarithromycin sensitive strains and that they might be capable of surviving an immune system attack for a prolonged period of time and as well develop resistance to clarithromycin that further attributes to eradication failure of *H. pylori.* In the experiments in the clinical part of the study on 8 patient's DCs stimulated with patient's own *H. pylori*, the difference between concentrations of cytokines between stimulation and inhibition of cathepsin X was not statistically significant. If we could increase the number of patients, we would most probably get a statistically significant difference in the concentrations of cytokines between the groups.

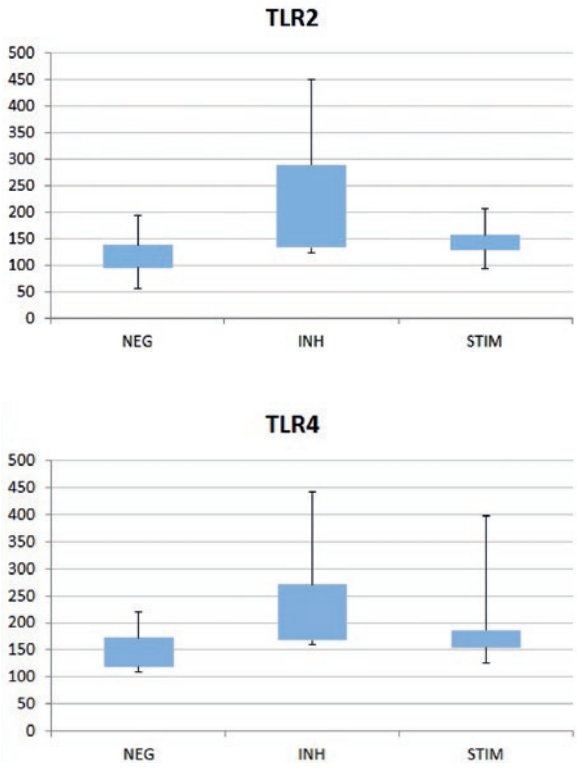

FIGURE 3. The expression of TLR-2 and TLR-4 on DCs (MFI - mean fluorescence intensity) in box plot. NEG negative control – un-stimulated DCs, INH DCs with *H. pylori* plus 2F12 - inhibition, STIM DCs with *H. pylori* - stimulation.

H. pylori is capable of suppressing the action of DCs and the host fails to prevent bacterial colonization. The failure to eradicate *H. pylori* during the acute phase may result in developing resistance to clarithromycin and further problems with eradication, chronic gastritis, development of peptic ulcer disease, or even gastric cancer.[17] *H. pylori*-specific response consists of both T helper 1 and 2 subsets with high levels of IL-10-secreting T regulatory cells. It seems that *H. pylori* induces a regulatory T cell response, possibly contributing to its commensal coexistence with the human host, and that chronic gastritis and peptic ulcer disease occur when this regulatory response is inadequate.[18] A similar effect was also seen in our study on THP-1 cells stimulated with *H. pylori.* Inhibited action of cathepsin X led to profoundly lower levels of IL-10 in the supernatant of THP-1 cells. In mice experiments *H. pylori* triggered an increase in the number of subepithelial lamina propria CD11c positive dendritic cells. Depletion of regulatory T cell numbers augmented *H. pylori*-specific effector helper T cell responses, which correlated with a lower degree of *H. pylori* colonization. Data imply that *H. pylori* targets the TLR-2 pathway to induce a regulatory T cell-skewed response.[19] The inhibition of cathepsin X activity during dendritic cell differentiation and maturation reduced the capacity of dendritic cells to stimulate T lymphocytes.[20] These observations are evidence that dendritic cells are involved in active editing of the immune response towards *H. pylori*. Cathepsin X may also be important in this process because some strains of *H. pylori* are able to lower the proportion of THP-1 cathepsin X positive cells. Such strains have the capability to persist in the stomach for a long time because they do not induce a strong immune response.[14] It was presented that the impaired cellular transmigration/invasion of cells lacking cathepsin X is most likely a consequence of changes in signal transduction mechanisms leading to cell cycle delay and phenotypic changes associated with cellular senescence. It seems that high levels of cathepsin X, as observed in certain tumours, may interfere with senescence pathways and/or promote pathways engaged in proliferation, thus stimulating tumor cell growth.[21] Recent work has suggested that defective signalling via TLR-4 may also result in an exaggerated immune response after the initial failure of innate immunity to control infection.[22] Once inside the host cell, CagA of *H. pylori* can disrupt signalling pathways by phosphorylation-dependent and -independent mechanisms, leading to abnormal proliferation, motility, and cytoskeletal change in gastric epithelial cells.[23] It was suggested that the eradication of CagA negative strains is harder than the eradication of CagA positive strains, because such strains are able to withstand eradication by not having important virulence factors such as CagA.[24]

We analysed the CagA/VacA status of the *H. pylori* strains in the clinical part of the study where DCs were stimulated with *H. pylori* strains. In our group of strains, CagA status is not as important for eradication success as in patients from Asia, where CagA status is relevant for the persistence of infection with *H. pylori*.

The immune response to *H. pylori* is also important for the development of gastric cancer. Recognition of pathogenic elements by TLRs and NLRs results in activation of kinases pathways and induces the synthesis and secretion of inflammatory cytokines. In the case of *H. pylori* infection, the resulting inflammation can lead to severe gastric immunopathology and cancer.[25] In one study, cathepsin X was also linked to colorectal cancer. The researchers still think that total serum levels of cathepsin X could be a useful prognostic indicator for determining survival of patients with colorectal cancer.[26] When the effect of inhibition of cathepsin X (also known as cathepsin Z) in mice was studied, the combined loss of cathepsin X and cathepsin B led to additive effects, resulting in significant and prominent delay of early and advanced tumour development.[27]

In conclusion the results of our study suggest that resistance to clarithromycin can be a problem for the eradication from the immune response point of view since such strains seem to be less immunogenic. We assume that the inhibition of cathepsin X to control the immune response to *H. pylori* in the cases where we have problems with eradication of *H. pylori* would not be beneficial. The immune response to infection would be delayed and this could lead to persistence of infection and possible development of resistance to antibiotics, atrophy, metaplasia and gastric cancer. On the other hand, when gastric cancer is already developed, inhibition of cathepsin X could be helpful since we could influence the process of cell senescence and also influence tumour cell growth.

References

1. Rad R, Ballhorn W, Voland P, Eisenächer K, Mages J, Rad L, et al. Extracellular and intracellular pattern recognition receptors cooperate in the recognition of *Helicobacter pylori*. *Gastroenterology* 2009; **136:** 2247-57.

2. Amieva MR, El-Omar EM. Host-bacterial interactions in *Helicobacter pylori* infection. *Gastroenterology* 2008; **134:** 306-23.
3. Borody T, Ren Z, Pang G, Clancy R. Impaired host immunity contributes to *Helicobacter pylori* eradication failure. *Am J Gastroenterol* 2002; **97:** 3032-7.
4. Mitchell P, Germain C, Fiori PL, Khamri W, Foster GR, Ghosh S, et al. Chronic exposure to *Helicobacter pylori* impairs dendritic cell function and inhibits Th1 development. *Infect Immun* 2007; **75:** 810-7.
5. Bühling F, Peitz U, Krüger S, Küster D, Vieth M, Gebert I et al. Cathepsins K, L ,B , X and W are differentially expressed in normal and chronically inflamed gastric mucosa. *Biol Chem* 2004; **385:** 439-45.
6. Krueger S, Kuester D, Bernhardt A, Wex T, Roessner A. Regulation of cathepsin X overexpression in *H. pylori*-infected gastric epithelial cells and macrophages. *J Pathol* 2009; **217:** 581-8.
7. Krueger S, Hundertmark T, Kalinski T, Peitz U, Wex T, Malfertheiner P, et al. Up-regulation of cathepsinX in *Helicobacter pylori* gastritis and gastric cancer. *J Pathol* 2005; **207:** 32-42.
8. Kos J, Sekirnik A, Premzl A, Zavasnik Bergant V, Langerholc T, Turk B, et al. Carboxypeptidases cathepsins X and B display distinct protein profile in human cells and tissues. *Exp Cell Res* 2005; **306:** 103-13.
9. Obermajer N, Premzl A, Zavasnik Bergant T, Turk B, Kos J. Carboxypeptidase cathepsin X mediates beta2-integrin-dependent adhesion of differentiated U-937 cells. *Exp Cell Res* 2006; **312:** 2515-27.
10. Obermajer N, Svajger U, Bogyo M, Jeras M, Kos J. Maturation of dendritic cells depends on proteolytic cleavage by cathepsinX. *J Leuk Biol* 2008; **84:** 1306-15.
11. Jevnikar Z, Obermajer N, Bogyo M, Kos J. The role of cathepsin X in the migration and invasiveness of T lymphocytes. *J Cell Sci* 2008; **121:** 2652-61.
12. Achtman M, Azuma T, Berg DE, Ito Y, Morelli G, Pan ZJ, et al. Recombination and clonal groupings within *Helicobacter pylori* from different geographical regions. *Mol Microbiol* 1999; **32:** 459-70.
13. Kopitar AN, Stegel V, Tepes B, Gubina M, Novaković S, Ihan A. Specific T cell responses to *Helicobacter pylori* predict successful eradication therapy. *J Infect* 2007; **54:** 257-61.
14. Obermajer N, Magister S, Kopitar AN, Tepes B, Ihan A, Kos J. Cathepsin X prevents an effective immune response against *Helicobacter pylori* infection. *Eur J Cell Biol* 2009; **88:** 461-71.
15. Cario E, Brown D, McKee M, Lynch-Devaney K, Gerken G, Podolsky DK. Commensal-associated molecular patterns induce selective toll-like receptor-trafficking from apical membrane to cytoplasmic compartments in polarized intestinal epithelium. *Am J Pathol* 2002; **160:** 165-73.
16. Hornef MW, Frisan T, Vandewalle A, Normark S, Richter-Dahlfors A. Toll-like receptor 4 resides in the Golgi apparatus and colocalizes with internalized lipopolysaccharide in intestinal epithelial cells. *J Exp Med* 2002; **195:** 559-70.
17. Wang X, Uto T, Sato K, Ide K, Akagi T, Okamoto M, et al. Potent activation of antigen-specific T cells by antigen-loaded nanospheres. *Immunol Lett* 2005; **98:** 123-30.
18. Robinson K, Kenefeck R, Pidgeon EL, Shakib S, Patel S, Polson RJ, et al. *Helicobacter pylori*-induced peptic ulcer disease is associated with inadequate regulatory T cell responses. *Gut* 2008; **57:** 1375-85.
19. Zhang M, Liu M, Luther J, Kao JY. *Helicobacter pylori* directs tolerogenic programming of dendritic cells. *Gut Microbes* 2010; **1:** 325-9.
20. Kos J, Jevnikar Z, Obermajer N. The role of cathepsin X in cell signaling. *Cell Adh Migr* 2009; **3:** 164-6.
21. Kraus S, Bunsen T, Schuster S, Cichoń MA, Tacke M, Reinheckel T, et al. Cellular senescence induced by cathepsin X downregulation. *Eur J Cell Biol* 2011; **90:** 678-86.
22. Higgins SC, Lavelle EC, McCann C, Keogh B, McNeela E, Byrne P, et al. Toll like receptor 4-mediated innate IL-10 activates antigen-specific regulatory T cells and confers resistance to *Bordetella pertussis* by inhibiting inflammatory pathology. *J Immunol* 2003; **171:** 3119-27.
23. Kurashima Y, Murata-Kamiya N, Kikuchi K, Higashi H, Azuma T, Kondo S, et al. Deregulation of beta-catenin signal by *Helicobacter pylori* CagA requires the CagA-multimerization sequence. *Int J Cancer* 2008; **122:** 823-31.
24. Sugimoto M, Yamaoka Y. Virulence factor genotypes of *Helicobacter pylori* affect cure rates of eradication therapy. *Arch Immunol Ther Exp* 2009; **57:** 45-56.
25. Patel MK, Trombly MI, Kurt-Jones EA. Innate immune responses to Helicobacter pylori infection: an overview. *Methods Mol Biol* 2012; **921:** 205-7.
26. Vizin T, Christensen IJ, Nielsen HJ, Kos J. Cathepsin X in serum from patients with colorectal cancer: relation to prognosis. *Radiol Oncol*. 2012; **46:** 207-12.
27. Sevenich L, Schurigt U, Sachse K, Gajda M, Werner F, Müller S et al. Synergistic antitumor effects of combined cathepsin B and cathepsin Z deficiencies on breast cancer progression and metastasis in mice. *Proc Natl Acad Sci U S A*. 2010; **107:** 2497-502.

research article

Early outcome in endoscopic extended endonasal approach for removal of supradiaphragmatic craniopharyngiomas: a case series and a comprehensive review

Roman Bosnjak[1], Mitja Benedicic[1], Alenka Vittori[1]

[1] Department of Neurosurgery, University Medical Centre, 1000 Ljubljana, Slovenia

Radiol Oncol 2013; 47(3): 266-279.

Received 5 October 2012
Accepted 2 December 2012

Correspondence to: Prof. Roman Bošnjak, MD, PhD, Department of Neurosurgery, University Medical Centre Ljubljana, Zaloška 7, 1000 Ljubljana, Slovenia. E-mail: roman.bosnjak@kclj.si

Disclosure: No potential conflicts of interest were disclosed.

Background. The choice of endoscopic expanded endonasal approach introduces the possibility of improved gross total resection of craniopharyngioma while minimizing surgical morbidity in a significant subset of patients.

Methods. From our trans-sphenoidal surgical series of 331 cases, we retrospectively reviewed visual, endocrine and neuro-cognitive outcomes in the first consecutive eight patients (median age 63 years; range 47–73 years) with newly diagnosed supradiaphragmatic craniopharyngioma (median tumour height 23 mm; range 15–34 mm), removed by expanded endonasal approach (median follow-up 27 months; range 10–69 months). Gross total resection was attempted in all patients.

Results. Gross total resection was achieved in 6 of 8 patients. Visual improvement was present in 6 of 8 patients of patients or in 14 of 16 eyes. New endocrinopathy, including diabetes insipidus, appeared in 5 of 8 patients. Stalk was preserved in 4 patients. Cognitive decline was present in 2 cases. Five of 8 patients retained previous quality of life.

Conclusions. Our early outcome results are comparable to the recent few expanded endonasal approach series, except for the incidence of new endocrinopathy and cerebrospinal fluid leak rate. This was influenced by higher number of transinfundibular tumours in our series, where stalk preservation is less likely, and not using nasoseptal flap or gasket closure in the first half of cases. Including data from the literature and ours, expanded endonasal approach shows a trend for improved gross total resection rate with less morbidity, more obviously for visual outcome and quality of life than for endocrine outcome. However, validity of expanded endonasal approach should be confirmed in a larger number of patients with a longer follow-up period.

Key words: extended endoscopic approach; craniopharyngioma; trans-sphenoidal approach

Introduction

Surgical treatment of craniopharyngiomas is a challenging issue owing to the delicate anatomical position related to the hypophyseal stalk and infundibulum and adherence to the important neurovascular structures in the suprasellar and retrochiasmatic region.[1-8] The current consensus about the optimal treatment strategy has reverted in the last 2 decades back to gross total resection (GTR) in contrast to more limited surgery, aimed at tumour debulking, decompressing the optic pathways and releasing cerebrospinal fluid (CSF) pathways, followed by radiotherapy (XRT).[4,9-11] Despite similar tumour control rates are reported with subtotal resection and adjuvant XRT, the surgery for recurrence is associated with unacceptably increased morbidity and mortality rates.[10-12] The challenge of more favourable long term recurrence rates in GTR is faced by increased risk of visual, pituitary and hypothalamic dysfunction; only pituitary insufficiency is nowadays acceptable with modern hor-

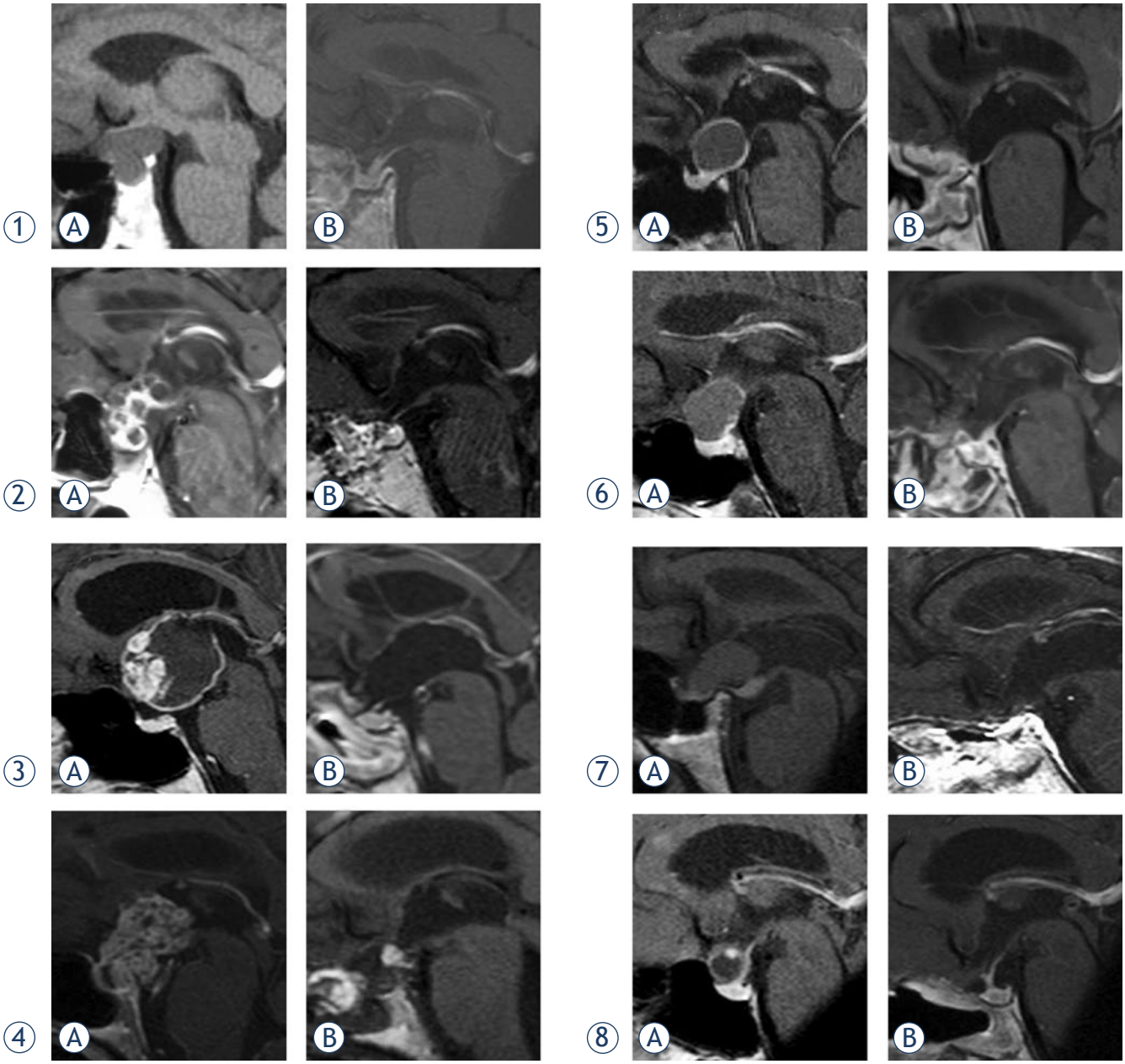

FIGURE 1. MRI scans (sagittal planes) of craniopharyngiomas in eight patients preoperatively **A** and postoperatively **B**.

monal substitution therapy. Several transcranial approaches have been established for maximum resection of craniopharyngiomas, many of them extending far beyond the sella.[9,13-17] In these principally lateral approaches, the direct visualization of suprasellar-retrochiasmatic region is incomplete on the contralateral side, resulting in a significant amount of blind dissection. The first 100 patients, published to date in a few series, have been operated on using endoscopic transplanum-transtuberculum approach for newly diagnosed or residual and recurrent supradiaphragmatic craniopharyngiomas.[18-24] The choice of endoscopic extended endonasal approach (EEA) as the minimally invasive access introduces the possibility of complete tumour resection while minimizing surgical morbidity in a significant subset of patients.[2,18-20,22,23] This midline approach has the advantage of providing direct visualisation of the suprasellar and third ventricle tumour extension and visually controlled in-line dissection at the plane between the tumour and the optic nerves, chiasm, stalk (if recognizable), hypothalamus and supraclinoidal internal carotid arteries with their branches.

TABLE 1. Clinical features of 8 patients with supradiaphragmatic craniopharingioma operated on by transplanum approach

Pt. No.	Sex, age	Signs and symptoms			Duration (months)	Tumor size (mm) W x H x L	Tumor Grade					Follow-up period
		Leading symptom(s)	Visual Right/Left eye	Endocrine function			Hoffman [ref. 13]	Samii [ref. 16]	Yasargil [ref. 17]	Kassam [ref. 26]	Songtao Qi [ref. 5]	
1	M, 66	Visual	BTH, ↓acuity	Normal	6	15x15x20	Subch	II	Suprasel	Retroinf	Extrav	5yr 9mo
2	M, 73	Visual, retrobulb. HA	Sup. BTQ	Normal	2,5	25x25x15	Intrav	III	Intrav	Transinf	Transinf	4yr
3	M, 51	HA,balance, psih	Normal	Normal	4	27x31x25	Intrav	IV	Intrav	Transinf	Extrav & Intrav	3yr 4mo
4	F, 71	V&N, visual	TH/Sup. TQ, ↓acuity L	Panh, no DI	4	17x34x21	Intrav	IV	Intrav	Transinf	Transinf	2yr 9mo
5	F, 60	Visual	BTH R > L	Normal	6	21x16x16	Retroch	III	Extrav	Preinf	Extrav & Intrav	1yr 9mo
6	F, 69	Visual	Sup. TQ/central scotoma, ↓acuity L	Normal	5	25x21x17	Retroch	III	Extrav	Preinf	Extrav & Intrav	18mo
7	M, 57	Visual	Inf. BTQ scotomas	Normal	5	22x20x15	Retroch	III	Extrav	Preinf	Extrav & Intrav	13mo
8	F, 47	Visual	Inf. NQ scotoma L	Normal	2	20x29x20	Subch	II	Suprasel	Preinf	Extrav	10mo

HA = headache; V&N = vomitus and nausea; BTH = bitemporal hemianopsia; BTQ = bitemporal quadrantanopsia; NQ = nasal quadrantanopsia; Panh = panhypopituitarysm; WxHxL = width, height, lenght; DI = diabetes insipidus; Subch = subchiasmatic; Retroch = retrochiasmatic; Intrav = intraventricular; Extrav = extraventricular; Suprasel = suprasellar; Preinf = preinfundibular; Retroinf = retroinfundibular; Transinf = transinfundibular

Improved GTR and less morbidity with EEA compared to transcranial surgery has not yet been proved as the number of publications on EEA is limited. The aim of this report is to contribute our experience in the endonasal endoscopic treatment of newly diagnosed supradiaphragmatic craniopharyngiomas with special attention to stalk preservation and postoperative visual, endocrine and cognitive/social outcomes. Results are compared to the recent series and the utilities and limitations of the EEA approach in supradiaphragmatic craniopharyngiomas are extracted.

Patients and methods

From our trans-sphenoidal series of 331 cases, we retrospectively reviewed records of 112 cases of patients with suprasellar lesions, treated with EEA at the Department of Neurosurgery, University Medical Centre Ljubljana, Slovenia (January 2007 – December 2011). The analysis revealed 8 consecutive adult patients with pure suprasellar craniopharyngioma that were treated with endoscopic EEA. GTR was attempted in all patients. All patients gave their informed consent and all surgeries were performed by the senior author (R. B.).

Patients underwent a comprehensive ophthalmological evaluation at the University Eye Clinic pre- and postoperatively, consisting of the assessment of visual acuity, visual field (Goldmann) and fundoscopy.

Endocrine evaluation was performed at the Department of Endocrinology at the University Medical Centre Ljubljana. Patients were evaluated with basal levels of prolactin (PRL), thyroid-stimulating hormone (TSH), free triiodothyronine (FT3),, free thyroxine (FT4), growth hormone (GH), insulin-like growth factor 1 (IGF-1), luteinizing hormone (LH), follicle-stimulating hormone (FSH), cortisol, testosteron (free, total) and adrenocorticotropic hormone (ACTH) test. If necessary, diabetes insipidus (DI) was diagnosed according to the freezing point depression osmometry of urine, fluid intake, urine volume and osmolality of urine (Table 1).

One patient (Patient 3) presented with moderate psychoorganic change, headache and balance problems from slowly developing hydrocephalus in the last 4 months. One patient (Patient 4) was wrongly diagnosed with a large pituitary adenoma 2 years ago in a peripheral hospital and denied surgery. She received complete hormonal substitutional therapy, but was referred to our department because of progressive visual loss and psychoorganic change during the last 4 months.

Postoperatively, hormonal status was evaluated at 3, 6 and 12 months and then yearly. Further endocrinological evaluation sheme was modified according to the presence of any hypothalamic-pituitary dysfuction. The extent of resection was independently evaluated by neuroradiologists comparing pre- and postoperative magnetic resonance images (MRI). T1-weighted contrast-enchanced,

T2-weighted and three-dimensional (3D) magnetization-prepared rapid gradient-echo images (MP-RAGE) were used for pre- and postoperative evaluation. Individual preoperative and postoperative MRI scans (sagittal planes) of craniopharyngiomas in 8 patients are presented in Figure 1.

Surgical technique

Under general anesthesia, the patient is placed in the supine position on the operating table with the head fixed into anteflexion for 30^0 and rotated toward the right shoulder for 30^0. In patients with a short neck, the shoulders and the upper back are supported with a cushion to achieve the desired neck anteflexion without jugular vein compression.

Patient's head is first registered with the neuronavigation device (Stealth Station 5.0, Medtronic, MN, USA).

The nostrils are washed with anstiseptic solution and temporarily packed with cottonoid strips soaked with 10% Xylocaine. The neurosurgeon is positioned face-to-face with the patient's right side while the assistant is at the right lateral side of the patient's head. The endoscopic tower with the high-resolution screen is positioned 1 m left lateral to the patients head in the line of sight of the neurosurgeon and the assistant. The scrub nurse is positioned on the left side of the patient. The binostril approach is more comfortable for the surgeon and provides less instruments collision with the use of 2 nostrils-four hands technique. A 0^0 and less frequently 45^0 or 70^0 rigid endoscope (180/4 mm) is used (Karl Storz, Tuttlingen, Germany).

Nasal phase

The endoscope is introduced into the left nasal cavity first. The middle turbinate (MT) is gently lateralized and the space between the MT and the nasal septum is gently widened. Only large and pneumatized MT is removed. The base of the MT, vomer and nasal septum are infiltrated with adrenaline (diluted 1:50.000) to promote vasoconstriction. The choana is identified and then sphenoidal opening is identified in superior direction about 1 cm above the inferior margin of MT and medial to the superior turbinate. A vascular pedicle nasoseptal flap is formed, turned inferiorly into the choana and saved for the subsequent sellar floor reconstruction.

On the right side, however, MT is only lateralized. The posterior third of septal mucosa is removed. A large opening is made in the posterior third of the denuded nasal septum. The lamina perpendicularis is removed in one large piece if possible and stored for sellar reconstruction. The endoscope is inserted through the right nostil and held by the assistant, while the neurosurgeon works through both nostrils bimanually, holding aspirator in the left hand and the drill handle, or bayonet microdissector or other fine instruments in the right hand.

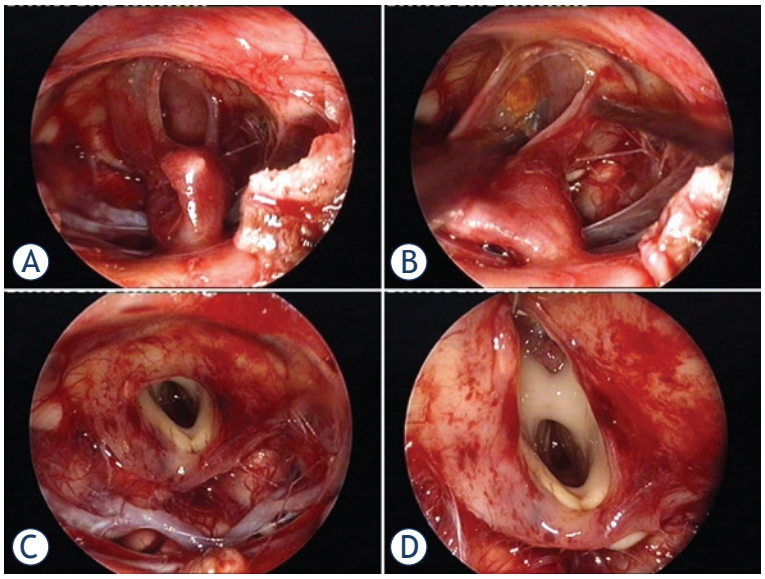

FIGURE 2. In this cystic craniopharyngioma (Patient 5), the stalk was centrally infiltrated close to the pituitary and could not be preserved **A**. The incipient third ventricle entrance is seen from intracavitary view. The slit into the third ventricle is still covered with tumour capsule **B**. Complete removal of the capsule opened the third ventricle **C**. Petehiae in the hypothalamus bilaterally resulted from apparently gentle traction and blunt dissection of the capsule away from the hypothalamus **D**. Psychoorganic change, disorientation and memory deficits were noticed in less than a week after surgery, the transient sleep disorder become apparent in the second week postoperatively (see also a supplemented video material 2).

Sphenoidal phase

The anterior wall of the sphenoidal sinus is widely opened and the septa removed. Inside the sphenoidal sinus, the sella is then localized. The posterior sphenoidal wall is denuded of the mucosa, which is removed or rolled in the lateral and the bottom part of the sphenoid sinus. Visualization of the sellar region is initially performed with a 0^0 endoscope. Sellar floor, bilateral protuberances of the anterior loop of the internal carotid arteries, major and minor optocarotid recesses (OCR), optic canals and paraclival carotid columns are identified. The use of neuronavigation in sphenoidal sinuses with atypical or blurred morphology, or occasionally with thick posterior wall is beneficial.

The remnants of the posterior ethmoidal cells, crushed lateraly from mucosal side, are gently punched off for sufficient midline exposure of the sphenoid ceiling and OCRs.

Sellar and planar phase

The sellar floor is opened with a highspeed drill or Kerrison rongeur. The blue line of the superior intercavernous sinus marks the transition from the anterior sellar wall to the planum sphenoidale. Here, the bone is removed in the superior direction for 1.5–2 cm and superolateral to OCR. The drilling around OCR and proximal parts of optic canals is gentle, intermittent and performed with constant irrigation of the diamond drill bit with cold saline to prevent the optic nerve from thermal injury.

The sellar and planar trephination together constitute the so-called "chief's hat" exposure of dura. This is generally sufficient to expose the planar dura up to the line of the dura propria traversing between the optic nerves.

The dura, exposed by the "chief's hat" trephination, is incized in T-shape: horizontally along the dura propria or a little above it, and vertically across the superior intercavernous sinus and along the midline over the pituitary and continued horizontally along the sellar floor on each side. The dural flaps are turned laterally (Supplement 1).

Intradural phase

When the arachnoid is dissected, CSF starts to leak and the dome of the craniopharyngioma is exposed, pushing up the chiasm and the optic nerves and displacing downward the remnants of the diaphragm sellae (in pure suprasellar craniopharyngiomas) and the pituitary. The cyst of the craniopharyngioma is punctured and the dark oily liquid pours out, immediately decompressing the chiasm and the optic nerves (Supplement 2).

Sometimes, the cyst is filled with cholesterine cristals. If the tumour is solid and calcified, it is first debulked. Tumour is entered by the longitudinal incision. The large calcifications have sometimes to be crunched first by micro-roungeur into smaller pieces. The solid part of the tumour with calcinations is removed by piecemeal technique, bearing in mind the stalk position when recognizable. The tumour is dissected extracapsularly in the clockwise direction along the tumour circumference from the superficial to the deep seated suprasellar structures. Following the arachnoid-tumour plane, the tumour capsule is detached first from the right supraclinoidal internal carotid artery (ICA) and the right optic nerve, from the undersurface of the chiasm, then from the left optic nerve and left ICA. Special attention is paid to perforators of the chiasm, hypophyseal and Dawson's arteries, originating from the supraclinoidal ICA. The striate structure of the stalk is carefully searched for around the surface of the cyst or grossly debulked tumour and from the inside aspect of the cystic craniopharyngioma. In supradiaphragmatic craniopharyngiomas, the stalk is first identifiable inferiorly at the pituitary, but should be traced up to the hypothalalmus and at least partially preserved if possible (Figure 2). This condition is rarely present (Supplement 3).

The surgeon must soon get the idea of a tumour growth type with stalk expansion (transinfundibular) or stalk dislocation (pre- and retroinfundibular). The stalk points toward the hypothalamus and the third ventricle floor, which may be displaced and distorted in extraventricular tumours or entered and split in extra- and intraventricular tumours.[2,6] The continuity of the stalk with the hypothalamus will result in functional integrity. In middle-sized and large transinfundibular tumours, the hypothalamus is split and tumour protrudes into the anterior third ventricle up to the foramina of Monro (Figure 3). Here the tumour is most adherents to the inner walls of infundibulum, which are most often dislocated inferolaterally. Meticulous sharp dissection of the tumour is necessary here at the exact tumour-glial plane.[3] Infiltration or severe adherence to the hypothalamus in the deep aspect of the dissection preclude partial resection to prevent hypothalamic injury (Figure 2). The rest of the tumour inside the third ventricle will be easier to detach from ventricular wall when infundibulum is passed. When the tumour is removed from the retrosellar region, corpora mamillaria, tip of the basilar artery, posterior cerebral arteries – P1 segments and the oculomotor nerves and the Liliequist's membrane will be exposed (Supplement 2).

Following tumour resection, both 0^0 and angled endoscopes are introduced into the surgical cavity to explore for any residual tumour (Figure 3).

In more favourable cases, the craniopharyngioma grows exophytically from the stalk, which can be partially preserved with careful dissection and avoiding traction. In true extraventricular craniopharyngioma, tumour can be severely adeherent to the the outer pial surface of the hypothalamus. Traction to the hypothalamic parenchyma and hypothalamic perforators should be avoided as much as possible (Figure 4, Supplement 2, Supplement 3).

For the reconstruction of the sellar floor, we use facia lata (FL) and Hadad's flap in a three-layer technique (suprasellar fat packing + inlay of FL + onlay FL + Hadad's flap + sealant) and gelfoam or fat are used as a buttress by packing the posterior sphenoid sinus (Supplement 1).[25,26] Lumbar drainage is applied postoperatively for 7–10 days.

Results

Eight patients were enrolled in the study (male:female = 4:4; median age 63 years; range 47–73 years). The follow-up period was 10–69 months (up to 5 years and 9 months, median 72 months).

Seven of 8 patients presented with a visual problem as a leading symptom, median duration of visual symptoms was 5 months (range 6–2 months). Except in Patient 4, there was no preoperative endocrine dysfunction in the other 7 patients and none of the patients had DI. The median tumour height was 23 mm (range 15–34 mm), six were equal or taller than 20 mm. All tumours were of adamantinomatous type.

Visual, endocrine, neurological and cognitive outcomes in 8 patients with craniopharingioma are revealed in Table 2.

Visual field defects were bilateral in 6/7 patients with visual disturbance (Table 1). Visual improvement was estimated according to the postoperative ophthalmological evaluation and subjective information from the patient. Visual status has improved, normalised or remained normal in 6 of 8 patients postoperatively or in 14/16 eyes; in 2 patients, improvement was unilateral only and new visual field deficits appeared in the other eye. In one patient (Patient 7), new visual field deficit appeared in a delayed fashion after initial improvement (on the postoperative day 4). There was no decline of visual acuity and all patients recover the reading capacity with correction (Table 2).

Stalk preservation was possible in 4/8 patients (Table 2). In 2 of them, endocrinological evaluation revealed normal pituitary function, in one panhypopituitarism (1/3 of the stalk thickness preserved; Patient 7) and in one partial hypopituitarism (substitution of tyroid hormon and ADH necessary, substitution of cortisol abandoned after 6 months postoperatively; Patient 6). The rates of DI and new endocrinopathy were 5/8 patients (Table 2).

Hypothalamic dysfunction was initially noted in 4 patients (Patients 3–6), but remained persistent in 2 patients (Patients 3 and 6). Short term memory deficits, confusion and spatial disorientation were recognized early within the first postoperative week. Three patients suffered from hyperphagia and gained 15–30 kg in the first 12 months postoperatively before stabilizing the body weight. Sleep rhythm was temporarely disturbed in 2 patients. It was observed in the second postoperative week and subsided spontaneously after 2–3 months. The psychoorganic syndrome was mild and transient in 2 patients (Patients 4 and 5) and more significant in another 2 (Patients 3 and 6). Memory deficit and emotional lability started to improve after one year as reported by the relatives, but were still observable in the follow-up period (Table 2).

The quality of life was retained in 5/8 patients. It was decreased in 2 patients due to cognitive problems (Patients 3 and 6) and in one due to new visual field deficit on one eye (Patient 7).

Despite the attempt at GTR in all patients, near total (>95%) removal was achieved in one patient (in Patient 7, a translucent capsule of 1.5x1 cm^2, firmly adherent to hypothalamus, was left in place; Figure 1 (1–7b)) and subtotal removal (approx. 90%)

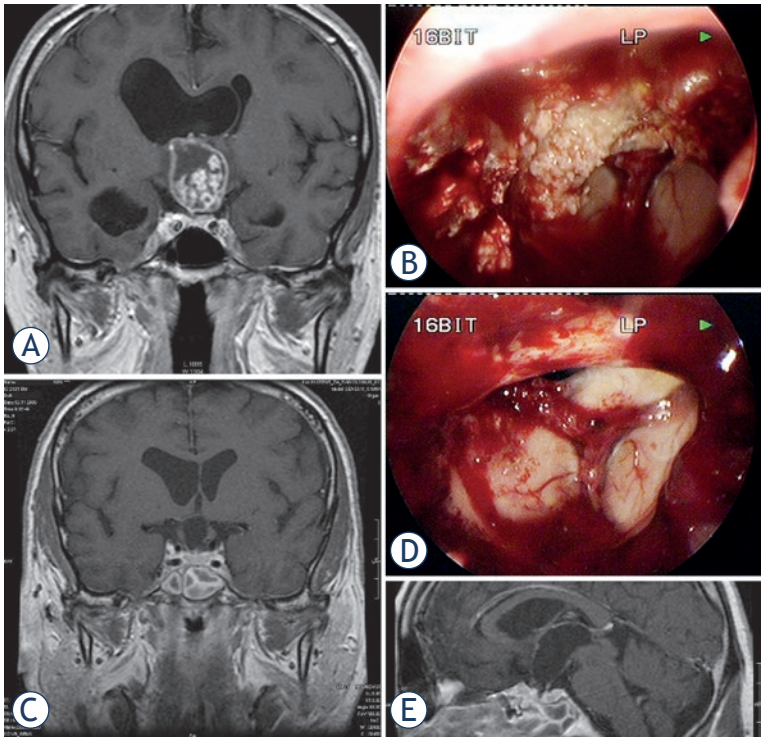

FIGURE 3. Large craniopharyngioma (Patient 3) produced unilateral hydrocephalus by obstructing the right formen of Monro **A**. The dome was filled with soft cholesterine cristals **B**, which were easily removed. Lower limbus of the right foramen of Monro is seen through the empty third ventricle **D**. Despite bilateral preservation of anteromedial hypothalamus **C** and stalk preservation **E**, the patient developed panhypopituitarism and diabetes insipidus with long lasting psychoorganic change.

TABLE 2. Visual, endocrine, neurological and cognitive outcomes in eight patients with craniopharingioma operated on by transplanum approach

Pt. No.	Sex, age	Visual outcome	Visual postop status	Endocrine outcome	Permanent diabetes insipidus	Stalk preservation	Neuro/cognitive consequences	Occupational/ life style resumed	Tumor removal
		Right/Left	Right/Left						
1	M,66	Normalised	Normal	Normal	No	Yes	No	Yes	GTR
2	M, 73	Normalised	Normal	Panh	Yes	No	No	Retired (same)	GTR
3	M, 51	Normal (same)	Normal	Panh	Yes	No	Obesity +30kg, memory, psih	No	GTR
4	F, 71	Improved	can read L+R, less bilat TH	Same (Panh)	Yes (triple response)	No	Mild psih (transit) Obesity +20kg	Retired (same)	NTR
5	F, 60	Improved R/ Worse L	R less temporal/ L TH + sup.NQ, can read L+R	Panh	Yes	No	Sleep (transit), mild psih (transit)	Housewife (same)	GTR
6	F, 69	Improved	can read L+R, R normal / L less central scotoma	Partial hypopituit.	No	Yes	Sleep (transit), psih, memory, obesity +15kg	No	GTR
7	M, 57	Improved R/ Worse L	R less inf.TQ/ L temporal complete	Panh	Yes	Yes	No	No	STR
8	F, 57	Normalised	Normal	Normal	No	Yes	No	Yes	GTR

Newly aquired visual deficit are undelined; TH = bitemporal hemianopsia; NQ = nasal quadrantanopsia; TQ = temporal quadrantanopsia; Panh = panhypopituitarism; hipopit = hypopituitarism; psih = psihoorganic symptomatology; transit = transitory; GRT = gross total removal; NTR = near total removal; STR = subtotal removal

in one patient (0.6 cm midline residual tumour in the optic recess was left in Patient 4, Figure 1 (1–4b)). GTR rate was achieved in 6/8 patients. None of the patients was referred for adjuvant XRT during the present follow-up period. In Patient 7, MRI after 7 months shows no tumour and no capsule, but some microcalcinations. In Patient 4, the subcentimeter residual tumour shows no progress (Figure 1).

The evolution of the sellar closure technique, implanted materials and exact closure in individual patients are revealed in Table 3.

The lumbar drainage was preventively inserted in all patient for the arbitrary 10 days. CSF leak reappeared in 2 patients after 11 (Patient 4) and 20 (Patient 5) days. The revision included an attempt to identify the leakage point using fluorescein dye and tamponade it with fat, followed by sphenoidal sinus obliteration. However, in Patient 4 a second revision was necessary with completely new sellar closure with bilayered fascia lata and a sealant (Table 3). Both patients suffered meningitis from prolonged CSF leak and lumbar drainage and were treated with antibiotics and needeed ventricular-peritoneal (VP) shunting.

In the first patient with CSF leak (Patient 4), the synthetic inlay of Neuropatch (B. Braun Melsungen AG, Melsungen, Germany) was combined with Tachosil (Takeda Pharmaceuticals International GmbH, Zurich, Switzerland) and obliteration of sphenoid sinus with Spongostan™ Absorbable Haemostatic Gelatin Sponge (Ethicon Biosurgery, Somerville, New Jersey, USA) and glue (Beriplast, CSL Behring, King of Prussia, Pennsylvania, USA).

In the second patient with CSF leak (Patient 5), the synthetic inlay (Neuropatch) was combined with Hadad's flap which did not completely cover it, resulting in a leakage point. Althrough efficient closure technique was reported in 2006, it was not usen in the first patients (Table 3).

The bad experience with these 2 patients precluded the use of autologous material (fascia lata) in bilayered sellar closure technique in combination with Hadad flap and sealant Duraseal™Exact (Covidien, Dublin, Ireland) in the following patients. In the last 3 consecutive patients there was no CSF leakage using Hadad's flap. In the last patient, only synthetic and heterologous material was successfully used in combination with the Hadad's flap (Table 3).

Discussion

Craniopharyngiomas are slowly growing epitelial tumours, originating from the epithelial remnants of the craniopharyngeal duct or Rathke's pouch (adamantinomatous subtype) or result from the metaplasia of squamous epitelial cell remnants (squamous papillary form).[12]

Craniopharyngiomas have bimodal incidence with the first peak in children at 5–14 years and second in adults at 65–75 years. Clinical signs and symptoms are diverse and usually appear

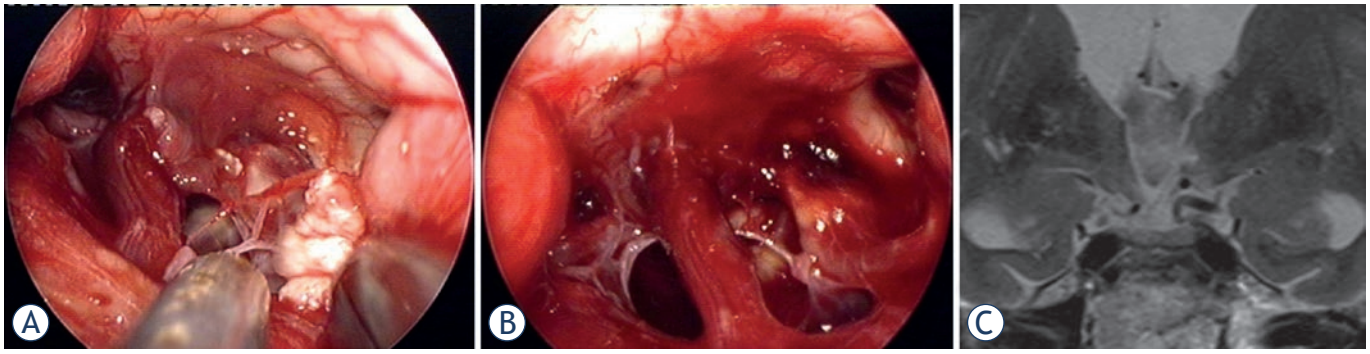

FIGURE 4. The capsule of the cystic craniopharyngioma was firmly attached to the left hypothalamus, the stalk was dislocated to the right side (Patient 6). The outgrowth of the craniopharyngioma from proximal stalk is recognizable **A**. Complete removal of the capsule was possible, but produced subpial blood injection over the left hypothalamic surface **B**. MRI scan revealed a small ischemic injury in the left hypothalamus **C**. This patient had transient sleep disorder, moderate hyperphagia and memory problems (see also a supplemented video material 1).

insidiously. Bitemporal hemianopsia from inferior compression of the chiasm is a typical visual disturbance. Endocrine dysfunction varies from indirect hyperprolactinemia, partial hypopituitarysm and panhypopituitarysm to precocious puberty in children. Large tumours can obstruct CSF pathways and produce obstructive hydrocephalus or affect the hypothalamus. Obesity, sleep disorders, apathy, emotional lability, short-term memory and thermoregulatory problems may accompany the altered neuropsychological profile and decrased mental performance at job or at school. Hydrocephalus and visual deterioration may also have an acute onset. The spontaneous rupture of cysts, containing dark oily liquid, may produce chemical meningitis.[4,12]

The radiological appearance of craniopharyngioma is most commonly that of a cystic/solid and calcified lesion in the suprasellar region. They physically originate from the stalk or the infundibulum. In contrary to pediatric population, only a small number of tumours in adults have infradiaphragmatic origin.[27] The extrasellar growth patterns are numerous.[6,9,13-15,17,28]

As the hypothalamic involvement is the single most important predictor of completness of removal and precludes surgical morbidity, MRI is the imaging method of choice to display dislocation or invasion of the hypothalamus in suprasellar retrochiasmatic growth.[3-6,8] However, the exact outgrowth of craniopharyngioma from the stalk or the infundibulum can not be precisely anticipated from MRI scans.[4-6]

Grading of craniopharyngiomas

Several grading systems were introduced to aid neurosurgeons in planning their surgical strategy either preoperatively from MRI scans and/or judging the feasibility of preservation of stalk and hypothalamus intraoperatively.[2,3,6-8,13,17,29] Hoffmanm proposed pre-, sub-, retrochiasmatic and intraventricular craniopharyngiomas.[13] Intra- or suprasellar, extra- or intraventricular tumour have been proposed by Yasargil, Wang and Steno.[6,7,8,17] Samii *et* Tatagiba proposed the following grading scale: I – intrasellar or infra-diaphragmatic, II – occupying the cistern with or without an intrasellar component, III – lower half of the third ventricle, IV – upper half of the third ventricle, and V – reaching the septum pellucidum or lateral ventricles.[16] Kassam based his classification on the infundibulum: preinfundibular, trans-infundibular, or retroinfundibular and isolated intraventricular.[2] Qi *et al*. studied the arachnoid envelope around the stalk.[5] They noticed that the arachnoid is more firmly attached to the proximal than distal stalk and divided craniopharyngiomas according to the 4 basic growth patterns: infradiaphragmatic, extraarachnoidal, intraarachnoidal and subarachnoidal. According to MRI analysis of 195 cases, these theoretical growth patterns were combined into 5 distinct locations of craniopharyngioma expansion: infradiaphragmatic, extraventricular, extra- and intraventricular, transinfundibular and infundibulo-tuberal.[5]

The protective role of the diaphragm sellae in craniopharyngiomas with infradiaphragmatic origin and suprasellar-retrochiasmatic extension is responsible for less hypothalamic morbidity because such tumour growth is essentially extra-arachnoidal.[7,8,27] In supradiaphragmatic craniopharyingiomas, the classification to extra- and intra ventricular and mixed-type has important clinical implications.[3,6,7] Steno *et al*. found in all 25 mixed tumours and in 3/18 considerably extraventricular tumours

TABLE 3. Sellar closure techniques and complications in transplanum transtuberculum approach for craniopharyngioma

Pt. No.	Sellar closure technique	Lumbar drainage (days)	CSF leak	Revision	Revision technique	Meningitis	Hydrocephalus / internal drainage
1	Neuropatch bilayer, Beriplast, Spongostan	10	No	None		No	No
2	Neuropatch bilayer, Beriplast, Sph obliteration (fat)	14	No	None		No	No
3	Neuropatch inlay, Beriplast, Neuropatch overlay, Tachosil, Spongostan	12	No	None		No	No
4	Neuropatch inlay, Tachosil overlay, Spongostan, Beriplast	11 (+13)	Yes	Twice	I. topic obliteration (Tachosil), Beriplast II. topic obliteration (fat), FL overlay, Sph obliteration (fat, Beriplast)	Yes (no bacteria)	Yes
5	Neuropatch bilayer, Tachosil, Hadad, Duraseal	20 (+14)	Yes	Once	Topic obliteration (fat), Beriplast, Sph obliteration (fat).	Yes (Ps. aer.)	Yes
6	Fat intrasell, FL bilayer, Hadad, Duraseal	12	No	None		No	No
7	Fat intrasell, FL bilayer, Hadad, Duraseal	11	No	None		No	No
8	Tachosil inlay, Duraform overlay (double), Tachosil overlay, Hadad, Duraseal	16	No	None		No	No

FL = fascia lata; Sph = sphenoid sinus; Neuropatch = microporic polyesther urethane (B. Braun Melsungen AG, Melsungen, Germany); Beriplast = fibrin glue CSL Behring, King of Prussia, Pennsylvania, USA); Duraseal = synthetic sealant (Covidien, Dublin, Ireland); Tachosil = animal derived collagen sponge with fibrinized surface (Takeda Pharmaceuticals International GmbH, Zurich, Switzerland); Spongostan = cellulose sponge (Ethicon Biosurgery, Somerville, New Jersey, USA); Hadad = nasal septal vascularized flap; Duraform = collagen-based biocompatible dural implant (Codman, Raynham, Maryland, USA); Ps. aer. = Pseudomonas Aeruginosa

a strip of firm adherence to the third ventricle walls around the equator of the tumour, separating extra- and intraventricular portions.[6] The tumour-glial interface, recognized by many authors and confirmed histologically, may provide a thin nonfunctional cleavage line which may preserve the function of the nuclei and alleviate hypothalamic morbidity.[5,30] The EEA may provide superior results in transinfundibular craniopharyngioma by enabling bilateral dissection at the cleavage line around the tumour circumference under direct vision and in the line of growth, with no blind retraction of the capsule from the hypothalamus on the contralateral side, as present in the lateral transcranial approaches, or upward, as present in transcallosal-transforminal removal. However, the preservation of the morphological integrity of the hypothalamic floor and the stalk is very rarely possible and does not guarantee the function (Figure 3).

We tried to grade our cases according to different classifications and compared the grade with our intraoperative findings (Figure 1, Table 1). None of our cases had an infradiaphragmatic component, although the inferior part of the tumour protruded into the sella in 5 cases (Patients 1, 2, 4, 6, 7). There was a significant discrepancy in medium sized tumours according to false and true intraventricular extension. Solely judged by MRI, the tumour of Patient 3 might also represent pure intraventricular craniopharyngioma or infundibulo-tuberal growth.[2,5] Such tumours are generally approached by transcallosal transforaminal or translaminar approach. Regardless of different classifications, MRI is often not conclusive about the stalk and hypothalamic dislocation or infiltration. The final surgical decision relies upon intraoperative details which are augmented by direct and bilateral visualization in EEA.

Gross total removal rate

GTR is related to a favourable long recurrence-free period and even cure. About 10–15% of totally resected craniopharyngiomas recur and up to 80% are symptoms free after 10 year after GTR without adjuvant XRT.[9,31-33]

GTR of craniopharyngioma is related to the origin of growth and pial and arachnoidal planes.[5,30] Virtually all craniopharyngiomas are related to the hypophyseal infundibulum and the removal of the adherent tumour is related to the high risk of hypothalamic injury (Supplements 1–3). In suprasellar extraventricular craniopharyngiomas, the surface of the tumour can be detached from the arachnoid with the preservation of subchiasmatic and hypothalamic arteries. However, when protruding inside the hypothalamus into the third ventricle, it becomes firmly adherent to its parenchyma inside the infundibulum (Figure 2b). GTR might become impossible in such cases and sharp excision should

be attempted to achieve near or subtotal removal (Patients 4 and 7).

The GTR rate in our series was 75% 6/8 patients, which is a solid result compared to recent series using EEA (Table 4).[18-24,31] We decided against immediate postoperative irradiation in Patient 4 (0.6 cm midline residual in the optic recess, old age) and in Patient 7 (only translucent capsule of 1.5 x 1 cm^2 was left attached to the hypothalamus). None of these 2 patients with near total removal (NTR) and subtotal resections (STR) subsequently deteriorated or showed progression on MRI during the follow-up period (Table 2).

Visual outcome

Vision improvement or normalisation is expected in most surgical cases, the rate of visual deterioration is around 15%.[31,33,34] Vision deterioration is less likely with trans-sphenoidal surgery, especially with preoperatively normal vision.[1,33]

EEA offers midline panoramic direct visualisation all around the tumour and is the most beneficial in dissecting the tumour dome from the undersurface of the chiasm and optic nerves. Special attention must be paid to the perforators of the chiasm which stem from distal supraclinoid internal carotid artery (ICA) and are pushed posteriorly by the tumour (Supplements 1–3). Mechanical trauma and vascular injury from blind dissection to contralateral structures which is more likely with lateral transcranial approaches. are minimized with EEA.

All patients recovered reading capability with correction on each eye, however in 2 patients new visual field deficit appeared or enlarged in one eye (but improved in the other eye). The visual improvement rate in our series was in 6/8 (75%) patients or 87.5% of eyes, which is in accordance with the recent series (average 79.4%, range 71–93; Table 4).[18-24] Vasospasm may be related to the delayed appearance of visual disturbance. After initial improvement, Patient 7 reported unilateral increase of visual field deficit on the postoperative day 4. Interestingly, central vision improved in all eyes, what may be related to the compensation by the fusion reflex of nasal halves of the visual fields.

Postoperative endocrinopathy

Stalk sacrifice is generally an acceptable price for GTR and long lasting recurrence-free time with modern hormonal replacement therapy, and is performed by many surgeons even in cases where stalk preservation is feasible.[10,13-17,31-33,35-38] Stalk preservation is related to 40–50% of thyroid and adrenal function.[10,18,38,39]

The retroinfundibular (Patient 1) and preinfundibular (Patients 6 and 8) variants of craniopharyngioma growth seem to be associated with the highest possibility of preservation of the stalk function. Longitudinal incision along portal vessels of the stalk after extracapsular dissection and surface observation may be the safest introduction into stalk-sparing surgery. However, in transinfundibular craniopharyngiomas (originating from the inside of the stalk and producing stalk expansion), the GTR can be achieved only with stalk resection.[2] This new panhypopituitarysm is not necessarily accompanied with diabetes insipidus in all cases.[37]

The overall rate of new endocrinopathy in craniopharyngioma surgery is reported at 37% for transcranial approaches and 25.7% in small series using EEA (Table 4).[18-24] Our results are comparable to the other few series of suprasellar craniopharyngiomas, removed by EEA, except for the incidence of new endocrinopathy and CSF leak (Table 4). New endocrinopathy (including DI) appeared in 5/8 (62.5%) patients. Stalk was preserved in 4 patients, resulting in normal endocrine status in 2 and partial hypopituitarism in one and panhypopituitarism in one of them. The preservation of the continuity of the stalk in extraventricular craniopharyngiomas enables the pituitary function, however, traction injury to the stalk and its intrinsic vessels or hypophyseal arteries can result in complete or partial pituitary failure. Vasospasm may also be responsible for some failures in pituitary function despite stalk preservation. In Patient 6 (Figure 4b; Supplement 1), the pituitary-suprarenal axis has recovered after 6 months, but not in other patients with partial stalk preservation (Patients 3 and 7). Only one patient had preexistent panhypopituitarism (Patient 4), but got new DI. Our results are at least partially influenced by a higher number of transinfundibular tumours, where stalk preservation is less likely.

Hypothalamic injury and quality of life

Cognitive, behavioral and social problems and re-employment rates are often neglected among surgical results in either transcranial or trans-sphenoidal series of adult patients with craniopharingioma, but are well-known in pediatric population.[4,10,24] The quality of life after craniopharyngioma surgery is determined by cognitive problems from hypothalamic injury and visual impairment. Infiltration of the hypothalamus and ill-defined

TABLE 4. Literature review of the outcomes in extended endonasal aproach for craniopharyngioma

Author, year, [reference]	No. of cases	GTR / NTR (%)	Vision improvement (%)	New DI / Panhypopituitarism (%)	Cognitve decline (%)	Occupational /life style Resumed (%)	CSF leak rate (%)
Frank et al., 2006, [21]	10	70/0	75	30/0	na	na	30
De Divitis et al., 2007, [20]	10	70/0	71	43/17	na	na	20
Gardner et al., 2008, [22]	16	50/25	93	8/18	na	na	69
Cavallo et al., 2009, [19]	22 (all reop.)	41/36	83	14/40	na	na	14
Campbell et al., 2010, [18]	14 (all new)	20/36	79	8/0	na	na	36
Jane et al., 2010, [23]	12	42/42	78	44/67	na	na	0
Leng at al., 2012, [24]	26	69/8 (86/19)*	77	42/38	12	69	3.8
Ikeda et al., 2012, [31]	15	60/0	93	20/67	na	na	0
Bošnjak *et al, current series*	8 (all new)	75/13*	75	63/57	25	63	25

GTR = gross total removal; NTR = near total removal; DI = diabetes insipidus; CSF = cerebrospinal fluid; reop = reoperation for residual or reccurent tumor; * primarily GTR attempted, na = data not available.

cleavage plane are the main intraoperative circumstance that may preclude partial resection to avoid hypothalamic injury. Hypothalamic injury is also possible in extraventricular craniopharyngiomas from the firm adeherence of the tumour to the hypothalamic surface and perforators (Figure 4, Supplement 1).

Hypothalamic injury can be lethal. Memory problems and psycho-organic change are the most disabling symptoms that affect re-employment and return to school. Up to 84% of patients can live independent life with social integration and retain professional occupation after transcranial surgery.[31] Obesity, hyperphagia and sleep disorders also represent hypothalamic injury. These were initially detected in 4/8 our patients (Patients 3, 4, 5 and 6). Petechiae of the inner walls of the infundibulum can be seen in Figure 2d, resulting from forced blunt dissection of the capsular dome (Supplement 2). Similarly, the subpial bleeding of the left outer hypothalamic surface resulted from forced blunt capsular detachment (Patient 6, Figure 1 (4b); Supplement 2). In this patient, unilateral millimeter-sized ischemic lesion in the deep of the left hypothalamus can be seen on the postoperative MRI (Patient 6, Figure 1 (4c)), possibly produced by traction of the hypothalamic perforators. Both patients (Patients 5 and 6) developed psycho-organic change and circadian rhythm sleep disorder, which became apparent in the second postoperative week; these patients presented with severe daytime somnolence. This symptomatic narcolepsy in some patients after removal of craniopharyngioma was found to be related to the low CSF hypocretin-1 level, resulting from injury to the hypocretin-producing neurons in the hypothalamus.[40] Sleep disorder was temporary in both patients and disappeared spontaneously in few months.

Two of 4 patients with postoperative hypothalamic dysfunction never regained their previous quality of life because of psycho-organic change and memory problems (Patients 3 and 6, but disappeared in Patients 4 and 5; Table 2). Additionally, one patient with no cognitive problems did not retain his occupation because of new visual field impairment in one eye (Patient 7; disturbing inferior half visual fields loss).

Cerebrospinal leak

CSF leak is the single most discrepant complication when comparing transcranial and endonasal approaches to craniopharyngiomas. This major drawback of transplanum transtubercle approach has been recently significantly reduced. The average rates from a small number of series, published in the last 5 years is about 24.7% (range 3.8–68%).[18-24] However, Jane *et al*. in 2010 and Leng *et al*. in 2012 reported rates of 0% and 3.8%, respectively.[23,24] Leng *et al*. suggested to use the gasket seal closure using fascia lata with Hadad's flap over it and sealant. Although effective closure techniques were published in 2006, these were not used in the first half of our cases. The CSF leak rate in our first 8 patients was 2/8 (25%) patients (Table 4), while there was no CSF leak in the last 3 patients, using Hadad's flap. However, the routine use of CSF diversion postoperatively for approximately 10 days has not yet been abadonded by us. There were no

subdural effusions or other complications using lumbar drainage of 250–300 mL of CSF outflow per day. Despite exposure of the third ventricle in some of our patients, postoperative antibiotics were not used routinely, except as a single bolus of cephalosphorine (2g) 30 minutes before surgery and after 3 hours of surgery if applicable. Two patients developed meningitis on postoperative day 14 (Patient 4; no bacteria) and 22 (Patient 5; *Pseudomonas aeruginosa*), respectively. Both were treated succesfully with antibiotics, but implantation of a ventriculo-peritoneal shunt was necessary to treat the hydrocephalus. We suggest immediate revision in recurrent CSF and a shorter lumbar drainage time to decrease the rate of CSF infection and hydrocephalus.

Residual tumours and radiation therapy

The management of a remnant tumour is also a point of controversy. A significant number of patients with residual tumours remain stable for a long time.[4] There is a growing evidence in recently published data that similar tumour control rates with less hypothalamic and hypophyseal morbidity can be achieved with STR combined with fractioned radiotherapy (fXTR) or radiosurgery (SRS) as compared to GTR.[10,11] Yang *et al*. studied control rates of different treatment modalities in 442 patients.[11] Progression free survival at 2 and 5 years did not differ between GTR (88 *vs*. 91%) and STR + XRT (67 *vs*. 69%) subgroups. Similar overall survival rates were found at 5 and 10 years (98 *vs*. 99% and 98 *vs*. 95%).[11] In meta-analysis by Sughrue *et al*., 540 patients, treated for craniopharyngioma (mean follow-up >4 years) were stratified into GTR, STR, STR + XTR, fXRT and SRS subgroups.[10] Overall, new endocrinopathy was expected in 37% and overall visual decline in 3.7%. All irradiated patients showed 2-fold increased rate of visual decline as compared to GTR alone. In contrast, GTR was associated with new endocrinopathy 2.5-fold more often (52%) than STR or STR+ XRT. Interestingly, adjuvant XTR in STR alone was not significantly related to visual deterioration.

The EEA may significantly improve the results either in GTR or STR (+ XRT) groups.

Transcranial approaches

Transcranial approaches include 9–90% GTR rate (on average 60–80%).[9,14-16,31,32,41] The transcranial approaches represent principally lateral, anterior and superior routes to craniopharyngiomas. Transpetrosal approach enables posterior route to retrochiasmatic region. A combination of approaches is applied in 10% of cases.[15,17,33] In the most commonly used pterional-transsylvian approach, certain amount of manipulation and mechanical stress to the contralateral neurovascular structures and blind resection are included.[9,14-16] The neurosurgeon removes the tumour between both optic nerve, optic nerve and the supraclinoid ICA, lateral to ICA and superior to ICA bifurcation. Intraventricular part of the tumour is approached anteriorly by trans-lamina terminalis (suitable in cases with a prefixed chiasm) or superiorly by interhemispheric transcallosal approaches. Basal trans-lamina terminalis approach is a midline transcranial approach which is the closest approximation to EEA.

As some recent transcranial series exist with similar high GTR rate over 80%, however, the comparisson between transcranial and endonasal cases in Table 4 is difficult, because transcranial series include complex and multicompartment craniopharingiomas.[1,15,17,34] The sum of >95% for GTR and NTR together has been reported with EEA recently (Table 4).[24] The advantage of direct bilateral visualization with EEA might become more apparent in functional outcomes and decreased major neurological risks (hemiparesis, cranial nerve deficit, intracranial hematoma, etc.) in more calibrated comparative studies in the future.

Utility and limitations

EEA is indicated to strictly midline supradiaphragmatic craniopharyngiomas. If GTR is the primary goal, extension lateral to ICA bifurcation and lateral to the optic nerve and tract are contraindications to EEA.[2] The advantages of EEA are mostly apparent in small to mid-sized centrally protruding supradiaphragmatic craniopharyngiomas. The intraventricular part of the tumour is also easily removable after passing the cleavage line at the infundibulum. Direct visualization in combination with bimanual microsurgical technique enables circumferential and more controlled tumour removal at the cleavage line bilaterally and perforators preservation, stalk-sparing surgery, better and earlier judgement of hypothalamic involvement and earlier switch to subtotal resection. The chances to preserve the integrity of the hypothalamus-stalk-pituitary complex and vascularity of the hypothalamo-chiasmatic region increase with direct multiangled inspection provided by the endoscopy-aided microsurgery.

However, large and giant tumours with lateral extensions into the basal ganglia and middle fossa, retroclivally, into cerebellopontine angle and towards foramen magnum or largely anteriorly projecting tumours or encircling neurovascular structures should be accessed with transcranial approaches.[2, 9, 14, 22]

All authors agree that pure intraventricular craniopharyngiomas (a rare entity) are not an indication for EEA, which would traverse and damage the functioning hypothalamus.[2,3,6,9,21,27] Because morbidity and mortality dramatically increase in reoperations for recurrent craniopharyngiomas, EEA is the first method of choice in recurrent and residual craniopharyngiomas after transcranial surgery, providing inferior "virgin" route as stated by Cavallo *et al*.[19]

Conclusions

Our early outcome results are comparable to the recent few series of patients with supradiaphragmatic craniopharyngiomas, removed by EEA, except for the incidence of new endocrinopathy and CSF leak rate (Table 4). This was influenced by a higher number of transinfundibular tumours in our series, where stalk preservation is less likely, and not using nasoseptal flap or gasket closure in the first half of cases.

There is a tendency of improved GTR rate with less morbidity in endonasal approaches as compared to transcranial approaches.[11,20,21,24] This is more obvious for visual outcome and quality of life than for endocrine outcome.[2,10,16-18,20-24] There is no current data of outcomes yet stratified for certain morphological subtypes of craniopharyngioma. It is intuitively expected in the future, that infradiaphragmatic and suprasellar extraventricular craniopharyngiomas will be agressively approached for GTR with EEA, while infundibulum-invading craniopharyngiomas will be treated with subtotal endoscopical resection and XTR. The first hundred of patients, published to date in a few series and including ours, have been operated using endoscopic transplanum-transtuberculum approach for newly diagnosed or recurrent and residual supradiaphragmatic craniopharyngiomas. The cumulative results of the last 8 series are promising, however, these hypotheses have to be tested on larger number of patients in the future, considering also a postoperative quality of life.[2,19-24,41]

Supplements

Supplement 1: Patient No. 6

http://www.degruyter.com/view/j/raon.2013.47.issue-3/raon-2013-0036/video_1_Patient_6.mov

Supplement 2: Patient No. 5

http://www.degruyter.com/view/j/raon.2013.47.issue-3/raon-2013-0036/video_2_Patient_5.mov

Supplement 3: Patient No. 8

http://www.degruyter.com/view/j/raon.2013.47.issue-3/raon-2013-0036/video_3_Patient_8.mov

Acknowledgment

The authors acknowledge the excellent cooperation with Endocrinology, Otorhinolaryngology and Ophthalmology teams.

References

1. Chakrabarti I, Amar AP, Couldwell W, Weiss MH. Long-term neurological, visual, and endocrine outcomes following transnasal resection of craniopharyngioma. *J Neurosurg* 2005; **102:** 650-7.
2. Kassam AB, Gardner PA, Snyderman CH, Carrau RL, Mintz AH, Prevedello DM. Expanded endonasal approach, a fully endoscopic transnasal approach for the resection of midline suprasellar craniopharyngiomas: a new classification based on the infundibulum. *J Neurosurg* 2008; **108:** 715-28.
3. Pascual JM, Carrasco R, Prieto R, Gonzalez-Llanos F, Alvarez F, Roda JM. Craniopharyngioma classification. *J Neurosurg* 2008; **109:** 1180-2; author reply 82-3.
4. Puget S, Garnett M, Wray A, Grill J, Habrand JL, Bodaert N, et al. Pediatric craniopharyngiomas: classification and treatment according to the degree of hypothalamic involvement. *J Neurosurg* 2007; **106:** 3-12.
5. Qi S, Lu Y, Pan J, Zhang X, Long H, Fan J. Anatomic relations of the arachnoidea around the pituitary stalk: relevance for surgical removal of craniopharyngiomas. *Acta Neurochir (Wien)* 2011; **153:** 785-96.
6. Steno J, Malacek M, Bizik I. Tumor-third ventricular relationships in supradiaphragmatic craniopharyngiomas: correlation of morphological, magnetic resonance imaging, and operative findings. *Neurosurgery* 2004; **54:** 1051-58; discussion 58-60.
7. Wang KC, Hong SH, Kim SK, Cho BK. Origin of craniopharyngiomas: implication on the growth pattern. *Childs Nerv Syst* 2005; **21:** 628-34.
8. Wang KC, Kim SK, Choe G, Chi JG, Cho BK. Growth patterns of craniopharyngioma in children: role of the diaphragm sellae and its surgical implication. *Surg Neurol* 2002; **57:** 25-33.
9. Honegger J, Tatagiba M. Craniopharyngioma surgery. *Pituitary* 2008; **11:** 361-73.
10. Sughrue ME, Yang I, Kane AJ, Fang S, Clark AJ, Aranda D, et al. Endocrinologic, neurologic, and visual morbidity after treatment for craniopharyngioma. *J Neurooncol* 2011; **101:** 463-76.
11. Yang I, Sughrue ME, Rutkowski MJ, Kaur R, Ivan ME, Aranda D, et al. Craniopharyngioma: a comparison of tumor control with various treatment strategies. *Neurosurg Focus* 2010; **28:** E5.

12. Garnett MR, Puget S, Grill J, Sainte-Rose C. Craniopharyngioma. *Orphanet J Rare Dis* 2007; **2:** 18.

13. Hoffman HJ. Surgical management of craniopharyngioma. *Pediatr Neurosurg* 1994; **21(Suppl 1):** 44-9.

14. Komotar RJ, Roguski M, Bruce JN. Surgical management of craniopharyngiomas. *J Neurooncol* 2009; **92:** 283-96.

15. Maira G, Anile C, Rossi GF, Colosimo C. Surgical treatment of craniopharyngiomas: an evaluation of the transsphenoidal and pterional approaches. *Neurosurgery* 1995; **36:** 715-24.

16. Samii M, Tatagiba M. Surgical management of craniopharyngiomas: a review. *Neurol Med Chir (Tokyo)* 1997; **37:** 141-9.

17. Yasargil MG, Curcic M, Kis M, Siegenthaler G, Teddy PJ, Roth P. Total removal of craniopharyngiomas. Approaches and long-term results in 144 patients. *J Neurosurg* 1990; **73:** 3-11.

18. Campbell PG, McGettigan B, Luginbuhl A, Yadla S, Rosen M, Evans JJ. Endocrinological and ophthalmological consequences of an initial endonasal endoscopic approach for resection of craniopharyngiomas. *Neurosurg Focus* 2010; **28:** E8.

19. Cavallo LM, Prevedello DM, Solari D, Gardner PA, Esposito F, Snyderman CH, et al. Extended endoscopic endonasal transsphenoidal approach for residual or recurrent craniopharyngiomas. *J Neurosurg* 2009; **111:** 578-89.

20. de Divitiis E, Cappabianca P, Cavallo LM, Esposito F, de Divitiis O, Messina A. Extended endoscopic transsphenoidal approach for extrasellar craniopharyngiomas. *Neurosurgery* 2007; **61:** 219-27; discussion 28.

21. Frank G, Pasquini E, Doglietto F, Mazzatenta D, Sciarretta V, Farneti G, et al. The endoscopic extended transsphenoidal approach for craniopharyngiomas. *Neurosurgery* 2006; **59:** ONS75-83; discussion ONS75-83.

22. Gardner PA, Kassam AB, Snyderman CH, Carrau RL, Mintz AH, Grahovac S, et al. Outcomes following endoscopic, expanded endonasal resection of suprasellar craniopharyngiomas: a case series. *J Neurosurg* 2008; **109:** 6-16.

23. Jane JA, Jr., Kiehna E, Payne SC, Early SV, Laws ER, Jr. Early outcomes of endoscopic transsphenoidal surgery for adult craniopharyngiomas. *Neurosurg Focus* 2010; **28:** E9.

24. Leng LZ, Greenfield JP, Souweidane MM, Anand VK, Schwartz TH. Endoscopic, endonasal resection of craniopharyngiomas: analysis of outcome including extent of resection, cerebrospinal fluid leak, return to preoperative productivity, and body mass index. *Neurosurgery* 2012; **70:** 110-23; discussion 23-4.

25. Kassam AB, Thomas A, Carrau RL, Snyderman CH, Vescan A, Prevedello D, et al. Endoscopic reconstruction of the cranial base using a pedicled nasoseptal flap. *Neurosurgery* 2008; **63:** ONS44-52; discussion ONS52-3.

26. Hadad G, Bassagasteguy L, Carrau RL, Mataza JC, Kassam A, Snyderman CH, et al. A novel reconstructive technique after endoscopic expanded endonasal approaches: vascular pedicle nasoseptal flap. *Laryngoscope* 2006; **116:** 1882-6.

27. Songtao Q, Yuntao L, Jun P, Chuanping H, Xiaofeng S. Membranous layers of the pituitary gland: histological anatomic study and related clinical issues. *Neurosurgery* 2009; **64:** 1-9; discussion 9-10.

28. Jane JA, Jr., Laws ER. Craniopharyngioma. *Pituitary* 2006; **9:** 323-6.

29. Kitano M, Taneda M. Extended transsphenoidal surgery for suprasellar craniopharyngiomas: infrachiasmatic radical resection combined with or without a suprachiasmatic trans-lamina terminalis approach. *Surg Neurol* 2009; **71:** 290-8, discussion 98.

30. Kawamata T, Kubo O, Hori T. Histological findings at the boundary of craniopharyngiomas. *Brain Tumor Pathol* 2005; **22:** 75-8.

31. Van Effenterre R, Boch AL. Craniopharyngioma in adults and children: a study of 122 surgical cases. *J Neurosurg* 2002; **97:** 3-11.

32. Weiner HL, Wisoff JH, Rosenberg ME, Kupersmith MJ, Cohen H, Zagzag D, et al. Craniopharyngiomas: a clinicopathological analysis of factors predictive of recurrence and functional outcome. *Neurosurgery* 1994; **35:** 1001-10; discussion 10-1.

33. Fahlbusch R, Honegger J, Paulus W, Huk W, Buchfelder M. Surgical treatment of craniopharyngiomas: experience with 168 patients. *J Neurosurg* 1999; **90:** 237-50.

34. Shi XE, Wu B, Zhou ZQ, Fan T, Zhang YL. Microsurgical treatment of craniopharyngiomas: report of 284 patients. *Chin Med J (Engl)* 2006; **119:** 1653-63.

35. Duff J, Meyer FB, Ilstrup DM, Laws ER, Jr., Schleck CD, Scheithauer BW. Long-term outcomes for surgically resected craniopharyngiomas. *Neurosurgery* 2000; **46:** 291-302; discussion 02-5.

36. Honegger J, Buchfelder M, Fahlbusch R, Daubler B, Dorr HG. Transsphenoidal microsurgery for craniopharyngioma. *Surg Neurol* 1992; **37:** 189-96.

37. Ikeda H, Gotoh H, Watanabe K. Outcome of endoscopy-assisted microscopic extended transsphenoidal surgery for suprasellar adult craniopharyngiomas. *Front Endocrinol (Lausanne)* 2012; **3:** 25.

38. Konig A, Ludecke DK, Herrmann HD. Transnasal surgery in the treatment of craniopharyngiomas. *Acta Neurochir (Wien)* 1986; **83:** 1-7.

39. Honegger J, Buchfelder M, Fahlbusch R. Surgical treatment of craniopharyngiomas: endocrinological results. *J Neurosurg* 1999; **90:** 251-7.

40. Tachibana N, Taniike M, Okinaga T, Ripley B, Mignot E, Nishino S. Hypersomnolence and increased REM sleep with low cerebrospinal fluid hypocretin level in a patient after removal of craniopharyngioma. *Sleep Med* 2005; **6:** 567-9.

41. Stamm AC, Vellutini E, Harvey RJ, Nogeira JF Jr, Herman DR. Endoscopic transnasal craniotomy and the resection of craniopharyngioma. *Laryngoscope* 2008; **118:** 1142-8.

research article

Definitive radiotherapy for uterine cervix cancer: long term results for patients treated in the period from 1998 till 2002 at the Institute of Oncology Ljubljana

Helena Barbara Zobec Logar, Barbara Segedin, Robert Hudej, Primoz Petric

Department of Radiotherapy, Institute of Oncology Ljubljana, Zaloška 2, 1000 Ljubljana, Slovenia;

Radiol Oncol 2013; 47(3): 280-288.

Received 26 December 2012
Accepted 24 January 2013

Correspondence to: Helena Barbara Zobec Logar, MD, MSc, Department of Radiotherapy, Institute of Oncology Ljubljana, Zaloška 2, 1000 Ljubljana, Slovenia. Phone: +386 1 5879 204; Fax: +386 1 5879 400; E-Mail: hlogar@onko-i.si

Disclosure: No potential conflicts of interest were disclosed.

Background. The aim of this retrospective study was to analyse results of the two-dimensional (2D) uterine cervix cancer treatment at the Institute of Oncology Ljubljana from 1998 till 2002, before the three-dimensional (3D) approach was introduced in our clinical practice.

Methods. Ninety-eight patients with the following FIGO stage distribution were analysed: 10% IB, 7% IIA, 37% IIB, 4% IIIA and 42% IIIB. The influence of age, haemoglobin level, histology, grade, stage, lymph node status, cumulative point A dose, and an overall treatment time on the survival and local control (LC) were evaluated. Acute and late side effects were assessed.

Results. Five and 8-year overall survival (OS), disease specific survival (DSS) and LC rate were as follows: 47.2% and 43.0%, 54.7% and 53.4%, 74.9% and 72.5%, respectively. Point A dose and histology of the tumour influenced OS, positive lymph nodes DSS and point A dose LC rate. Probability of grade three and four late complications in the first five years was 7.1% for gastrointestinal tract and 3.3% for genitourinary system and vagina.

Conclusions. Point A dose was independent predictor of OS and LC rate, lymph node status predicted DSS, while histology of the tumour influenced OS.

Key words: uterine cervix cancer; external beam radiotherapy; brachytherapy

Introduction

Brachytherapy (BT) in combination with external beam radiotherapy (EBRT) and chemotherapy plays a key role in the definitive treatment of locally advanced uterine cervix cancer.[1-6]

In the field of EBRT, sectional imaging has been widely implemented into the treatment planning process during recent decades. Three-dimensional (3D) conformal computed tomography (CT) based EBRT, employing megavoltage linear accelerators and customized shielding, nowadays represents a generally accepted approach to irradiation in the majority of tumours. Modern EBRT techniques, including intensity modulated radiotherapy and emerging new approaches, allow for increased dose conformity and a tight control over dose distribution in the irradiated tissues.

However, as far as gynaecological BT is concerned, treatment planning in the majority of institutions worldwide is currently still based on a two-dimensional (2D) approach, utilizing a geometrical system of points, defined on two orthogonal pelvic radiographs with the applicator in place.[6-11] In cervix cancer BT, this approach refers mainly to dose prescription at point A[6-9], while the dose to organs at risk (OAR) is most often reported at points as suggested by the International Commission on Radiation units and measurements (ICRU) Report 38 or their alternatives.[7,8] Due to the absence of

visual information on spatial interrelations between the applicator, the target volume and organs at risk, which differ from patient to patient, application to application and even within one application, the 2D approach is characterized by uncertainties regarding dose delivery to the irradiated tissues. In addition, the definition of point-related target and normal tissue dose constraints is controversial due to the steep dose gradient, dose inhomogeneity and non-contiguous high dose regions over the irradiated volume.[7-9] It is therefore clearly more appropriate and reliable to correlate the effects of radiation on tissues with doses, absorbed in certain volumes, rather than at specific points.[12-18] These correlations have been enabled by introduction of 3D sectional imaging into BT treatment planning.[12-14,17]

Nevertheless, a large amount of evidence that supports the correlation between conventional radiography based point doses and the clinical outcome exists.[7,8,12-14,17-25]

At the Institute of Oncology Ljubljana we have been performing 2D radiography based uterine cervix cancer BT until 2006. Subsequently, 3D MRI assisted BT treatment planning has been systematically implemented and currently represents our standard treatment approach.[26,27] When introducing a new method of planning, prescribing, recording and reporting the treatment, it is essential to have a thorough knowledge and understanding of existent traditional institutional techniques. Only by a careful analysis of long standing experience and by linking conventional dosimetric and clinical parameters to the sectional imaging based data, it is possible to avoid potentially hazardous deviations from 2D approach and to fully exploit the benefits of 3D sectional imaging based BT.

This report summarizes a single institutional experience with 2D radiography based treatment planning in uterine cervix cancer radiotherapy in a time period between 1998 and 2002. After 2002, 3D conformal CT-based EBRT was systematically introduced in our clinical practice.

Patients and methods

Patients and tumours

Ninety-eight patients with histologically confirmed uterine cervix cancer and complete medical records that were treated with curative intent with radiotherapy +/- chemotherapy at the Institute of Oncology Ljubljana in the period from January 1998 till December 2002 were enrolled and retrospectively analysed. The investigators followed recommendations of the Helsinki Declaration (1964, with later amendments) and of the European Council Convention on Protection of Human Rights in Bio-Medicine (Oviedo 1997).

Mean patient age was 60.1 (23 to 85) years. Pretreatment patient work-up consisted of gynaecological examination (all patients), chest radiography (98%), cystoscopy (42%), proctoscopy (32%), intravenous urography (19%), abdominal ultrasound (45%) and computed tomography (17%). Each patient was examined by at least three independent examiners, two gynaecologists and one radiation oncologist.

FIGO stage distribution was as follows: 10% IB, 7% IIA, 37% IIB, 4% IIIA and 42% IIIB.

The predominant histological type was squamous cell carcinoma (SCC), representing 92% of all tumours, followed by adenocarcinoma (3%) and other histologies (5%). The tumours were well, moderately and poorly differentiated in 10, 25 and 30%, respectively.

Treatment

The mean interval between the first presentation and the beginning of the treatment was 24 days (range 1-60). All patients were treated with a combination of EBRT +/- concurrent chemotherapy and BT. Mean overall treatment time was 52 days ± 11 days.

EBRT was delivered following conventional radiography-based simulation at a 5-15 MV linear accelerator in 99% and at a Cobalt-60 device in 1% of patients. A mean dose applied via pelvic fields was 40 Gy (20-60 Gy) (2 Gy per fraction, five fractions weekly). A four field technique was applied in 10% and the technique of two opposite fields in 90%.

Paraaortic radiotherapy (mean dose: 32 Gy; range: 20-40 Gy) was carried out in four (4.1%) patients with positive paraaortic (n = 3) and interiliac (n = 1) lymph nodes, as determined by ultrasound or CT.

Six (6.0%) patients received chemotherapy (weekly cisplatin, 40 mg/m^2) concurrent with EBRT.

Following completion of EBRT, low dose rate (LDR) brachytherapy with ^{137}Cs source was applied. A Henschke-type metallic applicator consisting of an intrauterine tandem and a pair of vaginal ovoids was utilized. In 95 (97%) patients, one insertion was performed. Three (3%) patients received two insertions after an interval from one to four weeks. Following insertion, two orthogonal pel-

vic radiographs with the applicator in place were taken. A mean nominal dose of 25 Gy (range 12-36 Gy) was prescribed to point A. Treatment planning was carried out using our in-house developed software application, and was based on the information obtained from the orthogonal radiography. Nominal doses at the ICRU-points for the rectum (ICRU-R) and bladder (ICRU-B) were calculated and recorded.[8]

For the purpose of adding doses from EBRT and BT, it was assumed that the EBRT dose to Manchester point A, point B (3 cm lateral to point A) and to the ICRU points for the bladder and rectum equalled the prescribed EBRT dose. In this study, at time of BT, the rate of dose delivery by the ^{137}Cs source was not equal to the reference dose rate (0.5 Gy/h). In addition, the dose rate was not equal for all patients due to a gradual decrease of ^{137}Cs source activity with time. Therefore, to enable meaningful comparisons of individual treatments, cumulative (EBRT + BT) biologically equivalent doses (EQD2) to the Manchester point A, point B and ICRU points for the bladder and rectum were calculated using the linear quadratic model (reference EBRT dose per fraction = 2 Gy, reference BT dose rate = 0.5 Gy/h, α/β for the tumour = 10 Gy, α/β for the organs at risk = 3 Gy, sublethal damage repair half time = 1.5h).[7] During treatment planning, we aimed at keeping the biological equivalent dose at the ICRU-R and ICRU-B points below our departmental limits of 70 Gy. No attempt was made to assess the dose to other organs at risk (*i.e.* sigmoid colon, small bowel and vagina).

Follow up

Acute treatment side effects were assessed during the treatment and recorded descriptively in the patient chart. For the purpose of this study the Radiation Therapy Oncology Group (RTOG) criteria[28] were employed in an attempt to retrospectively assign corresponding RTOG toxicity levels to individual cases, according to the descriptions in the patient charts. The haemoglobin level was recorded before, during and after the treatment.

Chronic side effects were evaluated at the time of each follow-up visit after the treatment and are reported here according to LENT-SOMA scale.[29] Follow-up investigations were performed respecting our institutional guidelines.[30-32]

Overall survival (OS), disease specific survival (DSS) and local control (LC) actuarial rates were defined as the period from the date of biopsy to the date of death, disease related death and first documented evidence of disease progression or recurrent tumour in true pelvis, respectively.

Statistical analysis

The data were analysed using SPSS 13.0 statistical software package (version 13 for Windows, Copyright© SPSS Inc., Chicago, Illinois). All statistical tests were double-sided; differences at $p < 0.05$ were considered statistically significant.

T-test was used to assess the statistical significance of differences between values of continuous variables. Kaplan-Meier method was applied to calculate actuarial survival and LC rates. Patients without recurrence were censored at time of the last follow-up, visit or death. Surviving patients were censored at time of the last follow-up. Frequencies of different grades of acute and chronic toxicity were calculated. Using the univariate statistical analysis, the influence of FIGO stage, age, nodal status, haemoglobin level, histological type, grade, cumulative EQD2 at point A and overall treatment time on the survival and LC rates were assessed by using a log-rank test. Variables such as age, haemoglobin level and overall treatment time were analysed as quantitative variables using arbitrary cut points (Hb < 100 g/l, Hb ≥ 100 g/l, overall treatment time ≤ 50 days and > 50 days, age < 60, ≥ 60 years). A multivariate analysis, based on the Cox form of the proportional hazards regression model, was performed to test possible predictive variables (method enters probability to enter 0.05, probability to remove 0.1).

Results

Dosimetric data

Cumulative (EBRT + BT) EQD2 at Manchester point A, B, ICRU-R and ICRU-B points are presented in Table 1. There were no statistically significant differences in the mean EQD2 delivered at point A between patients with different FIGO stages (Figure 1). The point A EQD2 was below 60 Gy in 26.0 %, between 60 and 80 Gy in 70.0 % and above 80 Gy in 5.0% of patients, respectively. The mean cumulative EQD2 at ICRU-B and ICRU-R point was 56.9 Gy (range 37.5-79.3) and 62.2 (range 38.3-82.5), respectively.

Survival and local control

The mean follow-up was 77 months (range 2-162 months). The 5-year OS and DSS rates were 47.2%

TABLE 1. Cumulative (EBRT + BT) biologically equivalent doses (EQD2) at Manchester point A, point B and ICRU points for the bladder and rectum (ICRU-B and ICRU-R)

Point	EQD2 mean [range] (GY)
A	66.5 [38.7 - 93.6]
B	60.1 [24.2 - 69.0]
ICRU-B	56.9 [37.5 - 79.3]
ICRU-R	62.2 [38.3 - 82.5]

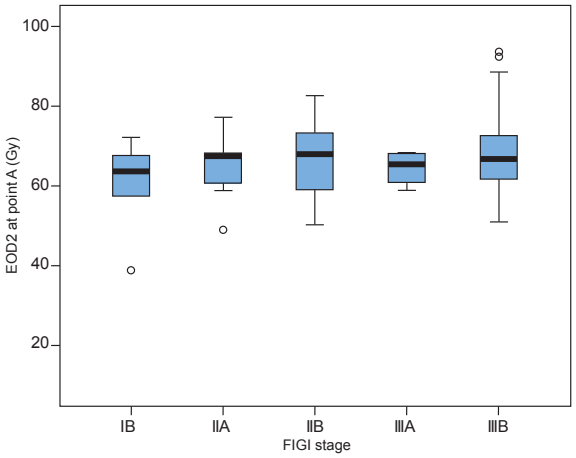

FIGURE 1. Cumulative EQD2 delivered at point A in different FIGO stages. Black horizontal lines represent mean values of EQD2 for each FIGO stage. The height of the box is equal to the interquartile range (IQR), which is the range within which the middle 50% of the ranked data are found. The whiskers indicate the range of the data. Dots represent extreme values.

and 54.7%. As expected, the 5-year OS rate was significantly lower for metastatic disease (patients with positive paraaortic lymph nodes and distant relapse), as for nonmetastatic disease (5.6% *versus* 54.7%, p = 0.000). OS, DSS and LC rates for different FIGO stages at five end eight years are represented in Figures 2 to 4.

The overall LC rate at five years was 74.9%. Six out of 98 patients (6%) had residual disease at the first follow-up (2 stage IIB, 1 stage IIIA and 3 stage IIIB). Two patients developed distant metastases during the treatment (both stage IIIB). All of these patients died.

Twenty-seven (28.0%) out of 98 patients developed a relapse, 11 (11%) in pelvis, 15 (15%) at distant sites and one (1%) in pelvis and distant sites simultaneously. A central pelvic relapse was observed in eight (8%) and a side wall relapse in three patients (3%). Seven patients were secondarily treated with salvage surgery or radiotherapy, but none of them survived.

The first sites of distant relapse were paraaortic lymph nodes in six, lung in four, liver in three, supraclavicular nodes in two and bone in one patient. For patterns of recurrence see Table 2.

The overall LC rate at eight years was 72.5%. After eight years of the follow up one more stage IIA patient developed a central pelvic relapse. One stage IIIB patient developed a distant relapse (paraaortic lymph nodes and lung) after 9.2 years of the follow up.

All three patients with positive paraaortic lymph nodes died within 14 months from the time of diagnosis. The only patient with enlarged lymph nodes, who survived to the time of analysis, was the one with positive interiliacal nodes.

Point A dose had an important role in LC and survival. The 5-year OS rate was 32.1% if the dose to point A was less than 65 Gy and 56.3% when point A dose was 65 Gy or more (p = 0.005). The same was true for DSS and LC. The 5-year DSS was 48.4% for the lower dose and 69.1% for the higher dose (p = 0.08). LC rate was 40.2% for the lower dose versus 84.0% for the higher dose (p = 0.03). The proportion of local recurrences was lower with a higher point A dose (Figure 5). Above 75 Gy no local recurrence was registered.

The histological type of the tumour influenced OS, which was better for SCC than for adenocarcinoma or adenosquamous carcinoma (46.3 *vs.* 0%; p ≤ 0.005). Positive lymph nodes were associated

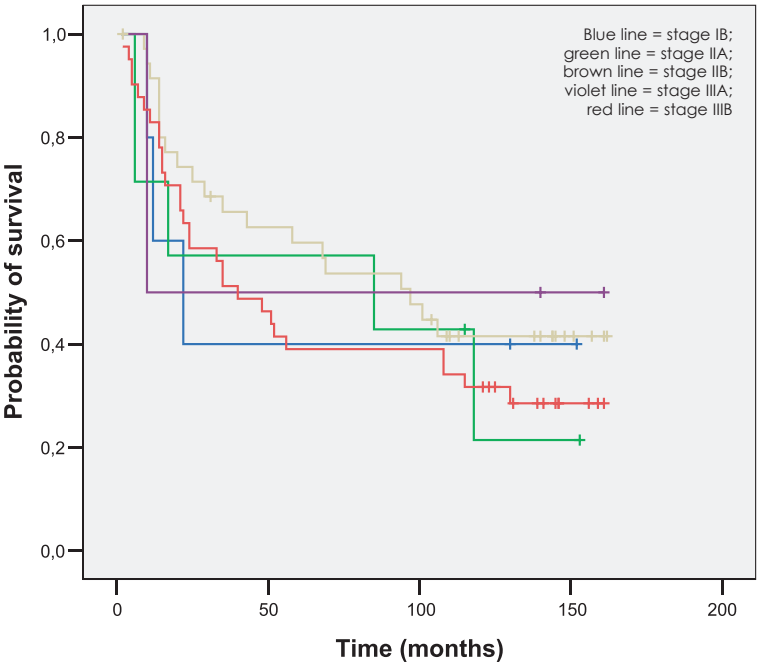

FIGURE 2. Overall survival according to FIGO stage.

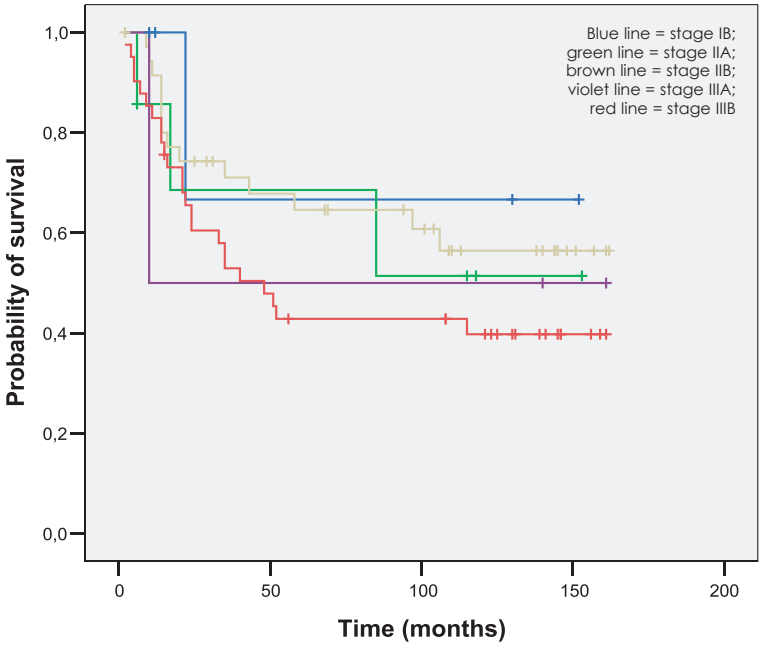

FIGURE 3. Disease specific survival according to FIGO stage.

with a drop in 5-year DSS. If the lymph nodes were negative DSS was 64.5%, vs. 18.8% in case of positive iliac or paraaortic lymph nodes (p = 0.01).

Variables such as age, grade, stage, haemoglobin level and overall treatment time didn't influence survival and LC.

In the multivariate analysis, point A dose retained its independent prognostic value for the OS (p = 0.03, hazard ratio (HR) = 0.5, confidence interval (CI) = 0.3-0.9).

Acute and late side effects

Acute gastrointestinal toxicity was reported in twelve (12.2%) patients. In general it was mild, with grade 1, 2 and 3 proctitis appearing in eight (8.3%) two (2.0%) and two (2.0%) patients, respectively. Acute urinary side effects were reported only in four (4.0%) patients, grade 1 in two (2.0%), and grade 3 in one (1.0%) patient. Only one patient (1.0%) experienced grade 4 acute toxicity.

The mean initial haemoglobin level was 120 (82-152) g/l, fell to 111 (59-150) g/l during the treatment and rose again after the treatment to a mean level of 120 (83-155) g/l in the next four months. The difference between initial and nadir haemoglobin levels was statistically significant (p < 0.005). Transfusion received 14.9% of the patients and erythropoietin received 3.1% of the patients on chemotherapy. There was no statistically significant difference in survival and LC in patients with a low haemoglobin level.

Chronic gastrointestinal side effects were reported by fifteen (15.3%) patients with eight (8.2%) experiencing grade 1, one (1.0%) grade 2, two (2.0%) grade 3 and four (4.1%) grade 4 late gastrointestinal toxicity. One patient developed a rectovaginal fistula, two patients developed ileus, *anus praeter* was formed in one patient.

Ten (10.2%) patients experienced late genitourinary tract toxicity: four (4.1%) grade 1, four (4.1%) grade 2 and two (2.0%) grade 4. Incontinence, haematuria, rise of serum creatinine level and mild hydronephrosis were the most common chronic genitourinary side effects. Rise of creatinine level and mild hydronephrosis developed independently of chemotherapy.

Twelve (12.2%) patients experienced late vaginal toxicity, five (5.1%) grade 1, five (5.1 %) grade 2, one (1.0%) grade 3 and one (1.0%) grade 4. Vaginal stenosis represented the most commonly reported complication.

The probability of developing late side effects of any grade in first five years was 16.6% for gastrointestinal tract, 15.7% for genitourinary system and 22.3% for the vagina. The probability of grade three and four late side effects in the first five years was

TABLE 2. Pattern of progression and relapse according to FIGO stage. The numbers represent numbers of patients which equals to per cent of patients

Stage	IB	IIA	IIB	IIIA	IIIB	Total
Total number	10	7	36	4	41	98
Local progression			2	1	3	6
Distant progression					2	2
Pelvic relapse (central/ side wall)		1 (1/0)	4 (3/1)	1 (1/0)	5 (3/2)	11 (8/3)
Distant relapse	2	1	4	1	7	15
Pelvic and distal relapse			1			1
Overall failure	2	2	11	3	17	35
No evidence of disease	8	5	25	1	24	63

7.1% for gastrointestinal tract and 3.3% for genitourinary system and vagina.

The mean interval before developing the late complication of any grade was 27.6 months (range 6-96 months) for gastrointestinal, 28.7 months (range 3-65 months) for genitourinary and 27.2 months (range 5-53 months) for late vaginal squeal. The mean interval before developing a serious late complication (grade 3 and 4) was 26.5 (range 3-94 months) for gastrointestinal tract, 21.5 months (range 16-27) for genitourinary tract and 21.5 months (range 16-27 months) for the vaginal complications.

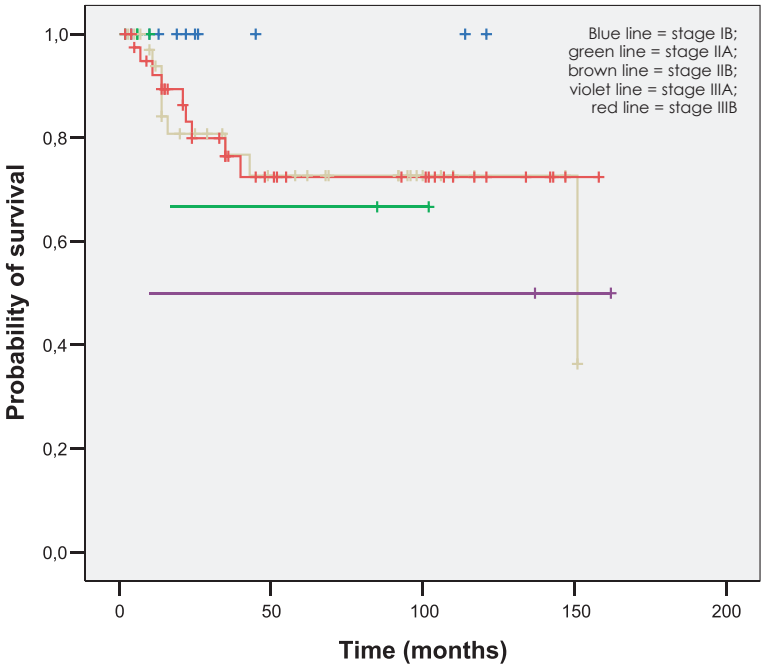

FIGURE 4. Local control according to FIGO stage.

Discussion

In the present study we evaluated historical data of combined EBRT and 2D LDR BT in the treatment of uterine cervix cancer. All the data were collected in a retrospective manner and only patients who received combined EBRT and BT treatment were included. There was no stage IVA disease patient treated with a combined therapy in the study. The weakness of the study was also uneven distribution of patients in different FIGO stages, especially a low number of stage IIA and IIIA patients, which was less than 10%.

The 5-year OS and DSS rates for all 98 patients were 47.2% and 54.7%. OS rate for stage IB was only 40.0%, which was lower than expected and lower than the reported survival rates for more advanced disease.[33-39] Mean age of patients with stage IB disease was higher when compared to the whole group (68.8 ±13.4 years compared to 60.1±14.2 years), so other age related comorbidity factors may have caused lower OS rate. In five out of ten patients in stage IB the death was not associated with primary disease, one patient died of breast cancer, two of metastatic disease due to uterine cervix cancer.

Five-year OS and DSS rates for stage IIA were 44.0% and 55.6%, with LC rate of 66.7%. Low LC rate (50.0%) was also observed in stage IIIA with DSS rate of 50.0%. The Vienna group reported 100.0% and 52.7% pelvic control rate for stage IIA and IIIA at three years, respectively, while Perez *et al*. reported a pelvic failure rate of 0-28% in stage IIA disease and 32-50% in stage III disease at ten years.[35,38] Barillot *et al*. reported 14.5% 5-year pelvic failure rate in stage IIA disease and 40% in stage IIIA disease.[39] We believe that rather high pelvic failure rates in these stages (33.3% in stage IIA, 50.0% in stage IIIA), were mainly due to the extension of the disease in the vagina and poor coverage of the primary tumour with the standard applicator at BT. This could have resulted in lower DSS and OS rates as it would be expected for these two stages.[33-39] Also the number of patients in both stages (seven in stage IIA, four in stage IIIA) was not big enough to make any definite conclusions.

LC rate in stage IIIB group, also the largest group of patients, was very good (72.4%). The Vienna group reported 69.1% LC rate at three years, while Ferrigno *et al*. reported 62 % in stage II and III patients and 58% in stage III at five years.[35,40,41] In the study of Barillot *et al*. the incidence of local failure at five years in stage IIIB was 48.5%.[39] The possible reason for high LC in stage IIIB and low LC rate in other stages (IIA and IIIA) can be explained by the lack of diagnostic procedures (CT and MRI) used to determine TNM stage.

Point A dose showed to be an important factor determining not only LC rate but also OS rate. If the dose was lower than 65 Gy, the 5-year survival rate was 32.2% and LC rate 59.8%, on the other hand if the dose was equal or higher than 65 Gy, OS was 55.1 % and LC rate as high as 89.2%. A rather high LC rate can be partly explained by the lack of stage IVA patients in the study. The Vienna group reported on OS and pelvic control rate at three years of 40% and 60% for stage IVA, and of 58.2% and 77.6% for all patients, respectively.[35] Perez *et al*. included 20 patients in stage IVA disease. There were

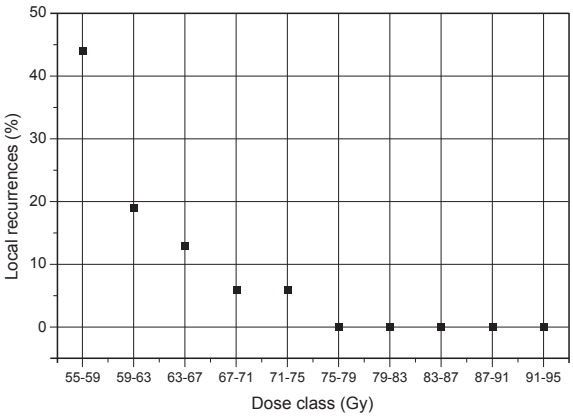

FIGURE 5. Proportion of local recurrences as a function of the point A dose. Point A dose is divided in ten dose classes with a class interval of 4 Gy.

no-long term survivors among them. The overall incidence of pelvic recurrences in stage IVA was 72%, and of distant metastases 55%, respectively.[38] Barillot *et al.* reported 5-year OS rate of 23% and local failure rate of 100% in stage IV, and of 68% in all stages, respectively.[39]

Dose is an important factor for the tumour cure. The optimal dose for the tumour is balanced with the dose to critical organs - sigmoid colon, rectum and bladder. The mean dose to point A in our patients was 66.5 Gy, while the mean dose to organs at risk was below our departmental constraints. Gastrointestinal late toxicities developed in 15.3%, 6.1% were grade 3 and 4 late reactions. Probability of grade three and four late side effects in the first five years was 7.1% for gastrointestinal tract. This is comparable with the Vienna group, which reported the incidence of 6.1% at three years.[35] Lorvidhaya reported 7% combined grade 3 and 4 late complication rate for bowel and bladder.[42] Based on our own experience with MRI based planning in BT and according to the literature, the dose to the rectum (D2cc) is usually lower than the dose to other critical organs.[12,13,27,43,44] Most of the published series report a higher dose to the sigmoid colon than to the rectum. In other words, late gastrointestinal toxicities could be mainly correlated to the high dose to the sigmoid colon rather than to the dose to the rectum.[45] In historical cases the dose to the sigmoid was not registered, so the correlation between the dose to the rectum and late toxicities is not straightforward. However, many studies that compared ICRU doses to critical organs and dose-volume histogram parameters (D2cc) proved a good correlation between ICRU dose and D2cc, especially for the rectal ICRU dose.[46-49]

Serious late bladder complications (grade 3 and 4) were rather rare and reported only in 2% of patients. Vaginal late toxicities grade 3 and 4 were also not as common as reported in the literature, probably because they were not systematically and prospectively recorded.[50] Vaginal late side effects are not commonly reported in the literature.[39,42] The Vienna group is one of the few who provide data on vaginal morbidity after definitive radiotherapy. They reported a 30.6% grade 3 and 4 vaginal complication rate.[35]

Fifteen out of 27 patients with recurrent disease developed relapse at distant sites. One of the reasons for a big proportion of distant failures could be, that CT/MRI were not yet systematically used in uterine cervix cancer patients at that time and only a minority of patients (6%) received concurrent chemotherapy with EBRT. The causes for omitting chemotherapy were advanced age, hydronephrosis, afunction/hypofunction of one or both kidneys, raised creatinin level and other comorbidities. A more systematic introduction of concurrent chemotherapy at our Institute started only after the year 2000.[1] It can be speculated that with the more wide implementation of sensitizing chemotherapy into the primary treatment of advanced disease distant failures can be further reduced and the survival improved.[50-53] Histology, point A dose and presence of positive lymph nodes proved to be critical factors that affect prognosis. Other variables such as age, grade, stage, overall treatment time and tumour size also influenced the survival and LC in other studies.[38,39,54] Their relevance was not confirmed in our study. The tumour size was not tested as the covariate in this study because it was not systematically monitored.

Conclusions

Results of the combined treatment (conventional 2D EBRT + LDR BT) of uterine cervix cancer at the Institute of Oncology Ljubljana were evaluated. 2D based BT approach was associated with good rates of LC in stage IIIB disease, which was the largest group in our study. Variables, influencing prognosis were histology, point A dose and lymph node status. Improved LC and reduced morbidity rates may be expected in the era of the systematic implementation of MRI-based adaptive BT at our department. Treatment results could be further improved with the development of new (individually tailored) applicators to enable the adequate dose-coverage of advanced tumours.

References

1. Morris M, Eifel PJ, Lu J, Grigsby PW, Levenback C, Stevens RE, et al. Pelvic radiation with concurrent chemotherapy compared with pelvic and para-aortic radiation for high-risk cervical cancer. *N Engl J Med* 1999; **340:** 1137-43.
2. Keys HM, Bundy BN, Stehman FB, Muderspach LI, Chafe WE, Suggs CL 3rd, et al. Cisplatin, radiation, and adjuvant hysterectomy for bulky stage IB cervical carcinoma. *N Engl J Med* 1999; **340:** 1154-61.
3. Whitney CW, Sause W, Bundy BN, Malfetano JH, Hannigan EV, Fowler WC Jr, et al. Randomized comparison of fluorouracil plus cisplatin versus hydroxyurea as an adjunct to radiation therapy in stage IIB-IVA carcinoma of the cervix with negative para-aortic lymph nodes: a Gynecologic Oncology Group and Southwest Oncology Group study. *J Clin Oncol* 1999; **17:** 1339-48.
4. Green JA, Kirwan JM, Tierney JF, Symonds P, Fresco L, Collingwood M, et al. Survival and recurrence after concomitant chemotherapy and radiotherapy for cancer of the uterine cervix: a systematic review and meta-analysis. *Lancet* 2001; **8:** 358(9284): 781-6.
5. Vale C. Reducing uncertainties about the effects of chemoradiotherapy for cervical cancer: A systematic review and meta-analysis of individual patient data from 18 randomized trials. *J Clin Oncol* 2008; **26:** 5802-12.
6. Gerbaulet A, Pötter R, Haie-Meder C. Cervix cancer. In: Gerbaulet A, Pötter R, Haie-Meder C, editors. *The GEC ESTRO handbook of brachytherapy*. Brussels: ESTRO; 2002. p. 301-63.
7. Pötter R, Van Limbergen E, Wambersie A. Reporting in brachytherapy: dose and volume specification. In: Gerbaulet A, Pötter R, Mazeron JJ, Meertens H, Van Limbergen E, editors. *The GEC ESTRO handbook of brachytherapy*. Brussels: ESTRO; 2002. p. 155-215.
8. ICRU, International Commission of Radiation Units and Measurements. Dose and volume specification for reporting intracavitary therapy in gynaecology. *ICRU Report 38*. Bethesda, MD: ICRU; 1985.
9. Massey JB, Pointon RS, Wilkinson JM. The Manchester System and the BCRU recommendations for brachytherapy source specification. *Br J Radiol* 1985; **58:** 911-3.
10. Guedea F, Ellison T, Venselaar J, Borras JP, Hoskin P, Poetter R, et al. Overview of brachytherapy resources in Europe: a survey of patterns of care study for brachytherapy in Europe. *Radiother Oncol* 2007; **82:** 50-4.
11. Guedea F, Ellison T, Hoskin P, Hellebust TP, Didier Peiffert D, Londres B, et al. Patterns of care of brachytherapy in Europe: updated results. *Radiother Oncol* 2010; **97:** 514-20.
12. Haie-Meder C, Pötter R, Van Limbergen E, Briot E, De Brabandere M, Dimopoulos J, et al. Recommendations from Gynaecological (GYN) GEC-ESTRO Working Group (I): concepts and terms in 3D image based 3D treatment planning in cervix cancer brachytherapy with emphasis on MRI assessment of GTV and CTV. *Radiother Oncol* 2005; **74:** 235-45.
13. Pötter R, Haie-Meder C, Van Limbergen E, Briot E, De Brabandere M, Dimopoulos J, et al. Recommendations from gynaecological (GYN) GEC ESTRO working group (II): concepts and terms in 3D image-based treatment planning in cervix cancer brachytherapy-3D dose volume parameters and aspects of 3D image-based anatomy, radiation physics, radiobiology. *Radiother Oncol* 2006; **78:** 67-77.
14. Wachter-Gerstner N, Wachter S, Reinstadler E, Fellner C, Knocke TH, Wambersie A, et al. Bladder and rectum dose defined from MRI based treatment planning for cervix cancer brachytherapy: comparison of dose-volume histograms for organ contours and organ wall, comparison with ICRU rectum and bladder reference point. *Radiother Oncol* 2003; **68:** 269-76.
15. Pötter R, VanLimbergen E, Gerstner N, Wambersie A. Survey of the use of the ICRU 38 in recording and reporting cervical cancer brachytherapy. *Radiother Oncol* 2001; **58:** 11-8.
16. Pötter R. Modern imaging in brachytherapy. In: Gerbaulet A, Pötter R, Mazeron JJ, Meertens H, Van Limbergen E, editors. The GEC ESTRO handbook of brachytherapy. Brussels: ESTRO; 2002. p. 123-51.
17. Barillot I, Horiot JC, Maingon P, Truc G, Chaplain G, Comte J, et al. Impact on treatment outcome and late effects of customized treatment planning in cervix carcinomas: baseline results to compare new strategies. *Int J Radiat Oncol Biol Phys* 2000; **48:** 189-200.
18. Perez CA, Grigsby PW, Lockett MA, Chao KS, Williamson J. Radiation therapy morbidity in carcinoma of the uterine cervix: dosimetric and clinical correlation. *Int J Radiat Oncol Biol Phys* 1999; **44:** 855-66.
19. Kovalic JJ, Perez CA, Grigsby PW, Lockett MA. The effect of volume of disease in patients with carcinoma of the uterine cervix. *Int J Radiat Oncol Biol Phys* 1991; **21:** 905-10.
20. Perez CA, Fox S, Lockett MA, Grigsby PW, Camel HM, Galakatos A, et al. Impact of dose in outcome of irradiation alone in carcinoma of the uterine cervix: analysis of two different methods. *Int J Radiat Oncol Biol Phys* 1991; **21:** 885-98.
21. Roeske JC, Mundt AJ, Halpern H, Sweeney P, Sutton H, Powers C, et al. Late rectal sequelae following definitive radiation therapy for carcinoma of the uterine cervix: A dosimetric analysis. *Int J Radiat Oncol Biol Phys* 1997; **37:** 351-8.
22. Chen SW, Liang JA, Yeh LS, Yang SN, Shiau AC, Lin FJ. Comparative study of reference points by dosimetric analyses for late complications after uniform external radiotherapy and high-dose-rate brachytherapy for cervical cancer. *Int J Radiat Oncol Biol Phys* 2004; **60:** 663-71.
23. Ogino I, Kitamura T, Okamoto N, Yamasita K, Aikawa Y, Okajima H, et al. Late rectal complication following high dose rate intracavitary brachytherapy in cancer of the cervix. *Int J Radiat Oncol Biol Phys* 1995; **31:** 725-34.
24. Ferrigno R, dos Santos Novaes PE, Pellizzon AC, Maia MA, Fogarolli RC, Gentil AC, et al. High-dose-rate brachytherapy in the treatment of uterine cervix cancer. Analysis of dose effectiveness and late complications. *Int J Radiat Oncol Biol Phys* 2001; **50:** 1123-35.
25. Kim HJ, Kim S, Ha SW, Wu HG. Are doses to ICRU reference points valuable for predicting late rectal and bladder morbidity after definitive radiotherapy in uterine cervix cancer? *Tumori* 2008; **94:** 327-32.
26. Petric P, Hudej R, Marolt-Mušič M. MRI assisted cervix cancer brachytherapy pre-planning, based on insertion of the applicator in para-cervical anaesthesia: preliminary results of a prospective study. *J Contemp Brachytherapy* 2009; **1:** 163-9.
27. Petric P, Hudej R, Rogelj P, Blas M, Segedin B, Zobec Logar HB, Dimopoulos JCA. Comparison of 3D MRI with high sampling efficiency and 2D multiplanar MRI for contouring in cervix cancer brachytherapy. *Radiol Oncol* 2012; **46:** 242-51.
28. Cox JD, Stetz J, Pajak TF. Toxicity criteria of the Radiation Therapy Oncology Group (RTOG) and the European Organization for Research and Treatment of Cancer (EORTC). *Int J Radiat Oncol Biol Phys* 1995; **31:** 1341-6.
29. LENT SOMA scales for all anatomic sites. *Int J Radiat Oncol Biol Phys* 1995; **31:** 1049-91.
30. Baškovič M, Cerar O, Kaučič M, Kocijan A, Kovačič J, Kuhelj J, et al. [Guidelines for the treatment of the gynaecological malignancies]. [Slovenian]. Ljubljana: Zveza slovenskih društev za boj proti raku; 1992.
31. Baškovič M, Bebar S, Cerar O, Fras AP, Kragelj B, Robič V, et al. [Gynaecological malignancies. Guidelines for the treatment at the Institute of Oncology Ljubljana and Gynaecological Clinic of the University Medical Centre Ljubljana]. [Slovenian]. 2nd revisioned edition. Ljubljana: Zveza slovenskih društev za boj proti raku; 2001.
32. Stržinar V, Baškovič M, Bebar S, Cerar O, Fras AP, Koritnik K, et al. [Gynaecological malignancies. Guidelines for the treatment at the Institute of Oncology Ljubljana and Gynaecological Clinic of the University Medical Centre Ljubljana]. [Slovenian]. 3rd revisioned edition. Ljubljana: Zveza slovenskih društev za boj proti raku, 2002.
33. Perez Ca, Breaux S, Bedwinek JM, Madoc-Jones H, Camel HM, Purdy JA, et al. Radiation therapy alone in the treatment of carcinoma of the uterine cervix. II. Analysis of complications. *Cancer* 1984; **54:** 235-46.
34. Fletcher GH, Hamburger AD. Female pelvis. Squamous cel carcinoma of the uterine cervix. In: Fletcher GH, editor. Textbook of radiotherapy. 3rd edition. Philadelphia: Lea and Febiger; 1980. p. 720-89.
35. Pötter R, Knocke TH, Fellner C, Baldass M, Reinthaller A, Kucera H. Definitive radiotherapy based on HDR brachytherapy with iridium 192 in uterine cervix carcinoma: report on the Vienna University Hospital findings (1993-1997) compared to the preceding period in the context of ICRU 38 recommendations. *Cancer Radiother* 2000; **4:** 159-72.
36. Horiot JC, Pigneux J, Pourquier H. Radiotherapy alone in carcinoma of the intact uterine cervix according to G. H. Fletcher guidelines: a French cooperative study of 1383 cases. *Int J Radiat Oncol Biol Phys* 1988; **14:** 605-11.
37. Pernot M, Hoffstetter S, Peiffert D, Carolus JM, Guillemin F, Verhaeghe JL, et al. Statistical study of a series of 672 cases of carcinoma of the uterine cervix. Results and complications according to age and modalities of treatment. *Bull Cancer* 1995; **82:** 568-81.

38. Perez CA, Grigsby PW, Chao KS, Mutch DG, Lockett MA. Tumor size, irradiation dose, and long-term outcome of carcinoma of uterine cervix. Int J Radiat Oncol Biol Phys 1998; 41: 307-17. Erratum in: *Int J Radiat Oncol Biol Phys* 1999; **45:** 1093.

39. Barillot I, Horiot JC, Pigneux J, Schraub S, Pourquier H, Daly N, et al. Carcinoma of the intact uterine cervix treated with radiotherapy alone: a French cooperative study: update and multivariate analysis of prognostics factors. *Int J Radiat Oncol Biol Phys* 1997; **38:** 969-78.

40. Ferrigno R, dos Santos Novaes PE, Pellizzon AC, Maia MA, Fogarolli RC, Gentil AC, et al. High-dose brachytherapy in the treatment of uterine cervix cancer. Analysis of dose effectiveness and late complications. *Int J Radiat Oncol Biol Phys* 2001; **50:** 1123-35.

41. Ferrigno R, Campos de Oliveira Faria SL, Weltman E, Salvajoli JV, Segreto RA, Pastore A, et al. Radiotherapy alone in the treatment of uterine cervix cancer with telecobalt and low-dose-rate brachytherapy: retrospective analysis of results and variables. *Int J Radiat Oncol Biol Phys* 2003; **55:** 695-706.

42. Lorvidhaya V, Tonusin A, Changwiwit W, Chitapanarux I, Srisomboon J, Wanwilairat S, et al. High-dose-rate afterloading brachytherapy in carcinoma of the cervix: an experience of 1992 patients. *Int J Radiat Oncol Biol Phys* 2000; **46:** 1185-91.

43. Dimopolus J, Schard G, Berger D, Lang S, Goldner G, Helbich T, et al. Systematic evaluation of MRI findings in different stages of treatment of cervical cancer: potential of MRI on delineation of target, patho-anatomical structures and organs at risk. *Int J Radiat Oncol Biol Phys* 2006; **64:** 1380-8.

44. Kirisits C, Lang S, Dimopoulos J, Berger D, Georg D, Pötter R. The Vienna applicator for combined intracavitary and interstitial brachytherapy of cervical cancer: Design, application, treatment planning, and dosimetric results. *Int J Radiat Oncol Biol Phys* 2006; **65:** 624-30.

45. Erickson B, Grossheim L, Mai J. Imaging the nondisplaced rectosigmoid during HDR brachytherapy for cervical cancer can alter dose specification. [Abstract]. *Radiother Oncology* 2004; **71(Suppl 2):** S9.

46. Pelloski CE, Palmer M, Chronowski GM, Jhingran A, Horton J, Eifel PJ. Comparison between CT-based volumetric calculations and ICRU reference-point estimates of radiation doses delivered to bladder and rectum during itracavitary radiotherapy for cervical cancer. *Int J Radiat Oncol Biol Phys* 2005; **62:** 131-7.

47. Kirisits C, Pötter R, Lang S, Dimopoulos J, Wachter-Gerstner N, Georg D. Dose and volume parameters for MRI-based treatment planning in intracavitary brachytherapy for cervical cancer. *Int J Radiat Oncol Biol Phys* 2005; **62:** 901-11.

48. Datta NR, Srivastava A, Maria Das KJ, Gupta A, Rastogi N. Comparative assessment of doses to tumor, rectum, and bladder as evaluated by orthogonal radiographs vs. computer enhanced computed tomography-based intracavitary brachytherapy in cervical cancer. *Brachytherapy* 2006; **5:** 223-9.

49. Cheng JC, Peng LC, Chen YH, Huang DY, Wu JK, Jian JJ. Unique role of proximal rectal dose in late rectal complications for patients with cervical cancer undergoing high-dose-rate intracavitary brachytherapy. *Int J Radiat Oncol Biol Phys* 2003; **57:** 1010-8.

50. Morris M, Eifel PJ, Lu J, Grigsby P, Levenback C, Stevens RE, et al. Pelvic radiation with concurrent chemotherapy compared with pelvic and para-aortic radiation for high-risk cervical cancer. *New Engl J Med* 1999; **340:** 1137-43.

51. Haie-Meder C, de Crevoisier R, Bruna A, Lhommé C, Pautier P, Morice P, et al. Concomitant chemoradiation in patients with cervix cancer. *Bull Cancer* 2005; **92:** 1032-8.

52. Heinzelmann F, Henke G, von Grafenstein M, Weidner M, Paulsen F, Staebler A, et al. Adjuvant radiochemotherapy in patients with locally advanced high-risk cervical cancer. *Strahlenther Onkol* 2012; **188:** 568-75.

53. Kim JY, Kim JY, Kim JH, Yoon MS, Kim J, Kim YS. Curative chemoradiotherapy in patients with stage IVB cervical cancer presenting with paraortic and left supraclavicular lymph node metastases. *Int J Radiat Oncol Biol Phys* 2012; **84:** 741-7.

54. Perez CA, Grigsby PW, Castro-Vita H, Lockett MA. Carcinoma of the uterine cervix. I. Impact of prolongation of overall treatment time and timing of brachytherapy on outcome of radiation therapy. *Int J Radiat Oncol Biol Phys* 1995; **32:** 1275-88.

research article

Evaluation of safety and analgesic consumption in patients with advanced cancer treated with zoledronic acid

Andrej Kmetec[1], Tine Hajdinjak[2]

[1] Department of Urology, University Medical Centre Ljubljana and Medical Faculty Ljubljana, Slovenia
[2] General Hospital Murska Sobota and Medical Faculty Maribor, Slovenia

Radiol Oncol 2013; 47(3): 289-295.

Received 18 February 2013
Accepted 28 March 2013

Correspondence to: Prof. Andrej Kmetec, MD, PhD, Department of Urology, University Medical Centre Ljubljana, Zaloška 7, 1000 Ljubljana, Slovenia. Phone: +386 522 3217; E-mail: andrej.kmetec@kclj.si or kmetec.andrej48@gmail.com

Disclosure: The potential conflict of interest was disclosed. The study was supported by Novartis Pharma Services Inc., Exp. Slovenia.

Background. The aim of the study was evaluation of zoledronic acid with regard to safety, effect on analgesic consumption and impact on occurrence of skeletal related events in patients with bone lesions from solid tumors and multiple myeloma.

Methods. We conducted an observational, 12-month, phase IV and multi-center study. One hundred and twenty-five symptomatic (pain) bone-metastatic patients were included between 2007 and 2009: 92 prostate cancers, 28 multiple myelomas, 5 others. They were prescribed monthly infusions of zoledronic acid in accordance to each disease's treatment guidelines. Analgesics consumption, pain and laboratory values were evaluated.

Results. Zoledronic acid was prescribed concurrent to initial therapy for myeloma and only in late stage of prostate cancer. With treatment, percentage of patients on analgesics decreased in myeloma group (from 57% to 24%) and increased in prostate cancer group (from 70% to 88%). In patients with any analgesics, the use of opiates' prescription dropped from 72.9% to 64%, percentages of non-steroidal analgesics and other mild analgesics increased slightly. Pain score (Visual Analog Scale, VAS) decreased non significantly (by 22%) in prostate cancer but significantly in myeloma (by 97%). Hypocalcaemia grade 3 or 4 was observed in 4% of patients. Deviations in creatinine remained stable throughout. A total of 31 skeletal related events were reported for 10 patients (8%).

Conclusions. Zoledronic acid was safe medication. Different response of pain was seen between prostate cancer and myeloma patients, which might be due to different stages of disease where it was prescribed according to present guidelines. Possibility of earlier start of treatment should be explored in prostate cancer.

Key words: diphosphonates; pain; neoplasm metastasis; bone; clinical trial; phase IV

Introduction

In patients with advanced cancer, bone metastases are a frequent occurrence. Pathological fracture and bone pain may be the first symptoms of the disease. In advanced prostate cancer, bone metastases occur in 74%, sometimes only several years after treatment, causing skeletal complications, pain, impaired mobility, increasing use of analgesics, all of which have a severe impact on the quality of life and survival of the patient.[1-3]. Bone pain affects 70% of multiple myeloma patients and is the most common symptom.

At additional risk are patients with advanced hormone sensitive cancers (most commonly prostate cancer, but also some gynaecological cancers) undergoing regular hormonal deprivation therapy. The therapy causes a decrease in bone mineral density and increases the risk of skeletal related events, particularly pathological fractures or spinal cord compression.[2,4] Further, although bone density loss is part of the aging process, cancer patients

are exposed to additional risk from cancer affecting bone metabolism, impairing patient mobility and causing calcium and vitamin D deficiency.[5]

To limit described damage from bone involvement of cancer, bisphosphonate treatment with its potential of inhibiting osteoclast activity and bone resorption in both osteolytic and osteoblastic bone metastases has evolved and was extensively justified for different cancers. For example, use of zoledronic acid in prostate cancer was established by work of Saad *et al*.[6], who in a 24-month placebo-controlled study confirmed that zoledronic acid reduced by 36% the incidence of all forms of skeletal related events. Moreover, the pain scores on a 10-level pain scale diminished by more than 2 points. The study revealed that the drug was effective even in cases when the patient had experienced a pathological bone fracture before the onset of treatment, reducing the risk of second or subsequent skeletal related events. When a skeletal related event occurs during zoledronic acid therapy, this is considered treatment failure by many urologists, and, consequently, the therapy is discontinued. However, literature reveals that continuation treatment nevertheless maintain its efficacy, preventing subsequent skeletal related events.[6,7] Furthermore, the pre-clinical studies demonstrated bisphosphonates' inhibiting effect on cancer development.[8] Some showed even increased survival in patients on regular treatment with zoledronic acid compared to the placebo group.[7]

After such extensive research work, bisphosphonates were included into treatment guidelines for different cancers.[9,10] Zoledronic acid is the only bisphosphonate to date demonstrating a statistically significant effect in reducing and delaying the time to first skeletal related event, and reducing the pain due to bone metastases in advanced prostate cancer.

As bisphosphonates are becoming every-day prescribed drug in all cancer treatment settings, it seems useful to verify results from laboratory and phase III trials also in the setting of widespread community use. The purpose of the study was evaluation of zoledronic acid treatment in patients with advanced cancer and bone metastases in relation to its safety, its effect on various serum laboratory values, specifically calcium, on analgesic prescription, bone pain and skeletal related events.

Patients and methods

This phase IV observational clinical study was designed, implemented and reported in accordance with the International Conference on Harmonisation of Technical Requirements for Registration of Pharmaceuticals for Human Use (ICH) which completed Tripartite Guidelines for Good Clinical Practice. The study was also conducted in accordance with the ethical principles laid down in the Declaration of Helsinki and was approved by the National Medical Ethics Committee, approval No 84/07/10.

The inclusion criteria were confirmed cancer (solid tumour) or multiple myeloma, objective evidence of bone metastases or lesions, presence of significant pain at baseline and age above 18 years. The inclusion took place between 2007 and 2009. Included patients received zoledronic acid (Zometa) at a dose of 4 mg once a month (dose could have been reduced to 3 mg according to product guidelines) and were monitored for 12 months. The pain status of the patients was assessed at each visit by using the Visual Analogue Scale (VAS) and recording analgesics drug prescription. Skeletal related events were recorded. As skeletal related events counted: pathological bone fractures (vertebral and non-vertebral), spinal cord compression, surgery to bone, radiotherapy to bone or change in anticancer therapy to palliate bone pain. At each visit, laboratory values were measured (serum creatinine, calcium, haemoglobin, albumins, alkaline phosphatase [ALP], aspartate aminotransferase [ASAT], alanine amino transferase [ALAT], bilirubin and, in prostate cancer patients, prostate-specific antigen [PSA]).

Statistical analysis was performed by using the confidence interval method; the percentage was calculated with a 95% confidence interval. Statistical analysis was performed using R v 2.10.1 (R Foundation for Statistical computing).

Results

Inclusion criteria were fulfilled by 125 patients (18 females and 107 males), mean age 69.2 years (from 47 to 89). According to cancer type, 92 patients (73.6%) had prostate cancer, 28 (22.4%) multiple myeloma, 3 (2.4%) kidney cancer and 2 (1.6%) other cancers. As the majority of the patients included were those with multiple myeloma and prostate cancer, the statistical analysis results for kidney cancer and other types of cancer were not sufficiently reliable so we focused on analysis of two groups: prostate cancer patients and multiple myeloma patients.

Reason for zoledronic acid prescription was mostly primary prevention of skeletal related

TABLE 1. Eastern Cooperative Oncology Group (ECOG) performance status of patients before prescription of zoledronic acid

ECOG	Multiple myeloma N (%)	Prostate cancer N (%)	Other N (%)	Total N (%)
0	4 (14)	24 (26%)	1 (20)	29 (23)
1	5 (18)	47 (51)	0	52 (42)
2	5 (18)	18 (20)	3 (60)	26 (21)
3	12 (43)	2 (2)	1 (20)	15 (12)
4	2 (7)	1 (1)	0	3 (2)

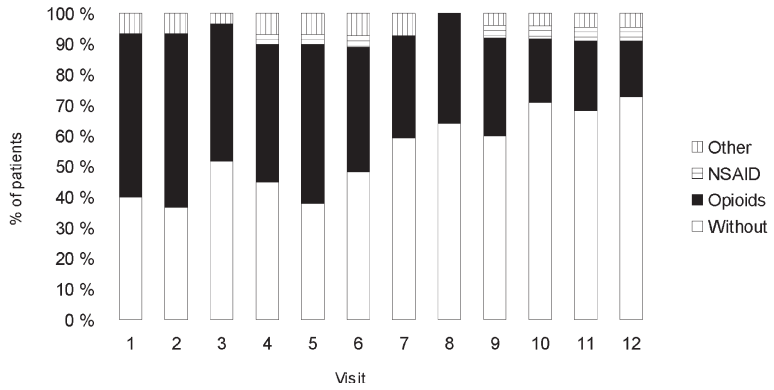

NSAID = non-steroidal antiinflammatory drugs

FIGURE 1. Use of different classes of pain medications by monthly visit in multiple myeloma patients during initial 12-month on zoledronic acid treatment.

events, but also secondary prevention (prescription to patients, who had skeletal related event before prescription).

Eastern Cooperative Oncology Group (ECOG) performance status of patients at the prescription of zoledronic acid is shown in Table 1.

Out of 125 patients who were included in the study, 100 (80%) finished 12 months observation period. Fourteen (11.2%) patients died and 2 (1.6%) stopped treatment due to progression of disease, 3 (2.4%) stopped treatment due to adverse events and 6 (5%) were lost to follow up. According to cancer type, 75% (21/28) of multiple myeloma patients and 82% (75/92) of prostate cancer patients finished study (not statistically significant difference, p=0.065).

Pain and analgesics use

For analysis of analgesic requirement, prescribed analgesics were grouped into 3 groups: opioid analgesics (tramadol, hydromorphone, oxycodone, transdermal fentanyl, piritramide, morphine sulphate), non-steroidal antiinflammatory drugs (diclofenac, ketoprofen) and others (paracetamol, metamizole, pregabalin). The total number of prescribed analgesics did not change significantly. The patients were prescribed a maximum of 4 different analgesics concomitantly. The most frequently prescribed analgesic was tramadol (weak opioid), followed by non-steroidal anti inflammatory drugs. During the follow up period, the percentage of patients receiving analgesic treatment increased slightly: 68% (85 subjects, CI 59.8%-76.2%) at Visit 1, 71.9% (82 subjects, CI 57.3%-73.9%) at Visit 6 and 75% (75 subjects, CI 66.5%-83.5%) at Visit 12. At Visit 1, out of those who received analgesic treatment, 72.9 % received opioids, 36.5% non-steroid analgesics, and 17.6% other analgesics and antipyretics. At Visit 6, the percentage of opioids dropped to 65.9%, non-steroid analgesics rose to 37.8%, while 20.7% received other analgesics. At Visit 12, 64% received opioids, 38.7% non-steroid analgesics, and 26.7% other analgesics.

In the multiple myeloma patients, the proportion of those without analgesic treatment increased during the follow-up period. At Visit 1, 16 (57.1%, CI 38.8%-75.5%) enrolled patients received analgesics, at Visit 6, the number of participants receiving analgesics was 13 (50%, CI: 30.8%-69.2%), and at the end of the period, there were only 5 (23.8%, CI 5.6%-42.0%) patients with multiple myeloma receiving analgesics. The number of opioid recipients diminished (at Visit 1, 16 out of 16 patients opioids were given, at Visit 6, 11 out of 13 patients with instituted analgesic therapy received opioids, and at Visit 12, only 4 out of 5 patients on analgesic treatment were still given opioids).

In the group of treatment recipients, the percentage of those receiving non-steroid anti inflammatory drugs and those on analgesics was on an increase as a result of a drop in the total number of analgesic recipients. Nevertheless, opioids were still the most frequently prescribed group of analgesics in patients on pain therapy. Analgesics requirements of multiple myeloma patients according to visit are shown in Figure 1.

In the group of prostate carcinoma patients, the percentage of patients without prescribed analgesics dropped during the follow-up period from 30.4 % (CI 21,0%- 39.8%) at Visit 1 to 12 % (CI 4.6%-19.4%) at Visit 12. At Visit 1, analgesic treatment was given to 69.6% of participants (CI 60.2%-79.0%), whereas at the end of the follow-up period, as many as 88% (CI 80.6%-95.4%) of the included patients with prostate carcinoma received analge-

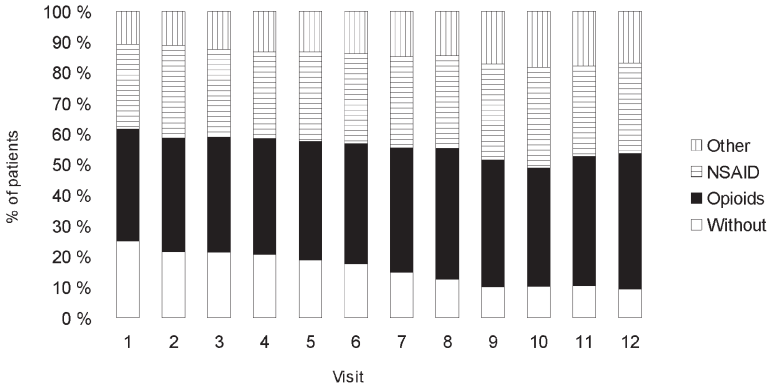

NSAID = non-steroidal anti inflammatory drugs

FIGURE 2. Use of different classes of pain medications by monthly visit in prostate cancer patients during initial 12-month on zoledronic acid treatment.

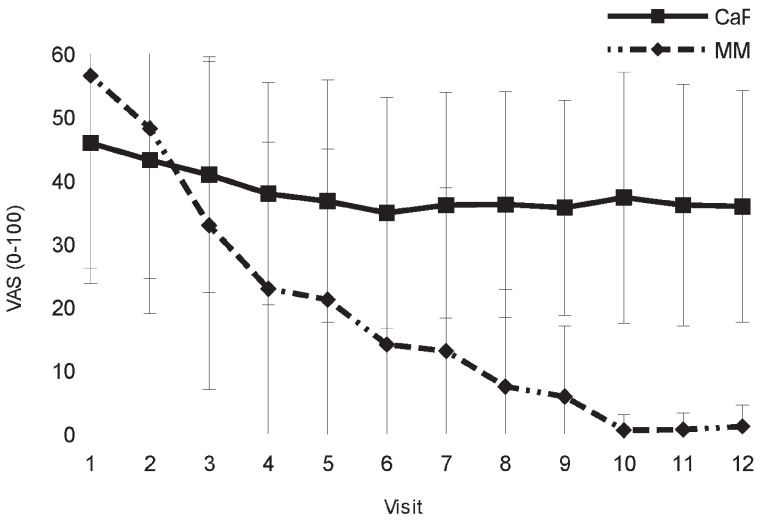

CaF = prostate cancer; MM = multiple myeloma

FIGURE 3. Visual analogue scale pains scores in prostate cancer and multiple myeloma patients during initial 12-month on zoledronic acid treatment.

sics. During the follow up, the percentage of opioid recipients did not vary significantly (at Visit 1, it was 64.1 % (CI 52.3%-75.8%), at Visit 6, it was 60.6 % (CI 48.8%-72.4%), and at Visit 12, it amounted to 63.6 % (CI 52.0%-75.2%). During the follow-up period, the proportion of patients receiving non-steroidal anti inflammatory drugs diminished: at Visit 1, 31 out of 64 patients with instituted pain therapy, i.e. 48.4% (CI 36.2%-60.7%), at Visit 6, 30 out of 66 patients with pain therapy, *i.e.* 45.5% (CI 33.4%-57.5%) and 28 out of 66 patients, *i.e.* 42.4% (CI 30.5%-54.3%) at the last visit. Analgesics prescription in prostate cancer patients according to visit is shown in Figure 2.

In multiple myeloma patients, pain sensation diminished during the follow-up, whereas in patients with prostate carcinoma, no significant changes were observed. In kidney cancer patients, VAS score decreased after Visit 5. Graph of mean VAS score and standard deviation according in prostate cancer and multiple myeloma patients during 12 months of study is shown in Figure 3.

Skeletal related events

During one year of zoledronic acid treatment, new skeletal related events (31 events) were recorded in 10 patients (8%, CI 3.2%-12.8%): 2 with multiple myeloma, 6 with prostate cancer and 2 with other cancers. During the observation period 93.5% of prostate cancer patients and 92.8% of multiple myeloma patients did not experience skeletal related events.

Bone fracture was reported for one patient with multiple myeloma and for 3 patients with prostate cancer. Two bone fractures experienced by one patient with other carcinoma Spinal cord compression was reported for 4 prostate cancer patients, one patient with kidney cancer and one patient with other carcinoma. Bone radiotherapy was performed for one multiple myeloma and one prostate cancer patient. Bone surgery was performed for 3 prostate cancer and one multiple myeloma patients. Change in treatment was related to event in one patient. No cases of hypercalcaemia of malignancy were reported.

Safety

At least one potential adverse event was reported for 101 patients (80.8 %, CI 73.9%-87.0%). One or more potential adverse events were reported for 18 multiple myeloma patients (64.3%, CI 46.5%-82.0%), 79 prostate cancer patients (85.9 %, CI 78.8%-93.0%) and 4 of 5 other cancer patients (3 patients with kidney cancer, 1 patient with unknown primary). Among very common adverse events, increased serum creatinine was observed in 17.9% multiple myeloma and 32.6% prostate cancer patients. There were 4 occasions of creatinine increase Grade 3 or 4.

At first visit, 54% of multiple myeloma patients and 3.5% of prostate cancer patients had abnormal (increased) serum calcium values. For multiple myeloma patients, serum calcium values normalized (decreased) in all patients with available data at visit 10 and remained within normal ranges till the end of observation period. For prostate cancer

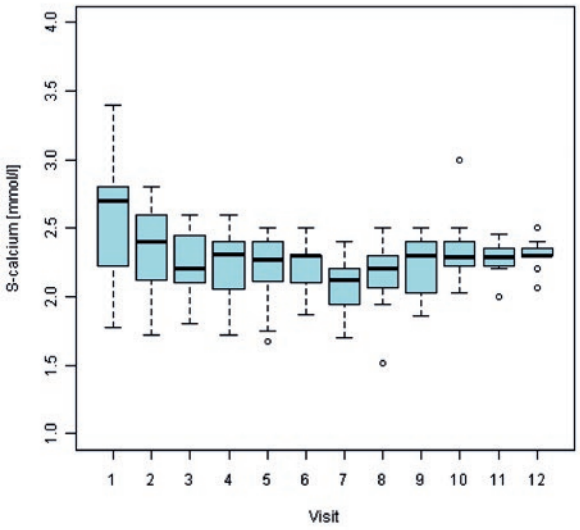

S = serum

FIGURE 4. Mean values and variability of serum calcium concentrations by monthly visit from the beginning of zoledronic acid treatment in multiple myeloma patients.

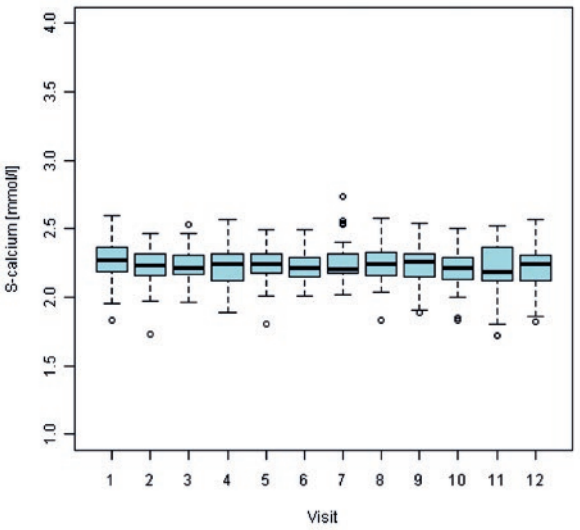

S = serum

FIGURE 5. Mean values and variability of serum calcium concentrations by monthly visit from the beginning of zoledronic acid treatment in prostate cancer patients.

patients, proportion of abnormally low serum calcium values increased during the study period and reached 16.7% at the end of observation period. Overall, hypocalcaemia was observed in 17.9% multiple myeloma patients and in 18.5% prostate cancer patients. There were 5 occasions (5/125; 4%) of hypocalcaemia Grade 3 or 4. Figures 4 and 5 show box plots of serum calcium values by visit for multiple myeloma and prostate cancer patients, respectively.

None of the patients experienced osteonecrosis of the jaw.

Other adverse events (anaemia, elevated PSA) were mainly associated with the primary disease and most cannot be directly linked to zoledronic acid therapy.

Discussion

Patients with bone metastases experience pain and zoledronic acid treatment is aimed also at improving pain control, which was monitored by recording analgesic prescription pattern. In individual patient groups, the most significant reduction in the overall use of analgesics was recorded for the multiple myeloma group, *i.e.* from 57.1% to 23.8%. Accordingly, sensation of pain diminished in multiple myeloma patients, the reduction being more significant than in other types of carcinoma with bone metastases. The results showed well known fact that with the beginning of treatment, analgesics use and pain scores decrease in multiple myeloma patients. This is observed also in multiple myeloma patients, who do not receive zoledronic acid treatment, but at a lesser extent compared to patients who receive treatment.[11] Without bisphosphonate treatment 31%-76% pain amelioration is expected.[12] In our series of multiple myeloma patients, treated with zoledronic acid, much more prominent reduction of pain was observed – 97% if looking at VAS score, mean score decreased from 56.5 (SD 32.8) to 1.2 (SD 3.4). However, this takes into account only patients who remained in trial. In prostate cancer patients, only stabilization of pain score, non-significant reduction of VAS score for 22% was observed (from 46 to 36). In prostate cancer, the percentage of patients requiring analgesic treatment increased from 67% to 88%. The share of opioids remained mostly unchanged. A slight decrease was recorded in the use of non-steroidal analgesics, whereas the share of other, additionally prescribed analgesics increased. Regarding percentage of patients without analgesics, it increased in accordance to decrease in VAS score in group of multiple myeloma patients from 43% to 76%. Percentage of patients without analgesics in prostate cancer group decreased from 33% to 12%, which negates observed (although not significant) decrease in VAS score.

Comparing responses to pain for multiple myeloma and prostate cancer, although obviously dif-

ferent diseases have different progression, it stands out that in multiple myeloma, bisphosphonate treatment is introduced much earlier in the course of disease, synchronously with primary treatment for all patients, irrespectively of bone mineral density, calculations and predictions of future skeletal-related events or confirmation of bone lesions.[10] In prostate cancer patients, bisphosphonates treatment was indicated only after confirmation of bone lesions and at the same time presence of hormone-refractory disease.[13] This may be much too late in the progression of disease. If approached similarly to multiple myeloma, all patients who are treated systemically (hormonally) for prostate cancer would be treated with bisphosphonates, perhaps sparing only patients on watchful waiting, which is equivalent disease stage to smouldering myeloma.

Some older prostate cancer patients (older than 70 year of age with lower body mass index) can get low-dose bisphosphonate treatment without bone metastases, if receive androgen deprivation therapy. At this age and taking into account secondary osteoporosis as risk factor, Fracture Risk Assessment Tool (FRAX) calculator for most shows 3% 10 year risk of hip fracture.[13] Effects of this prophylactic treatment have not been widely studied and should be explored in the future.

The laboratory values for multiple myeloma patients were characterized by a decrease in the percentage of patients with abnormal serum calcium and haemoglobin values, which can be attributed to successful treatment of primary disease as well as to the effect of zoledronic acid. Alkaline phosphatase value in prostate cancer patients remained mostly unchanged throughout the follow-up period. Low haemoglobin values were observed often. In prostate cancer, bone metastases are most frequently found in flat bones which contain bone marrow. Consequently, these patients are diagnosed with anaemia. Among patients with prostate cancer, PSA values were above 4 at the beginning of the study in 78.6% of included patients – this value decreased to 73.6% after one year (of course excluding drop-outs), which cannot be attributed merely to the specific cancer therapy but also to zoledronic acid treatment.

Zoledronic acid is considered safer compared to newer drug for prevention of skeletal related events in cancer patients, denosumab, in regard to frequency of severe hypocalcaemia (grade 3 or 4 according to Common Toxicity Criteria [CTC]).[14] We observed 4% of grade 3 or 4 hypocalcaemia. This result is in line with literature reports - 4.9% of hypocalcaemia grade 3 or 4 was reported in recent meta-analysis for zoledronic acid treated patients, significantly less than for denosumab, a new drug, with comparable therapeutic effect and with less nephrotoxicity.[15,16] Regarding all measurements of serum calcium below normal limits, we observed 16.8% grade 1 and 2 hypocalcaemias at final visit in prostate cancer patients and 0% at final visit in multiple myeloma patients. For prostate cancer patients, higher percentage of measured low grade hypocalcaemia may be attributed also to less attention to need for monitoring and correcting serum calcium (with enough supplementary calcium and vitamin D) by urologists, who were prescribing zoledronic acid to prostate cancer patients compared to haematologists, who were prescribing zoledronic acid to multiple myeloma patients. In the future, as denosumab is becoming one of opinions for prevention of skeletal related events in prostate cancer patients and as denosumab is known to have twice higher rate of hypocalcaemia compared to zoledronic acid, careful monitoring of serum calcium will become even more important.[16] On the other side, at the time of writing, this seems not to be a problem for multiple myeloma patients, where denusomab is not approved due to observed lower survival compared to zoledronic acid according to one trial[17] and remains for this indication strictly investigational.

Zoledronic acid reduces all types of skeletal related events compared to placebo in cancers, metastatic to bone, by 36%.[7,8] Prostate cancer patients are at an even greater risk of skeletal related events than other cancer patients with bone metastases due to hormonal treatment induced secondary osteoporosis. Bisphosphonates were confirmed in many trials to help also in this regard.[18] In our study, during the observation period, skeletal related events were identified in 8% of the patients (10/125). Trial, similar to ours, which included US prostate cancer patients, reported 11.9% skeletal-related events[19], which is within the confidence interval of our observation (3.2%–12.8%).

Frequency of suspected adverse events reported (80.8%) is also similar to the observation in US population, where 84% of suspected adverse events were reported.[19] Adverse events were mainly associated with the primary disease and most cannot be directly linked to zoledronic acid therapy. PSA in prostate cancer patients as a group remained unchanged or even decreased during the observation period which may indirectly support reports of zoledronic acid anticancer activity.[20,21]

Limitation of this observational study is lack of the comparator group receiving no zoledronic ac-

id, however, we believe that this would be ethically inappropriate for the time being.

Similar rate of skeletal related events and of potential adverse events in studies from different parts of the world indicate safe and consistent adverse events profile of zoledronic acid. Zoledronic acid is prescribed in different malignancies in different stages of disease: for multiple myeloma at an early stage and for prostate cancer at a late stage of disease, which correlates with pain response, which is much more favourable when drug is prescribed at earlier stage of disease. Further work should explore potential, efficiency and usefulness of zoledronic acid prescription in earlier phase of disease also in solid tumours, specifically those, where it is already used for secondary osteoporosis treatment.

Acknowledgments

Participating urologists and haematologists : Kisner K, Bratuš D, Hlebič G, Pavlović M, Lah R, Kolenc A, Stanonik GJ, Kacjan U, Jagodič K, Poteko S, Erklavec M, Hawlina S, Štrus B, Lovšin M, Tršinar B, Cotič D, Vrhovec A, Sterle I, Bizjak I, Šutar B, Stanisavlijević ŠS, Bricman IU, Grat M, Fikfak N, Jelenko T, Rotdajč R, Glaser M.

References

1. Coleman RE. Metastatic bone disease: clinical features, pathophysiology and treatment strategies. *Cancer Treat Rev* 2001; **27:** 165-76.
2. Rajer M, Kovač V. Malignant spinal cord compression. *Radiol Oncol* 2008; **42:** 23-31.
3. Gojkovič Horvat A, Kovač V, Strojan P. Radiotherapy in palliative treatment of painful bone metastases. *Radiol Oncol* 2009; **43:** 213-24.
4. Maillefert JF, Sibilia J, Michel F, Saussine C, Javier RM, Tavernier C. Bone mineral density in men treated with synthetic gonadotropin-releasing hormone agonists for prostatic carcinoma. *J Urol* 1999; **161:** 1219-22.
5. Daniell HW, Dunn SR, Ferguson DW, Lomas G, Niazi Z, Stratte PT. Progressive osteoporosis during androgen deprivation therapy for prostate cancer. *J Urol* 2000; **163:** 181-6.
6. Saad F, Gleason DM, Murray R, Tchekmedyian S, Venner P, Lacombe L, et al. A randomized, placebo-controlled trial of zoledronic acid in patients with hormone-refractory metastatic prostate carcinoma. *J Natl Cancer Inst* 2002; **94:** 1458-68.
7. Saad F, Gleason DM, Murray R, Tchekmedyian S, Venner P, Lacombe L, et al. Long-term efficacy of zoledronic acid for the prevention of skeletal complications in patients with metastatic hormone-refractory prostate cancer. *J Natl Cancer Inst* 2004; **96:** 879-82.
8. Aapro M, Saad F. Bone-modifying agents in the treatment of bone metastases in patients with advanced genitourinary malignancies: a focus on zoledronic acid. *Ther Adv Urol* 2012; **4:** 85-101.
9. Mottet N, Bellmunt J, Bolla M, Joniau S, Mason M, Matveev V, et al. EAU guidelines on prostate cancer. Part II: Treatment of advanced, relapsing, and castration-resistant prostate cancer. *Eur Urol* 2011; **59:** 572-83.
10. Anderson KC, Alsina M, Bensinger W, Biermann JS, Cohen AD, Steven Devine S, et al. NCCN Guidelines version 1.2013. Multiple Myeloma. *J Natl Compr Canc Netw* 2013; **11:** 11-7.
11. Tamburrelli FC, Proietti L, Scaramuzzo L, De Stefano V, Logroscino CA. Bisphosphonate therapy in multiple myeloma in preventing vertebral collapses: preliminary report. *Eur Spine J* 2012; **21(Suppl 1):** S141-5.
12. Mhaskar R, Redzepovic J, Wheatley K, Clark OAC, Miladinovic B, Glasmacher A, et al. Bisphosphonates in multiple myeloma: a network meta-analysis. *Cochrane Database Syst Rev* 2012; **5:** CD003188.
13. Mohler, JL, Armstrong AJ, Bahnson RR, Boston B, Busby EJ, D'Amico AV, et al. Prostate cancer, Version 3.2012: featured updates to the NCCN guidelines. *J Natl Compr Canc Netw* 2012; **10:** 1081-7
14. NCI Common Terminology Criteria for Adverse Events (CTCAE) v.4 data files. Availabele 15th February, 2013: http://ctep.cancer.gov/protocolDevelopment/electronic_applications/ctc.htm#ctc_40
15. Peddi P, Lopez-Olivo MA, Pratt GF, Suarez-Almazor ME. Denosumab in patients with cancer and skeletal metastases: a systematic review and meta-analysis. *Cancer Treat Rev* 2013; **39:** 97-104.
16. Fizazi K, Carducci M, Smith M, Damião R, Brown J, Karsh L, et al. Denosumab versus zoledronic acid for treatment of bone metastases in men with castration-resistant prostate cancer: a randomised, double-blind study. *Lancet* 2011; **377:** 813-22.
17. Henry DH, Costa L, Goldwasser F, Hirsh V, Hungria V, Prausova J, et al. Randomized, double-blind study of denosumab versus zoledronic acid in the treatment of bone metastases in patients with advanced cancer (excluding breast and prostate cancer) or multiple myeloma. *J Clin Oncol* 2011; **29:** 1125-32.
18. Serpa Neto A, Tobias-Machado M, Esteves MA, Senra MD, Wroclawski ML, Fonseca FLA, et al. Bisphosphonate therapy in patients under androgen deprivation therapy for prostate cancer: a systematic review and meta-analysis. *Prostate Cancer Prostatic Dis* 2012; **15:** 36-44.
19. Polascik TJ, Given RW, Metzger C, Julian SR, Vestal JC, Karlin GS, et al. Open-label trial evaluating the safety and efficacy of zoledronic acid in preventing bone loss in patients with hormone-sensitive prostate cancer and bone metastases. *Urology* 2005; **66:** 1054-9.
20. Pouessel D, Culine S. Complete clinical and biological response to zoledronic acid in castrate-resistant prostate cancer metastatic to bone. *Anticancer Drugs* 2012; 23: 141-2.
21. Coleman R, Cook R, Hirsh V, Major P, Lipton A. Zoledronic acid use in cancer patients: more than just supportive care? *Cancer* 2011; **117:** 11-23.

research article

Usability application of multiplex polymerase chain reaction in the diagnosis of microorganisms isolated from urine of patients treated in cancer hospital

Zefiryn Cybulski[1], Katarzyna Schmidt[2], Alicja Grabiec[1], Zofia Talaga[1], Piotr Bociąg[2], Jacek Wojciechowicz[2], Andrzej Roszak[3,4], Witold Kycler[5]

[1] Department of Microbiology, Greater Poland Cancer Centre, Poznań, Poland
[2] Genetic Medicine Laboratory CBDNA Research Centre, Poznań, Poland
[3] Department of Radiotherapy and Gynaecologic Oncology, Greater Poland Cancer Centre, Poznań, Poland
[4] Department of Electroradiology, University of Medical Sciences Poznań, Poland
[5] Department of Oncological Surgery II, Greater Poland Cancer Centre, Poznań, Poland

Radiol Oncol 2013; 47(3): 296-303.

Received 17 January 2013
Accepted 11 May 2013

Correspondence to: Zefiryn Cybulski, Department of Microbiology, Greater Poland Cancer Centre, Poznań, Poland. E-mail: zefiryn.cybulski@wco.pl

Disclosure: No potential conflicts of interest were disclosed.

Background. The objective of this study was: i) to compare the results of urine culture with polymerase chain reaction (PCR) -based detection of microorganisms using two commercially available kits, ii) to assess antimicrobial susceptibility of urine isolates from cancer patients to chosen antimicrobial drugs and, if necessary, to update the recommendation of empirical therapy.

Materials and methods. A one-year hospital-based prospective study has been conducted in Greater Poland Cancer Centre and Genetic Medicine Laboratory CBDNA Research Centre in 2011. Urine cultures and urine PCR assay from 72 patients were examined

Results. Urine cultures and urine PCR assay from 72 patients were examined. Urine samples were positive for 128 strains from which 95 (74%) were identical in both tests. The most frequently isolated bacteria in both culture and PCR assay were coliform organisms and *Enterococcus spp*. The Gram negative bacilli were most resistant to cotrimoxazol. 77.2% of these bacilli and 100% of *E. faecalis* and *S. agalactiae* were sensitive to amoxicillin-clavulanic acid. 4.7% of Gram positive cocci were resistant to nitrofurantoin.

Conclusions. The PCR method quickly finds the causative agent of urinary tract infection (UTI) and, therefore, it can help with making the choice of the proper antimicrobial therapy at an early stage. It appears to be a viable alternative to the recommendations made in general treatment guidelines, in cases where diversified sensitivity patterns of microorganisms have been found.

Key words: significant bacteriuria; PCR; microbiological culture; susceptibility tests

Intoduction

The most frequently isolated bacteria responsible for urinary tract infection (UTI) are coliform organisms – about 70% of all bacterial strains isolated from urine samples, followed by *Enterococcus spp*. – about 15.0%, coagulase-negative staphylococci - about 10% and *Pseudomonas aeruginosa*- about 5%. Among the coliforms, *E. coli* comprise about 75% of isolates.[1]

UTI may arise as a nosocomial infection and this is the most frequently observed form of this infection.[2-4] The clinical view of UTI can be symptomatic or asymptomatic, all types of the infection may cause serious effects or prolonged stays in hospital. Significant bacteriuria is one of the most important

factors in UTI. The immediately introduced empirical UTI therapy may prevent severe complications, for example urosepsis, which is especially dangerous for immunocompromised patients, including cancer patients. Side effects after the treatment of cancer: the soft tissue damage after external radiotherapy or brachytherapy causes serious effects and may have a negative influence for the patient's immune system.[5] The most often used antimicrobial drugs for initial, empirical UTI therapy are ciprofloxacin, cotrimoxazole, nitrofurantoin and amoxicillin-clavulanic acid.[6] The PCR method for the detection of the etiologic infection factor can help when choosing appropriate antimicrobial drugs within a few hours. This rapid method is commonly used in diagnosis of bacteremia.[7] Therefore, in our study we wanted to investigate two commercially available kits for urine specimen and compare the results with urine culture.

The objectives of the present study were: 1) to compare the results of urine culture with PCR-based detection of urine sample microorganisms and 2) to assess antimicrobial susceptibility of urine isolates to ciprofloxacin, cotrimoxazole, nitrofurantoin and amoxicillin-clavulanic acid and, if necessary, to update the recommendation of empirical therapy of UTI according to results of these analyses.

Materials and methods

A one-year hospital-based prospective study has been conducted in Greater Poland Cancer Centre and Genetic Medicine Laboratory CBDNA Research Centre in 2011. Urine cultures and urine PCR assay from 72 patients were examined. The study was approved by the ethic commission of University of Medical Sciences Poznan, Poland.

Urine culture and sensitivity tests

The present analysis was carried out on all urinary specimens with bacteriuria of $\geq 10^4$ colony forming units (CFU)/mL, including only the first isolate for each patient per two weeks. There was no information on whether the submitted urine samples came from patients with symptomatic upper or lower UTI or asymptomatic bacteriuria. Urine samples were taken as part of the standard patient care and collected with the use of special urine collection system- UriSwab (Copan). The sponge applicators were dipped into urine samples and transported at once to the laboratory in sterile conditions (sterile plastic preservatives). This procedure protected the urine samples from the infection both in the preanalytical and analytical phase as well.

The qualitative and quantitative analysis of urine included urine cultures on the following media for isolation and diagnosis of microorganisms: ChromID CPS chromogenic agar, D-Coccosel medium, Cetrimide agar, Albicans ID2 agar. All 'under bed' tests were produced by the firm bioMerieux. Cultures were prepared using quantitative loops and incubated at 35°C overnight.

Microorganisms were identified according to standard biochemical tests, which identified most isolated strains to genus level and many to species level. The Vitek identification system (bioMérieux, Marcy l'Etoile, France) was used for confirmation. *In vitro* susceptibility was determined primarily by Vitek AST GP and AST N0 systems.

Extended-Spectrum Beta-Lactamases (ESBL) detection

For ESBL detection the combined method of disc diffusion with the use of discs with ceftazidime (30 μg), ceftazidime/clavulanic acid (30/10 μg) and cefotaxime (30 μg), cefotaxime clavulanic acid (30/10 μg) was used. The discs were placed on a Mueller Hinton agar plate on which a 0.5 McFarland of test organism was swabbed. An organism was considered to be an ESBL producer if there was ≥ 5 mm increase in zone diameter between the cephalosporins with the clavulanate disc and that of the cephalosporins disc alone.[8]

DNA isolation

DNA from urine was isolated using NucleoSpin Tissue Macherey – Nagel (MN) firm. Urine samples were collected into the special urine collection system- UriSwab (Copan). The sponge applicators were dipped into urine samples and transported to the laboratory using special plastic preservatives. The sponge applicator absorbed about 2 mL urine. Then 180 μL T1 buffer and 25 μL proteinase K was added to the urine's sediment and incubated for one hour at 56°C. Then 200 μL of B3 buffer was added and incubated for 10 minutes at 70°C to lyse the samples. 210 μL of 96% ethanol was added to the mixture, which was then loaded onto the column and centrifuged for 1 minute at 11000 g to bind the DNA. To wash the silica membrane, first 500 μL of BW buffer and then 600 μL of B5 buffer was used. This was then centrifuged for 1 minute at 11000 g. The DNA was eluted in 100 μL of TE buff-

TABLE 1. Patient's characteristics

Cancer types	Number	Gender		Age (mean age)	
		Female	Male	Female	Male
Stomach cancer	2	1	1	71	65
Colorectal cancer	4	3	1	72 (63-80)	64
Uterine cervix cancer	3	3	-	52 (39-66)	-
Prostate cancer	11	-	11	-	67 (56-79)
Brain cancer	2	2	-	44 (20-67)	-
Bladder cancer	15	4	11	73 (64-82)	66 (52-81)
Mamma cancer	4	4	-	51 (42-60)	-
Colon cancer	3	2	1	70 (64-76)	83
Kidney cancer	2	2	-	74 (63-84)	-
Maxilla cancer	1	-	1	-	67
Vagina cancer	1	1	-	76	-
Lymphoma amygdale	2	2	-	64	-
Duodenum cancer	1	1	-	57	-
Lung cancer	1	-	1	-	69
Sigmoid cancer	2	1	1	78	58
Nasopharyngeal cancer	1	1	-	70	-
Pancreatic cancer	1	1	-	78	-
Hepatic cancer	2	1	1	70	63
Thyroid cancer	1	1	-	80	-
Breast cancer	1	1	-	80	-
Non-cancer patient	12	6	6	53 (26–80)	71 (63–80)
Total	**72**	**37**	**35**		

er (Tris-EDTA, pH=8). The DNA concentration was measured using spectrophotometric method by NanoDrop. The concentration of the eluted DNA was between 5-50 ng/μL.

Multiplex PCR

Multiplex PCR was performed by using two commercially available diagnostic kits: Seeplex UTI ACE Detection and Seeplex Sepsis DNA (Seegene). Both of these kits are intended for diagnosis of urine specimens. The bacteria target genes were identified according to manufacturer's instructions. The target regions for bacterial genes were not specified by the multiplex PCR producer's. Using the Seeplex UTI ACE detection kit it is possible to detect the following bacteria: Urophathogenic *E. coli* (UPEC), *Proteus mirabilis, Klebsiella pneumoniae, Staphylococcus saprophyticus, Pseudomonas aeruginosa* and *Enterococcus faecalis.* Seeplex Sepsis DNA kit was used for the detection of *Enterococcus faecium/faecalis*, *Staphylococcus aureus*, *Staphylococcus epidermidis*, *Staphylococcus haemolyticus* and other gram positive cocci from *Staphylococcus spp.* then *Streptococcus agalactiae*, *Streptococcus pneumoniae, Streptococcus pyogenes* and *Streptococcus mitis.*

Moreover, this system also detects some gram negative bacteria like: *Enterobacter aerogenes*, *Serratia marcescens, Klebsiella pneumoniae, Enterobacter cloacae, Klebsiella oxytoca, Pseudomonas aeroginosa, Escherichia coli, Proteus mirabilis, Stenotrophomonas maltophilia* and *Acinetobacter baumannii.* The PCR reaction was prepared according to the producer's instructions. The concentration of the eluted DNA was between 5-50 ng/μL. The PCR solution contained DNA polymerase, dNTPs, $MgCl_2$, DNA internal control, primers to internal control and pairs of primers specific to the DNA of the microorganisms. The PCR reaction was amplified in a DNA Engine® thermal cycler (Bio-Rad). 40 thermocycles were performed, each consisting of a 30 s denaturation step at 94°C, a 90 s annealing step at 63°C and a 90 s elongation step at 72°C. In each PCR reaction a positive, negative and internal control were used. The amplified product was visualized under UV light after electrophoresis in a 2% agarose gel

TABLE 2. Number of microorganisms from urine samples detected in molecular and cultural method. Microorganisms: 1-8 Gram negative bacilli; 9-19 Gram positive cocci; 20 Yeast

Nr	Microorganisms	Both tests	PCR only	Culture only
1	*E. coli*	41	5	1
2	*K. pneumoniae*	3	1	-
3	*P. mirabilis*	2	1	-
4	*E. aerogenes*	1	1	-
5	*E. cloacae*	3	-	-
6	*C. freundii**	-	-	1
7	*M. morganii**	-	-	2
8	*P. aeruginosa*	3	4	-
9	*E. faecalis*	20	6	1
10	*E. faecium*	6	-	-
11	*E. gallinarum**	-	-	1
12	*S. aureus*	2	-	2
13	*S. haemolyticus*	2	-	-
14	*S. epidermidis*	3	2	-
15	*S. agalactiae*	8	-	-
16	*S. mitis*	1	-	1
17	*S. group C**	-	-	1
18	*A. viridans**	-	-	1
19	*A. hydrophila**	-	-	1
20	*C. lusitaniae**	-	-	1
	Total	**95**	**20**	**13**

* Pathogens not included in the multiplex panel

containing GelRed (Biotium). Fragment sizes were determined according to marker 100-500 (ABO) (Figure 1).

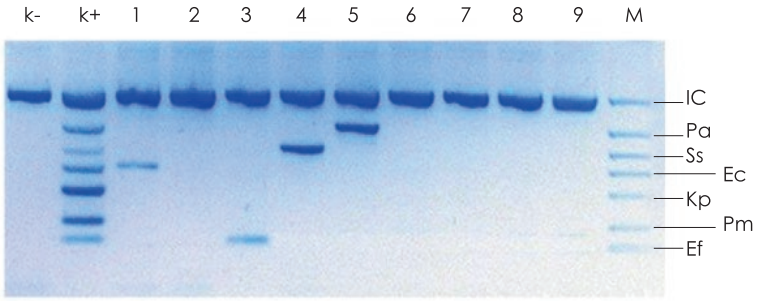

FIGURE 1. Agarose gel elektrophoresis of PCR amplified products generated from patients DNA urine samples. Lane k- is negative control showing no infection any of the detected pathogens, lane k+ is positive control, lane M is the DNA size marker (UTI DNA ladder supplying by producer).

IC = (1000 bp) internal control (DNA plasmid); Pa = (655bp) *P. aeruginosa*; Ss = (526 bp) *S. saprophyticus;* Ec = (401 bp) uropathogenic *E. coli*; Kp = (350 bp) *K. pneumoniae*; Pm = (265 bp) *P. mirabilis*; Ef = (206 bp) *E. faecalis*. Lane 2, 6, 7, 8, 9 shows negative samples, lane 1, 3, 4, 5 shows positive samples: 1 = *E. coli;* 3 = *E. faecalis;* 4 = *S. saprophyticus;* 5 = *P. aeruginosa*

Results

The characteristic of patients group

Urine cultures and urine PCR assay from 72 patients were examined. 60 from them were cancer patients, 31 women and 29 men. The other 12 patients were a heterogeneous group in which cancer was ruled out. The characteristics of the patient group are described in Table 1.

Comparison of PCR and urine culture results

Urine samples were positive for 128 strains of 20 species of microorganisms from which 95 (74%) were identical in both tests (Table 2).

The multiplex PCR method used here proved to be highly specific since it gave only 3.1% of false positive results in comparison with urine cultures of monomicrobial infections and infections caused with two bacterial strains. It was found that urine samples were infected with one, two or three pathogens (Table 3 and 4). The most frequent were mixed infections of *E. coli* and *Enterococcus spp.* The most frequently isolated bacteria in both culture and PCR assay were coliform organisms from the *Enterobacteriaceae* family: 53 cases (56%) from all bacteria strains, then *Enterococcus spp.*: 26 cases (27%). 17% strains were *Streptococcus spp.* and *Staphyloccus spp. E. coli* constituted 42 strains from culture, including two ESBL positive, which were isolated after two weeks of time interval. Infections caused by only one microorganism were detected in 50 urine samples by PCR and 53 urine samples by culture (Table 3).Two strains were found in 23 urine samples by PCR and 24 urine samples by culture (Table 4).

The susceptibility of isolates to antimicrobial drugs

Our investigations involved 20 species of microorganisms, including strains of methicillin resistant *S. aureus* (MRSA) and ESBL.

MRSA strain isolated from one urine sample was sensitive to vancomycin, linezolid, quinupristin/dalfopristin, tigecyclin, rifampicin and nitrofurantoin. Besides beta - lactam antibiotics resistance, this strain was resistant to aminoglycosides, tetracyclines, clindamycin and ciprofloxacin, as well.

TABLE 3. Concordance of detectable pathogens in mono- and polymicrobial infections. 1-6 Gram negative bacilli; 7- 13 Gram positive cocci

Nr	Pathogen	Monomicrobial	Infection 2 pathogens	Infection 3 pathogens
		PCR/culture	PCR/culture	PCR/culture
1	*E. coli*	25/23	19/17	2/2
2	*K. pneumoniae*	1/2	1/1	2/0
3	*P. mirabilis*	2/2	0/0	1/0
4	*E. aerogenes*	1/1	0/0	1/0
5	*E. cloacae*	1/1	1/2	1/0
6	*P. aeruginosa*	2/1	2/1	3/1
7	*E. faecalis*	8/8	13/11	5/2
8	*E. faecium*	3/3	3/3	0/0
9	*S. aureus*	0/2	2/2	0/0
10	*S. haemolyticus*	1/2	1/0	0/0
11	*S. epidermidis*	3/3	1/0	1/0
12	*S. agalactiae*	3/5	4/3	1/0
13	*S. mitis*	0/0	1/2	0/0
	Total	**50/53**	**48/42**	**17/5**

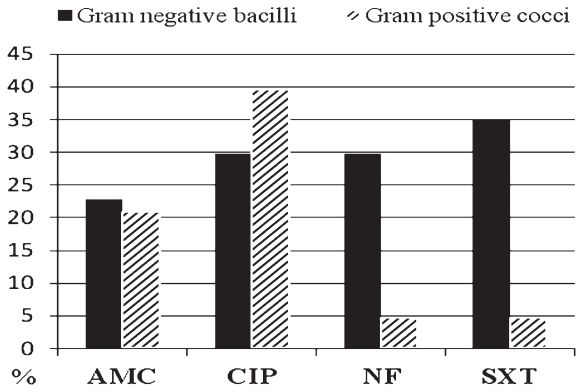

FIGURE 2. The percentage of strains resistant to antimicrobial drugs.

AMC = amoxicillin-clavulanic acid; NF – nitrofurantoin = CIP – ciprofloxacin; SXT = cotrimoxazole

The Gram negative bacilli were most resistant to cotrimoxazol (Figure 2). 29.8% of them were resistant to nitrofurantoin and ciprofloxacin excluding three *P. aeruginosa* strains which were sensitive to chinolons; 77.2% of bacilli and 100% of *E. faecalis* and *S. agalactiae* strains were sensitive to amoxicillin-clavulanic acid. Generally, 4.7% of Gram positive cocci were resistant to nitrofurantoin.

Discussion

Rapid, sensitive and specific methods for the identification of microorganisms causing urinary tract infections are required at hospitals, in clinical laboratories and for epidemiological purposes. Several urine screening techniques have been described, including Gram stain, quantitative leukocyte counts, direct testing of urine sediment, various biochemical methods and automated systems.[9] Each of these techniques has many disadvantages limiting significantly their use in a diagnostic laboratory. The urine culture is still the "gold standard" for diagnosis of UTI.[10,11] It is simple and inexpensive. Moreover, many bacteria which are responsible for UTI can easily grow on the medium. However, sensitivity, quality of the medium, risk of interpretation errors by culture and time consuming growing are limitations. The cultures require 24 to 48 hours to provide results after pure cultures are obtained.[12,13] Even with automated systems such a long incubation is necessary and some additional tests may have to be carried out to differentiate species.[12] The development of molecular techniques has considerably improved the rapidity and accuracy of the microbiological diagnostics. PCR is simple, highly specific, sensitive and amenable to

TABLE 4. Number of infected patients detected by culture and PCR

Methods	Patients' infected 2 pathogens	Patients' infected 3 pathogens
Culture	24	2
PCR	23	6

full automation.[14] It has been successfully used to detect bacterial DNA from different biological fluids. Compared with the classical urine culture, PCR is more rapid and the results are available 5 hours after the specimen collection. However, the use of PCR in diagnostic laboratories is limited by cost, availability of adequate diagnostic kits and availability of appropriate biological materials.[14] To overcome these shortcomings and to increase the uses of PCR, multiplex PCR has been described.[14] According to multiplex PCR, which uses several pairs of specific primers to target bacteria sequences, it is possible to detect more than one pathogen in one reaction. It saves considerable time and costs in diagnosis and allows the treatment with a specific antibiotic to be started more quickly.

However, it should be emphasized a need for the critical evaluation of the role of multiplex PCR in the diagnosis of significant bacteriuria. Conventional PCR gives only a presence or absence result of the specific pathogens. On the other hand a small, insignificant number of bacteria may give a positive result in PCR technique. Therefore, a future development of quantitative real time multiplex PCR assays with pathogens specific probes can overcome the limitations of conventional PCR and can be used to quantitative research. In our investigation we used two commercially available kits that are resisted to the dual priming oligonucleotide (DPO) technology (Seegene, Seoul, Korea). This DPO system is structurally and functionally different from the traditional primer available system. It has two separate primer segments with distinct annealing properties incorporated into a single primer, which are joined by poly(I) linker. This blocks the extension of nonspecifically primed templates and achieved consistently high specifically of the assay.[15,16]

In the present study multiplex PCR allowed the detection of more pathogens than the cultures, as shown in Tables 2 and 3. According to Lehmann *et al.*, such divergence of the results might be interpreted as false positive PCR assays or false negative microbiological findings.[13] False positive PCR results can be related to the amplification of free DNA released from unviable or killed bacteria, whereas cultural methods detect only viable and reproductive organisms.[13] However, two samples with *S. aureus* and one sample with *S. mitis* detected by culture in our investigation showed negative results in PCR. This might be explained by the degradation of DNA.

Karupati *et al.* reported that PCR assays detected low numbers of bacteria in tissues or body fluids that were difficult to culture or that were serologically similar. This might be one of the reasons why multiplex PCR detected more mixed infections than culture.[7] Knowing that normal human urine microorganisms include numerous opportunistic bacteria and fungi, fastidious and anaerobic microbes, which are potentially pathogenic[17-21], an early detection and identification of etiological factors causing UTI is, therefore, crucial in the clinical setting of the immunocompromised patient.

The diagnosis of UTI is usually based on quantitation of uropathogens in voided urine. Significant bacteriuria is one of the most important. For the criterion of a significant bacteriuria a concentration of $\geq 10^5$, 10^4 or 10^3 CFU/mL may be considered.[22,23] We used $\geq 10^4$ CFU/mL for purposes of this investigation.

Although microbiological culture takes more time to get results, it is still the best way to generate the sensitivity test which is necessary for the further treatment. The results of antibiotic resistance by PCR are insufficient. Bacterial resistance tests found only mecA gene in MRSA and vanA/vanB/vanC gene in *Enterococcus spp.* We found one MRSA strain. The infections caused by MRSA are particularly dangerous because of a very high resistance of these bacteria to antibiotics.

PCR method cannot yet replace the traditional microbiological urine culture, but can supplement it and greatly reduce the time needed to obtain results in urgent cases. Rapid and sensitive methods for the identification of pathogens initiated before the empirical therapy may be helpful in choosing the effective treatment, decreasing clinical symptoms and decreasing the proportion of resistant pathogens. Furthermore, the development of DNA based assays may reduce costs by decreasing the length of hospitalization and conserving hospital resources.

Breast and lung cancer are the leading cancer type among women and men, respectively and lung cancer is the most common cause of cancer death worldwide.[24-28] On the other hand, urinary bladder cancer continues to pose a significant global health challenge.[29] It was most frequently observed cancer between our patients, as well (Table 1).

Choosing the appropriate treatment based on the results of sensitivity tests seemed to be the best means of avoiding the use of unnecessary antibiotics and decreasing the risk of serious complications occurring. There is no publication date suggesting the use PCR method for an early diagnosis of the etiological UTI factor in immunocompromised patients. The described method allows differentiating

coliform bacilli from *P. aeruginosa* what is crucial for the proper treatment of patients. *P. aeruginosa* is an opportunistic human pathogen. It is known for its ability to inhabit diverse habitats ranging from soil to immunocompromised individuals.[30,31] We isolated three *P. aeruginosa* strains which were genetically resistant to nitrofurantoin, while 70.2% coliform strains were sensitive to this drug. Because of this the early differentiation between *P. aeruginosa* and coliform is important when nitrofurantoin is introduced into the treatment. Moreover, used PCR methods differentiated *E. faecalis* and *S. agalactiae* that were sensitive to amoxicillin/clavulanic acid from *E. faecium* mostly resistant to this antibacterial drug. Our results draw attention to the emergence of organisms resistant to ciprofloxacin and cotrimoxazole, many authors list drugs as standard treatments for UTI.[6,32] Local UTI treatment guidelines seem to be very important. However, there are substantial differences even between high-standard guidelines on the same well defined clinical entity for UTI management.[33] The selection of a specific antimicrobial drug for the treatment of a symptomatic UTI episode will be determined by known or suspected susceptibilities of the infecting organism, clinical presentation, patient tolerance, documented efficacy of the agent in the treatment of urinary tract infection, as well as administrative factors such as formulary availability or cost. While the empirical therapy has been initiated, the response to therapy and antimicrobial selection should be re-evaluated after 48 to 72 hours, when culture results are available.[34,35] The results of cultures and sensitivity tests may be used to verify the treatment.

In this study, it was found that most microorganisms remained susceptible to nitrofurantoin (Figure 2). However, this drug was licensed for lower UTIs only, and should be administered for a minimum of 7 days for the empirical therapy.[35,36] Cotrimoxazole was not recommended for the treatment of UTI caused by *Enterococcus sp.* According to our knowledge, there were no available data in the literature concerning rapid diagnostics of bacteriuria in the cancer patients. On the other hand, high risk of serious UTI complications has been well documented in the cancer patients.[37]

Conclusions

The PCR method quickly identified the causative agent of UTI infection and because of this significantly helped in making the choice of proper antimicrobial therapy at an early stage. It seems it is the better way than recommendation of general treatment guidelines when diversified sensitivity patterns of microorganisms have been found. The multiplex PCR method used here proved to be highly specific since it gave only 3.1% of false positive results in comparison with urine cultures of monomicrobial infections and infections caused with two bacterial strains.

Acknowledgements

This study was supported by Grant 3/2012(45) from Greater Poland Cancer Centre, Poznan, Poland.

References

1. Cybulski Z, Kjaeldgaard P. Resistance to oral antibiotics in urinary coliform strains isolated between 2000 and 2008 in Sønderborg area, Denmark. *Int J Antimicrob Agents* 2010; **35:** 516-7.
2. Bouza E, San Juan R, Muñoz P, Voss A, Kluytmans J. Co-operative Group of the European Study Group on Nosocomial Infections: A European perspective on nosocomial urinary tract infections I. Report on the microbiology workload, etiology and antimicrobial susceptibility (ESGNI-003 study). European Study Group on Nosocomial Infections. *Clin Microbiol Infect* 2001; **7:** 523-31.
3. Laupland KB, Zygun DA, Davies HD, Church DL, Louie TJ, Doig CJ. Incidence and risk factors for acquiring nosocomial urinary tract infection in the critically ill. *J Crit Care* 2002; **17:** 50-7.
4. Warren JW. Catheter-associated urinary tract infections. *Int J Antimicrob* 2001; **17:** 299-303.
5. Conde S, Borrego M, TeixeiraT, Teixeira R, Corbal M, Sá A, *et al.* Impact of neoadjuvant chemoradiation on pathologic response and survival of patients with locally advanced rectal cancer. *Rep Pract Oncol Radiother* 2010; **15:** 51-9.
6. Geerlings SE, van den Broek PJ, van Haarst EP, Vleming LJ, van Haaren KM, Janknegt R, et al. Optimisation of the antibiotic policy in the Netherlands. X. The SWAB guideline for antimicrobial treatment of complicated urinary tract infections. *Ned Tijdschr Geneeskd* 2006; **150:** 2370-6.
7. Karupati P, Chow C, Kumarasinghe G, Poh CL. Rapid detection of *Klebsiella pneumoniae* from blood culture bottles by real time PCR. *J Clin Microbiol* 2004; **42:** 1337-40.
8. Clinical and Laboratory Standards Institute. Performance standards for antimicrobial susceptibility testing. *CLSI Document M100- S17*. **Vol. 27 No 1.** Wayne PA; 2007.
9. Church D, Gregson D. Screening urine samples for significant bacteriuria in the clinical microbiology laboratory. *Clin Microbiol Newsletter* 2004; **26:** 179-83.
10. Bartges JW. Diagnosis of urinary tract infections. *Vet Clin North Am Small Anim Pract* 2004; **34:** 923-33.
11. Lehmann LE, Hauser S, Malinka T, Klaschik S, Weber SU, Schewe JC, et al. Rapid qualitative urinary tract infection pathogen identification by SeptiFast Real-time PCR. *PLoS One* 2011; **6(2):** e17146.
12. Ke D, Picard FJ, Martineau F, Ménard C, Roy PH, Ouellette M, et al. Development of a PCR assay for rapid detection of *enterococci. J Clin Microbiol* 1999; **37:** 3497-503.
13. Lehmann LE, Hauser S, Malinka T, Klaschik S, Stüber F, Book M. Real-time polymerase chain- reaction detection of pathogens is feasible to suplement the diagnostic sequence for urinary tract infections. *BJU Int* 2010; **106:** 114-20.
14. Elnifro EM, Ashi AM, Cooper RJ, Klapper PE. Multiplex PCR: optimization and application in diagnostic virology. *Clin Microb Rev* 2000; **13:** 559-70.

15. Chun JY, Kim KJ, Hwang IT, Kim YJ, Lee DH, Lee IK, et al. Dual priming oligonucleotide system for the multiplet detection of respiratory viruses and SNP genotyping of CYP2C19 gene. *Nucleic Acids Res.* 2007; **35(6):** e40.

16. Horii T, Ohtsuka H, Osaki M, Ohkuni H. Use of a dual priming oligonucleotide system to detect multiple sexually transmitted pathogens in clinical specimens. *Lett Appl Microbiol* 2009; **49**: 46-52.

17. Siddiqui H, Lagesen K, Nederbragt AJ, Jeansson SL, Jakobsen KS. Alterations of microbiota in urine from women with interstitial cystitis. *BMC Microbiol* 2012; **12:** 205.

18. Siddiqui H, Nederbragt AJ, Lagesen K, Jeansson SL, Jakobsen KS. Assessing diversityof the female urine microbiota by high throughput sequencing of 16S rDNA amplicons. *BMC Microbiol* 2011; **11**: 244.

19. Nelson DE, Van Der Pol B, Dong Q, Revanna KV, Fan B, Easwaran S, et al. Characteristic male urine microbiomes associated with asymptomatic sexually transmitted infection. *PLoS One* 2010; **5(11):** e14116.

20. Dong Q, Nelson DE, Toh E, Diao L, Gao X, Fortenberry JD, et al. The microbial communities in male first catch urine are highly similar to those in paired urethral swab specimens. *PLoS One* 2011; **6(5):** e19709.

21. Wolfe AJ, Toh E, Shibata N, Rong R, Kenton K, Fitzgerald M, et al. Evidence of uncultivated bacteria in theadult female bladder. *J Clin Microbiol* 2012; **50:** 1376-83.

22. Tan CK, Ulett KB, Steele M, Benjamin WH Jr, Ulett GC. Prognostic value of semi-quantitative bacteruria counts in the diagnosis of group B streptococcus urinary tract infection: a 4-year retrospective study in adult patients. *BMC Infect Dis* 2012; **12:** 273.

23. Thue G, Baerheim A, Bjelkaroy WI, Digranes A. Urindyppekultur i allmennpraksis. *Tidsskr Nor Legeforen* 2010; **130:** 483-6.

24. Algara M, Arenas M, De las Peñas D, Bayo E, Muñoz J, Carceller JA, et al. Radiation techniques used in patients with breast cancer: Results of a survey in Spain. *Rep Pract Oncol Radiother* 2012; **17:** 122-8.

25. Lekic M, Kovac V, Triller N, Knez L, Sadikov A, Cufer T. Outcome of small cell lung cancer (SCLC) patients with brain metastases in a routine clinical setting. *Radiol Oncol* 2012; **46:** 54-9.

26. Ovcaricek T, Frkovic SG, Matos E, Mozina B, Borstnar S. Triple negative breast cancer - prognostic factors and survival. *Radiol Oncol* 2011; **45:** 46-52.

27. Parkin DM, Bray FI, Devesa SS. Cancer burden in the year 2000: The global picture. *Eur J Cancer* 2001; **37(Suppl 8):** 4-66.

28. Ulukaya E, Karaagac E, Ari F, Oral AY, Adim SB, Tokullugil AH, et al. Chemotherapy increases caspase-cleaved cytokeratin 18 in the serum of breast cancer patients. *Radiol Oncol* 2011; **45:** 116-22.

29. Khader J, Farah N, Salem A. Bladder preservation by concurrent chemoradiation for muscle-invasive bladder cancer: Applicability in low-income countries. *Rep Pract Oncol Radiother* 2011; **16:** 23-6.

30. Gupta R, Schuster M. Quorum sensing modulates colony morphology through alkyl quinolones in Pseudomonas aeruginosa. *BMC Microbiology* 2012; **12**: 30

31. Kerr KG, Snelling AM. *Pseudomonas aeruginosa*: a formidable and ever-present adversary. *J Hosp Infect* 2009; **73:** 338-44.

32. Cybulski Z, Roszak A, Talaga Z, Grabiec A, Kaźmierska J. Urinary tract infections in patients with malignant neoplasms of the genitourinary system. *Rep Pract Oncol Radiother* 2005, **10:** 23-6.

33. Christiaens T, De Backer D, Burgers J, Baerheim A. Guidelines, evidence, and cultural factors. *Scand J Prim Health Care* 2004; **22:** 141-5.

34. Nicolle LE. A practical guide to antimicrobial management of complicated urinary tract infection. *Drug Aging* 2001; **18:** 243-54.

35. Pallett A, Hand K. Complicated urinary tract infections: practical solutions for the treatment of multiresistant Gram-negative bacteria. *J Antimicrob Chemother* 2010; **65(Suppl 3):** 25-33.

36. Karlowsky JA, Lagace´-Wiens PRS, Simner PJ, DeCorby MR, Adam HJ, Walkty A, et al. Antimicrobial resistance in urinary tract pathogens in Canada from 2007 to 2009: CANWARD Surveillance Study. *Antimicrob Agents Chemother* 2011; **55:** 3169-75.

37. van der Starre WE, van Nieuwkoop C, Paltansing S, van't Wout JW, Groeneveld GH, Becker MJ, et al. Risk factors for bacteremia with uropathogen not cultured from urine in adults with febrile urinary tract infection. *Clin Infect Dis* 2010; **50(11):** e69-72.

research article

Estimated collective effective dose to the population from nuclear medicine examinations in Slovenia

Damijan Skrk[1], Dejan Zontar[1,2]

[1] Slovenian Radiation Protection Administration, Ljubljana, Slovenia
[2] "Jožef Stefan" Institute, Ljubljana, Slovenia

Radiol Oncol 2013; 47(3): 304-310.

Received 12 October 2012
Accepted 14 May 2013

Correspondence to: Assist. Prof. Damijan Škrk, PhD, Slovenian Radiation Protection Administration Ljubljana, Ajdovščina 4, SI-1000 Ljubljana, Slovenia, EU. Phone: +368 1 478 87 09; Fax: +386 1 478 87 15; E-mail: damijan.skrk@gov.si

Disclosure: No potential conflicts of interest were disclosed.

Background. A national survey of patient exposure from nuclear medicine diagnostic procedures was performed by Slovenian Radiation Protection Administration in order to estimate their contribution to the collective effective dose to the population of Slovenia.

Methods. A set of 36 examinations with the highest contributions to the collective effective dose was identified. Data about frequencies and average administered activities of radioisotopes used for those examinations were collected from all nuclear medicine departments in Slovenia. A collective effective dose to the population and an effective dose per capita were estimated from the collected data using dose conversion factors.

Results. The total collective effective dose to the population from nuclear medicine diagnostic procedures in 2011 was estimated to 102 manSv, giving an effective dose per capita of 0.05 mSv.

Conclusions. The comparison of results of this study with studies performed in other countries indicates that the nuclear medicine providers in Slovenia are well aware of the importance of patient protection measures and of optimisation of procedures.

Key words: nuclear medicine; diagnostic procedures; collective effective dose; population exposure; dose per capita

Introduction

The exposure of the global population to ionizing radiation is rising rapidly, nearly exclusively due to increasing medical use of radiation. Diagnostic X-rays is by far the largest source of medical exposure in most developed countries, while the contribution of nuclear medicine examinations is between 4% and 14%.[1] For that reason also legislation of European Union requires that the Member States determine the distribution of individual doses from medical exposure for their population.[2,3]

Based on findings of the "DOSE DATAMED" project European Commission prepared and published European Guidance on Estimating Population Doses from Medical X-ray Procedures in 2008.[1] In the beginning of 2011 a follow-up project, named "Study on European Population Doses From Medical Exposure", or "DOSE DATAMED2" (DDM2) was launched. The objective of the DDM2 project is to collect available data on the patient doses from the radiodiagnostic procedures in the European Union.

An estimate of doses to patients from nuclear medicine examinations in Slovenia as a whole has not been carried out previously. Therefore in 2011 Slovenian Radiation Protection Administration (SRPA) performed a survey about the population exposure from nuclear medicine procedures. This article summarizes the results of the survey and shows the impact of nuclear medicine examinations on the population dose.

Materials and methods

In order to assess population exposure from nuclear medicine in terms of the collective or per capita effective dose, it is necessary to estimate frequency and mean effective dose for each type of examination that makes a significant contribution to the annual collective effective dose in a country. At the European level a set of 28 diagnostic procedures that are contributing most significantly to the collective effective dose (Table 1) were identified by DDM2 project.[3]

All nuclear medicine departments in Slovenia were asked to report their annual workload and the average administered activity of the radiopharmaceutical for the 28 nuclear medicine procedures. Data about additional examinations that were not included in the list but are frequently performed at their departments were also requested. All requested data were received from all nuclear medicine departments in Slovenia. Additional 20 examinations were reported together with the relevant data.

Among the 28 examinations listed by the DDM2 project, myocardial perfusion (PET) with radioisotope ^{15}O and dopamine transporter imaging (parkinsonism) with radioisotope ^{123}I in chemical form β-CIT were not performed in Slovenia. The final analysis thus included 26 examinations proposed by the DDM2 project and additional 20 procedures that made a significant contribution to the collective effective dose. Ten out of the 20 additional examinations identified during the project contribute less than 0.5% to the total collective dose and are consequently not presented in Table 2, while the ten most relevant ones are.

The collected data were verified by comparing them to information available from licensing and inspection procedures and with the amounts of imported radiopharmaceuticals. Results from all those approaches were found to be consistent.

Mean activity per examination in Slovenia was derived from the mean activities as reported from each department, weighted by relative number of examinations performed at any given department.

The typical effective dose per nuclear medicine examination was estimated by multiplying mean activity administered per examination with a conversion factor (mSv/MBq) as given in product specifications of radiopharmaceuticals or as published by International Commission on Radiological Protection (ICRP). Relevant publications are ICRP 53[4] and its updated and extended editions ICRP 80[5] and ICRP 106.[6] Conversion factors for examinations listed in Table 1 are taken from ICRP publications, while in Table 2 product specifications of radiopharmaceuticals provided by nuclear medicine departments are used. The collective effective dose from each examination was calculated by multiplying the number of performed examinations with the typical effective dose and the total collective effective dose is a sum of collective effective doses for each examination.

The effective dose per capita was calculated by dividing the total collective effective dose with the total population of Slovenia that was taken as 2.05 million (end of 2011 data).[7]

Obtaining information from all nuclear medicine departments ensures a representative data sample. Thereby the major source of error is uncertainties in the number of performed examinations as reported from nuclear medicine departments. Uncertainties of the results will be further elaborated in the next section.

Results

Based on the gathered data, the analysis of the 36 nuclear medicine examinations was performed in order to estimate the typical effective dose of each type of examination as well as the collective dose of each group of examinations and their contribution to the total collective dose. In addition, relative contributions of different radioisotopes and workloads of different departments are presented.

Data about the 26 nuclear medicine examinations as selected by the DDM2 project are presented in Table 1 and in Table 2 the additional ten examinations are listed. The first three columns list types of examinations with radionuclide and chemical form of radiopharmaceutical used. The next four columns list number of examinations performed yearly, average administered activity per examination with the range of average activities (in brackets), conversion factors and the effective dose per examination as calculated from the listed data. In the last column contributions of each examination to the collective effective dose from nuclear medicine procedures in Slovenia in 2011 are presented.

The remaining ten examinations (a total of 1170 examinations performed in 2011) are not listed as they contribute less than 0.5% (0.41 manSv) to the total collective effective dose from nuclear medicine procedures.

Five examinations with the highest contribution to the total collective effective dose (bone imaging and four myocardial procedures) contribute nearly

TABLE 1. Data about the 26 nuclear medicine examinations as selected by the Study on European Population Doses From Medical Exposure (DDM2) project

Examination	Radionuclide	Chemical form	Number of examinations	Mean activity (MBq) per examination (min-max)	Conversion factor (mSv/MBq)	Effective dose per examination(mSv)	Collective effective dose (manSv)
Bone imaging	^{99m}Tc	Phosphates, phosphonates	7542	683 (550-700)	5.70E-03[5]	3.89	29.36
Myocardial perfusion, rest	^{99m}Tc	Tetrofosmin	2700	591 (520-600)	7.60E-03[5]	4.49	12.13
Myocardial perfusion, exercise	^{99m}Tc	MIBI	1936	583 (520-630)	7.90E-03[5]	4.61	8.92
Myocardial perfusion, rest	^{99m}Tc	MIBI	1577	582 (520-630)	9.00E-03[5]	5.24	8.26
Thyroid imaging (oral administration, no blocking)	^{99m}Tc	Pertechnetate	4546	97 (74-120)	1.30E-02[5]	1.26	5.73
Myocardial perfusion, exercise	^{99m}Tc	Tetrofosmin	1370	580 (520-600)	7.00E-03[5]	4.06	5.56
MUGA, cardiac blood pool, flow (equilibrium)	^{99m}Tc	Tc-labelled erythrocytes	608	923 (740-925)	7.00E-03[5]	6.46	3.93
Myocardial perfusion	^{201}Tl	Chloride	250	111 (111-111)	1.40E-01[6]	15.54	3.89
Lung perfusion	^{99m}Tc	MAA	1518	143 (115-185)	1.10E-02[5]	1.57	2.38
Infection/inflammation imaging	^{99m}Tc	labbelled white blood cells	303	483 (450-650)	1.10E-02[5]	5.31	1.61
Parathyroid imaging	^{99m}Tc	MIBI	279	624 (444-777)	9.00E-03[5]	5.61	1.57
Thyroid metastases (after ablation, uptake 0%)	^{131}I	Iodide	118	148 (148-148)	6.10E-02[4]	9.03	1.07
Tumor imaging (PET)	^{18}F	FDG	1350	370 (370-370)	1.90E-03[4]	0.70	0.95
Renal imaging	^{99m}Tc	MAG 3	1126	116 (100-185)	7.00E-03[5]	0.81	0.92
Dopamine transporter imaging (parkinsonism)	^{123}I	Ioflupane (DaTscan)	223	121 (115-125)	2.40E-02[6]	2.89	0.65
Neuroendocrine tumors/somatostatin receptors imaging	^{111}In	Pentetreotide (OctreoScan)	30	222 (222-222)	5.40E-02[5]	11.99	0.36
Infection/inflammation imaging	^{67}Ga	Gallium citrate	16	177 (120-200)	1.00E-01[5]	17.68	0.27
Infection/inflammation imaging	^{99m}Tc	Monoclonal antibody (LeucoScan)	48	553 (550-555)	8.00E-03[6]	4.42	0.21
Myocardial perfusion (PET)	^{18}F	FDG	30	300 (300-300)	1.90E-02[4]	5.70	0.17
Cerebral blood flow	^{99m}Tc	ECD (Neurolite)	119	657 (555-700)	2.20E-03[6]	1.45	0.17
Cerebral blood flow	^{99m}Tc	Exametazime (HMPAO,Ceretec)	22	700 (700-700)	9.30E-03[5]	6.51	0.14
Thyroid imaging (thyroid uptake 35%)	^{123}I	Iodide	278	15 (15-15)	2.20E-02[5]	0.34	0.09
MUGA, cardiac blood pool, flow (equilibrium)	^{99m}Tc	DTPA	20	740 (740-740)	4.90E-03[5]	3.63	0.07
Renal imaging	^{99m}Tc	DTPA	80	185 (185-185)	4.90E-03[5]	0.91	0.07
Tumor imaging (PET) + Diagnostic CT	^{18}F	FDG	81	370 (370-370)	1.90E-03[5]	0.70	0.06
Renal imaging	^{99m}Tc	DMSA	32	91 (80-100)	8.80E-03[5]	0.80	0.03
Total			**26202**				**88.57**

DMSA = dimercaptosuccinic acid; DTPA = diethylene triamine pentaacetic acid; ECD = Neurolite; FDG = Fluorodeoxyglucose (^{18}F); MAA = technetium ^{99m}Tc albumin aggregated; MIBI = technetium (^{99m}Tc) sestamibi; MUGA = multi gated acquisition scan

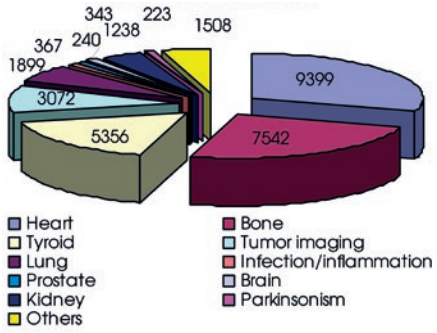

FIGURE 1. Number of nuclear medicine examinations grouped according to the organ, target or closely similar objectives.

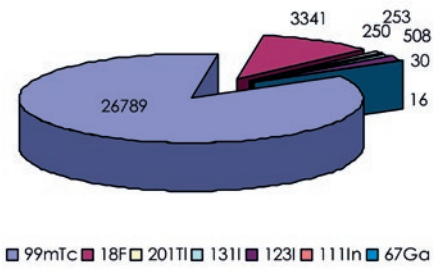

FIGURE 3. Number of nuclear medicine examinations according to the isotope used.

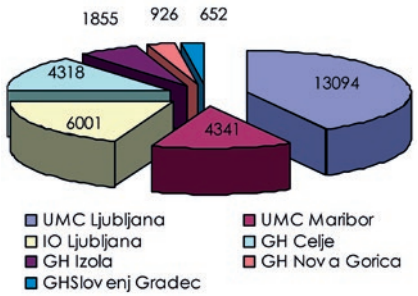

FIGURE 5. Number of examinations per nuclear medicine department.

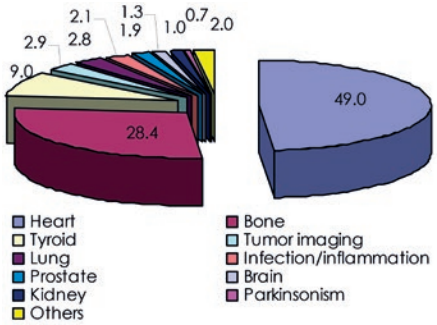

FIGURE 2. Collective effective dose from nuclear medicine examinations grouped according to the organ, target or closely similar objectives.

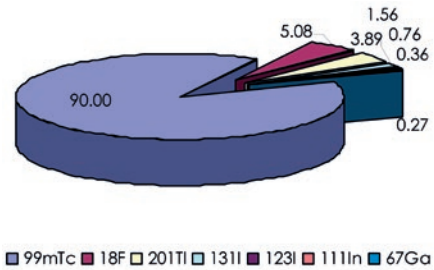

FIGURE 4. Collective effective dose from nuclear medicine examinations according to the isotope used.

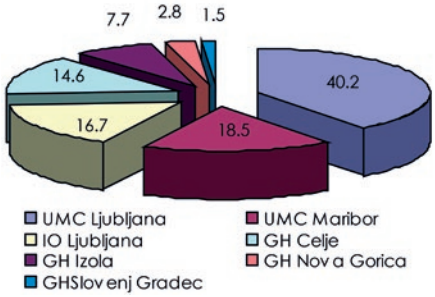

FIGURE 6. Collective effective dose (manSv) per nuclear medicine department.

64%, while the top ten examinations contribute 85% and top twenty examinations contribute 96%. Based on the collected data that include 31,187 nuclear medicine examinations, the collective effective dose from nuclear medicine procedures in 2011 was estimated to be 102 manSv, *i.e.* 0.05 mSv per inhabitant.

To determine contributions to the total collective dose from different examination groups, examinations were grouped together according to the organ, target or closely similar objectives. Examinations were grouped into the following categories: heart, bone, tyroid, lung, prostate, brain, kidney, infection/inflammation, tumor imaging and parkinsonism. Bone scans, heart and tyroid examinations contribute more than 70% to the total annual number of nuclear medicine examinations and over 85% to the total collective dose. Numbers of nuclear medicine examinations in different categories are shown in Figure 1 and their contributions to the total collective dose in Figure 2.

In Slovenian nuclear medicine departments the following isotopes are used for diagnostic purposes: ^{99m}Tc, ^{18}F, ^{201}Tl, ^{131}I, ^{123}I, ^{111}In and ^{67}Ga. Isotope ^{99m}Tc is used in all nuclear medicine departments, ^{123}I is used in three, ^{18}F, ^{111}In and ^{67}Ga in two, while ^{201}Tl and ^{131}I are used in only one department each. Most procedures were performed with ^{99m}Tc and ^{18}F, with ^{99m}Tc being used in 86% and ^{18}F in 11% of all procedures. The full list is shown in Figure 3 and their contributions to total collective effective dose from nuclear medicine examinations are shown in Figure 4. By far the largest contribution to the collective effective dose from nuclear medicine examinations is from the use of ^{99m}Tc (90%) and radiopharmaceuticals with isotope ^{18}F contribute another 5%. Radiopharmaceuticals with ^{111}In and ^{67}Ga have almost negligible contribution to the collective dose. The contributions are expected to change in the future as the number of PET examinations is expected to increase and use of ^{201}Tl radiopharmaceuticals to decrease.

The analysis of the workload distribution among the departments showed that nearly 42% of all examinations were performed in Nuclear medicine department of the University Medical Center Ljubljana. Nuclear medicine departments of the University Medical Center Maribor, the Institute

TABLE 2. Data about the 10 additional nuclear medicine examinations with the highest contribution to the collective effective dose to the population from nuclear medicine procedures in Slovenia

Examination	Radionuclide	Chemical form	Number of examinations	Mean activity (MBq) per examination (min-max)	Conversion factor (mSv/MBq)	Effective dose per examination (mSv)	Collective effective dose (manSv)
Myocardial perfusion, persantin	^{99m}Tc	Tetrofosmin	908	600 (600-600)	1.12E-02	6.72	6.10
Prostate imaging (PET)	^{18}F	Choline	240	250 (250-250)	3.13E-02	7.83	1.88
Tumor imaging (PET) + Low dose CT	^{18}F	FDG	1437	370 (370-370)	1.90E-03	0.70	1.01
Brain imaging (PET)	^{18}F	FDG	203	250 (250-250)	2.00E-02	5.00	1.01
Labelled erythrocytes	^{99m}Tc	Tc-labelled erythrocytes	96	569 (450-600)	1.40E-02	7.97	0.76
Neuroendocrine tumors/somatostatin receptors imaging	^{99m}Tc	EDDA/ HYNIC-TOC	174	600 (600-600)	5.00E-03	3.00	0.52
Pre-ablation thyroid remnant imaging (oral administration, no blocking)	^{131}I	Iodide	135	4 (4-4)	1.00E+00	3.70	0.50
Liver hemangiom	^{99m}Tc	Tc-labelled erythrocytes	66	450 (450-450)	1.40E-02	6.30	0.42
Lung ventilation	^{99m}Tc	Tc-technegas	380	40 (40-40)	2.43E-02	0.97	0.37
Sentinel node	^{99m}Tc	Nanocoll	176	124 (74-133)	1.70E-02	2.11	0.37
Total			3815				12.94

EDDA/HYNIC-TOC = EDDA/HYNIC-Tyr3-octreotide; FDG = Fluorodeoxyglucose (^{18}F)

of Oncology Ljubljana and General hospital Celje, with comparable workloads, contributed together close to 47%, with the remaining three departments accounting for less than 12%. Numbers of nuclear medicine examinations per department are shown in Figure 5 and their contributions to the total collective dose in Figure 6.

Uncertainties of the results

The collected data are a representative sample of nuclear medicine practice in Slovenia. Analysed procedures were estimated to contribute over 99% to the total collective effective dose from diagnostic procedures in nuclear medicine in Slovenia.

The only recognized source of uncertainty that could considerably influence the reliability of the results was uncertainties in the number of performed examinations. Information from two departments which reported exact values were assumed to be very precise as they were extracted from the local databases. Uncertainties on total number of procedures from four departments which reported rounded values were conservatively estimated to be 3% to 15%, while uncertainty of values scaled to the yearly level from one department was estimated to 8%. The total uncertainty estimation took into account relative contributions and conservative assumptions of uncertainties for each department. Under such assumptions the total uncertainty on the collective effective dose was estimated to be less than 4% (CL 95%). Possible uncertainties from incorrect matching of procedures and incorrect reported mean activities per examination were checked for by comparison with independent data from official SRPA records. Based on the findings their contribution was assumed to be negligible.

Discussion

In Slovenia the collective effective dose to the population from radiological examinations is not being estimated regularly. The presented survey is the first attempt to gather data about all nuclear medi-

cine examinations performed in all departments in order to estimate their contribution to the total collective effective dose. Gathered data also enable the comparison of the frequencies and the annual per capita doses from medical nuclear medicine examinations in Slovenia with other countries.[1] In the future, gathered data will enable observation of trends in the frequencies, annual collective dose and/or per capita dose from nuclear medicine examinations in Slovenia.

The total annual number of nuclear medicine examinations per 1000 inhabitants in Slovenia in 2011 was found to be 15 and the average annual effective dose per capita was 0.05 mSv. Taking into account an unpublished SRPA study of radiological procedures, the contribution of nuclear medicine examinations to the collective effective dose from diagnostic medical exposures was 7%, while in European countries it is between 4% and 14%.[1] The total annual number of nuclear medicine examinations per 1000 inhabitants in European countries ranges from 8 to 56. The number of nuclear medicine examinations per 1000 population in Slovenia is lower compared to Belgium (56), Germany (42), Luxemburg (38) and Netherlands (18) and slightly higher than in Switzerland (13), Norway (12), Sweden (12), Untied Kingdom (11) and Finland (8) [(1,8)]. As a result of a lower annual number of nuclear medicine examinations as well due to optimised levels of administered activities of radioisotopes per examination, the level of annual effective dose per capita in Slovenia is relatively low compared to European average.

The total average annual effective dose from nuclear medicine procedures per capita in European countries ranges from 0.03 mSv to 0.20 mSv. The average annual effective dose in Slovenia is lower compared to Belgium (0.20 mSv, 1999), Luxembourg (0.16 mSv, 2002), Germany (0.11 mSv, 2002), Netherlands (0.07 mSv, 2002), Switzerland (0.07 mSv, 2004), the same as in Norway (0.05 mSv, 2004) and higher than in Sweden (0.04 mSv, 2005), United Kingdom (0.03 mSv, 2004) and in Finland (0.03 mSv, 2009).[(1,8)]

Bone scans and heart examinations were most frequent procedures both in Slovenia and in other countries for which authors had available data. A higher number of tyroid examination in Slovenia is due to the iodine deficiency, the same reason as for its higher contribution in Germany and Luxemburg.

Average ratio between maximal and minimal average administered activity between departments for any particular examination was found to be 1.4, which seems not to be a substantial difference[1]. Nevertheless, factors such as poor performance of imaging instrumentation and procedure parameters that influence the image quality and may result in higher average administered activities should be carefully investigated in close collaboration with the professional bodies in the nuclear medicine field. In addition special attention should be given to nuclear medicine examinations causing higher patient exposures, especially to those which are performed frequently. Evaluation of new available radiopharmaceuticals offering better performance or causing lower patient exposure should be performed regularly.

Frequent updates of information about nuclear medicine practice are essential as rapid technological development, new techniques and instrumentation as well as new procedures would affect both administered activity and frequency of particular examinations. Although the resources required to perform such surveys and analyses are considerable, it is proposed that they should be repeated at least every 5 years.[1]

Conclusions

In Slovenia the total collective effective dose from nuclear medicine procedures was estimated to be 102 manSv in 2011, while the estimated effective dose per inhabitant was 0.05 mSv. This presents 7% of the total collective dose from all medical exposure examinations.

Nearly half of the collective effective dose from nuclear medicine examinations was caused by heart examinations. It is shown that procedures with ^{99m}Tc were the major source of the total collective dose from nuclear medicine procedures, contributing almost 90%, while combined contribution of ^{131}I, ^{123}I, ^{111}In and ^{67}Ga procedures was less than 3%. The contribution of PET examinations was 5% in 2011 and is anticipated to increase in the future.

Presented results show that the nuclear medicine practice in Slovenia is close to the level of European countries where the awareness of patient protection and need for optimisation procedures is assumed to be high. Nevertheless, there is always room for improvement and optimisation. Regularly updating written procedures for examinations and establishment of national diagnostic reference levels in close cooperation with nuclear medicine professional bodies would be recommended.

Due to a rapid technological development, surveys and analysis of the doses from medical expo-

sure procedures should be performed regularly. Availability of updated information will enable the proper optimisation process of nuclear medicine procedures and the adequate decision-making in the field of radiation protection on the national as well as on the international level in the future.

Acknowledgement

The authors would like to express gratitude to all nuclear medicine departments in Slovenia for making the data of nuclear medicine procedures available for publication.

References

1. European Commission. *European Commission guidance on estimating population doses from medical X-ray procedures (Radiation Protection No 154)*. Luxemburg: Office for Official Publications of the European Communities; 2008.
2. European Commission. *Council Directive 97/43/EURATOM of 30 June 1997 on health protection of individuals against the danger of ionizing radiation in relation to medical exposure* (*Official Journal of the European Commission, No- L 180).* Luxemburg: Office for Official Publications of the European Communities; 1997.
3. International Commission on Radiological Protection ICRP. *The 2007 recommendations of the International Commission on Radiological Protection.* Orlando: Elsevier, published for the International Commission on Radiological Protection; 2007.
4. International Commission on Radiological Protection ICRP. *Radiation dose to patients from radiopharmaceuticals (ICRP Publication 53, Ann ICRP **18**(1-4)).* Oxford: Pergamon Press; 1988.
5. International Commission on Radiological Protection ICRP. *Radiation dose to patients from radiopharmaceuticals (Addendum to ICRP Publication 53, ICRP Publication 80, Ann ICRP **28**(3)).* Oxford: Pergamon Press; 1998.
6. International Commission on Radiological Protection ICRP. *Radiation dose to patients from radiopharmaceuticals (Addendum 3 to ICRP Publication 53, ICRP Publication 106, Ann ICRP **38**(1-2)).* Amsterdam: Elsevier Press; 2008.
7. Statistical office of the Republic of Slovenia. *Slovenia in figures 2012,* Ljubljana: Littera picta d.o.o.; 2012.
8. Bly R, Järvinen H, Korpela M H, Tenkanen-Rautakoski P, Mäkinen A. Estimated collective effective dose to the population from X-ray and niclear medicine examinations in Finland. *Radiat Prot Dosimy* 2011; **147:** 233-6.

Radiol Oncol 2013; 47(3): 197-205.
doi:10.2478/raon-2013-0037

Pomen zunajceličnih veziklov v rakasti transformaciji celic

Ogorevc E, Kralj-Iglič V, Veranič P

Izhodišča. Rak se tradicionalno obravnava kot bolezen, ki nastane zaradi genskih mutacij. Nova biološka dognanja dopolnjujejo genetske razlage napredovanja raka z negenetskimi vplivi. Znano je, da igra medcelična komunikacija pomembno vlogo pri napredovanju raka. V tem pogledu je še posebej zanimiva komunikacija s pomočjo zunajceličnih veziklov. Zunajcelični vezikli so membranske strukture, ki nastanejo kot produkt brstenja celične membrane različnih tipov celic. Po odcepu od materinske celice postanejo zunajcelični vezikli mobilni in lahko potujejo iz zunajceličnega prostora v kri in druge telesne tekočine.

Zaključki. Novejše ugotovitve kažejo, da so tumorske celice še posebej nagnjene k vezikulaciji in da zunajcelični vezikli iz tumorskih celic prenašajo proteine, lipide in nukleinske kisline, povezane z napredovanjem bolezni. Privzem tumorskih zunajceličnih veziklov lahko v normalnih celicah povzroči fenotipske rakave spremembe. Zaviranje vezikulacije celic bi torej lahko upočasnilo rast tumorja in napredovanje bolezni. Namen preglednega članka je povzeti znanje o doslej odkritih fenotipskih vzrokih rakavih transformacij, posredovanih z zunajceličnimi vezikli.

Radiol Oncol 2013; 47(3): 206-218.
doi:10.2478/raon-2013-0007

Primerjava med MRI celega telesa in Fluor-18-Fluorodeoksiglukozo PET ali PET/CT v onkologiji. Sistematični pregled

Ciliberto M, Maggi F, Treglia G, Padovano F, Calandriello L, Giordano A, Bonomo L

Izhodišča. Namen članka je sistematični pregled objavljenih podatkov o uporabi pozitronske emisijske tomografije (PET) ali PET računalniške tomografije (PET/CT) z uporabo Fluor-18-Fluorodeoksiglukoze (FGD) in magnetne resonance celega telesa (WB-MRI) pri bolnikih z različnimi tumorji.

Metode. Naredili smo obširen pregled literature na podatkovnih bazah PubMed/MEDLINE, Scopus in Embase. Upoštevali smo klinične raziskave, ki so bile objavljene do aprila 2012 ter so primerjale uporabo FDG-PET ali PET/CT in WB-MRI pri bolnikih z različnimi vrstami tumorjev.

Rezultati. V sistematični pregled smo vključili 44 raziskovalnih člankov, ki so obravnavali 2287 bolnikov. Veliko objav je analiziralo obe diagnostični metodi pri mešanih tumorjih. Glede na vrsto tumorjev smo ugotovili največ podatkov za limfome, kostne tumorje, tumorje glave in vratu in pljučne tumorje, za ostale vrste tumorjev pa je manj podatkov.

Zaključki. Iz analizirane literature lahko sklepamo, da bi lahko bila WB-MRI primerna alternativna metoda PET/CT v onkologiji. Za boljšo oceno vloge WB-MRI v primerjavi z FGD-PET ali PET/CT pri specifičnih tumorjih pa so potrebne večje, prospektivne klinične raziskave in tudi ocena stroškov preiskav.

RadiolOncol 2013; 47(3): 219-223.
doi:10.2478/raon-2013-0023

Napoved 2-letnega preživetja pri bolnikih s stadijem I in II nedrobnoceličnega pljučnega raka ob uporabi kvantifikacije vrednosti standardnega privzema (SUV) ^{18}F-FDG PET/CT

Cistaro A, Quartuccio N, Mojtahedi A, Fania P, Filosso PL, Campennì A, Ficola U, Baldari S

Izhodišča. Namen raziskave je bil opredeliti povezavo med največjo vrednostjo standardnega privzema (SUVmax) in velikostjo primarnega tumorja ter preživetjem brez bolezni in celokupnim preživetjem pri bolnikih s stadijem I in II nedrobnoceličnega raka pljuč ob 2-letnem opazovanju.

Bolniki in metode. V raziskavo smo vključili 49 bolnikov s stadijem I in II nedrobnoceličnega raka pljuč. Pred operacijo smo naredili preiskavo s ^{18}FDG-PET/CT. Ugotavljali smo povezavo med SUVmax in velikostjo tumorja ter kliničnim potekom bolezni. Izračunali smo mejno vrednost za SUVmax in za velikost tumorja z najboljšim kliničnim potekom bolezni glede na verjetnostj preživetja brez bolezni ter povezavo med SUVmax in celokupnim preživetjem.

Rezultati. Ugotovili smo statistično značilno povezavo med SUVmax in preživetjem brez bolezni (p=0,029). Mejna vrednost za SUVmax je bila 9 (p=0,0013), mejna vrednost za velikost tumorja pa 30 mm (p=0,0028). Bolniki s SUVmax >9 in velikostjo primarnega tumorja >30 mm so imeli 37,5% 2-letno pričakovano preživetje brez ponovitve bolezni, medtem ko se je verjetnost dvignila na 90%, če je bil SUVmax <9 in tumor <30 mm.

Zaključki. Pri bolnikih s stadijem I in II nedrobnoceličnega pljučnega raka lahko SUVmax in velikost tumorja napovesta podskupino tistih bolnikov, ki imajo večjo verjetnost za ponovitev bolezni.

Radiol Oncol 2013; 47(3): 224-229.
doi:10.2478/raon-2013-0033

Sodobne ultrazvočne tehnologije za določevanje učinkov radiofrekvenčne ablacije pri hepatocelularnem raku

Toshikuni N, Shiroeda H, Ozaki K, Matsue Y, Minato T, Nomura T, Hayashi N, Arisawa T, Tsutsumi M

Izhodišča. Radiofrekvenčna ablacija (RFA) je terapija z namenom ozdravitve bolnikov s hepatocelularnim rakom. Pri izvajanju RFA in ocenjevanju njenega učinka uporabljamo različne metode. Ko ciljano punktiramo tumor, najpogosteje uporabljamo ultrazvok (UZ), za ocenjevanje učinka RFA pa pogosteje uporabljamo dinamično računalniško tomografijo ali magnetno resonanco. Razvili smo novo metodo za določevanje učinkov RFA pri hepatocelularnem raku, pri njej uporabljamo kombinacijo UZ s kontrastom in virtualnega UZ s tridimenzionalnimi ultrazvočnimi podatki v realnem času.

Bolniki in metode. Za pripravo tridimenzionalnih ultrazvočnih podatkov smo pred RFA naredili običajni ultrazvočni pregled tarčnih nodulov hepatocelularnega raka in okoliškega parenhima jeter. Po RFA smo sinhronizirali rekonstruirane večplanarne slike. Te smo pridobili s tridimenzionalnim ultrazvočnimi slikami UZ v realnem času na istem ultrazvočnem monitorju; nato smo naredili UZ s kontrastom in virtualni UZ v realnem času. Z uporabo funkcije označevanja smo narisali krožni označevalec vzdolž tarčnega nodula hepatocelularnega raka na večplanarnih rekonstruiranih ultrazvočnih slikah pred zdravljenjem. Avtomatično sinhroniziran označevalec je predstavljal originalno označen nodul hepatocelularnega raka na ultrazvočnih slikah s kontrastom, ki so bile narejene po zdravljenju. Če je avaskularno območje z robom nekaj milimetrov v vseh smereh obkrožalo označevalec na ultrazvočnih slikah s kontrastom, je bila albacija uspešna.

Rezultati. Predstavljena metoda je bila izvedljiva in primerna za ocenjevanje terapevtskega učinka pri 13 zaporednih bolnikih s hepatocelularnim rakom, pri katerih smo naredili RFA. Pri 2 bolnikih, ki sta imela več aplikacij RFA, smo na ultrazvočnih slikah zlahka določili, kateri predeli nodulov hepatocelularnega raka so zahtevali dodatno RFA.

Zaključki. Predstavljena metoda sodobne ultrazvočne tehnologije bo olajšala določevanje učinkov RFA pri hepatocelularnem raku.

Radiol Oncol 2013; 47(3): 230-238.
doi:10.2478/raon-2013-0047

Intratorakalni maligni periferni tumorji živčnih ovojnic. Slikovna diagnostika in zdravljenje

Kamran SC, Shinagare AB, Howard SA, Nishino M, Hornick JL, Krajewski KM, Ramaiya NH

Izhodišča. Namen raziskave je bil analizirati klinične in slikovnodiagnostične značilnosti primarnih intratorakalnih malignih perifernih tumorjev živčnih ovojnic.

Bolniki in metode. Retrospektivno klinično raziskavo je odobrila Komisija za raziskave v ustanovi, kjer smo raziskavo izvedli. Ovrednotili smo klinične in slikovnodiagnostične značilnosti 15 bolnikov (8 moških in 7 žensk; srednja starost 50 let [18–83]). Vsi so imeli patomorfološko dokazan maligni periferni tumor živčnih ovojnic, zdravljeni pa so bili od januarja 1999 do decembra 2011. Rezultate slikovnodiagnostičnih preiskav so ocenjevali trije radiologi in jih primerjali s kliničnimi podatki. Predhodno smo pri 15 bolnikih naredili CT, pri 5 MRI in pri 4 bolnikih PET/CT.

Rezultati. Od 15 tumorjev jih je 6 ležalo v mediastinu (2 v sprednjem, 2 v srednjem in 2 v zadnjem), 4 tumorje smo ugotovili v torakalni steni, 2 paraspinalno in 3 v pljučih. Nevrofibromatozo 1 smo odkrili pri 4 bolnikih, heterologno rabdomioblastično diferenciacijo pa pri 4 bolnikih. Tumorske mase so značilno potekale vzdolž živcev, srednja velikost je bila 11 cm. Tumorji so bili hipo- ali izodenzni glede na mišice pri preiskavi s CT-jem; izointenzivni na obtežitvi T1 in hiperintenzivni na obtežitvi T2 pri preiskavi z MRI-jem; intenzivno so kopičili fluorodeoksiglukozo (FDG) pri preiskavi s PET/CT-jem (srednja največja standardizirana vrednost privzema [SUV]max je bila 10,5 [4,4–23,6]). Nekrozo smo videli pri 4 tumorjih in kalcifikacije prav tako pri 4 tumorjih. Širitev tumorja v sosednje strukture smo ugotovili pri 7 bolnikih, kar je spremenilo načrt zdravljenja in bolnike smo najprej zdravili s kemoterapijo.

Zaključki. Intratorakalnih maligni periferni tumorji živčnih ovojnic se pojavljajo kot velike tumorske mase, ki zajemajo mediastinum, prsno steno ali pljuča. Radiološka ugotovitev širjenja tumorja v sosednje organe bistveno vpliva na spremembo načrta zdravljenja. Pri takšnih bolnikih se odločamo za neoadjuvantno in adjuvantno kemoradioterapijo.

Radiol Oncol 2013; 47(3): 239-243.
doi:10.2478/raon-2013-0029

Zdravljenje embolije zgornje mezenterične arterije s perkutano mehansko trombektomijo

Kuhelj D, Kavčič P, Popovič P

Izhodišča. Embolija zgornje mezenterične arterije je redko urgentno stanje, ki pogosto vodi v infarkt črevesja in je mnogokrat smrtna. Pravočasna diagnoza in hitro ukrepanje sta bistvenega pomena za učinkovito zdravljenje. V prispevku predstavljamo uspešno perkutano metodo zdravljenja embolije zgornje mezenterične arterije.

Prikaz primerov. Tri zaporedne bolnike z embolijo v srednjem delu debla SMA smo zdravili z mehansko trombektomijo. Pri dveh bolnikih smo uporabili kateter Aspirex®, velikosti 6F, pri enem pa kateter Rotarex®, velikosti 6F. Po posegu so vsi bolniki občutili takojšnje olajšanje bolečine v trebuhu, brez kliničnih znakov infarkta črevesja. Pri enem bolniku smo med zdravljenjem s katetrom Aspirex® poškodovali manjšo arterijsko vejo in krvavitev uspešno pozdravili z žilno opornico. Pri enem bolniku je po posegu nastal paralitični ileus, ki je izzvenel spontano. Vsi bolniki so ostali asimptomatski med sledenjem bolezni, ki pri prvem bolniku traja že 45 mesecev.

Zaključki. Perkutana mehanska trombektomija je hitro in učinkovito zdravljenje embolije zgornje mezenterične arterije v srednjem delu debla, kadar ni znakov nekroze črevesja. Sledenje bolnikov je pokazalo odlične kratkoročne in dolgoročne rezultate.

Radiol Oncol 2013; 47(3): 244-246.
doi:10.2478/raon-2013-0039

Magnetno resonančno slikanje protuberantnega dermatofibrosarkoma vulve – prikaz primera

Ozmen E, Güney G, Algin O

Izhodišča. Protuberantni dermatofibrosarkom vulve je redek nizko maligen sarkom mehkih tkiv. Poročil o slikovnih značilnostih protuberantnega dermatofibrosarkoma vulve pridobljenih z magnetno resonance (MRI) v literature ni najti.

Prikaz primera. Poročamo o kliničnih, histoloških in MRI značilnostih protuberantnega dermatofibrosarkoma vulve. Glede na pregledano literature je to prvi primer histološko potrjenega protuberantnega dermatofibrosarkoma vulve, ki je predstavljen z MRI slikovno diagnostiko. Diagnozo protuberantnega dermatofibrosarkoma običajno postavimo na osnovi histopatoloških in kliničnih značilnosti.

Zaključki. MRI je uporabna tako za diagnozo protuberantnega dermatofibrosarkoma kot tudi za sledenje bolnika, saj ima metoda dobro ločljivost za mehka tkiva in bolnika ne izpostavlja sevanju. Z MRI lahko prikažemo odnos do sosednjih anatomskih struktur, razširjenost in globino tumorja ter morebitno zajetost bezgavk.

Radiol Oncol 2013; 47(3): 247-257.
doi:10.2478/raon-2013-0045

Uporaba nevtralnega testa komet in testa žarišč γH2AX za ocenjevanje radiosenzitivnosti z ogljikovimi ioni na humanih celičnih linijah

Zhao J, Guo Z, Zhang H, Wang Z, Song L, Ma J, Pei S, Wang C

Izhodišča. Ogljikovi ioni ($^{12}C^{6+}$) so sevalci z visokim linearnim prenosom energije in visoko relativno biološko učinkovitostjo. Dobra ocena radiosenzitivnosti celic bi pripomogla k boljši napovedi primerne doze za obsevanje tumorjev. Namen raziskave je bil ocena uporabe nevtralnega testa komet in testa tvorjenja žarišč γH2AX za določanje radiosenzitivnosti celic pri obsevanju z ogljikovimi ioni.

Materiali in metode. Uporabljali smo dozi 2 in 4 Gy ogljikovih ionov ($^{12}C^{6+}$) in žarkov X. Delež preživelih celic, delež dvojnih prelomov DNA in kinetiko poprave le teh smo ocenjevali z uporabo testa klonogenosti, nevtralnega testa komet in tvorjenja žarišč γH2AX. Teste smo uporabili na celicah HeLa humanega karcinoma materničnega vratu, jetrnih celicah HepG2 in karcinomskih celicah MEC-1 ob različnih časovnih intervalih po obsevanju z ogljikovimi ioni in žarki X.

Rezultati. Delež preživelih celic je bil veliko manjši po obsevanju z ogljikovimi ioni, kot po obsevanju z žarki X ($p < 0,05$) pri vseh treh testiranih celičnih linijah. Nevtralni test komet je pokazal statistično značilno več poznih poškodb na celicah ($p < 0,05$). Najvišjo stopnjo poškodb smo ugotovili 0,5 in 4 ure po obsevanju, tako z ogljikovimi ioni kot z žarki X. Pri celicah HeLa smo našli značilno več kasnih poškodb po obsevanju z ogljikovimi ioni v primerjavi z žarki X ($p < 0,05$). Največji delež žarišč γH2AX smo zaznali 30 minut po obsevanju pri vseh treh celičnih linijah ($p < 0,01$). Delež žarišč γH2AX smo opazovali še vse do 24 ur po obsevanju; na celicah HeLa in MEC-1 je bil delež žarišč večji po obsevanju z ogljikovimi ioni kot žarki X ($p < 0,05$). Korelacija med klonogenim testom, nevtralnim testom komet in testom žarišč γH2AX ni bila statistično značilna, razen pri nekaterih celičnih linijah ob določeni sevalni dozi.

Zaključki. Rezultati raziskave kažejo, da bi bilo možno uporabljati nevtralni test komet in test določanja žarišč γ-H2AX pri ocenjevanju radiosensitivnosti celic na obsevanje z $^{12}C^{6+}$.

Radiol Oncol 2013; 47(3): 258-265.
doi:10.2478/raon-2013-0043

Imunski odziv celic THP-1 in dendritičnih celic na okužbo s *Helicobacter pylori* je okrnjen, če inhibiramo delovanje encima katepsina X

Skvarč M, Štubljar D, Kopitar AN, Jeverica S, Tepeš B, Kos J, Ihan A

Izhodišče. Imunski odziv na okužbo z bakterijo *Helicobacter pylori* poleg antibiotične terapije odločilno pripomore k odstranitvi bakterije iz želodčne sluznice. V članku je predstavljena vloga katepsina X, cisteinske proteaze, v procesu imunskega odziva na okužbo.

Materiali in metode. Preučevali smo, kako vpliva inhibicija delovanja katepsina X na imunski odziv. Celice THP-1 in dendritične celice bolnikov smo stimulirali s *H. pylori* ali s *H. pylori* in inhibitorjem katepsina X 2F12. Preučevali smo izražanje toll-like receptorjev 2 in 4 (receptorji TLR-2 in TLR-4) na membranah celic in izražanje vnetnih citokinov. V študijo smo vključili 48 sevov H. pylori bolnikov, ki so imeli težave z eradikacijo bakterije. Vzorce smo analizirali s pomočjo pretočnega citometra.

Rezultati. Dokazali smo, da je ob inhibiciji delovanja katepsina X povečano izražanje receptorjev TLR-4 na membranah celic THP-1 in izražanje receptorjev TLR-2 in TLR-4 na membranah dendritičnih celic. V prisotnosti inhibitorjev katepsina X je zmanjšana količina izločenih vnetnih citokinov v supernatantu THP-1 celic.

Zaključki. Dokazali smo, da inhibicija katepsina X vpliva na proces internalizacije TLR-2 in TLR-4, saj inhibicija vpliva na fluidnost membrane in fagocitozo imunskih kompleksov, kar posredno vpliva na koncentracijo vnetnih citokinov v supernatantu vnetnih celic. Imunski odziv je okrnjen in *H. pylori* se lahko izogne eradikaciji.

Radiol Oncol 2013; 47(3): 266-279.
doi: 10.2478/raon-2013-0036

Zgodnji rezultati endoskopskega razširjenega endonazalnega pristopa pri odstranitvi supradiafragmalnih kraniofaringiomov - prikaz primerov in pregled področja

Bošnjak R, Benedičič M, Vittori A

Izhodišča. Izbira endoskopskega razširjenega endonazalnega pristopa ponuja možnost boljše odstranitve kraniofaringiomov in zmanjšanja kirurške obolevnosti pri pomembno veliki podskupini bolnikov.

Metode. Izmed 331 bolnikov, ki smo jih operirali transfenoidno, smo pri prvih osmih bolnikih (mediana starost 63 let; razpon 47–73 let) proučili vidne, endokrinološke in nevrološko-kognitivne izhode po endoskopski endonazalni odstranitvi supradiafragmalnega kraniofaringioma (mediana višina tumorja 23 mm; razpon 15–34 mm; mediana opazovalnega obdobja 27 mesecev, razpon 10–69 mesecev). Pri vseh smo pokušali tumor odstraniti v celoti.

Rezultati. Tumor smo odstranili v celoti pri 6 od 8 bolnikov. Vid se je izboljšal obojestransko pri 6 od 8 bolnikov oziroma pri 14 od 16 očes. Novi endokrinološki izpadi, vključujoč diabetes insipidus, so se pojavili pri 5 od 8 bolnikov. Kognitivni upad je bil prisoten pri 2 bolnikih. Pet od 8 bolnikov je ohranilo prejšnjo kakovost življenja.

Zaključki. Naši rezultati so primerljivi z rezultati podobnih raziskav, razen pogostost novih endokrinoloških izpadov in rinolikvorej. Vzroka sta verjetno dva: večji delež transinfundibularnih tumorjev, kjer je ohranitev hipofiznega peclja malo verjetna, ter neuporaba nazoseptalnega režnja in načina "košarica" pri prvi polovici bolnikov. Upoštevajoč podatke iz literature in naše rezultate razširjeni endonazalni pristop nakazuje boljšo odstranitev tumorja in manj kirurške obolevnosti kot pri transkranialnih pristopih. Endonazalni pristop omogoča manj motenj vida in boljšo kakovost življenja, manj izrazita pa je razlika v endokrinološki funkciji. Potrebno je nadaljnje preučevanje večjega števila bolnikov v daljšem opazovalnem obdobju.

Radiol Oncol 2013; 47(3): 280-288.
doi:10.2478/raon-2013-0025

Radikalno zdravljenje raka materničnega vratu z obsevanjem na Onkološkem inštitutu v Ljubljani v letih 1998-2002

Zobec Logar HB, Šegedin B, Hudej R, Petrič P

Izhodišča. Namen retrospektivne klinične raziskave je bil analizirati uspešnost zdravljenja raka materničnega vratu z dvodimenzionalnim (2D) načinom obsevanja in predpisovanjem doze na točko A. Kljub trodimenzionalnemu (3D) načinu obsevanja, ki smo ga kasneje uvedli na Onkološkem inštitutu, je namreč dvodimenzionalen pristop v svetu še vedno široko v uporabi.

Metode. V retrospektivno raziskavo smo vključili 98 bolnic z rakom materničnega vratu, ki smo jih zdravili na Onkološkem inštitutu v letih od 1998-2002. Analizirali smo vpliv starosti, hemoglobina, histologije, stopnje diferenciacije tumorja, stadija bolezni, prizadetosti bezgavk, doze na točko A in trajanja zdravljenja na preživetje in lokalno kontrolo. Ovrednotili smo zgodnje in pozne posledice zdravljenja.

Rezultati. 5 in 8-letno celokupno preživetje, preživetje brez bolezni in lokalna kontrola bolezni so bili: 47,2 % in 43,0%, 54,7 % in 53,4 %, 74,9 % in 72,5 %. Doza na točko A, pozitivne bezgavke in histologija tumorja so neodvisno vplivali na lokalno kontrolo bolezni ali preživetje. Verjetnost hujših poznih posledic zdravljenja (stopnje tri ali štiri) v prvih petih letih je bila 7,1 % za gastrointestinalni ter 3,3 % za genitourinarni sistem in nožnico.

Zaključki. Doza na točko A je bila neodvisen napovedni dejavnik za celokupno preživetje in lokalno kontrolo bolezni, pozitivne bezgavke za preživetje povezano z boleznijo, histologija pa je bila neodvisni napovedni dejavnik za celokupno preživetje.

Radiol Oncol 2013; 47(3): 289-295.
doi:10.2478/raon-2013-0041

Varnost in poraba analgetikov pri bolnikih z napredovalim rakom, zdravljenih z zoledronsko kislino

Kmetec A, Hajdinjak T

Izhodišča. Ocenili smo uporabo zoledronske kisline pri bolnikih s kostnimi zasevki solidnih tumorjev in multiplega mieloma glede na varnost ter učinek na porabo analgetikov in vpliv na pojav kostnih dogodkov.

Metode. Raziskava je bila opazovalna, multicentrična v IV. fazi in je trajala 12 mesecev. Med leti 2007 in 2009 je bilo vključenih 125 simptomatskih bolnikov z bolečino in s kostnimi zasevki: 92 z rakom prostate, 28 z multiplim mielom in 5 z drugimi vrstami raka. Mesečno so prejemali zoledronsko kislino v infuziji skladno s smernicami za posamezno vrsto bolezni. Ocenjevali smo porabo analgetikov, stopnjo bolečine ter ovrednotili laboratorijske vrednosti.

Rezultati. Pri multiplem mielomu smo predpisali zoledronsko kislino istočasno z začetnim zdravljenjem, pri raku prostate pa šele v napredovalem stadiju. Med zdravljenjem se je pri skupini bolnikov z multiplim mielomom znižal odstotek bolnikov, ki so potrebovali analgetike (od 57 % na 24 %) in zvišal pri skupini bolnikov z rakom prostate (od 70 % na 88 %). Med bolniki, ki so potrebovali katerikoli analgetik, se je skupni delež bolnikov, ki so dobivali opiate, znižal iz 72,9 % na 64 %, nekoliko pa se je zvišal odstotek predpisanih nesteroidnih in drugih blažjih analgetikov. Ocena bolečine po vizualno analogni skali se je pri raku prostate statistično neznačilno znižala za 22 %, pri multiplem mielomu pa statistično značilno za 97 %. Hipokalcemijo 3. ali 4. stopnje smo ugotovili pri 4 % opazovanih bolnikov. Odstopanja pri vrednostih serumskega kreatinina so bile ves čas opazovanja enakomerna. Pri 10 (8 %) bolnikih smo ugotovili 31 s skeletom povezanih dogodkov.

Zaključki. Zoledronska kislina je varno zdravilo. Ugotovili smo različen odgovor bolnikov na zdravljenje bolečine med skupinama bolnikov z rakom prostate in multiplim mielomom, kar je lahko posledica različnega stadija bolezni, v katerem smo uvedli zdravljenje po sedaj uveljavljenih smernicah. V prihodnjih raziskavah bi bilo smiselno proučiti zgodnejše uvajanje zoledronske kisline pri bolnikih z rakom prostate.

Radiol Oncol 2013; 47(3): 269-303.
doi:10.2478/raon-2013-0044

Uporaba multipleksne polimerazne verižne reakcije pri ugotavljanju mikroorganizmov, izoliranih iz urina hospitaliziranih bolnikov z rakom

Cybulski Z, Schmidt K, Grabiec A, Talaga Z, Bociąg P, Wojciechowicz J, Roszak A, Kycler W

Izhodišča. Cilji raziskave so bili: i) primerjava rezultatov določanja mikroorganizmov v urinu s polimerazno verižno reakcijo (PCR) ob uporabi dveh komercialno dostopnih testov, ii) določiti občutljivost mikrobnih izolatov iz urina bolnikov z rakom na izbrane antimikrobne učinkovine in pripraviti priporočila za empirično terapijo.

Materiali in metode. Enoletno prospektivno raziskavo smo izvedli v letu 2011 v Velikem poljskem centru za raka v Poznanju in v Gentskem laboratoriju Raziskovalnega centra CBDNA v Poznanju. Preiskali smo urin pri 72 bolnikih.

Rezultati. Urinske kulture in urin smo preiskovali z metodo PCR pri 72 bolnikih. Vzorci urina so bili pozitivni na 128 sevov bakterij, od katerih je bilo 95 (74%) enakih pri obeh testih. Najpogosteje smo s testoma kulture in PCR izolirali koliformne bakterije in *Enterococcus spp.* Gram negativne bakterije so bile najpogosteje odporne na cotrimoxazol. 77,2% od teh bacilov ter 100% od *E. faecalis* in *S. agalactiae* so bili občutljivi na amoksicilin-klavulansko kislino. 4,7% Gram pozitivnih kokov je bilo neobčutljivih na nitrofurantoin.

Zaključki. Metoda PCR je hitra metoda za ugotavljanje povzročiteljev okužbe sečil in nam lahko pomaga pri ustreznejši izbiri zgodnjega protimikrobnega zdravljenja. Metoda bi lahko bila primerna alternativa standardni metodi gojenja in bi jo lahko vključili v smernice, predvsem v primerih, ko odkrijemo različno občutljivost na enaka zdravila.

Radiol Oncol 2013; 47(3): 304-310.
doi:10.2478/raon-2013-0048

Ocena kolektivne efektivne doze zaradi nuklearnomedicinskih preiskav v Sloveniji

Škrk D, Žontar D

Izhodišča. Uprava Republike Slovenije za varstvo pred sevanji je zbirala podatke o nuklearnomedicinskih preiskavah in jih analizirala. Želeli smo oceniti, koliko nuklearnomedicinske preiskave prispevajo h kolektvni efektivni dozi pri prebivalstvu Slovenije.

Metode. Izbrali smo 36 nuklearnomedicinskih preiskav, ki prispevajo največji delež h kolektivni efektivni dozi. Zbrali smo podatke o pogostosti in povprečni aplicirani aktivnosti radioizotopa za vsako izmed določenih preiskav na vseh nuklearno medicinskih oddelkih v Sloveniji. Na podlagi zbranih podatkov ter uporabe konverzijskih količnikov smo ocenili kolektivno efektivno dozo za prebivalstvo in za posameznika.

Rezultati. Ocenjena skupna kolektivna doza za prebivalstvo v letu 2011 zaradi nuklearnomedicinskih preiskav je bila 102 človekSv. Kolektivna doza na prebivalca pa je bila ocenjena na 0,05 mSv.

Zaključek. Primerjava rezultatov opravljene analize z rezultati analiz v drugih državah pokaže, da se izvajalci nuklearnomedicinskih posegov v Sloveniji zavedajo pomena ukrepov za varstvo bolnikov in optimizacije postopkov.

Fundacija "Docent dr. J. Cholewa"
je neprofitno, neinstitucionalno in nestrankarsko
združenje posameznikov, ustanov in organizacij, ki želijo
materialno spodbujati in poglabljati raziskovalno
dejavnost v onkologiji.

Dunajska 106
1000 Ljubljana

ŽR: 02033-0017879431

Activity of "Dr. J. Cholewa" Foundation for Cancer Research and Education – a report for the second quarter of 2013

The Dr. J. Cholewa Foundation for Cancer Research and Education is a non-profit, non-political and non-government that unites individuals, professionals, institutions and organisations thorough their common goal of achieving optimal results in cancer research, cancer education, cancer treatment and prevention. It provides financial support for physicians and other experts interested in all the subjects associated with cancer, resulting in a number of successful initiatives and projects.

The Foundation continues to provide financial support of "Radiology and Oncology", an international scientific journal that is edited, published and printed in Ljubljana, Slovenia. "Radiology and Oncology" publishes scientific articles, reviews, case reports, short reports and letters to the editor about research and studies in experimental and clinical oncology, supportive therapy, experimental and clinical research in radiology, radiophyics, and prevention and early diagnostics of different types of cancer. It is an open access journal available in pdf format and with an important Science Citation Index Impact factor (for the year 2012 is 1.602). All the abstracts in "Radiology and Oncology" are translated in Slovenian and the journal can thus provide sufficient scientific information from various fields of high quality cancer research to interested lay public in Slovenia.

The Foundation also continues to provide financial support for the publication of a number of information materials and brochures published by Slovenian Cancer Association, a member of European Cancer Leagues and UICC and most important lay association and organization involved in cancer education of lay and professional public in Slovenia. The Foundation has also continued to provide financial support for "Janez Plečnik Memorial Meeting and International Symposium" that has been organized by the Medical Faculty of University of Ljubljana for a number of years and it took part in the preparation and organization of "Briški izzivi", an annual meeting of physicians at the start of their careers held in Šmartno in the Goriška Brda region of Slovenia, and in the year 2012 dedicated to surgical proceedings in the treatment of rare tumours of digestive organs.

The Dr. J. Cholewa Foundation for Cancer Research and Education continues to provide financial and other means of support to all in Slovenia interested in the fight against cancer to organise scientific and other meetings of specific interest in different fields of cancer research and education.

Tomaž Benulič, MD
Borut Štabuc, MD, PhD
Andrej Plesničar, MD, MSc
Viljem Kovač, MD, PhD

Kakovost • Izbira • Zadovoljstvo

THE

Natrelle™

COLLECTION

Prsni vsadki in ekspanderji tkiv

Individualne ženske

Individualen izbor

ALLERGAN

DISTRIBUCIJA IN PRODAJA:
SANOLABOR, d.d.,
Leskoškova 4, 1000 Ljubljana, Slovenija
Tel:+386 (0)1 585-42-11
Fax:+386 (0)1 585-42-98
www.sanolabor.si

Sanolabor

PROMOCIJA, MARKETING IN STROKOVNA PODPORA:
EWOPHARMA d.o.o., Cesta 24.junija 23, 1000 Ljubljana, Slovenija
Jurij Pivka, vodja poslovne enote -Medicinska estetika
Tel: +386 (0) 59 084 845, mobilnik: +386 (0) 51 326 058
Fax: +386 (0) 59 084 849

SKRAJŠAN POVZETEK GLAVNIH ZNAČILNOSTI ZDRAVILA

Ime zdravila ALIMTA 100 mg prašek za koncentrat za raztopino za infundiranje in ALIMTA 500 mg prašek za koncentrat za raztopino za infundiranje **Kakovostna in količinska sestava** ALIMTA 100 mg: vsaka viala vsebuje 100 mg pemetrekseda (v obliki dinatrijevega pemetrekseda). Po pripravi vsebuje vsaka viala 25 mg/ml pemetrekseda. Pomožne snovi: Vsaka viala vsebuje približno 11 mg natrija, manitol, klorovodikova kislina, natrijev hidroksid. ALIMTA 500 mg: vsaka viala vsebuje 500 mg pemetrekseda (v obliki dinatrijevega pemetrekseda). Po pripravi vsebuje vsaka viala 25 mg/ml pemetrekseda. Pomožne snovi: Vsaka viala vsebuje približno 54 mg natrija, manitol, klorovodikova kislina, natrijev hidroksid. **Terapevtske indikacije:** ALIMTA je v kombinaciji s cisplatinom indicirana za zdravljenje bolnikov z neresektabilnim malignim plevralnim mezoteliomom, ki jih še nismo zdravili s kemoterapijo. ALIMTA je v kombinaciji s cisplatinom indicirana kot zdravljenje prvega izbora za bolnike z lokalno napredovalim ali metastatskim nedrobnoceličnim karcinomom pljuč, ki nima pretežno ploščatocelične histologije. ALIMTA je indicirana kot monoterapija za zdravljenje lokalno napredovalega ali metastatskega nedrobnoceličnega pljučnega karcinoma, ki nima pretežno ploščatocelične histologije pri bolnikih, pri katerih bolezen ni napredovala neposredno po kemoterapiji na osnovi platine. ALIMTA je indicirana kot monoterapija za zdravljenje drugega izbora bolnikov z lokalno napredovalim ali metastatskim nedrobnoceličnim pljučnim karcinomom, ki nima pretežno ploščatocelične histologije. **Odmerjanje in način uporabe:** *Odmerjanje:* ALIMTO smemo dajati le pod nadzorom zdravnika, usposobljenega za uporabo kemoterapije za zdravljenje raka. ALIMTA v kombinaciji s cisplatinom Priporočeni odmerek ALIMTE je 500 mg/m2 telesne površine (TP), dan kot intravenska infuzija v 10 minutah prvi dan vsakega 21-dnevnega ciklusa. Priporočeni odmerek cisplatina je 75 mg/m2 TP, infundiran v dveh urah približno 30 minut po zaključku infuzije pemetrekseda prvi dan vsakega 21 dnevnega ciklusa. Bolniki morajo prejeti zadostno antiemetično zdravljenje, pred in/ali po prejemanju cisplatina jih moramo tudi ustrezno hidrirati. *ALIMTA kot samostojno zdravilo* Priporočeni odmerek ALIMTE je 500 mg/m2 TP, dan kot intravenska infuzija v 10 minutah prvi dan vsakega 21 dnevnega ciklusa. *Režim premedikacije* Da zmanjšamo incidenco in resnost kožnih reakcij, dajemo kortikosteroid dan pred dajanjem pemetrekseda, na dan dajanja pemetrekseda in naslednji dan. Kortikosteroid naj ustreza 4 mg deksametazona, danega peroralno dvakrat dnevno. Za zmanjšanje toksičnosti morajo bolniki dnevno jemati tudi peroralno folno kislino ali multivitaminski pripravek, ki jo vsebuje (350 do 1000 mikrogramov). V sedmih dneh pred prvim odmerkom pemetrekseda morajo vzeti vsaj pet odmerkov folne kisline, odmerjanje pa morajo nadaljevati ves čas zdravljenja in še 21 dni po zadnjem odmerku pemetrekseda. Bolniki morajo prejeti tudi intramuskularno injekcijo vitamina B12 (1000 mikrogramov) v tednu pred prvim odmerkom pemetrekseda in enkrat vsake tri cikluse zatem. Kasnejše injekcije vitamina B12 lahko dajemo isti dan kot pemetrekseda. **Kontraindikacije:** Preobčutljivost za zdravilno učinkovino ali katerokoli pomožno snov. Dojenje. Sočasno cepljenje proti rumeni mrzlici. **Posebna opozorila in previdnostni ukrepi:** Pemetreksed lahko zavre delovanje kostnega mozga, kar se kaže kot nevtropenija, trombocitopenija in anemija (ali pancitopenija). Mielosupresija običajno predstavlja toksičnost za omejitev odmerka. Pri bolnikih, ki pred zdravljenjem niso prejemali kortikosteroidov, so poročali o kožnih reakcijah. Uporabe pemetrekseda pri bolnikih z očistkom kreatinina < 45 ml/min ne priporočamo. Bolniki z blagim do zmernim popuščanjem delovanja ledvic naj se izogibajo jemanju nesteroidnih protivnetnih zdravil (NSAID), denimo, ibuprofena in acetilsalicilne kisline 2 dni pred dajanjem pemetrekseda, na dan dajanja in še 2 dni po dajanju pemetrekseda. Vsi bolniki, ki jih lahko zdravimo s pemetreksedom, naj se izogibajo jemanju NSAID-ov z dolgimi razpolovnimi časi izločanja vsaj 5 dni pred dajanjem pemetrekseda, na dan dajanja in še vsaj 2 dni po dajanju pemetrekseda. Poročali so o resnih ledvičnih primerih, vključno z akutno ledvično odpovedjo, s pemetreksedom samim ali v povezavi z drugimi kemoterapevtiki. Pri bolnikih s klinično pomembno tekočino tretjega prostora moramo razmisliti o drenaži izliva pred dajanjem pemetrekseda. Kot posledico toksičnosti pemetrekseda v kombinaciji s cisplatinom za prebavila so opažali hudo dehidracijo, zato moramo bolnike pred prejemanjem terapije in/ali po njej ustrezno hidrirati, prejeti morajo zadostno antiemetično zdravljenje. Občasno so v kliničnih študijah pemetrekseda, običajno ob sočasnem dajanju z drugo citotoksično učinkovino, poročali o resnih srčnožilnih dogodkih, vključno z miokardnim infarktom in možganskožilnimi dogodki. Odsvetujemo uporabo živih oslabljenih cepiv. Spolno zrelim moškim odsvetujemo zaploditev otroka v času zdravljenja in še 6 mesecev zatem. Priporočamo ukrepe proti zanositvi ali vzdržnost. Zaradi možnosti, da zdravljenje s pemetreksedom povzroči trajno neplodnost, naj se moški pred začetkom zdravljenja posvetujejo o shranjevanju semena. Ženske v rodni dobi morajo v času zdravljenja s pemetreksedom uporabljati učinkovito kontracepcijo. Poročali so o primerih radiacijske pljučnice pri bolnikih, ki so jih zdravili z radiacijo pred, med ali po zdravljenju s pemetreksedom. Poročali so o radiacijskem izpuščaju pri bolnikih, ki so se zdravili z radioterapijo pred tedni ali leti. **Medsebojno delovanje z drugimi zdravili in druge oblike interakcij:** Sočasno dajanje nefrotoksičnih zdravil (denimo, aminoglikozidov, diuretikov zanke, spojin platine, ciklosporina) lahko potencialno povzroči zakasnjeni očistek pemetrekseda. Sočasno dajanje snovi, ki se tudi izločajo s tubulno sekrecijo (denimo, probenecid, penicilin), lahko potencialno povzroči zakasnjeni očistek pemetrekseda. Pri bolnikih z normalnim delovanjem ledvic lahko visoki odmerki nesteroidnih protivnetnih zdravil (NSAID-i, denimo, ibuprofen) in acetilsalicilna kislina v visokih odmerkih zmanjšajo eliminacijo pemetrekseda in tako lahko povečajo pojavnost neželenih učinkov pemetrekseda. Pri bolnikih z blagim do zmernim popuščanjem delovanja ledvic se moramo izogibati sočasnemu dajanju pemetrekseda z NSAID-i (denimo, ibuprofenom) ali acetilsalicilne kisline v visokih odmerkih 2 dni pred dajanjem pemetrekseda, na dan dajanja in še 2 dni po dajanju pemetrekseda. Sočasnemu dajanju NSAID-ov z daljšimi razpolovnimi časi s pemetreksedom se moramo izogibati vsaj 5 dni pred dajanjem pemetrekseda, na dan dajanja in še vsaj 2 dni po dajanju pemetrekseda.Velika različnost med posamezniki v koagulacijskem statusu v času bolezni ter možnost medsebojnega delovanja med peroralnimi antikoagulacijskimi učinkovinami ter kemoterapijo proti raku zahtevata povečano pogostnost spremljanja INR. **Kontraindicirana sočasna uporaba:** Cepivo proti rumeni mrzlici: tveganje za smrtno generalizirano bolezen po cepljenju. **Odsvetovana sočasna uporaba:** Živa oslabljena cepiva (razen proti rumeni mrzlici): tveganje za sistemsko, potencialno smrtno bolezen. **Neželeni učinki** Klinične študije malignega plevralnega mezotelioma *Zelo pogosto:* znižani nevtrofilci/granulociti, znižani levkociti, znižan hemoglobin, znižani trombociti, nevropatija-senzorna, diareja, bruhanje, stomatitis/faringitis, slabost, anoreksija, zaprtje, izpuščaj, alopecija, povišan kreatinin, znižan očistek kreatinina, utrujenost. *Pogosti:* dehidracija, motnje okusa, konjuktivitis, dispepsija. Klinične študije nedrobnoceličnega pljučnega karcinoma - ALIMTA monoterapija, zdravljenje 2. izbora: *Zelo pogosti:* znižan nevtrofilci/granulociti, znižani levkocitit, znižan hemoglobin, diareja, bruhanje, stomatitis/faringitis, slabost, anoreksija, izpuščaj/luščenje, utrujenost. *Pogosti:* znižani trombociti, zaprtje, povišanje SGPT (ALT), povišanje SGOT (AST), srbenje, alopecija, povišana telesna temperatura. Klinične študije nedrobnoceličnega pljučnega karcinoma - ALIMTA v kombinaciji s cisplatinom, zdravljenje 1. izbora: *Zelo pogosti:* znižan hemoglobin, znižani nevtrofilci/granulociti, znižani levkocitit, znižani trombociti, slabost, bruhanje, anoreksija, zaprtje, stomatitis/faringitis, diareja brez kolostomije, alopecija, izpuščaj/luščenje, povišan kreatinin, utrujenost. *Pogosti:* nevropatija-senzorična, motnje okusa, dispepsija/zgaga. Klinične študije nedrobnoceličnega pljučnega karcinoma - ALIMTA monoterapija, vzdrževalno in nadaljevalno zdravljenje: *Zelo pogosti:* znižan hemoglobin, slabost, anoreksija, utrujenost. *Pogosti:* znižani levkociti, znižani nevtrofilci, nevropatija-senzorična, bruhanje, mukozitis/stomatitis, povišanje ALT (SGPT), povišanje AST (SGOT), izpuščaj/luščenje, bolečina. Občasno so v kliničnih študijah pemetrekseda poročali o primerih resnih srčnožilnih in možganskožilnih dogodkov, vključno z miokardnim infarktom, angino pektoris, cerebrovaskularnim insultom in prehodnimi ishemičnimi atakami; primerih kolitisa ter o primerih intersticijske pljučnice z respiratorno insuficience, primerih edema, o ezofagitisu/radiacijskem ezofagitisu in o primerih sepse. Redkeje pa o primerih potencialno resnega hepatitisa in pancitopenije. Po uvedbi zdravila na trg so poročali o primerih akutne odpovedi ledvic s pemetreksedom samim ali v povezavi z drugimi kemoterapevtiki, primerih radiacijske pljučnice pri bolnikih, ki so jih zdravili z radiacijo pred, med ali po njihovem zdravljenju s pemetreksedom, primerih radiacijskega izpuščaja pri bolnikih, ki so se v preteklosti zdravili z radioterapijo, o primerih periferne ishemije, ki je včasih vodila v nekrozo okončin, redkih primerih buloznih stanj, kot sta Stevens-Johnsonov sindrom in toksična epidermalna nekroliza, ki so bila v nekaterih primerih usodna in o redkih primerih hemolitične anemije. Poročali so o redkih primerih anafilaktičnega šoka. **Imetnik dovoljenja za promet** Eli Lilly Nederland B.V., Grootslag 1 5, NL 3991 RA, Houten, Nizozemska. Datum zadnje revizije besedila 23. 07. 2012. **Način izdaje zdravila:** H. SAMO ZA STROKOVNO JAVNOST.
Podrobnejše informacije o zdravilu Alimta, so dostopne na spletni strani Evropske agencije za zdravila EMA http://www.ema.europa.eu in na lokalnem predstavništvu.

SIALM00056

Eli Lilly Farmacevtska družba, d.o.o.
Brnčičeva 41G, 1231 Ljubljana - Črnuče, Slovenija
Telefon: +386 (0)1 5800 010
Faks: +386 (0)1 5691 705

XGEVA®: PRVI IN EDINI ZAVIRALEC LIGANDA RANK, KI PREPREČUJE ZAPLETE KOSTNIH ZASEVKOV

Razvrščeno na pozitivno (P 100*) listo.[2] Na voljo od decembra 2012.

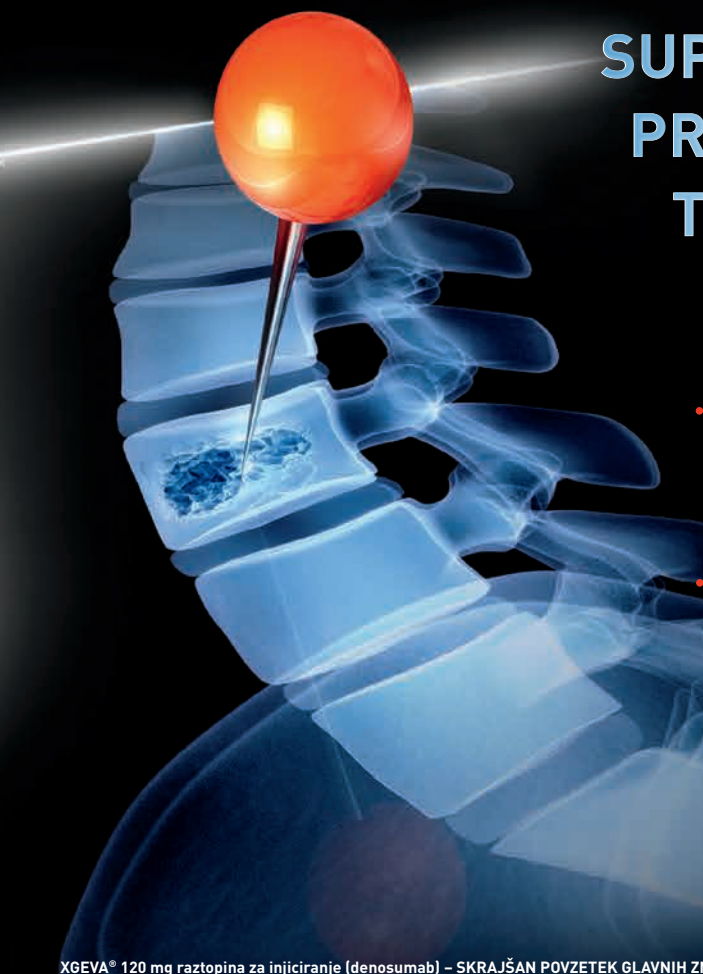

SUPERIORNO PREPREČEVANJE.[1] TARČNO DELOVANJE.[1] SUBKUTANO INJICIRANJE.[1]

- Zdravilo XGEVA® je indicirano za preprečevanje zapletov kostnih zasevkov pri odraslih s kostnimi zasevki solidnih tumorjev.
- Priporočen odmerek zdravila XGEVA® je 120 mg v enkratni subkutani injekciji, enkrat na 4 tedne.[1]

XGEVA®
(denosumab)
NATANČEN. MOČAN. DOKAZAN.

XGEVA® 120 mg raztopina za injiciranje (denosumab) – SKRAJŠAN POVZETEK GLAVNIH ZNAČILNOSTI ZDRAVILA
Samo za strokovno javnost.
Pred predpisovanjem si preberite celoten povzetek glavnih značilnosti zdravila.

SESTAVA ZDRAVILA: Ena viala vsebuje 120 mg denosumaba v 1,7 ml raztopine (70 mg/ml). Pomožne snovi s prepoznavnim delovanjem: 1,7 ml raztopine vsebuje 78 mg sorbitola (E420). **TERAPEVTSKE INDIKACIJE:** Preprečevanje skeletnih dogodkov (patoloških zlomov, obsevanja kosti, kompresije hrbtenjače ali operacije kosti) pri odraslih s kostnimi metastazami solidnih tumorjev. **ODMERJANJE IN NAČIN UPORABE:** Priporočeni odmerek zdravila XGEVA® je 120 mg enkrat na 4 tedne v enkratni subkutani injekciji v stegno, trebuh ali nadlaket. Vsi bolniki morajo prejemati dodatek vsaj 500 mg kalcija in 400 i.e. vitamina D dnevno, razen če ima bolnik hiperkalciemijo. *Bolniki z okvaro ledvic:* Prilagoditev odmerka ni potrebna. Izkušnje pri bolnikih na dializi ali s hudo okvaro ledvic (očistek kreatinina < 30 ml/min) so omejene. *Bolniki z okvaro jeter:* Varnost in učinkovitost denosumaba nista raziskani. *Starejši bolniki (stari ³ 65 let):* Prilagoditev odmerka ni potrebna. *Pediatrični bolniki:* Uporaba zdravila XGEVA® ni priporočljiva za pediatrične bolnike (stare < 18 let), ker njegovi učinkovitost in varnost pri teh bolnikih nista dokazani.
Za subkutano uporabo. Zdravilo XGEVA® mora aplicirati zdravstveni delavec. **KONTRAINDIKACIJE:** Preobčutljivost na zdravilno učinkovino ali katero koli pomožno snov. Huda, nezdravljena hipokalciemija. **POSEBNA OPOZORILA IN PREVIDNOSTNI UKREPI:** Vsi bolniki morajo prejemati dodatek kalcija in vitamina D, razen če ima bolnik hiperkalciemijo. Obstoječo hipokalciemijo je treba odpraviti še pred začetkom zdravljenja z zdravilom XGEVA®. Hipokalciemija se lahko pojavi kadarkoli med zdravljenjem z zdravilom XGEVA®. Najpogosteje se pojavi v prvih 6 mesecih zdravljenja. Bolniki s hudo okvaro ledvic (očistek kreatinina < 30 ml/min) ali na dializi imajo večje tveganje za pojav hipokalciemije, tem bolnikom je priporočljivo kontrolirati koncentracijo kalcija. če se med prejemanjem zdravila XGEVA® pojavi hipokalciemija, je lahko potrebno dodatno dodajanje kalcija. Bolniki z aktivnimi zobnimi boleznimi ali boleznimi čeljustnice morajo pred zdravljenjem z zdravilom XGEVA® opraviti zobozdravstveni pregled, vključno z ustreznimi preventivnimi zobozdravstvenimi ukrepi. Med zdravljenjem se morajo bolniki izogniti invazivnim zobozdravstvenim posegom, če je to mogoče, ter skrbeti za dobro ustno higieno. Bolnike, pri katerih med zdravljenjem z zdravilom XGEVA® obstaja sum na osteonekrozo čeljustnice ali se jim ta razvije, mora zdraviti zobozdravnik ali ustni kirurg. Pri takšnih bolnikih lahko obsežna zobna operacija za zdravljenje osteonekroze čeljustnice stanje še poslabša. Preden zdravnik predpiše zdravilo XGEVA® bolniku z neugodnimi dejavniki tveganja za osteonekrozo čeljustnice in če se med zdravljenjem z zdravilom XGEVA® pojavi osteonekroza čeljustnice, je treba narediti individualno oceno koristi in tveganja. Bolnikom je treba naročiti, naj takoj poiščejo zdravniško pomoč, če se jim pojavijo znaki ali simptomi celulitisa. Atipični zlomi stegnenice se lahko pojavijo že ob majhni poškodbi ali celo brez poškodbe, in sicer v subtrohanternem in diafiznem predelu stegnenice. Za te dogodke so značilni specifični radiografski izvidi. O njih so poročali tudi pri bolnikih z določenimi sočasnimi bolezenskimi stanji (npr. s pomanjkanjem vitamina D, revmatoidnim artritisom, hipofosfatazijo) in med uporabo določenih zdravil (npr. difosfonatov, glukokortikoidov, zaviralcev protonske črpalke). Ti dogodki so se pojavili tudi brez antiresorpcijskega zdravljenja. Podobni zlomi, opisani v zvezi z difosfonati, so pogosto obojestranski, zato je treba pri bolnikih, ki se zdravijo z denosumabom in so imeli zlom srednjega dela stegnenice, opraviti tudi pregled druge stegnenice. Pri bolnikih, pri katerih obstaja sum na atipičen zlom stegnenice, je treba razmisliti o prenehanju uporabe zdravila XGEVA® ob vrednotenju bolnika glede na individualno oceno koristi in tveganja. Bolnikom je treba naročiti, da morajo med zdravljenjem z zdravilom XGEVA® zdravniku poročati o novi ali nenavadni bolečini v stegnu, kolku ali dimljah. Bolnike s takšnimi simptomi je treba preiskati glede nepopolnega zloma stegnenice. Bolniki, zdravljeni z zdravilom XGEVA®, sočasno ne smejo prejemati drugih zdravil, ki vsebujejo denosumab (za indikacije pri osteoporozi), in difosfonatov. Bolniki z redko prirojeno motnjo intolerance za fruktozo ne smejo uporabljati zdravila XGEVA®. **INTERAKCIJE:** Študij medsebojnega delovanja niso izvedli. V kliničnih preskušanjih sočasna kemoterapija in/ali hormonsko zdravljenje ali predhodna intravenska izpostavljenost difosfonatom niso klinično pomembno spremenili najmanjše koncentracije denosumaba v serumu in farmakodinamike denosumaba (N-telopeptid v urinu, prilagojen na kreatinin, uNTx/Cr). **POVZETEK NEŽELENIH UČINKOV:** Občasni (≥ 1/1.000 do < 1/100): celulitis, preobčutljivost na zdravilo. Pogosti (≥ 1/100 do < 1/10): hipokalciemija, hipofosfatemija, ekstrakcija zoba, hiperhidroza, osteonekroza čeljustnice. Zelo pogosti (≥ 1/10): dispneja, driska. Redki (≥ 1/10.000 do < 1/1.000): anafilaktična reakcija, atipični zlom stegnenice. **FARMACEVTSKI PODATKI:** Shranjujte v hladilniku (2 °C - 8 °C). Ne zamrzujte. **NAČIN IN REŽIM PREDPISOVANJA TER IZDAJE ZDRAVILA:** Predpisovanje in izdaja zdravila je le na recept s posebnim režimom – ZZ. **IMETNIK DOVOLJENJA ZA PROMET:** Amgen Europe B.V., Minervum 7061, NL-4817 ZK Breda, Nizozemska. **Dodatna pojasnila lahko dobite v lokalni pisarni:** Amgen zdravila d.o.o., Šmartinska 140, SI-1000 Ljubljana. **DATUM ZADNJE REVIZIJE BESEDILA:** 25. april 2013. **Datum priprave informacije:** junij 2013.
Literatura: 1. Povzetek glavnih značilnosti zdravila XGEVA® (denosumab), Amgen 2013. 2. Spremembe liste zdravil, december 2012, objava dne 6.12.2012, ZZZS.

AMGEN®

SLO-DO-AMG-013-2013-JUN

Samo za strokovno javnost.

Nova indikacija

Pravočasno je vse

Za bolnike z metastatskim, na kastracijo odpornim rakom prostate, ki nimajo simptomov ali imajo blage simptome po neuspešnem zdravljenju z deprivacijo androgenov in pri katerih kemoterapija še ni indicirana.[1]

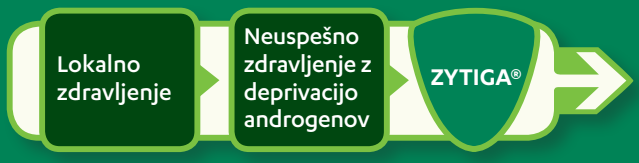

- za **47 %** zmanjša tveganje za radiografsko potrjeno napredovanje bolezni ($p < 0,001$),[2]
- za **8,4 mesece** podaljša čas do uvedbe citotoksične kemoterapije ($p < 0,001$).[2]

Zdravilo ZYTIGA je v obliki tablet, bolnik jih jemlje enkrat na dan.[1]

Čas je vse

SKRAJŠANO NAVODILO ZA PREDPISOVANJE ZDRAVILA:

Ime zdravila: ZYTIGA 250 mg tablete **Kakovostna in količinska sestava:** 250 mg abirateronacetata; pomožne snovi: mikrokristalna celuloza, premreženi natrijev karmelozat, laktoza monohidrat, magnezijev stearat, povidon, brezvodni koloidni silicijev dioksid, natrijev lavrilsulfat. **Indikacije:** uporaba skupaj s prednizonom ali prednizolonom za zdravljenje na kastracijo odpornega metastatskega raka prostate pri odraslih bolnikih, ki nimajo ali imajo blage simptome po neuspešnem zdravljenju z deprivacijo androgenov in pri katerih kemoterapija še ni klinično indicirana; ter pri odraslih bolnikih, pri katerih je bolezen napredovala med ali po zdravljenju s kemoterapijo z docetakselom. **Odmerjanje:** priporočeni odmerek: 1.000 mg (štiri 250 mg tablete v enem odmerku), 10 mg prednizona ali prednizolona/dan, najmanj dve uri po obroku. Pri bolnikih s hudo okvaro jeter ali ledvic je potrebna previdnost. **Kontraindikacije:** preobčutljivost na zdravilno učinkovino ali katero koli pomožno snov, uporaba zdravila pri ženskah, huda okvara jeter. **Posebna opozorila:** Pri uporabi zdravila pri bolnikih z anamnezo kardiovaskularne bolezni je potrebna previdnost. Pri bolnikih z iztisnim deležem levega prekata < 50% ali s srčnim popuščanjem razreda III ali IV po NYHA varnost uporabe zdravila ni dokazana. Pred začetkom zdravljenja je treba urediti hipertenzijo, zastajanje tekočin in odpraviti hipokaliemijo. Če kadarkoli med zdravljenjem pride do pojava hude hepatotoksičnosti je treba z zdravljenjem prenehati in se ga ne sme ponovno uvesti. Pri bolnikih, ki prejemajo prednizon ali prednizolon in so v stresni situaciji, je lahko pred in med stresno situacijo ter po njej indiciran zvečan odmerek kortikosteroidov. Pri bolnikih z napredovanim metastatskim rakom prostate (rezistentnim na kastracijo) lahko pride do zmanjšanja kostne gostote. Jemanje zdravila v kombinaciji z glukokortikoidi lahko ta učinek poveča. Pri bolnikih z rakom prostate, zdravljenih s ketokonazolom, lahko pričakujemo nižjo stopnjo odziva na zdravljenje. Uporaba glukokortikoidov lahko poslabša hiperglikemijo. Varnost in učinkovitost sočasne uporabe zdravila ZYTIGA in citotoksične kemoterapije ni bila ugotovljena. Bolniki z redko dedno intoleranco za galaktozo, laponsko obliko zmanjšane aktivnosti laktaze ali malabsorpcijo glukoze/galaktoze ne smejo jemati tega zdravila. Zdravilo vsebuje tudi več kot 1 mmol (oziroma 27,2 mg) natrija na odmerek (v štirih tabletah), kar je treba upoštevati pri bolnikih na dieti z nadzorovanim vnosom natrija. Pri bolnikih, ki se zdravijo z zdravilom ZYTIGA se lahko pojavita anemija in spolna disfunkcija. **Interakcije:** zdravila se ne sme jemati s hrano, ker se bistveno poveča absorpcija abirateronacetata. Pri sočasni uporabi z zdravili, ki jih aktivira ali presnavlja CYP2D6, zlasti tistih z majhno terapevtsko širino je potrebna previdnost. In vitro podatki kažejo, da je zdravilo substrat CYP3A4. Med zdravljenjem se uporabi močnih zaviralcev in induktorjev CYP3A4 izogibajte ali bodite še posebej previdni. **Nosečnost in dojenje:** Ženske, ki so noseče in ženske, ki bi lahko bile noseče, morajo v primeru stika ali rokovanja z zdravilom, nositi zaščitne rokavice. V študijah na živalih so ugotovili toksične učinke na sposobnost razmnoževanja. **Neželeni učinki:** okužba sečil, periferni edemi, hipokaliemija, hipertenzija, hipertrigliceridemija, hepatotoksičnost z zvišanimi vrednostmi ALT, AST in celokupnega bilirubina, srčno popuščanje, angina pektoris, aritmija, atrijska fibrilacija, tahikardija, zlomi, dispepsija, izpuščaj, hematurija, adrenalna insufi cienca. **Imetnik dovoljenja za promet:** Janssen-Cilag International NV, Turnhoutseweg 30, 2340 Beerse, Belgija, Predstavnik v Sloveniji: Johnson & Johnson d.o.o., Šmartinska 53, Ljubljana **Režim izdajanja zdravila:** Rp/Spec. **Datum zadnje revizije besedila:** 18. 12. 2012

Literatura:
1. Povzetek glavnih značilnosti zdravila Zytiga, 18. 12. 2012
2. Ryan CJ et al. N Engl J Med 2013; 368: 138 - 148

ZYT-SLO-A-051-040313

janssen
PHARMACEUTICAL COMPANIES OF Johnson&Johnson

Zytiga®
abirateronacetat

CLINIPORATOR

LEADING CLINICAL ELECTROPORATION

Electrochemotherapy

Effective, safe, simple.

For local tumours control

Before electrochemotherapy

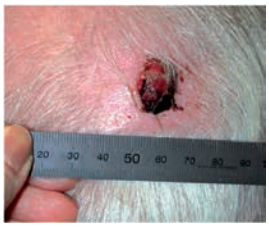

10 weeks after electrochemotherapy

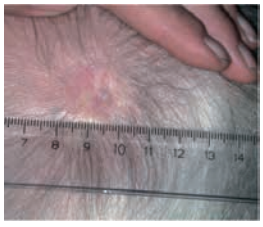

Gehl J, EJC Supplements, Volume 4, N° 11:35-37, 2006

Before electrochemotherapy

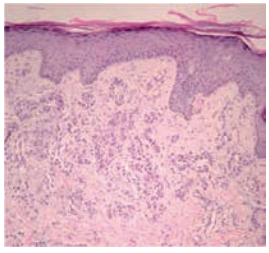

60 days after electrochemotherapy

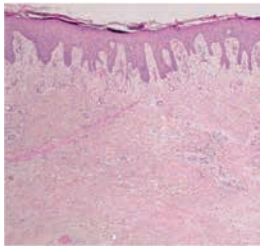

Quaglino P, Annals Of Surgical Oncology. 15 (8):2215-2222. 2008

CLINICAL INDICATIONS

- Melanoma and other skin tumors
- Local recurrences and cutaneous metastases from breast cancer
- Head and neck cancers

High response rate
Preservation of normal tissue and organ function
Efficacy in areas previously treated with radiation therapy
Palliation of painful, ulcerated or bleeding lesions
Improved quality of life and cosmetic results

IGEA SpA, Carpi, Italy | www.igeamedical.com | info@igeamedical.com

IGEA® CLINICAL BIOPHYSICS

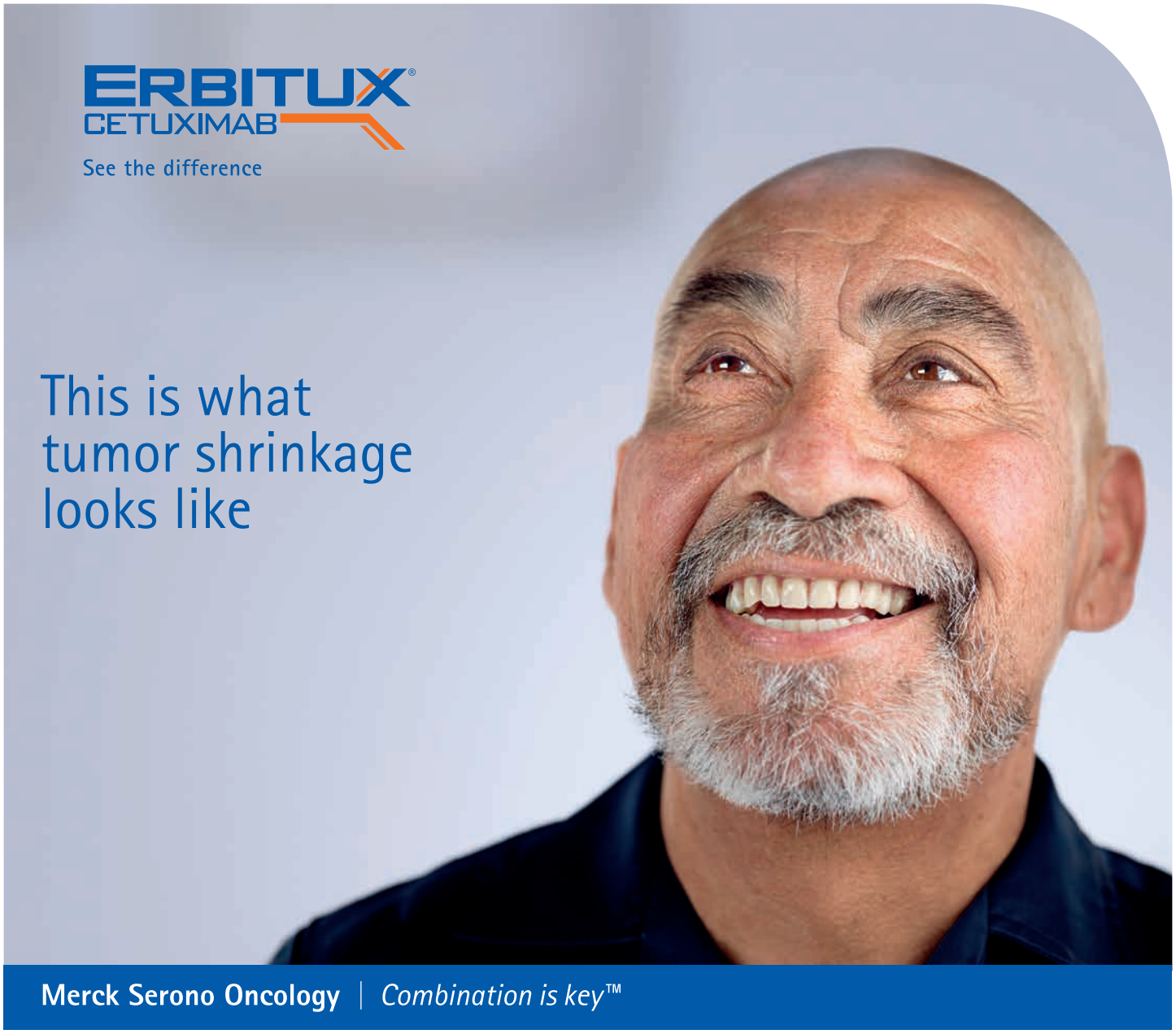

Erbitux 5 mg/ml raztopina za infundiranje
Skrajšan povzetek glavnih značilnosti zdravila

Sestava: En ml raztopine za infundiranje vsebuje 5 mg cetuximaba in pomožne snovi. Cetuksimab je himerno monoklonsko IgG1 protitelo. **Terapevtske indikacije:** Zdravilo Erbitux je indicirano za zdravljenje bolnikov z metastatskim kolorektalnim rakom z ekspresijo receptorjev EGFR in nemutiranim tipom KRAS v kombinaciji s kemoterapijo na osnovi irinotekana, kot primarno zdravljenje v kombinaciji s FOLFOX in kot samostojno zdravilo pri bolnikih, pri katerih zdravljenje z oksaliplatinom in irinotekanom ni bilo uspešno ter pri bolnikih, ki ne prenašajo irinotekana. Zdravilo Erbitux je indicirano za zdravljenje bolnikov z rakom skvamoznih celic glave in vratu v kombinaciji z radioterapijo za lokalno napredovalo bolezen in v kombinaciji s kemoterapijo na osnovi platine za ponavljajočo se in/ali metastatsko bolezen. **Odmerjanje in način uporabe:** Zdravilo Erbitux pri vseh indikacijah infundirajte enkrat na teden. Pred prvo infuzijo mora bolnik prejeti premedikacijo z antihistaminikom in kortikosteroidom. Začetni odmerek je 400 mg cetuksimaba na m2 telesne površine. Vsi naslednji tedenski odmerki so vsak po 250 mg/m2. **Kontraindikacije:** Zdravilo Erbitux je kontraindicirano pri bolnikih z znano hudo preobčutljivostno reakcijo (3. ali 4. stopnje) na cetuksimab. Kombinacija zdravila Erbitux s kemoterapijo, ki vsebuje oksaliplatin, je kontraindicirana pri bolnikih z metastatskim kolorektalnim rakom z mutiranim tipom KRAS ali kadar status KRAS ni znan. **Posebna opozorila in previdnostni ukrepi:** Če pri bolniku nastopi blaga ali zmerna reakcija, povezana z infundiranjem, lahko zmanjšate hitrost infundiranja. Priporočljivo je, da ostane hitrost infundiranja na nižji vrednosti tudi pri vseh naslednjih infuzijah. Če se pri bolniku pojavi kožna reakcija, ki je ne more prenašati, ali huda kožna reakcija (≥ 3. stopnje po kriterijih CTCAE), morate prekiniti terapijo s cetuksimabom. Z zdravljenjem smete nadaljevati le, če se je reakcija izboljšala do 2. stopnje. Če ugotovite intersticijsko bolezen pljuč, morate zdravljenje s cetuksimabom prekiniti, in bolnika ustrezno zdraviti. Zaradi možnosti pojava znižanja nivoja magnezija v serumu se pred in periodično med zdravljenjem priporoča določanje koncentracije elektrolitov. Če se pojavi sum na nevtropenijo, je potrebno bolnika skrbno nadzorovati. Potrebno je upoštevati kardiovaskularno stanje bolnika in sočasno dajanje kardiotoksičnih učinkovin kot so fluoropirimidini. Cetuksimab je treba uporabljati previdno pri bolnikih z anamnezo keratitisa, ulcerativnega keratitisa ali zelo suhih oči. **Interakcije:** Pri kombinaciji s fluoropirimidini se je povečala pogostnost srčne ishemije, vključno z miokardnim infarktom in kongestivno srčno odpovedjo ter pogostnost sindroma dlani in stopal. V kombinaciji s kemoterapijo na osnovi platine se lahko poveča pogostnost hude levkopenije ali hude nevtropenije. V kombinaciji s kapecitabinom in oksaliplatinom (XELOX) se lahko poveča pogostnost hude driske. **Neželeni učinki:** Zelo pogosti (≥ 1/10): hipomagneziemija, povečanje ravni jetrnih encimov, kožne reakcije, blage ali zmerne reakcije povezane z infundiranjem, mukozitis, v nekaterih primerih resen. Pogosti (≥ 1/100, < 1/10): dehidracija, hipokalciemija, anoreksija, glavobol, konjunktivitis, driska, navzeja, bruhanje, hude reakcije povezane z infundiranjem, utrujenost. **Posebna navodila za shranjevanje:** Shranjujte v hladilniku (2 °C - 8 °C). **Pakiranje:** 1 viala z 20 ml ali 100 ml raztopine. **Način in režim izdaje:** H.
Imetnik dovoljenja za promet: Merck KGaA, 64271 Darmstadt, Nemčija.
Datum zadnje revizije besedila: Februar 2013.
Pred predpisovanjem zdravila natančno preberite celoten Povzetek glavnih značilnosti zdravila.
Podrobnejše informacije so na voljo pri predstavniku imetnika dovoljenja za promet z zdravilom:
Merck d.o.o., Ameriška ulica 8, 1000 Ljubljana, tel.: 01 560 3810, faks: 01 560 3830,
el. pošta: info@merck.si

www.merckserono.net
www.Erbitux-international.com

PM-ONC-06/13/26.04.2013

Merck Serono

Merck Serono is a division of Merck

MERCK

Skrajšan povzetek glavnih značilnosti zdravila ZELBORAF

Samo za strokovno javnost.

Ime zdravila: Zelboraf 240 mg filmsko obložene tablete
Kakovostna in količinska sestava: Ena tableta vsebuje 240 mg vemurafeniba (v obliki precipitata vemurafeniba in hipromeloze acetat sukcinata). **Terapevtske indikacije:** Vemurafenib je indiciran za samostojno zdravljenje odraslih bolnikov z neresektabilnim ali metastatskim melanomom, s pozitivno mutacijo BRAF V600. **Odmerjanje in način uporabe:** Zdravljenje z vemurafenibom mora uvesti in nadzorovati usposobljen zdravnik, ki ima izkušnje z uporabo zdravil za zdravljenje raka. Odmerjanje: Priporočeni odmerek vemurafeniba je 960 mg (4 tablete po 240 mg) dvakrat na dan (to ustreza celotnemu dnevnemu odmerku 1920 mg). Vemurafenib lahko vzamemo s hrano ali brez nje, izogibati pa se moramo stalnemu jemanju obeh dnevnih odmerkov na prazen želodec. Zdravljenje z vemurafenibom moramo nadaljevati do napredovanja bolezni ali pojava nesprejemljive toksičnosti. Če bolnik izpusti odmerek, ga lahko vzame do 4 ure pred naslednjim odmerkom za ohranitev sheme dvakrat na dan. Obeh odmerkov pa ne sme vzeti hkrati. Če bolnik po zaužitju vemurafeniba bruha, ne sme vzeti dodatnega odmerka zdravila, ampak mora z zdravljenjem normalno nadaljevati. Prilagoditve odmerjanja: Za obvladovanje neželenih učinkov ali ob podaljšanju intervala QTc je potrebno zmanjšanje odmerka, začasna prekinitev in/ali dokončno prenehanje zdravljenja (za podrobnosti o prilagoditvi odmerka, prosimo glejte SmPC zdravila). Zmanjšanje odmerka pod 480 mg dvakrat na dan ni priporočljivo. Če se pri bolniku pojavi ploščatocelični karcinom kože, priporočamo nadaljevanje zdravljenja brez zmanjšanja odmerka vemurafeniba. *Posebne populacije*: Za bolnike, starejše od 65 let, prilagajanje odmerka ni potrebno. O bolnikih z okvaro ledvic ali jeter je na voljo malo podatkov. Bolnike s hudo okvaro ledvic ali z zmerno do hudo okvaro jeter je treba pozorno spremljati. Varnost in učinkovitost vemurafeniba pri otrocih in mladostnikih, mlajših od 18 let, še nista bili dokazani. Podatkov ni na voljo. Način uporabe: Tablete vemurafeniba je treba zaužiti cele, z vodo. Ne sme se jih žvečiti ali zdrobiti. **Kontraindikacije:** Preobčutljivost na zdravilno učinkovino ali katerokoli pomožno snov. **Posebna opozorila in previdnostni ukrepi:** Pred uporabo vemurafeniba je treba z validirano preiskavo potrditi, da ima bolnik tumor s pozitivno mutacijo BRAF V600. Dokazi o učinkovitosti in varnosti vemurafeniba pri bolnikih s tumorji z izraženo redko BRAF V600 mutacijo, ki ni V600E ali V600K, niso prepričljivi. Vemurafeniba se ne sme uporabljati pri bolnikih z malignim melanomom, ki ima divji tip BRAF. *Preobčutljivostne reakcije:* V povezavi z vemurafenibom so bile opisane resne preobčutljivostne reakcije, vključno z anafilaksijo. Hude preobčutljivostne reakcije lahko vključujejo Stevens-Johnsonov sindrom, generaliziran izpuščaj, eritem ali hipotenzijo. Pri bolnikih, pri katerih se pojavijo resne preobčutljivostne reakcije, je treba zdravljenje z vemurafenibom dokončno opustiti. *Kožne reakcije:* Pri bolnikih, ki so prejemali vemurafenib, so v ključnem kliničnem preskušanju poročali o hudih kožnih reakcijah, vključno z redkim Stevens-Johnsonovim sindromom in toksično epidermalno nekrolizo. Pri bolnikih, pri katerih se pojavi huda kožna reakcija, je treba zdravljenje z vemurafenibom dokončno opustiti. *Podaljšanje intervala QT:* V nekontrolirani, odprti študiji faze II pri predhodno zdravljenih bolnikih z metastatskim melanomom, so opazili podaljšanje intervala QT, odvisnega od izpostavljenosti vemurafenibu. Podaljšanje intervala QT lahko poveča tveganje za ventrikularne aritmije, vključno s t. i. *Torsade de Pointes*. Z vemurafenibom ni priporočljivo zdraviti bolnikov z elektrolitskimi motnjami (vključno z magnezijem), ki jih ni mogoče odpraviti, bolnikov s sindromom dolgega intervala QT in bolnikov, zdravljenih z zdravili, ki podaljšajo interval QT. Pred zdravljenjem z vemurafenibom, en mesec po zdravljenju in po spremembi odmerka je treba pri vseh bolnikih posneti elektrokardiogram (EKG) in kontrolirati elektrolite (vključno z magnezijem). Nadaljnje kontrole so priporočljive predvsem pri bolnikih z zmerno do hudo jetrno okvaro, in sicer mesečno prve 3 mesece zdravljenja, potem pa na 3 mesece oziroma pogosteje, če je to klinično indicirano. Zdravljenja z vemurafenibom ni priporočljivo uvesti pri bolnikih, ki imajo interval QTc > 500 milisekund (ms). *Bolezni oči:* Poročali so o resnih neželenih učinkih na očeh, vključno z uveitisom, iritisom in zaporo mrežnične vene. Bolnikom je treba oči redno kontrolirati glede morebitnih neželenih učinkov na očeh. *Ploščatocelični karcinom kože:* Pri bolnikih, zdravljenih z vemurafenibom, so bili opisani primeri ploščatoceličnega karcinoma kože, vključno s ploščatoceličnim karcinomom, opredeljenim kot keratoakantom ali mešani keratoakantom. Priporočljivo je, da vsi bolniki pred uvedbo zdravljenja opravijo dermatološki pregled in da so med zdravljenjem deležni rednih kontrol. Vsako sumljivo spremembo je treba izrezati, poslati na histopatološko oceno in jo zdraviti v skladu z lokalnimi smernicami. Med zdravljenjem in do šest mesecev po zdravljenju ploščatoceličnega karcinoma mora zdravnik enkrat mesečno pregledati bolnika. Pri bolnikih, ki se jim pojavi ploščatocelični karcinom kože, je priporočljivo nadaljevati zdravljenje brez zmanjšanja odmerka. Nadzor se mora nadaljevati še 6 mesecev po prenehanju zdravljenja z vemurafenibom ali do uvedbe drugega antineoplastičnega zdravljenja. Bolnikom je treba naročiti, naj svojega zdravnika obvestijo o pojavu kakršnih koli sprememb na koži. *Ploščatocelični karcinom, ki se ne nahaja na koži:* Pri bolnikih, ki so prejemali vemurafenib v kliničnih preskušanjih, so poročali o primerih ploščatoceličnega karcinoma, ki se ne nahaja na koži. Bolnikom je treba pred uvedbo zdravljenja in na 3 mesece med zdravljenjem pregledati glavo in vrat (pregled mora obsegati vsaj ogled ustne sluznice in palpacijo bezgavk). Poleg tega morajo bolniki pred zdravljenjem in na 6 mesecev med zdravljenjem opraviti računalniško tomografijo (CT) prsnega koša. Pred in po končanem zdravljenju ali kadar je klinično indicirano, je priporočljivo opraviti pregled zadnjika in ginekološki pregled (pri ženskah). Po prenehanju zdravljenja z vemurafenibom se mora nadzor glede ploščatoceličnega karcinoma, ki se ne nahaja na koži, nadaljevati še 6 mesecev ali do uvedbe drugega antineoplastičnega zdravljenja. Nenormalne spremembe je treba obravnavati v skladu s klinično prakso. *Novi primarni melanom:* V kliničnih preskušanjih so poročali o novih primarnih melanomih. Bolnike s takšnimi primeri so zdravili z ekscizijo, bolniki pa so nadaljevali z zdravljenjem brez prilagoditve odmerka. Nadzor nad pojavom kožnih lezij je treba izvajati, kot je navedeno zgoraj pri ploščatoceličnem karcinomu kože. *Poškodbe jeter:* Med uporabo vemurafeniba se lahko pojavijo jetrne laboratorijske nepravilnosti (zvišanje GGT, ALT, alkalne fosfataze, bilirubina, AST). Pred uvedbo zdravljenja in mesečno med zdravljenjem oz. kot je klinično indicirano, je treba kontrolirati jetrne encime (transaminaze in alkalno fosfatazo) ter bilirubin. Laboratorijske nepravilnosti je treba obvladati z zmanjšanjem odmerka, prekinitvijo zdravljenja ali prenehanjem zdravljenja (za podrobnosti o prilagoditvi odmerka, prosimo glejte SmPC zdravila). *Jetrna okvara:* Bolnikom z jetrno okvaro začetnih odmerkov ni treba prilagajati. Bolnike, ki imajo zaradi metastaz v jetrih blago jetrno okvaro in nimajo hiperbilirubinemije, se lahko nadzoruje v skladu s splošnimi priporočili. Podatkov o bolnikih z zmerno do hudo jetrno okvaro je le malo; pri takih bolnikih je izpostavljenost lahko večja. Tako je posebej po prvih tednih zdravljenja potreben skrben nadzor, saj lahko po daljšem obdobju (več tednih) pride do kopičenja. *Ledvična okvara:* Bolnikom z blago ali zmerno ledvično okvaro začetnih odmerkov ni treba prilagajati. Pri bolnikih z hudo ledvično okvaro je treba vemurafenib uporabljati previdno ter jih pozorno spremljati. *Fotosenzibilnost:* Pri bolnikih, ki so v kliničnih študijah prejemali vemurafenib, je bila opisana blaga do huda fotosenzibilnost. Vsem bolnikom je treba naročiti, naj se med jemanjem vemurafeniba ne izpostavljajo soncu. V primeru fotosenzibilnosti stopnje 2 (neprenosljivo) ali več so priporočljive prilagoditve odmerka. *Ženske v rodni dobi* morajo med zdravljenjem in vsaj še 6 mesecev po zdravljenju uporabljati učinkovito kontracepcijsko zaščito. Vemurafenib lahko zmanjša učinkovitost hormonskih kontraceptivov. *Sočasno dajanje ipilimumaba* Pri sočasni uporabi ipilimumaba in vemurafeniba so v preskušanju faze I poročali o asimptomatskih zvišanjih transaminaz in bilirubina stopnje 3. Glede na te preliminarne podatke sočasna uporaba ipilimumaba in vemurafeniba ni priporočljiva. **Medsebojno delovanje z drugimi zdravili in druge oblike interakcij:** *Vplivi vemurafeniba na substrate CYP* Vemurafenib lahko poveča izpostavljenost v plazmi tistih snovi, ki se presnavljajo pretežno s CYP1A2; v takem primeru je treba razmisliti o prilagoditvi odmerka. Vemurafenib lahko zmanjša plazemsko izpostavljenost zdravilom, ki se presnavljajo pretežno s CYP3A4. Tako je lahko učinkovitost kontracepcijskih tablet, ki se presnavljajo s CYP3A4 in se uporabljajo sočasno z vemurafenibom, zmanjšana. Pri substratih CYP3A4, ki imajo ozko terapevtsko okno, je treba razmisliti o prilagoditvi odmerka. Zaenkrat še ni znano ali lahko vemurafenib pri 100 µM koncentraciji v plazmi, ki je bila opažena pri bolnikih v stanju dinamičnega ravnovesja (približno 50 µg/ml), zmanjša plazemske koncentracije sočasno dajanih substratov CYP2B6, kot je bupropion. Kadar se vemurafenib pri bolnikih z melanonom uporabi hkrati z varfarinom (CYP2C9), je potrebna previdnost.Tveganja za klinično pomemben učinek na sočasno uporabljene učinkovine, ki so substrati CYP2C8, pa ni mogoče izključiti. Zaradi dolge razpolovne dobe vemurafeniba je mogoče, da popolnega inhibitornega učinka vemurafeniba na sočasno dajano zdravilo ne opazimo, dokler ne mine 8 dni zdravljenja z vemurafenibom. Po končanem zdravljenju z vemurafenibom bo morda potreben 8-dnevni premor, da se izognemo interakcijam z nadaljnjim zdravljenjem. *Vpliv vemurafeniba na transportne sisteme zdravil* Možnosti, da vemurafenib morda poveča izpostavljenost drugih zdravil, ki se prenašajo s P-gp, ni mogoče izključiti. Možen vpliv vemurafeniba na druge prenašalce (npr. BCRP) trenutno ni znan. *Vplivi sočasno uporabljenih zdravil na vemurafenib* Študije *in vitro* kažejo, da sta presnova s CYP3A4 in glukuronidacija odgovorni za presnovo vemurafeniba. Zdi se, da je tudi izločanje z žolčem pomembna pot izločanja. Vemurafenib je treba uporabljati previdno v kombinaciji z močnimi inhibitorji CYP3A4, glukuronidacije in/ali prenašalnih beljakovin (npr. ritonavirjem, sakvinavirjem, telitromicinom, ketokonazolom, itrakonazolom, vorikonazolom, posakonazolom, nefazodonom, atazanavirjem). Sočasna uporaba močnih induktorjev P-gp, glukuronidacije, in/ali CYP3A4 (npr. rifampicina, rifabutina, karbamazepina, fenitoina ali šentjanževke [hypericum perforatum]) lahko vodi v suboptimalno izpostavljenost vemurafenibu in se ji je treba izogibati. Študije *in vitro* so pokazale, da je vemurafenib substrat sekretornega prenašalca, P-gp. Vplivi induktorjev in inhibitorjev P-gp na izpostavljenost vemurafenibu niso znani. Ne moremo pa izključiti možnosti, da imajo lahko zdravila, ki inhibirajo ali vplivajo na P-gp (npr. verapamil, klaritromicin, ciklosporin, ritonavir, kinidin, dronedaron, amiodaron, itrakonazol, ranolazin) vpliv na farmakokinetiko vemurafeniba. Za zdaj ni znano, ali je vemurafenib substrat tudi za druge beljakovinske prenašalce.
Neželeni učinki: Med najpogostejšimi neželenimi učinki (> 30 %), o katerih so poročali v zvezi z vemurafenibom, so artralgija, utrujenost, kožni izpuščaj, fotosenzibilnostna reakcija, navzea, alopecija in srbenje. Zelo pogosto je bil opisan ploščatocelični karcinom kože. Sledijo najpogostejši neželeni učinki, ki so se pojavili pri bolnikih, zdravljenih z vemurafenibom v študiji faze II in III in dogodki iz varnostnih poročil vseh preskušanj. *Zelo pogosti:* ploščatocelični karcinom kože, seboroična keratoza, kožni papilom, zmanjšanje teka, glavobol, disgevzija, kašelj, driska, bruhanje, slabost, zaprtost, fotosenzibilna reakcija, aktinična keratoza, kožni izpuščaj, makulo-papulozen izpuščaj, papulozen izpuščaj, srbenje, hiperkeratoza, eritem, alopecija, suha koža, sončne opekline, artralgija, mialgija, bolečina v okončini, mišično-skeletne bolečine, bolečine v hrbtu, utrujenost, pireksija, periferni edem, astenija, zvišanje GGT. *Pogosti*: folikulitis, bazalnocelični karcinom, novi primarni melanom, ohromelost sedmega živca, omotica, uveitis, sindrom palmarno-plantarne eritrodisestezije, nodozni eritem, pilarna keratoza, artritis, zvišanje ALT, alkalne fosfataze, bilirubina in izguba telesne mase, podaljšanje QT. *Posebne populacije*: Pri starejših bolnikih (≥ 65 let) je možna večja verjetnost neželenih učinkov, vključno s ploščatoceličnim karcinomom kože, zmanjšanjem teka in motnjami srčnega ritma. Med neželene učinke stopnje 3, ki so bili med kliničnimi preskušanji vemurafeniba pri ženskah opisani pogosteje kot pri moških, spadajo kožni izpuščaj, artralgija in fotosenzibilnost.

Režim izdaje zdravila: Rp/Spec
Imetnik dovoljenja za promet: Roche Registration Limited, 6 Falcon Way, Shire Park, Welwyn Garden City, AL7 1TW, Velika Britanija
Verzija: 3.0/13 Informacija pripravljena: julij 2013

DODATNE INFORMACIJE SO NA VOLJO PRI:
Roche farmacevtska družba d.o.o., Vodovodna cesta 109, 1000 Ljubljana
Povzetek glavnih značilnosti zdravila je dosegljiv na www.roche.si

009-13-ZEL

Zelboraf®
vemurafenib

Roche

Posamezniku prilagojeno zdravljenje metastatskega melanoma

Vsak bolnik z metastatskim melanomom je drugačen.

S pravilnim izborom bolnikov in tarčnim zdravljenjem bolnikov z neresektabilnim ali metastatskim melanomom s potrjeno mutacijo $BRAF^{V600}$ z zdravilom ZELBORAF®, se lahko bistveno izboljša odziv na zdravljenje in celokupno preživetje v primerjavi z dakarbazinom. Neželeni učinki zdravljenja z zdravilom ZELBORAF® so obvladljivi.[1]

Zelboraf®
vemurafenib

1 Povzetek glavnih značilnosti zdravila Zelboraf® 27.6.2013. Dosegljiv na www.ema.europa.eu; dostopano: julij 2013.

TANTUM VERDE®

Lajšanje bolečine in oteklin pri vnetju v ustni votlini in žrelu, ki nastanejo zaradi okužb in stanj po operaciji in kot posledica radioterapije (t.i. radiomukozitis).

CSC ANGELINI

Imetnik dovoljenja za promet
CSC Pharma d.o.o.
Jana Husa 1a
1000 Ljubljana

www.tantum-verde.si

Tantum Verde 1,5 mg/ml oralno pršilo, raztopina

Terapevtske indikacije
Samozdravljenje: lajšanje bolečine in oteklin pri vnetju v ustni votlini in žrelu, ki so lahko posledica okužb in stanj po operaciji. Po nasvetu in navodilu zdravnika: lajšanje bolečine in oteklin v ustni votlini in žrelu, ki so posledica radiomukozitisa.

Odmerjanje in način uporabe
Uporaba 2- do 6-krat na dan (vsake 1,5 do 3 ure). Odrasli: 4 do 8 razprškov 2- do 6-krat na dan. Otroci od 6 do 12 let: 4 razprški 2- do 6-krat na dan. Otroci, mlajši od 6 let: 1 razpršek na 4 kg telesne mase; do največ 4 razprške 2 do 6-krat na dan.

Posebna opozorila in previdnostni ukrepi
Pri manjšini bolnikov lahko resne bolezni povzročijo ustne/žrelne ulceracije.
Če se simptomi v treh dneh ne izboljšajo, se mora bolnik posvetovati z zdravnikom ali zobozdravnikom, kot je primerno. Zdravilo vsebuje aspartam (E951) (vir fenilalanina), ki je lahko škodljiv za bolnike s fenilketonurijo. Zdravilo vsebuje izomalt (E953) (sinonim: izomaltitol (E953)). Bolniki z redko dedno intoleranco za fruktozo ne smejo jemati tega zdravila. Uporaba benzidamina ni priporočljiva za bolnike s preobčutljivostjo za salicilno kislino ali druga nesteroidna protivnetna zdravila. Pri bolnikih, ki imajo ali so imeli bronhialno astmo, lahko pride do bronhospazma. Pri takih bolnikih je potrebna previdnost.

Neželeni učinki
Bolezni prebavil Redki: pekoč občutek v ustih, suha usta.
Bolezni imunskega sistema Redki: preobčutljivostna reakcija.
Bolezni dihal, prsnega koša in mediastinalnega prostora Zelo redki: laringospazem.
Bolezni kože in podkožja Občasni: fotosenzitivnost. Zelo redki: angioedem.

Rok uporabnosti
4 leta. Zdravila ne smete uporabljati po datumu izteka roka uporabnosti, ki je naveden na ovojnini. Posebna navodila za shranjevanje Za shranjevanje pastil niso potrebna posebna navodila. Plastenko z raztopino shranjujte v zunanji ovojnini za zagotovitev zaščite pred svetlobo. Shranjujte pri temperaturi do 25°C. Shranjujte v originalni ovojnini in nedosegljivo otrokom.

Instructions for authors

The editorial policy

Radiology and Oncology is a multidisciplinary journal devoted to the publishing original and high quality scientific papers, professional papers, review articles, case reports and varia (editorials, short communications, professional information, book reviews, letters, etc.) pertinent to diagnostic and interventional radiology, computerized tomography, magnetic resonance, ultrasound, nuclear medicine, radiotherapy, clinical and experimental oncology, radiobiology, radiophysics and radiation protection. Therefore, the scope of the journal is to cover beside radiology the diagnostic and therapeutic aspects in oncology, which distinguishes it from other journals in the field.

The Editorial Board requires that the paper has not been published or submitted for publication elsewhere; the authors are responsible for all statements in their papers. Accepted articles become the property of the journal and, therefore cannot be published elsewhere without the written permission of the editors.

Submission of the manuscript

The manuscript written in English should be submitted to the journal via online submission system Editorial Manager available for this journal at: www.radioloncol.com.

In case of problems, please contact Sašo Trupej at saso.trupej@computing.si or the Editor of this journal at gsersa@onko-i.si

All articles are subjected to the editorial review and the review by independent referees.

Authors are requested to suggest persons competent to review their manuscript. However, please note that this will be treated only as a suggestion, the final selection of reviewers is exclusively the Editor's decision. The authors' names are revealed to the referees, but not vice versa.

Manuscripts which do not comply with the technical requirements stated herein will be returned to the authors for the correction before peer-review. The editorial board reserves the right to ask authors to make appropriate changes of the contents as well as grammatical and stylistic corrections when necessary. Page charges will be charged for manuscripts exceeding the recommended page number, as well as additional editorial work and requests for printed reprints.

All articles are published printed and on-line as the open access. To support the open access policy of the journal, the authors are encouraged to pay the open access charge of 500 EUR.

Manuscripts submitted under multiple authorship are reviewed on the assumption that all listed authors concur in the submission and are responsible for its content; they must have agreed to its publication and have given the corresponding author the authority to act on their behalf in all matters pertaining to publication. The corresponding author is responsible for informing the coauthors of the manuscript status throughout the submission, review, and production process.

Preparation of manuscripts

Radiology and Oncology will consider manuscripts prepared according to the Uniform Requirements for Manuscripts Submitted to Biomedical Journals by International Committee of Medical Journal Editors (www.icmje.org). The manuscript should be typed double-spaced with a 3-cm margin at the top and left-hand side of the sheet. The manuscript should be written in grammatically and stylistically correct language. Abbreviations should be avoided. If their use is neccessary, they should be explained at the first time mentioned. The technical data should conform to the SI system. The manuscript, including the references, must not exceed 15 typewritten pages, and the number of figures and tables is limited to 8. If appropriate, organize the text so that it includes: Introduction, Materials and methods, Results and Discussion. Exceptionally, the results and discussion can be combined in a single section. Start each section on a new page, and number each page consecutively with Arabic numerals.

The Title page should include a concise and informative title, followed by the full name(s) of the author(s); the institutional affiliation of each author; the name and address of the corresponding author (including telephone, fax and E-mail), and an abbreviated title. This should be followed by the abstract page, summarizing in less than 250 words the reasons for the study, experimental approach, the major findings (with specific data if possible), and the principal conclusions, and providing 3-6 key words for indexing purposes. Structured abstracts are preferred. Slovene authors are requested to provide title and the abstract in Slovene language in a separate file. The text of the research article should then proceed as follows:

Introduction should summarize the rationale for the study or observation, citing only the essential references and stating the aim of the study.

Materials and methods should provide enough information to enable experiments to be repeated. New methods should be described in detail.

Results should be presented clearly and concisely without repeating the data in the figures and tables. Emphasis should be on clear and precise presentation of results and their significance in relation to the aim of the investigation.

Discussion should explain the results rather than simply repeating them and interpret their significance and draw conclusions. It should discuss the results of the study in the light of previously published work.

Charts, Illustrations, Photographs and Tables must be numbered and referred to in the text, with the appropriate location indicated. Charts, illustrations and photographs, provided electronically, should be of appropriate quality for good reproduction. Illustrations and charts must be vector image, created in CMYK colour space, used font familie are encouraged "Century Gothic" and saved as .AI, .EPS or .PDF format. Color charts, illustrations and photographs are encouraged. Picture (image) size must be 2.000 pixels on the longer side and saved as .JPG (maximum quality) format. In photographs, mask the identities of the patients. Tables should be typed double-spaced, with a descriptive title and, if appropriate, units of numerical measurements included in the column heading. The files with the figures can be uploaded as separate files.

References must be numbered in the order in which they appear in the text and their corresponding numbers quoted in the text. Authors are responsible for the accuracy of their references. References to the Abstracts and Letters to the Editor must be identified as such. Citation of papers in preparation or submitted for publication, unpublished observations, and personal communications should not be included in the reference list. If essential, such material may be incorporated in the appropriate place in the text. References follow the style of Index Medicus. All authors should be listed when their number does not exceed six; when there are seven or more authors, the first six listed are followed by "et al.". The following are some examples of references from articles, books and book chapters:

Dent RAG, Cole P. *In vitro* maturation of monocytes in squamous carcinoma of the lung. *Br J Cancer* 1981; **43:** 486-95.

Chapman S, Nakielny R. *A guide to radiological procedures.* London: Bailliere Tindall; 1986.

Evans R, Alexander P. Mechanisms of extracellular killing of nucleated mammalian cells by macrophages. In: Nelson DS, editor. *Immunobiology of macrophage.* New York: Academic Press; 1976. p. 45-74.

Authorization for the use of human subjects or experimental animals

Manuscripts containing information related to human or animal use should clearly state that the research has complied with all relevant national regulations and institutional policies and has been approved by the authors' institutional review board or equivalent committee. These statements should appear in the Materials and methods section (or for contributions without this section, within the main text or in the captions of relevant figures or tables).

When reporting experiments on human subjects, authors should indicate whether the procedures followed were in accordance with the Helsinki Declaration. Patients have the right to privacy; therefore the identifying information (patient's names, hospital unit numbers) should not be published unless it is essential. In such cases the patient's informed consent for publication is needed, and should appear as an appropriate statement in the article.

The research using animal subjects should be conducted according to the EU Directive 2010/63/EU and following the Guidelines for the welfare and use of animals in cancer research (*Br J Cancer 2010;* **102:** 1555 – 77). Authors must identify the committee approving the experiments, and must confirm that all experiments were performed in accordance with relevant regulations.

Transfer of copyright agreement

For the publication of accepted articles, authors are required to send the Transfer of Copyright Agreement to the publisher on the address of the editorial office. A properly completed Transfer of Copyright Agreement, signed by the Corresponding Author on behalf of all the authors, must be provided for each submitted manuscript. The non-commercial use of each article will be governed by the Creative Commons Attribution-NonCommercial-NoDerivs license.

Conflict of interest

When the manuscript is submitted for publication, the authors are expected to disclose any relationship that might pose real, apparent or potential conflict of interest with respect to the results reported in that manuscript. Potential conflicts of interest include not only financial relationships but also other, non-financial relationships. In the Acknowledgement section the source of funding support should be mentioned. The Editors will make effort to ensure that conflicts of interest will not compromise the evaluation process of the submitted manuscripts; potential editors and reviewers will exempt themselves from review process when such conflict of interest exists. The statement of disclosure must be in the Cover letter accompanying the manuscript or submitted on the form available on www.icmje.org/coi_disclosure.pdf

Page proofs will be sent by E-mail or faxed to the corresponding author. It is their responsibility to check the proofs carefully and return a list of essential corrections to the editorial office within three days of receipt. Only grammatical corrections are acceptable at this time.

Reprints: The electronic version of the published papers will be available on www.versitaopen.com/ro free of charge.

SUTENT® kapsule
sunitinibijev malat

ODPIRANJE NOVIH MOŽNOSTI

Zdravljenje metastatskega karcinoma ledvičnih celic (mRCC), gastrointestinalnega stromalnega tumorja (GIST) in nevroendokrinih tumorjev trebušne slinavke (pNET)

BISTVENI PODATKI IZ POVZETKA GLAVNIH ZNAČILNOSTI ZDRAVILA

SUTENT 12,5 mg, 25 mg, 37,5 mg, 50 mg trde kapsule
Sestava in oblika zdravila: Ena kapsula vsebuje 12,5 mg, 25 mg, 37,5 mg ali 50 mg sunitiniba (v obliki sunitinibijevega malata). **Indikacije:** Zdravljenje neizrezljivega in/ali metastatskega malignega gastrointestinalnega stromalnega tumorja (GIST) pri odraslih, če zdravljenje z imatinibom zaradi odpornosti ali neprenašanja ni bilo uspešno. Zdravljenje napredovalega in/ali metastatskega karcinoma ledvičnih celic (MRCC) pri odraslih. Zdravljenje neizrezljivih ali metastatskih, dobro diferenciranih nevroendokrinih tumorjev trebušne slinavke (pNET), kadar gre za napredovanje bolezni pri odraslih (izkušnje z zdravilom Sutent kot zdravilom prve izbire so omejene). **Odmerjanje in način uporabe:** Terapijo mora uvesti zdravnik, ki ima izkušnje z uporabo zdravil za zdravljenje rakavih bolezni. *GIST in MRCC:* Priporočeni odmerek je 50 mg peroralno enkrat na dan, 4 tedne zapored; temu sledi 2-tedenski premor (Shema 4/2), tako da celotni ciklus traja 6 tednov. *pNET:* Priporočeni odmerek je 37,5 mg peroralno enkrat na dan, brez načrtovanega premora. *Prilagajanje odmerka*: Odmerek je mogoče prilagajati v povečanjih po 12,5 mg, upoštevaje individualno varnost in prenašanje. Pri GIST in MRCC dnevni odmerek ne sme preseči 75 mg in ne sme biti manjši od 25 mg; pri pNET je največji odmerek 50 mg na dan, z možnimi prekinitvami zdravljenja. Pri sočasni uporabi z močnimi zaviralci ali induktorji CYP3A4 je treba odmerek ustrezno prilagoditi. *Pediatrična populacija:* Uporaba sunitiniba ni priporočljiva. *Starejši bolniki (≥ 65 let):* Med starejšimi in mlajšimi bolniki niso opazili pomembnih razlik v varnosti in učinkovitosti. *Okvara jeter:* Pri bolnikih z jetrno okvaro razreda A in B po Child-Pughu prilagoditev odmerka ni potrebna; pri bolnikih z okvaro razreda C sunitinib ni bil preizkušen, zato njegova uporaba ni priporočljiva. *Okvara ledvic:* Prilagajanje začetnega odmerka ni potrebno, nadaljnje prilagajanje odmerka naj temelji na varnosti in prenašanju pri posameznem bolniku. *Način uporabe:* Zdravilo Sutent se uporablja peroralno, bolnik ga lahko vzame s hrano ali brez nje. Če pozabi vzeti odmerek, ne sme dobiti dodatnega, temveč naj vzame običajni predpisani odmerek naslednji dan. **Kontraindikacije:** Preobčutljivost na zdravilno učinkovino ali katero koli pomožno snov. **Posebna opozorila in previdnostni ukrepi:** *Bolezni kože in tkiv:* obarvanje kože, bolečine/draženje v ustih. Redko so poročali o primerih gangrenozne pioderme (običajno izgine po prekinitvi zdravljenja) ter o hudih kožnih reakcijah (multiforni eritem (EM), Stevens-Johnsonov sindrom (SJS) in toksična epidermalna nekroliza (TEN)). Če so prisotni znaki EM, SJS ali TEN, je treba zdravljenje prekiniti. *Krvavitve* v prebavilih, dihalih, sečilih, možganih; najpogosteje epistaksa; krvavitve tumorja, včasih s smrtnim izidom. Pri bolnikih, ki se sočasno zdravijo z antikoagulanti, se lahko redno spremlja celotna krvna slika (trombociti), koagulacijski faktorji (PT / INR) in opravi telesni pregled. *Bolezni prebavil:* poleg navzeje, diareje, stomatitisa, dispepsije, bruhanja in ezofagitisa tudi resni zapleti (včasih s smrtnim izidom), vključno z gastrointestinalno perforacijo. *Hipertenzija,* povezana z zdravljenjem; pri bolnikih s hudo hipertenzijo, ki je ni mogoče urediti z zdravili, je priporočljivo začasno prenehanje zdravljenja. *Hematološke bolezni:* zmanjšanje števila nevtrofilcev, trombocitov, anemija. *Bolezni srca in ožilja:* srčno-žilni dogodki, vključno s srčnim popuščanjem, kardiomiopatijo in motnjami v delovanju miokarda, v nekaterih primerih s smrtnim izidom. Sunitinib povečuje tveganje za pojav kardiomiopatije. *Podaljšanje intervala QT*: previdna uporaba pri bolnikih z znano anamnezo podaljšanja intervala QT, tistih, ki jemljejo antiaritmike, in tistih z relevantno, že obstoječo srčno boleznijo, bradikardijo ali elektrolitskimi motnjami. *Venski in arterijski trombembolični dogodki*; arterijski včasih s smrtnim izidom. *Dogodki na dihalih:* dispneja, plevralni izliv, pljučna embolija ali pljučni edem; redki primeri s smrtnim izidom. *Moteno delovanje ščitnice:* bolnike je treba med zdravljenjem rutinsko spremljati glede delovanja ščitnice vsake 3 mesece. *Pankreatitis*, tudi resni primeri s smrtnim izidom. *Hepatotoksičnost*, nekateri primeri s smrtnim izidom. *H*olecistitis, vključno z akalkuloznim in emfizemskim holecistitisom. *Delovanje ledvic:* primeri zmanjšanega delovanja ledvic, odpovedi ledvic in/ali akutne odpovedi ledvic, v nekaterih primerih s smrtnim izidom. *Fistula:* če nastane fistula, je treba zdravljenje s sunitinibom prekiniti. *Oteženo celjenje ran:* pri bolnikih, pri katerih naj bi bil opravljen večji kirurški poseg, je priporočljiva začasna prekinitev zdravljenja s sunitinibom. *Osteonekroza čeljustnic:* pri sočasnem ali zaporednem dajanju zdravila Sutent in intravenskih difosfonatov je potrebna previdnost; invazivni zobozdravstveni posegi predstavljajo dodatni dejavnik tveganja. *Preobčutljivost/angioedem*. *Motnje okušanja*. *Konvulzije:* obstajajo poročila, nekatera s smrtnim izidom, o preiskovancih s konvulzijami in radiološkimi znaki reverzibilnega posteriornega levkoencefalopatskega sindroma. *Sindrom lize tumorja*, v nekaterih primerih s smrtnim izidom. *Okužbe:* hude okužbe z ali brez nevtropenije (okužbe dihal, sečil, kože in sepsa), vključno z nekaterimi s smrtnim izidom. **Medsebojno delovanje z drugimi zdravili:** (Študije so izvedli le pri odraslih.) Zdravila, ki lahko zvišajo koncentracijo sunitiniba v plazmi (ketokonazol, ritonavir, itrakonazol, eritromicin, klaritromicin ali sok grenivke). Zdravila, ki lahko znižajo koncentracijo sunitiniba v plazmi (deksametazon, fenitoin, karbamazepin, rifampin, fenobarbital, *Hypericum perforatum* oz. šentjanževka). **Plodnost, nosečnost in dojenje:** Zdravila Sutent ne smemo uporabljati med nosečnostjo in tudi ne pri ženskah, ki ne uporabljajo ustrezne kontracepcije, razen če možna korist odtehta možno tveganje za plod. Ženske v rodni dobi naj med zdravljenjem z zdravilom Sutent ne zanosijo. Ženske, ki jemljejo zdravilo Sutent, ne smejo dojiti. Neklinični izsledki kažejo, da lahko zdravljenje s sunitinibom poslabša plodnost samcev in samic. **Vpliv na sposobnost vožnje in upravljanja s stroji:** Sutent lahko povzroči omotico. **Neželeni učinki:** Najbolj resni neželeni učinki (nekateri s smrtnim izidom) so odpoved ledvic, srčno popuščanje, pljučna embolija, gastrointestinalna perforacija in krvavitve (npr. v dihalih, prebavilih, tumorju, sečilih in možganih). Najpogostejši neželeni učinki (ki so se pojavili pri vsaj 20 % bolnikov v registracijskih preskušanjih) so: zmanjšan apetit, motnje okušanja, hipertenzija, utrujenost, prebavne motnje (npr. driska, slabost, stomatitis, dispepsija in bruhanje), sprememba barve kože/motnje pigmentacije in sindrom palmarno-plantarne eritrodisestezije. Med najbolj pogostimi neželenimi učinki so hematološke motnje (nevtropenija, trombocitopenija in anemija). Ostali zelo pogosti (≥ 1/10) neželeni učinki so: glavobol, epistaksa, bolečina v trebuhu/napihnjenost, zaprtje, glosodinija, izpuščaj, spremembe barve las, suha koža, bolečine v udih, vnetje sluznice, edemi. **Način in režim izdaje:** Predpisovanje in zdaja zdravila je le na recept, zdravilo pa se uporablja samo v bolnišnicah. Izjemoma se lahko uporablja pri nadaljevanju zdravljenja na domu ob odpustu iz bolnišnice in nadaljnjem zdravljenju. **Imetnik dovoljenja za promet:** Pfizer Limited, Ramsgate Road, Sandwich, Kent, CT13 9NJ, Velika Britanija. **Datum zadnje revizije besedila:** 21.3.2013
Pred predpisovanjem se seznanite s celotnim povzetkom glavnih značilnosti zdravila.

SAMO ZA STROKOVNO JAVNOST

Pfizer Luxembourg SARL, Grand Duchy of Luxembourg, 51, Avenue J.F. Kennedy, L-1855,
PFIZER, Podružnica za svetovanje s področja farmacevtske dejavnosti, Ljubljana,
Letališka 3c, 1000 Ljubljana, SLOVENIJA

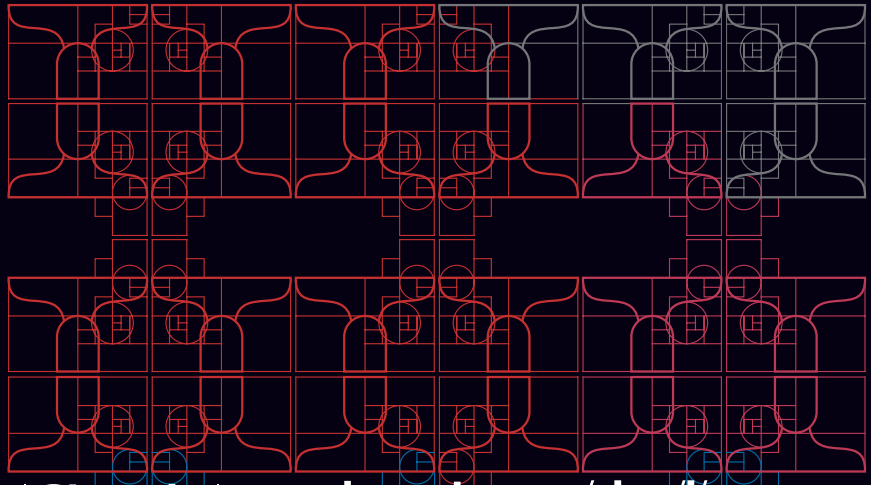

Radiology and Oncology | Ljubljana | Slovenia | www.degruyter.com/view/j/raon

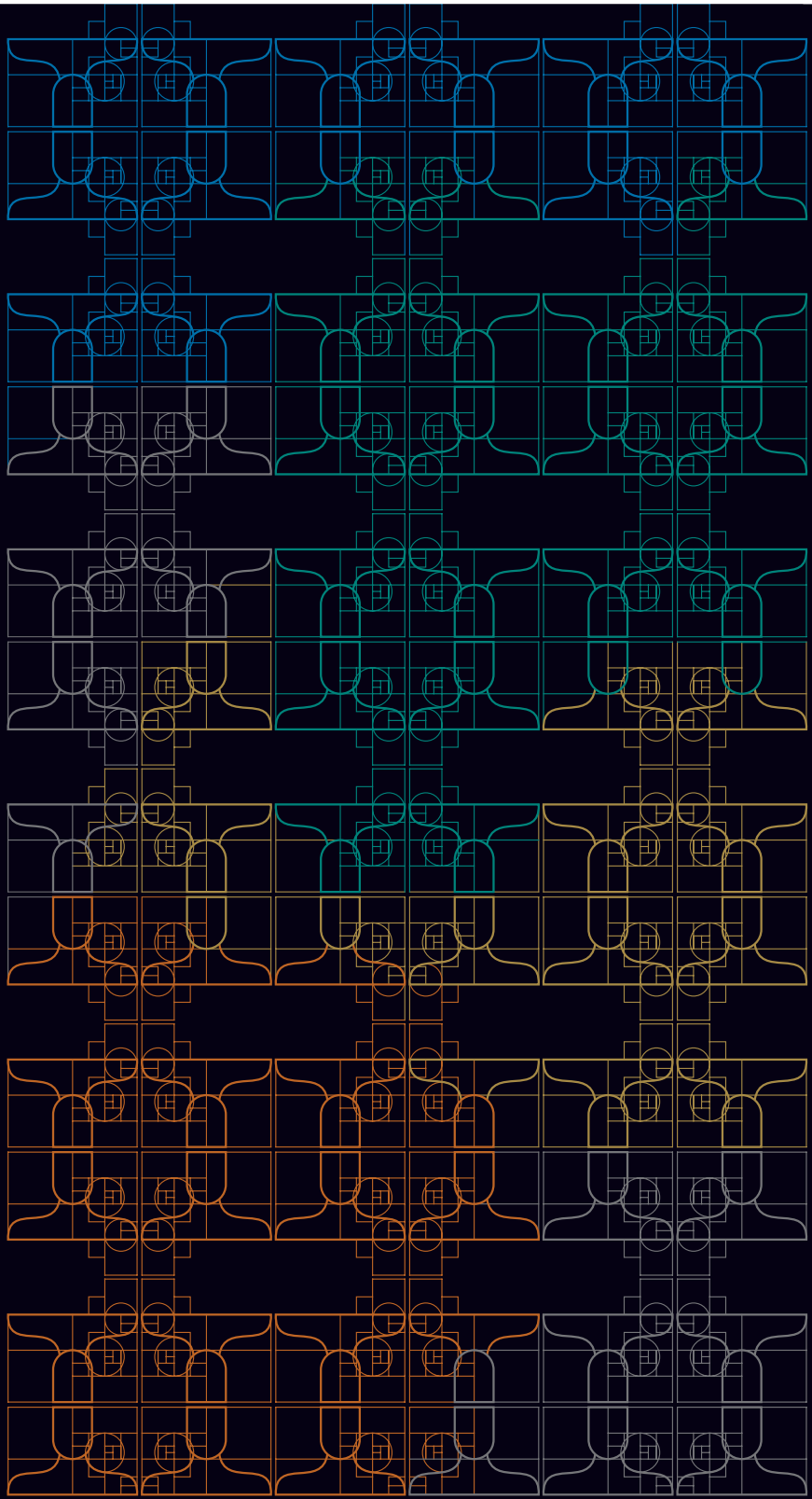

ISSN 1318 - 2099